AD_____

Grant Number DAMD17-97-1-7007

TITLE: Transgenic Engineering of Cholinesterases: Tools for Exploring Cholinergic Responses

PRINCIPAL INVESTIGATOR: Hermona Soreq, Ph.D.

CONTRACTING ORGANIZATION: Hebrew University of Jerusalem
91904 Jerusalem, Israel

REPORT DATE: January 1998

TYPE OF REPORT: Annual

PREPARED FOR: U.S. Army Medical Research and Materiel Command
Fort Detrick, Maryland 21702-5012

REPORT DOCUMENTATION PAGE

Form Approved
OMB No. 0704-0188

1. AGENCY USE ONLY *(Leave blank)*	2. REPORT DATE	3. REPORT TYPE AND DATES COVERED
	January 1998	Annual (30 Dec 96 - 29 Dec 97)

4. TITLE AND SUBTITLE
Transgenic Engineering of Cholinesterases: Tools for Exploring Cholinergic Responses

5. FUNDING NUMBERS
DAMD17-97-1-7007

6. AUTHOR(S)
Hermona Soreq, Ph.D.

7. PERFORMING ORGANIZATION NAME(S) AND ADDRESS(ES)
Hebrew University of Jerusalem
91904 Jerusalem, Israel

8. PERFORMING ORGANIZATION REPORT NUMBER

9. SPONSORING/MONITORING AGENCY NAME(S) AND ADDRESS(ES)
U.S. Army Medical Research and Materiel Command
Fort Detrick, Maryland 21702-5012

10. SPONSORING/MONITORING AGENCY REPORT NUMBER

11. SUPPLEMENTARY NOTES

12a. DISTRIBUTION / AVAILABILITY STATEMENT
Approved for public release; distribution unlimited

12b. DISTRIBUTION CODE

13. ABSTRACT *(Maximum 200*

The long-term objective of the research in the laboratory is to understand the molecular and cellular mechanisms that mediate the coupling of short-term changes in cholinergic neurotransmission to long-term consequences in motor, cognitive and autonomous functions. To study the pathways by which cholinergic inputs control neuritic and synaptic cytoarchitecture and determine changes in downstream-regulated genes, we have developed transgenic and antisense models which enable gain- and loss-of-function modulation in several acetylcholinesterase (AChE) variants. These led to the observation that AChE expression is essential for neurite growth and affects synaptic development through its catalytic function, core protein and variable C-termini domains. In transgenic mice, we found that AChE overproduction alters expression of the neuronal circuitry-related members of the neurexin gene family and causes late onset, progressive deterioration in dendrite branching, neuromotor and cognitive faculties. Using hippocampal brain slices and an *in vivo* stress protocol, we demonstrated that both acute stress and exposure to anti-cholinesterases disrupt the blood-brain barrier and promote long-lasting changes in cholinergic gene expression. Currently, cosmid sequencing and genotyping studies are being employed to explore the association of intragenic and neighboring sequences with regulation of the expression of the AChE gene, which is essential for responses to drugs and scavenging of poisons.

14. SUBJECT TERMS	15. NUMBER OF PAGES
Gulf War Illness acetylcholinesterase animal models anti-cholinesterase antisense butyrylcholinesterase human ribozyme	141
	16. PRICE CODE

17. SECURITY CLASSIFICATION OF REPORT	18. SECURITY CLASSIFICATION OF THIS PAGE	19. SECURITY CLASSIFICATION OF ABSTRACT	20. LIMITATION OF ABSTRACT
Unclassified	Unclassified	Unclassified	Unlimited

FOREWORD

Opinions, interpretations, conclusions and recommendations are those of the author and are not necessarily endorsed by the U.S. Army.

____ Where copyrighted material is quoted, permission has been obtained to use such material.

____ Where material from documents designated for limited distribution is quoted, permission has been obtained to use the material.

____ Citations of commercial organizations and trade names in this report do not constitute an official Department of Army endorsement or approval of the products or services of these organizations.

__X__ In conducting research using animals, the investigator(s) adhered to the "Guide for the Care and Use of Laboratory Animals," prepared by the Committee on Care and Use of Laboratory Animals of the Institute of Laboratory Resources, National Research Council (NIH Publication No. 86-23, Revised 1985).

__X__ For the protection of human subjects, the investigator(s) adhered to policies of applicable Federal Law 45 CFR 46.

__X__ In conducting research utilizing recombinant DNA technology, the investigator(s) adhered to current guidelines promulgated by the National Institutes of Health.

__X__ In the conduct of research utilizing recombinant DNA, the investigator(s) adhered to the NIH Guidelines for Research Involving Recombinant DNA Molecules.

__X__ In the conduct of research involving hazardous organisms, the investigator(s) adhered to the CDC-NIH Guide for Biosafety in Microbiological and Biomedical Laboratories.

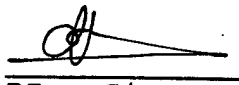

Jan. 7, 1998

PI - Signature Date

Table of Contents

The Report

Tasks indicated for the grant:

Task 1, year 1: Create transgenic BuChE and AChE *Xenopus* tadpoles with different efficiencies of expression and the cell-type management of the resultant enzyme.

Task 2, year 1: Characterize the sensitivity to OPs of the transgenic tadpoles (task 1).

Task 3, years 1 and 2: Create transgenic BuChE- and AChE-mice with optimum DNA construct s (task 2).

Task 4, years 2 and 3: Test transgenic mice (task 3) in behavioral tests and hypothermic responses with or without exposure to OPs and LD_{50}.

In 1997, progress is reported in tasks

Task 1: Because it was found that *Xenopus* embryos are more resistant to OPs than are mammalian cells, it was decided to concentrate on 3' splicing variants of AChE, those which generate characteristic proteins. This is reported in the manuscript by Sternfeld et al.

Task 2: The work on characterizing the OP sensitivities of the variant AChEs is in progress. Results will not be available until next year.

Task 3: Several lines of AChE-transgenic mice have been created and characterization has been initiated.

In 1998, work is planned on tasks

Task 3: Characterization of OP sensitivities will be continued.

Task 4: Creation and characterization of mice expression AChE variants in behavioral tests will be initiated.

Introduction

Work under current grant support has focused on several specific topics. First, we wished to address the question of whether changes in the levels and/or properties of AChE may cause deleterious effects on cognitive or neuromotor functions in mammals. To answer this question, we have investigated a line of transgenic mice which overexpress human AChE in brain neurons and have studied their neuronal circuitry, neuromuscular junctions and spinal cord synapses at the microscopic and electron microscopic levels, in conjunction with their neuromotor and cognitive functioning on the one hand, and metabolic changes in their cholinergic neurotransmission elements on the other.

The second question addressed in our research refers to the long-argued issue of non-catalytic functions (s) of AChE. To unequivocally demonstrate that such functions exist and that they affect neurogenesis and synaptogenesis, we created an insertion-inactivated AChE by genetic engineering, expressed this enzyme in developing *Xenopus* motoneurons , and compared the results of this expression with those obtained with a series of catalytically active AChE variants with modified C-termini. The outcome of this study indicates that non-catalytic role(s) of AChE should be taken into consideration also when the catalytically active enzyme is overexpressed, as in the case of the transgenic mice.

To further explore the subject of post-transcriptional control of AChE properties, we investigated the potential of phosphorylation agent(s) to affect the catalytic activity of this enzyme. To unravel the physiological basis of the paradoxical appearance of CNS symptoms in response to the peripherally acting AChE inhibitor pyridostigmine, we considered the possibility that the blood-brain barrier may be corrupted under acute psychological stress.

The non-catalytic functions of AChE are not necessarily blocked by chemical inhibitors, which demands that some of our previous conclusions and assumptions must be viewed with caution. This, in turn, called for development of novel experimental means for suppression not only of AChE activity, but also of the protein's presence in any form. To

this end, we initiated the antisense approach, based on prevention of protein production through sequence-targeted destruction of the mRNAs which encode them.

Along these lines, the body of this report is organized in 5 distinct parts, each with its own focused introduction and experimental results and each reflecting one or more publications:

A. The role of AChE in inducing a genetically programmed neurodeterioration in AChE-transgenic mice
   Andres et al., (1997) Proc. Natl. Acad. Sci. USA 94, 8173-8178.
   Andres et al., Neurochem. Internatl. (in press)
B. Non-catalytic functions of AChE in *Xenopus* embryos and in mice
   Sternfeld et al., J. Neurosci. (in press)
   Beeri et al. (1997) J. Neurochem. 69, 2441-2451.
C. The increase of specific catalytic activity of AChE in response to phosphorylation
   Grifman et al. (1997) Mol. Brain Res. 51, 179-187.
D. The physiological basis of the paradoxical appearance of CNS symptoms in response to pyridostigmine, a peripherally acting AChE inhibitor
   Friedman et al., (1996) Nature Med. 2, 1382-1385.
E. AS-ODN suppression of *ACHE* expression in cultured cells.
   Grifman et al. (1997) in *Concepts in Gene Research*, M. Strauss, J.A. Barranger, eds., de Gruyter, Berlin, 141-167.

A. The role of AChE in genetically programmed neurodeterioration in AChE-transgenic mice

1. Transgenic mice display embryonic modulation of spinal cord choline acetyltransferase and neurexin Iβ expression and post-natal neurodeterioration

Introduction

Mammalian synapses are continuously remodeled to adjust to growth and the demands of use (Burns and Augustine, 1995; Grinell, 1995). Various diseases of the central and peripheral nervous systems that are associated with postnatal or adult-onset, progressive deterioration reflect deficiencies in the remodeling processes of cholinergic synapses. Examples include Alzheimer's disease (AD) (Coyle et al., 1983), spinal muscular atrophy (Crawford and Pardo, 1996), congenital myasthenias (Shillito et al., 1993) and amyotrophic lateral sclerosis (Robert and Brown, 1995). A simple model to explain the delayed-onset of pathology in these degenerative conditions views the decline toward disease as a gradual accumulation of damage which results in pathology when it passes a threshold. In such a model, built-in margins of safety protect the system, and hence the organism, for a period of time that reflects the margins of safety. An alternative, or supplemental approach to understanding late-onset disease is to postulate the existence of mechanisms that adjust the levels of other proteins and assure normal function during embryonic, postnatal, and young adulthood periods, but which falter or fail during aging. In that case, the age of onset will depend on the limits of adjustment and on the functional integrity of the cellular and molecular mechanisms which regulate feedback pathways. To distinguish between these possibilities and to search for putative age-limited adjustment mechanisms, animal models with late-onset nervous system defects are required.

Imbalanced cholinergic neurotransmission can be induced in animal models by acetylcholinesterase (AChE) over-production. Changes in synaptic AChE density, in particular, are predicted to modulate synaptic levels of acetylcholine (ACh) as well as postsynaptic miniature endplate potentials (MEPPS, Anglister et al., 1994). Transient overexpression of AChE indeed exerts a morphogenic effect on the development of neuromuscular junctions (NMJ) in AChE-transgenic *Xenopus* embryos (Seidman et al. 1995). The morphogenic effects of overexpressed AChE were attributed, at least in part, to subtle alterations in cholinergic neurotransmission. However, while the overall normal development of AChE-transgenic tadpoles suggested that developing NMJs can tolerate some deviation from normal cholinergic activity, the short time course of those experiments (3-5 days) precluded an investigation into the long-term effects of deregulated AChE expression on neuromuscular integrity and function. To this end, AChE-transgenic mice provide an intriguing model in which the effects of chronic AChE excesses can be examined in depth.

Transgenic overexpression of acetylcholinesterase (AChE) in cholinergic brain neurons of transgenic mice promotes late-onset progressive impairments in learning and memory (Beeri et al., 1995) as well as in neuromotor functioning (Andres et al., 1997). The cognitive defects observed in these mice could potentially reflect a cholinergic deficit which is caused by excessive hydrolysis of ACh and a consequent cholinergic hypofunction. In this sense, the adult-onset loss-of-function observed in AChE transgenic mice can serve as a model for the loss of cholinergic faculties observed in Alzheimer's disease (AD) patients (Coyle et al., 1983). However, the neuromotor deficiency in these AChE-overexpressing transgenic mice was preceded by changes in the expression of both choline acetyl transferase and neurexin Ib, reflecting feedback processes affecting non-cholinergic functions in addition to the cholinergic ones (Andres et al., 1997). This, in turn, predicted changes in the properties and/or cytoarchitecture of specific synapses that were associated with the delayed onset of AChE-promoted neurodeterioration in these transgenic mice. To define which synapses were thus affected, we have undertaken a comparative ultrastructure

analysis of neuromuscular junction (NMJ) and cholinergic spinal cord axo-dendritic synapses in the AChE-transgenic mice.

Formation of NMJs differs from that of inter-neuronal synapses in that it involves the differentiation of precisely defined domains on the surface of muscle fibers (Hall and Sanes, 1993; Carbonetto and Lindenbaum, 1995). Mammalian NMJ formation depends on several important neuron-derived proteins including agrin, which stimulates the formation of subneural clusters of ACh receptors (AChR) and AChE (reviewed by Grinnell, 1995 and Gautam et al., 1996) and neuregulin, which promotes the expression of several of the AChR subunit genes (Jo et al., 1995; Carraway and Burden, 1995). Experimental elimination of either of these proteins drastically reduces or abolishes NMJ formation during embryogenesis and results in prenatal or perinatal death (Gautam et al., 1996, Glass et al., 1996). Global interference with NMJ formation has also been achieved experimentally by genomic disruption or overexpression of other key NMJ proteins, CNTF (Masu et al., 1993), laminin b2, (Noakes et al., 1995), GAP-43 (Aigner et al., 1995), rapsyn (Gautam et al., 1995), and MuSK (Dechiarra et al., 1996). However, the early onset and severity of the neuromuscular defects obtained in knock-out studies precludes investigation into the role of these molecules in the long-term maintenance of synaptic ultrastructure and function during adulthood.

AChE-transgenic mice express a modest excess of human AChE in spinal cord but not muscle (Beeri et al., 1995; Andres et al., 1997). We now report that the ultrastructure of spinal cord cholinergic synapses is largely retained in spite of this excess, unlike NMJs of AChE transgenic mice which undergo dramatic cytoarchitectural changes. AChE-transgenic mice thus can be used for dissecting the molecular and cellular chains of events which lead from AChE excess toward postnatal neuromuscular pathology. Moreover, they can be employed to differentiate between effects of impaired cholinergic neurotransmission and those due to modified cell-cell interactions. Therefore, they may establish a valid paradigm for approaching delayed-onset human diseases of environmental (e.g. insecticide poisoning) and/or multigenic origin such as congenital myasthenias that are associated with AChE mal-or overproduction.

Experimental Results

To explore the possibility that overproduction of neuronal AChE confers changes in both cholinergic and morphogenic, intercellular interactions, we studied developmental responses to neuronal AChE overexpression in motoneurons and neuromuscular (NMJ) junctions of AChE-transgenic mice. The transgene is expressed in spinal cord neurons, but not in muscle (Fig. 1). Perikarya of spinal cord motoneurons were consistently enlarged from embryonic through adult stages in AChE-transgenic mice (Fig. 2). Atypical motoneuron development was accompanied by premature enhancement in the embryonic spinal cord expression of choline acetyltransferase (ChAT) mRNA, encoding the acetylcholine synthesizing enzyme (Fig. 3). In contrast, the mRNA encoding neurexin-Iβ, the heterophilic ligand of the AChE-homologous neuronal cell surface protein neuroligin, was drastically lower in embryonic transgenic spinal cord than in controls (Fig. 4). Postnatal cessation of these dual transcriptional responses was followed by late-onset deterioration in neuromotor performance that was associated with gross aberrations in NMJ ultrastructure and with pronounced amyotrophy (Figs. 5, 6). These findings demonstrate embryonic feedback mechanisms to neuronal AChE overexpression that are attributable to both cholinergic and cell-cell interaction pathways, suggest that embryonic neurexin Iβ expression is concerted *in vivo* with AChE levels, and indicate that postnatal changes in neuronal AChE-associated proteins may be involved in late-onset neuromotor pathologies.

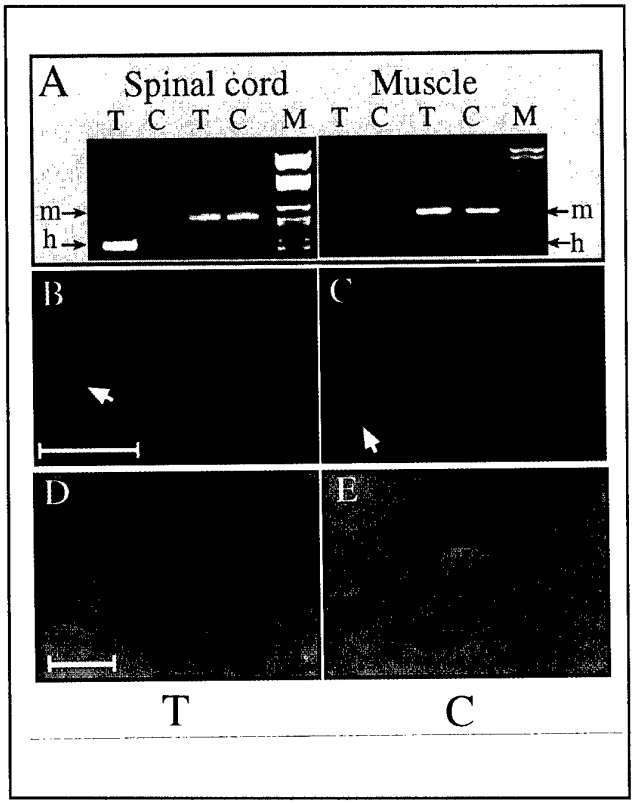

Fig. 1. Human AChE cDNA is expressed in spinal cord neurons but not muscle. A: RT-PCR analyses. Primers specific for mouse (m) or human (h) AChEmRNA induced expression of the transgene in transgenic (T) spinal cord but not muscle. Control (C) mice express the endogenous mRNA in both tissues. B,C: *In situ* hybridization. A probe which detects both mouse and human AChEmRNAs labeled neurons in 50 μm cervical spinal cord sections from both transgenic (B) and control (C) mice. Black arrows indicate large polygonal α-motoneurons; white arrows indicate γ motoneurons and/or interneurons. Size bar equals 50 μm. Note that labeling is restricted to cells with neuronal morphology. D,E: Enzyme activity. Fixed sections from the anterior horn of lumbar spinal cord of transgenic (D) or control (E) mice were cytochemically stained for catalytically active AChE. Note the enhanced activity in nerve fibers and cell bodies from the transgenic spinal cord. Size bar equals 100 μm.

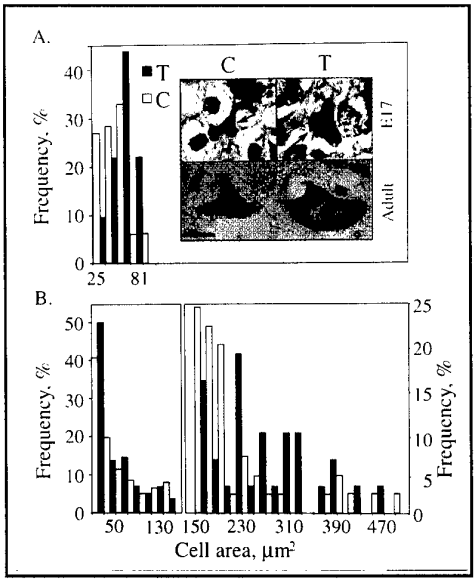

Fig. 2. AChE overexpression is associated with enlarged motoneuron perikarya. A. Embryonic enlargement. Thoracic spinal cord sections from E17 transgenic (T) and control (C) mice were stained with cresyl violet and the perikaryal areas in μm^2 of ventral horn cells measured. Presented are percent fractions of the total number of cresyl violet-positive cells in each size group (67 control and 32 transgenic cells were measured). This analysis revealed overall enlargement of neurons in transgenic embryonic spinal cord ($p<0.05$). Inset. Representative cresyl violet-positive control (C) and transgenic (T) neurons from embryonic (E17) and 3 month-old (adult) mice are presented. Note that the enlarged neurons characteristic of transgenic animals maintain the normal polygonal morphology. Size bar = 10 μm. Arrows indicate motoneurons. B. Adult enlargement. Separate size distributions for ventral horn neurons up to 150 μm^2 (left) and larger than 150 μm^2 (right) from adult mice are presented. Smaller cells (202 control and 186 transgenic cells), presumably interneurons and γ-motoneurons showed similar perikaryal area distributions in transgenic and control animals. In contrast, the larger ventral horn cells, presumably α-motorneurons (44 control and 27 transgenic cells), preserved the embryonic trend of enlarged perikarya observed in transgenic animals ($p<0.02$).

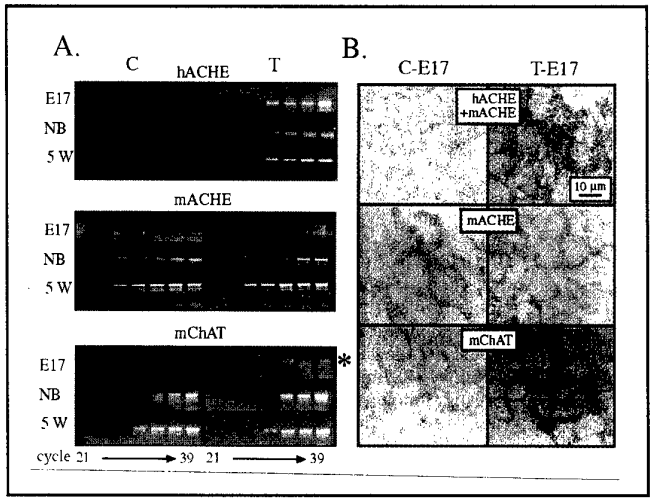

Fig. 3. Transgenic hAChEmRNA expression induces a transient embryonic enhancement in ChATmRNA levels. A. RT-PCR analyses. RNA extracted from spinal cord of control (C) and transgenic (T) mice at the noted ages was subjected to kinetic RT-PCR using primers for the noted mRNAs. Aliquots of amplified DNA representing human (h) or mouse (m) ACHE or ChAT mRNAs were removed every third cycle from cycle 21, representing differences of ca. 8-fold between samples. Products were electrophoresed and stained with ethidium bromide. Note that hAChEmRNA is present only in transgenic mice, that endogenous AChE mRNA levels are similar in control and transgenic animals, and that while mChAT levels are undetectable in control E17 embryos, a prominent signal, marked by a star, is observed in transgenic embryos. In postnatal mice, ChAT mRNA levels in transgenic and control spinal cord are indistinguishable. NB = newborn. B. *In situ* hybridization. 7 µm sections from the lumbar spinal cord of control (C) and transgenic (T) E17 embryos were subjected to *in situ* hybridization. Fast-red red (Boehringer-Mannheim, Germany) served for detection. Note the intense AChE and ChAT mRNA signals in transgenic cell bodies.

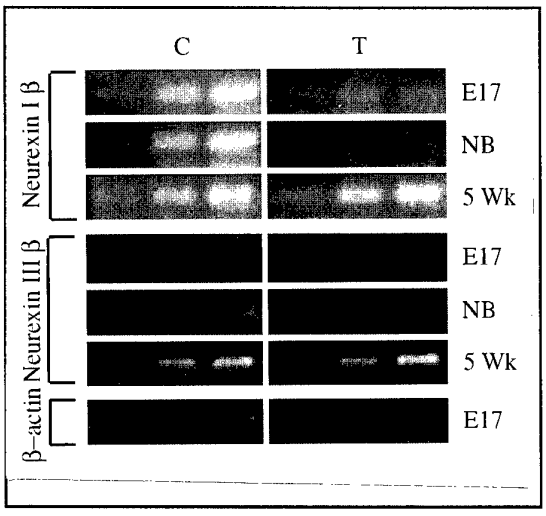

Fig. 4. Neurexin Iβ mRNA is dramatically suppressed in embryonic and newborn transgenic mice. Primers specific for neurexin Iβ and IIIβ mRNAs were used in semi-quantitative RT-PCR on spinal cord RNA from control (C) and transgenic (T) mice at the noted ages. Note the dramatic reduction in signal intensities for neurexin Iβ in embryonic (E17) and newborn (NB) transgenic mice compared to controls and to 5 week-old (5 Wk) mice. Primers for β-actin mRNA served to verify quantity and quality of RNA in each sample. Shown are PCR products sampled every third cycle (i.e., reflecting 8-fold differences) from cycle 21 for β-actin and cycle 24 for neurexins.

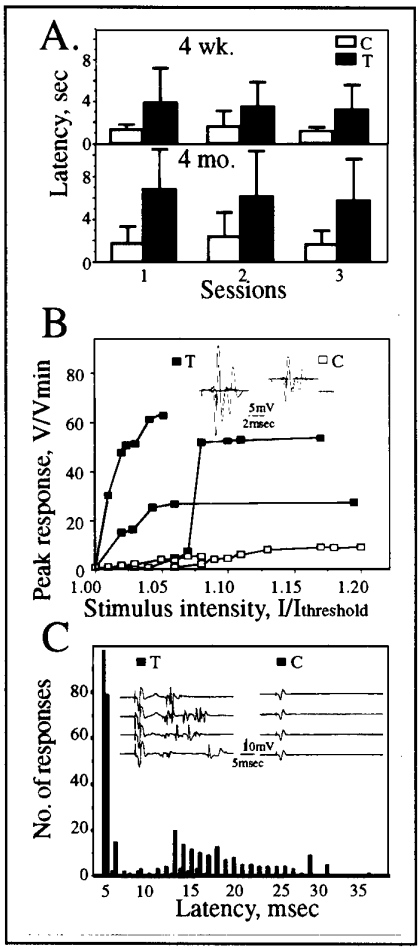

Fig. 5. Postnatal motor function impairments worsen with age.
Groups of 5-10 mice at the ages of 4 week- and 4 month-old transgenic (T) and control (C)) were suspended with their forelegs on a 3 mm diameter rope and the time taken to securely grip the rope with their hindlegs was noted (latency). Presented are escape latencies in sec (avg ± SD). Note the slower performance of transgenics as compared with controls at both age groups and the worsening of this phenotype with age. B. Electromyographic profiles. Evoked muscle fiber potentials (V/V_{min}) following sciatic nerve stimulation were recorded by a microelectrode placed on the surface of the gastrocnemius muscle in 3 transgenic (filled squares) and 3 control (empty squares) mice. Inset. Superposition of responses evoked by increasing stimulus intensity up to 1.0 mA at 1 Hz as in the enclosed scale. Saturation of response occurred only at high stimulus intensities and required more stimuli in transgenics than in controls. Note that in the transgenic muscle several negative peaks were observed in response to a single stimulus. C: Delayed repetitive firing of action potentials. Following 100 supramaximal stimulations at 1 Hz, abnormal late potentials (filled bars) appeared in 4 transgenic animals for up to 40 msec post-stimulation as compared with a few signals in 4 control animals (empty bars). Presented are numbers of response spikes as a function of latency time for 10 different measurements.

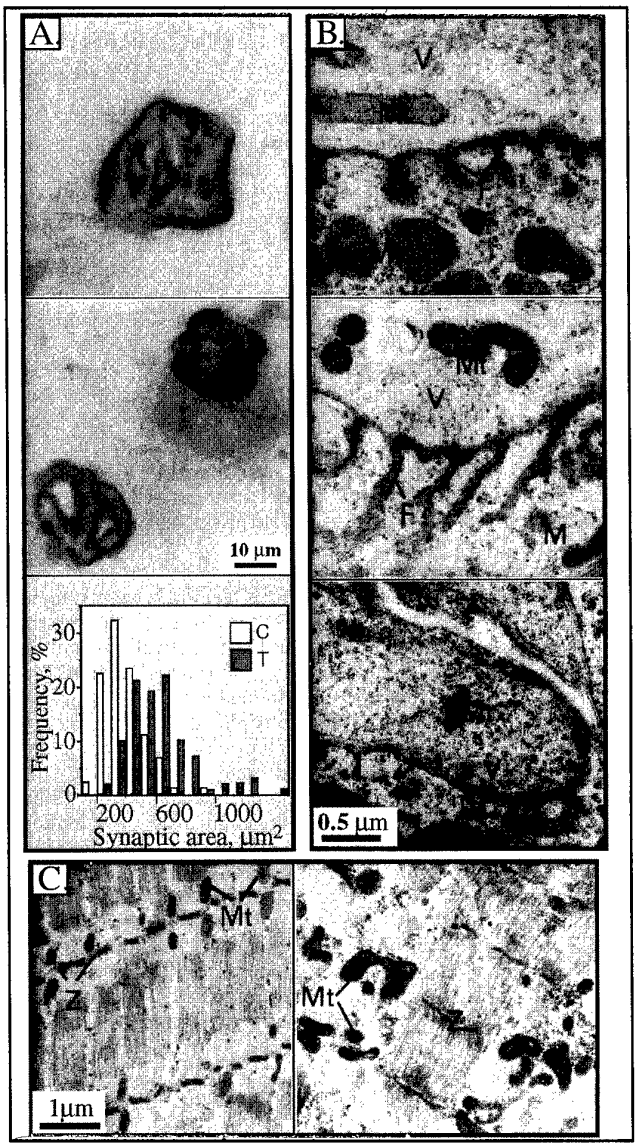

Fig. 6. Enlargement and shape modifications in diaphragm neuromuscular junctions of transgenic animals. A. NMJ surface changes. Wholemount cytochemical staining of AChE activity was performed on fixed diaphragms from 4 month-old transgenic (top) and control (center) animals. Transgenic NMJs displayed larger circumference and fading boundaries as compared with the complex, sharp contours in controls. Representative endplates from 12 control and transgenic mice. Similar results were obtained using methylene blue staining for total protein (not shown). Bottom: Stained areas in μm^2 for motor endplates illustrated above (for 90 control, 100 transgenic terminals) are presented as a frequency distribution plot. B. Post-synaptic fold changes. Electron microscopy of 80 nm cross-sections of terminal diaphragm zones reveals variable deformities in NMJ from transgenic mice. Top. Normal NMJ. Center. Transgenic NMJ with exaggerated post-synaptic folds. Bottom. Transgenic NMJ with short, undeveloped folds marked by arrowheads. V = vesicles; M = muscle; V = vesicles; F = post-synaptic folds. C: Muscle abnormalities. Left: Longitudinal section from normal diaphragm muscle. Note the organization of mitochondria (Mt) at well-aligned Z bands (Z). Right. Transgenic diaphragm muscle with fiber atrophy, loss of muscle fiber organization and swelling of mitochondria at disrupted Z bands.

2. Transgenic acetylcholinesterase induces enlargement of murine neuromuscular junctions but leaves spinal cord synapses intact

Introduction

Animal models for studying late-onset disorders associated with cholinergic deterioration, and most notably Alzheimer's disease (AD) should display progressive deterioration of memory and learning, as well as senile plaques and neurofibrillary tangles (Price et al., 1995), a hypofunctional cholinergic system (Bierer et al., 1995), and breakdown in cortical circuitry related to cell and synaptic loss (Davies & Maloney, 1976; DeKosky and Sheff, 1990; Terry et al., 1992; Honer et al., 1992). Aged, cognitively-impaired animal models displayed the expected behavioral, neuroanatomical, and/or neurochemical changes in their cholinergic system (Bartus and Uehara, 1979). Several physical or pharmacological modulations also resulted in loss of cholinergic synapses and impaired memory (Fischer et al., 1989 ; Zhi et al., 1995). Subsequent transgenic APP mouse models (LaFerla et al., 1995; Games et al., 1995; Moran et al., 1995; Hsiao et al., 1995, 1996) demonstrated development of Ab deposits, neuritic plaques, synaptic loss and late-onset spatial memory deficits. However, in AD, amyloid plaques and tangles are particularly concentrated in brain regions where cholinergic circuits operate (Coyle et al., 1983). Also, synaptic loss but not the presence of amyloid plaques or neurofibrillary tangles could be convincingly correlated with cognitive impairment in AD (Terry et al., 1992). Yet, correlation between high levels of β-amyloid deposits and progressive severity of the cognitive defect was only shown in part of the above transgenic models (Hsiao et al., 1996) . Therefore, it remained unresolved whether the learning deficits in these mice were caused by- or only correlated with increased brain β-amyloid levels and amyloid depositions.

In AD, structural changes in brain cholinergic synapses (DeKosky and Scheff, 1990) are associated with loss of neuronal nicotinic binding sites (Nordberg et al., 1988), with death of ACh-producing neurons (Davies and Maloney, 1976; Whitehouse et al., 1986), and with the consequent disruption of cholinergic neurotransmission (Coyle et al., 1983; Fibiger, 1991). The resultant hypocholinergic condition is characterized by a relative excess of the ACh-hydrolyzing enzyme, acetylcholinesterase (AChE). To define the contribution of cholinergic malfunction toward the AD phenotype ,we have recently used the authentic promoter from the human *ACHE* gene in conjunction with the AChE-coding sequence to create transgenic mice expressing human AChE in central nervous system (CNS) neurons. Manual use of the Morris water maze, revealed a progressively severe decline in the spatial learning and memory capabilities of these transgenic mice (Beeri et al., 1995). It was therefore of interest to carefully dissect the learning and memory impairments in AChE transgenic mice and examine in them which of the morphometric and/or biochemical correlates of AD can be causally associated with cholinergic malfunction.

Cortical neurons in normal aged humans may develop longer and more branched dendritic trees than either young adults or individuals with senile dementia (Buell and Coleman, 1981). Cognitive deficiencies are further associated with dysgenesis of dendritic spines, on which most cortical synapses reside (Purpura, 1974; Braak and Braak, 1985). We therefore wished to evaluate the state of dendrite arborizations and spine density in adult transgenic mice with excess brain AChE. Also, we explored the transport of choline, which is used by cholinergic neurons, both for reforming metabolized membrane phosphatidylcholine and for synthesizing the neurotransmitter acetylcholine (ACh). The levels of the high affinity Na^+-dependent choline transporter unique to these cells can be quantified using [^{3}H] hemicholinium-3 (Vickroy et al., 1984). The concentration of available choline is the rate limiting factor for ACh synthesis; when choline is in short supply, active cholinergic neurons were reported to sustain neurotransmission at the expense of membrane building (Wurtman, 1992). Indeed, cerebral cortical areas in AD

brains exhibited marked decreases in choline acetyltransferase (ChAT) activity and significant enhancement in [^{3}H] hemicholinium-3 binding. In the AD frontal cortex, transporter overexpression exceeded the level which is needed to compensate for the loss of synaptic terminals, presumably accelerating membrane turnover and neurodegeneration (Slotkin et al., 1994).

In search for behavioral, morphological and molecular correlates common to AD and the AChE-transgenic mice we employed video imaging to carefully assess the memory impairment in these mice. We further examined in them the dendritic branching and spine density in cortical neurons, the mRNA and protein levels of ACh-receptors and the levels of [^{3}H]-hemicholinium-3 binding. Our findings demonstrate complex cognitive failure, attenuated dendrite branching, declined spine density and Imbalanced choline metabolism in AChE transgenic mice, attributing all of these phenomena to AChE excess and the associated cholinergic malfunction.

Experimental Results

AChE produced by spinal cord motoneurons accumulates within axo-dendritic spinal cord synapses (Fig. 1) It is also secreted from motoneuron cell bodies, through their axons, into the region of neuromuscular junctions, where it terminates cholinergic neurotransmission. We have shown that transgenic mice expressing human AChE in their spinal cord motoneurons display primarily normal axo-dendritic spinal cord cholinergic synapses in spite of the clear excess of transgenic over host AChE within these synapses (Fig. 2). This is in contrast to our recent observation that a modest excess of AChE drastically affects the structure and long-term functioning of NMJs in these mice although they express human AChE in their spinal cord, but not muscle (above). Enlarged muscle endplates with either exaggerated or drastically shortened post-synaptic folds (Tables 1, 2) then lead to a progressive neuromotor decline and massive amyotrophy. These findings demonstrate that excess neuronal AChE may cause distinct effects on spinal cord and neuromuscular synapses, and attribute the late-onset neuromotor deterioration observed in AChE transgenic mice to NMJ abnormalities.

Table 1. Morphometric parameters of hAChE-expressing spinal cord synapses[a]

parameter 2	control	transgenic	
AChE stained area, μm^2	0.05 ± 0.04 (43)	0.34 ± 0.90 (47)	$p < 0.03$
area occupied by vesicles, μm^2	0.47 ± 0.3 (37)	0.39 ± 0.29 (44)	n.s.
vesicles/ μm^2	95.8 ± 33.9 (16)	107.9 ± 27.9 (16)	n.s.
axon minimal diameter, μm	0.93 ± 0.34 (40)	0.74 ± 0.28 (44)	n.s.
axonal mitochondria area, μm^2	0.23 ± 0.13 (37)	0.19 ± 0.1 (31)	n.s
dendrite minimal diameter, μm	2.44 ± 2.3 (20)	1.61 ± 0.9 (15)	n.s.
dendritic mitochondria area, μm^2	0.52 ± 0.52 (19)	0.35 ± 0.21 (13)	n.s.

[a]Morphometric parameters were derived from photographs taken using light or electron microscopy for the numbers of axo-dendritic cholinergic synapses from the anterior spinal cord of at least 5 adult control and transgenic mice. Statistical significance (Student's t test) is noted wherever relevant; n.s., not significant.

Table 2. Morphometric parameters of hAChE-expressing neuromuscular junctions[a]

parameter	control	transgenic	
AChE stained area, μm^2	398 ± 136.4 (90)	625.6 ± 227.7 (100)	$p < 0.001$
methylene blue-stained area, μm^2	301 ± 92.1 (38)	723.7 ± 495.3 (33)	$p < 0.001$
mean length of post-synaptic folds/ length of NMJ	0.56 ± 0.12(14)	0.65 ± 0.37 (16)	n.s.
vesicles/μm^2	122.5 ± 30.7 (12)	161.4 ± 41.8 (9)	$p < 0.02$
muscle fiber diameter, µm	30.8 ± 7.45 (69)	35.6 ± 5.17 (75)	$p < 0.005$

[a]Morphometric parameters were determined as detailed in Table 1 for the numbers noted of NMJs, analyzed folds or muscle fibers from the diaphragm muscle of control and transgenic mice.

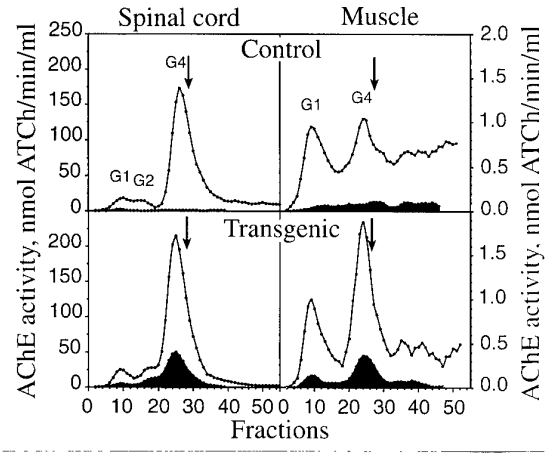

Fig. 1. Transgenic human AChE is found in spinal cord and muscle homogenates. Detergent-soluble homogenates of spinal cord and muscle were fractionated by sucrose gradient centrifugation and AChE activity determined in each fraction prior to (line) or after binding to a specific anti-human AChE monoclonal antibody (shaded area) (Seidman et al., 1995). Note the different activity scales for spinal cord (left) and muscle (right hand side). Arrows denote sedimentation of an internal marker, bovine catalase (11.4 S). Activity peaks reflecting globular monomers, dimers and tetramers are labeled G1, G2 and G4, respectively. Fractions drawn from the top of each tube represented by fraction 1.

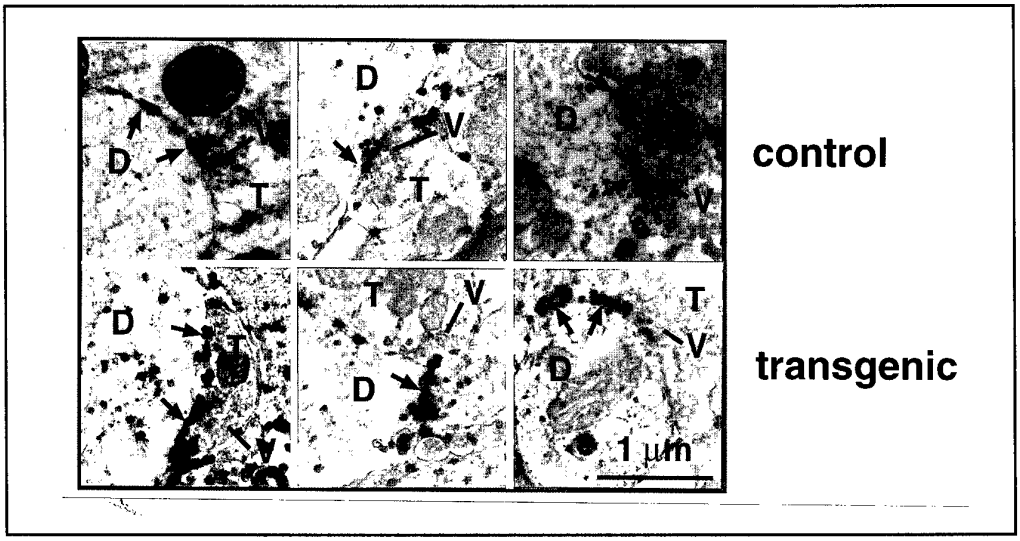

Fig. 2. AChE overexpression in axo-dendritic synapses from anterior spinal cord of transgenic mice. Electron micrographs of three representative synapses from transgenic and control (C) mice are presented. Acetylthiocholine hydrolysis products representing sites of AChE accumulation appear as dark crystals, particularly conspicuous in the synaptic cleft between axon terminals (T) and dendrites (D). V = vesicles. Size bar equals 1 µm.

B. Non-catalytic functions of AChE in *Xenopus* embryos and in mice

1. Acetylcholinesterase enhances neurite growth and synapse development through alternate contributions of its hydrolytic capacity, core protein and variable C-termini

Introduction

Acetylcholinesterase (AChE) hydrolyzes the neurotransmitter acetylcholine (ACh) released from nerve terminals at neuromuscular junctions (NMJs) and brain cholinergic synapses, thus terminating synaptic transmission (Salpeter, 1967). Potential non-catalytic function(s) of AChE were implicated by findings that certain AChE inhibitors decrease chick neurite outgrowth in culture and that externally added AChE stimulates this process regardless of the presence of specific inhibitors (Layer et al., 1993; Small et al., 1995; Jones et al., 1995). Sequence homology between AChE and several adhesion molecules (de La Escalera et al., 1990; Ichtchenko et al., 1995) and the early appearance of AChE in developing embryos before the onset of cholinergic neurotransmission (Layer and Willbold , 1995) also suggest that AChE may play a developmental function in cellular development and in neuronal growth, that is unrelated to its classical ACh hydrolyzing activity. However, experiments addressed at the non-catalytic nature of the neurogenic activity of AChE were all based on the indirect use of inhibitors or involved external addition of AChE to the culture medium (Jones et al., 1995) or the solid substrate (Layer et al., 1993, Small et al., 1995). This called for studies where the mode or level of the autologous expression of AChE would be changed within the tested neurons themselves.

The human AChEmRNA transcript may be alternatively spliced at its 3'-end to yield 3 mature AChEmRNAs encoding protein products with three distinct C-termini (Ben Aziz-Aloya et al., 1993; Karpel et al., 1994). These include the brain-abundant exon 6-encoded C-terminal peptide, the hematopoietic exon 5-encoded C-terminus which enables glycophospholipid conjugation and the C-terminus derived from the open reading frame of the tumor-abundant pseudointron 4. The brain and muscle human (h) AChE form (hAChE-E6), overexpressed in developing *Xenopus laevis* embryos, accumulates in and enlarges the post-synaptic length of neuromuscular junctions (Seidman et al., 1994; 1995). Injection of h*ACHE*DNA encoding the readthrough form of AChEmRNA (*ACHE*-I4/E5) to *Xenopus* embryos, caused selective production and secretion of an enzyme C-terminated by the I4-encoded peptide (AChE-I4) in ciliated and secretory epidermal cells. However, AChE-I4 did not reach neuromuscular junctions or affect their length (Seidman et al., 1995). In cultured glioma cells microinjected or stably transfected with the *ACHE*-E6 vector, overexpression caused cell body enlargement and rapid process extension. Stable transfection with *ACHE*-I4/E5, in contrast, caused the appearance of small, process-less round cells (Karpel et al., 1996). However, no experiments explored the potential effects of these alternative C-termini on AChE-induced process extension from primary neurons. To address these questions, we constructed two novel hAChEDNA vectors. One of these encodes a truncated form of the enzyme, devoid of any of the natural C-termini; the other encodes an insert-disrupted form of the enzyme, incapable of hydrolyzing ACh yet recognized by anti-AChE antibodies. These two constructs and the above *ACHE*-E6 and *ACHE*-I4/E5 DNAs were microinjected into *Xenopus* oocytes and embryos and were used to test the biochemical and hydrodynamic properties of the resultant proteins and compare these properties with the effects of each of these AChE variants on neurite extension of *Xenopus* spinal neurons.

Experimental Results

Accumulated indirect evidence suggests nerve-growth promoting activities for AChE. To unequivocally define whether such activities exist, whether they are related to this enzyme's capacity to hydrolyze acetylcholine, and whether they are associated with specific alternative splicing products of the *ACHE* gene, we employed four biochemically distinct recombinant human AChEs (Fig. 1). First, *Xenopus laevis* embryos were injected with

human *ACHE* DNA for characterization of the expression products. When expressing the synapse-characteristic AChE-E6 which contains the exon 6-derived C-terminus, cultured spinal neurons grew 3-fold faster than co-cultured control neurons (Figs. 2, 3, Table 1). Similar enhancement occurred in neurons expressing an insertion-inactivated human AChE-E6-IN protein, which displays immunochemical and electrophoretic migration properties indistinguishable from those of the normal synaptic enzyme, but is not capable of hydrolyzing acetylcholine. In contrast, the non-synaptic secretory human AChE-I4 variant, which contains the pseudointron 4-derived C-terminus did not affect neurite growth. Moreover, no growth-promotion occurred in neurons which express the soluble, catalytically active C-terminally truncated human AChE -E4, demonstrating a dominant-positive role of the E6-derived C-terminus and an inert role for the I4-derived alternative C-terminus in neurite extension. Of all three active enzyme variants employed, AChE-E6 was the only one to be associated with *Xenopus* membranes (Figs. 4, 5). These findings prove an autologous, evolutionarily conserved and exon 6-dependent growth-promoting activity for neuronal AChE. Furthermore, this study directly reveals that the morphogenic activity of AChE is spatially limited and unrelated to its hydrolytic capacity and points at a mechanism of enzyme association with the cell membrane for this function .

Table 1. Effects of AChE on neurote growth *in vitro*

construct injected[a]		total neurite length per cell (μm)		growth rate (μm/hr)	number of branches	number of cells (embryos)
		at 6-7 hr	at 9-10 hr			
ACHE-E6	+	64.6 ± 6.5	124.0 ±11.7	37.9 ± 5.2*	1.8 ± 0.1	32 (7)
	-	55.2 ± 5.9	88.2 ± 10.3	12.9 ± 2.7	1.6 ± 0.1	33 (7)
ACHE-I4/E5	+	62.0 ± 10.6	77.5 ± 8.2	11.6 ± 2.1	1.7 ± 0.1	27 (8)
	-	52.9 ± 5.0	92.7 ± 6.2	14.7 ± 1.9	1.6 ± 0.1	31 (8)
ACHE-E6-IN	+	91.2 ± 9.8*	156.9 ± 13.6*	33.6 ± 3.7*	2.0 ± 0.1	25 (3)
	-	47.4 ± 5.1	62.5 ± 9.6	11.2 ± 2.1	1.5 ± 0.1	28 (3)
ACHE-E4	+	48.0 ± 7.0	94.2 ± 9.1	11.9 ± 3.7	1.7 ± 0.2	16 (4)
	-	51.6 ± 7.4	126.2 ± 20.4	13.0 ± 4.2	1.8 ± 0.2	20 (4)

[a]cDNA vectors were injected into *Xenopus* embryos at the 2-cell stage using rhodamine-dextran as a marker. Cultures were made from injected embryos 1 day later. "+" indicates rhodamine-dextran-positive neurons, "-" indicates rhodamine-dextran-negative neurons in the same cultures.

*Significant difference was found between + and - groups (two-tailed t test; $p < 0.005$).

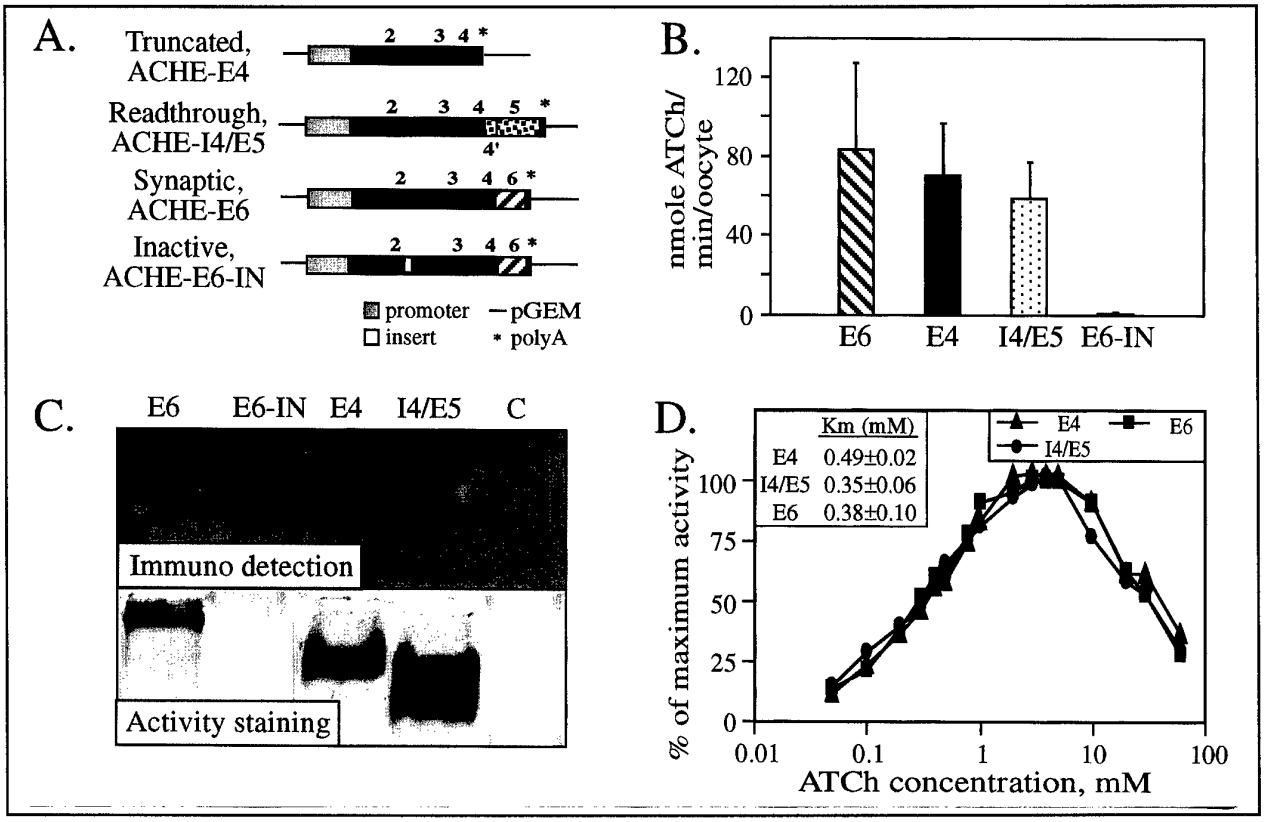

Fig. 1. Biochemical properties of recombinant AChE variants. A. Analyzed AChE DNAs. The DNA constructs which encode each of the examined AChE variants. Common exons are designated by black boxes, exon 6 by a hatched box, and pseudointron 4 and exon 5 by dotted boxes. B. Hydrolytic cholinesterase activities. ATCh-hydrolyzing activities of each of the enzyme forms encoded by the above ACHE constructs were tested in homogenates of microinjected *Xenopus* oocytes. Presented are average results of 3 experiments for each construct. Endogenous *Xenopus* AChE activities were subtracted from activities found for cDNA injected oocytes. Note that AChE-E4 activity levels are comparable with those of AChE-E6 and AChE-I4 and AChE-E6-IN displayed no significant catalytic activity. C. Electrophoretic and activity properties of the AChE variants. Homogenates of *Xenopus* oocytes microinjected with each of the ACHE cDNA constructs and of buffer injected oocytes (C) were subjected to denaturing gel electrophoresis followed by protein blot and immunodetection (above) and to non-denaturing gel electrophoresis followed by AChE activity staining (below). Each lane represents ca. 50 ng AChE. Note that AChE-E6-IN is highly immunoreactive but displays no catalytic activity, and that AChE-E4 migrates faster than the other variants in the denaturing gel. In the lower panel, note that AChE-I4 displays heterogeneous bands, and migrates faster than AChE-E6 and AChE-E4. D. Substrate inhibition. The above oocyte homogenates were assayed for cholinesterase activity in the presence of 0.05-60 mM ATCh as substrate. Cholinesterase activity in each substrate concentration is shown as percentage of the highest activity for each homogenate, after subtraction of spontaneous ATCh hydrolysis. Shown is one representative of two experiments. Inset: Km values of the recombinant hAChE variants.

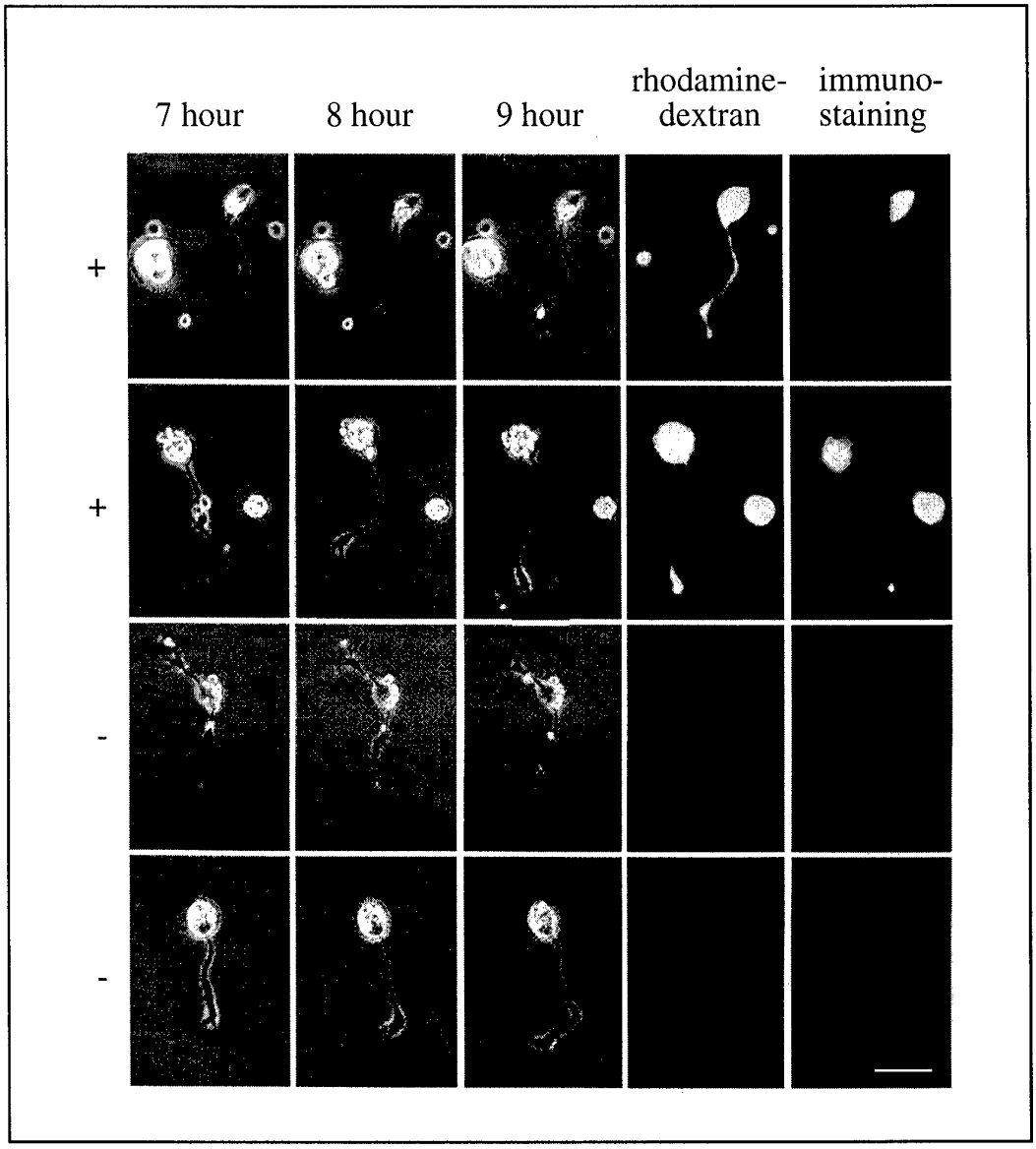

Fig. 2. Neurons which express human AChE-E6 (+) and control neurons (-) in *Xenopus* cultures. *Xenopus* embryos were co-injected with AChE-E6 DNA and rhodamine-dextran complexes and their spinal neurons dissociated into culture 1 day later. Bright-field images were taken at 7, 8, and 9 h after cell plating. Both the total neurite length and the rate of neurite growth were measured during this period. Fluorescence micrographs on the right of the 9 h photographs depict the rhodamine fluorescence of dextran complexes, which were co-injected with the cDNA. Indirect fluorescein immunofluorescence staining of AChE, observed at the end of the experiment is shown on the last right panel. Note the correlation between dextran fluorescence and AChE staining. Staining and imaging conditions were identical for all 4 cells, which were from the same culture. Fluorescent cells (+) were positive with both red and green filters, whereas negative (-) cells remained invisible in both. Bar = 20 μm.

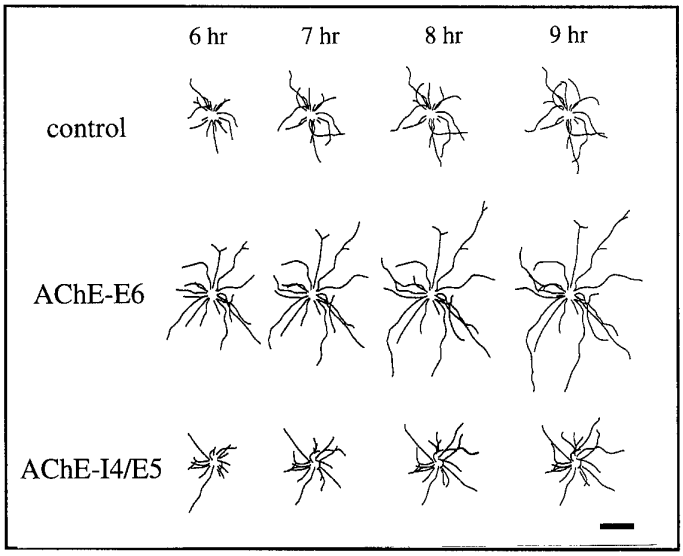

Fig. 3. Effects of expressing human AChE on the growth of *Xenopus* spinal neurons. Composite concentric line drawings were made from video images of 12 isolated spinal neurons at 6, 7, 8 and 9 h after cell plating. The center of the neuronal soma was placed in the center of each drawing. Note consistent overall neurite length promotion in neurons that expressed AChE-E6, but not AChE-I4. Neurons derived from uninjected blastomeres served as controls. Bar = 20 μm.

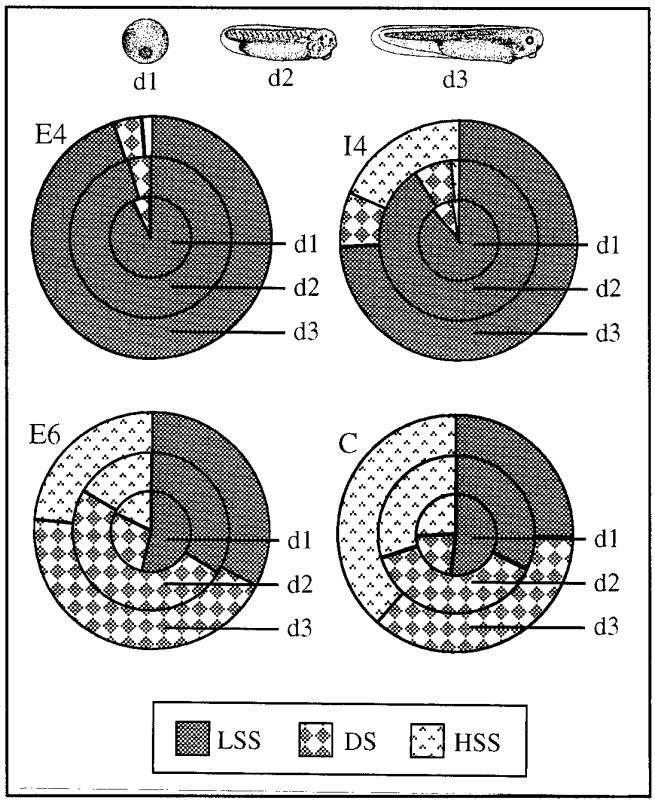

Fi.g. 4. AChE-E6 exhibits developmentally increased membrane association *in vivo*. Cleaving *Xenopus* embryos were injected with the various *ACHE* DNA vectors or with buffer (C) and sequential extractions into low salt-soluble (LSS), low salt-detergent-soluble (DS), and high salt-soluble (HSS) fractions were performed. Indogenous *Xenopus* AChE activities were subtracted from activities of all other embryo samples. Slices, therefore, represent the net relative fractions of the total summed activities for the host enzyme and each hAChE varient. Note that AChE-E6 is similar to *Xenopus* AChE in its lower solubility under low salt extraction, whereas AChE-E4 and AChE-I4 are both predominantly low salt-soluble. Top, schemattic drawings of 1-, 2- and 3-day old *Xenopus* embryos modeled after those of Deuchar (1966).

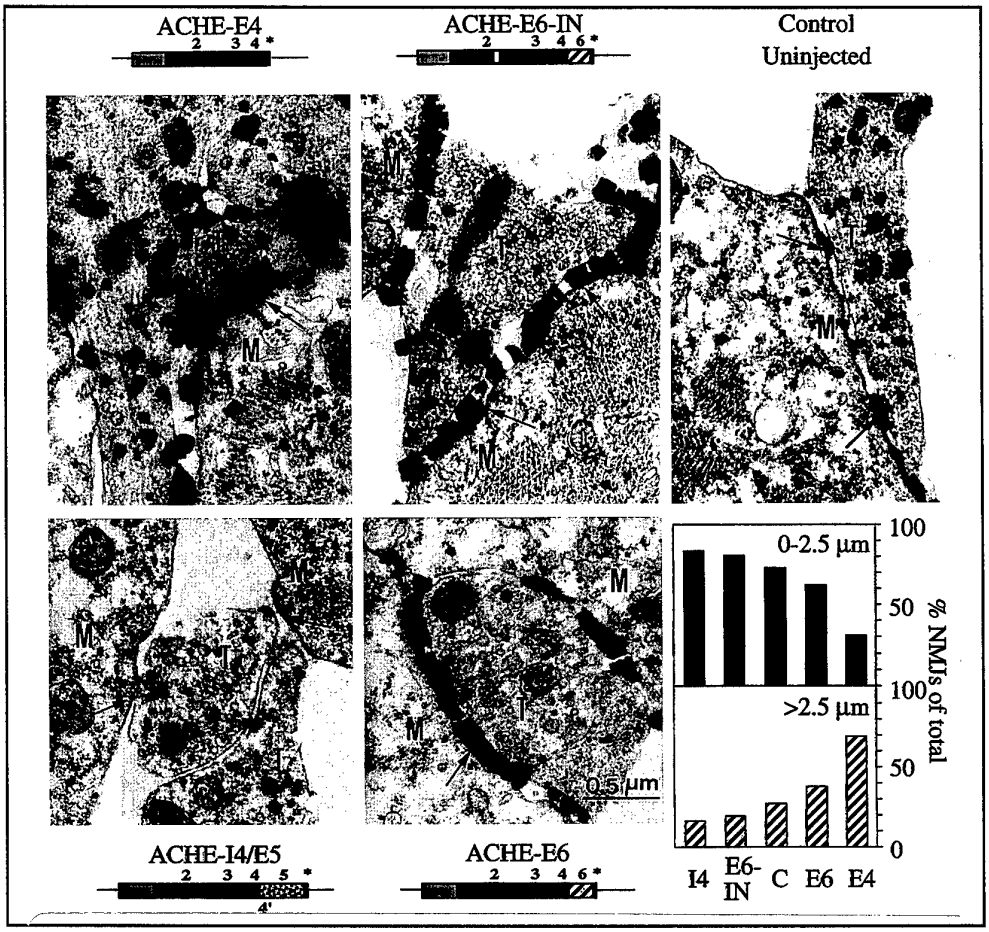

Fig. 5. AChE-E6 and AChE-E4 enhance NMJ length, whereas AChE-I4 and AChE-E6-IN do not. Two day-old DNA-injectied and control uninjected *Xenopus* embryos were stained for catalytically active AChE and examined by electron microscopy. Representative images of NMJs from embryos with each of the vectors are shown. Note the enhanced staining apparent as dark electron-dense deposits in NMJs from AChE-E6-, AChE-E6-IN- and AChE-E4-injeced embryos as compared with controls. T, nerve terminal; M, muscle cell; *arrows* point to synaptic clefts. *Bottom right panel*, NMJ population analysis. Electron microscope NMJ images (16, 31, 43 and 66 sections from AChE-E4-, -E6-IN-, -I4- and -E6-injected and 55 sections from control uninjected embryos, respectively) were used for postsynaptic length measurements. The percentages of synapses with lengths shorter or longer than 2.5 µm are presented for NMJs from embryhos injected with each vector. Note that expression of AChE-E6 and AChE-E4 increases postsynaptic length as compared with controls.

2. Enhanced hemicholinium binding and attenuated dendrite branching in cognitively impaired ACHE-transgenic mice

Introduction

Animal models for studying late-onset disorders associated with cholinergic deterioration, and most notably Alzheimer's disease (AD) should display progressive deterioration of memory and learning, as well as senile plaques and neurofibrillary tangles (Price et al., 1995), a hypofunctional cholinergic system (Bierer et al., 1995), and breakdown in cortical circuitry related to cell and synaptic loss (Davies & Maloney, 1976; DeKosky and Sheff, 1990; Terry et al., 1992; Honer et al., 1992). Aged, cognitively-impaired animal models displayed the expected behavioral, neuroanatomical, and/or neurochemical changes in their cholinergic system (Bartus and Uehara, 1979). Several physical or pharmacological modulations also resulted in loss of cholinergic synapses and impaired memory (Fischer et al., 1989 ; Zhi et al., 1995). Subsequent transgenic APP mouse models (LaFerla et al., 1995; Games et al., 1995; Moran et al., 1995; Hsiao et al., 1995, 1996) demonstrated development of Aβ deposits, neuritic plaques, synaptic loss and late-onset spatial memory deficits. However, in AD, amyloid plaques and tangles are particularly concentrated in brain regions where cholinergic circuits operate (Coyle et al., 1983). Also, synaptic loss but not the presence of amyloid plaques or neurofibrillary tangles could be convincingly correlated with cognitive impairment in AD (Terry et al., 1992). Yet, correlation between high levels of β-amyloid deposits and progressive severity of the cognitive defect was only shown in part of the above transgenic models (Hsiao et al., 1996) . Therefore, it remained unresolved whether the learning deficits in these mice were caused by, or only correlated with increased brain Aβ levels and amyloid depositions.

In AD, structural changes in brain cholinergic synapses (DeKosky and Scheff, 1990) are associated with loss of neuronal nicotinic binding sites (Nordberg et al., 1988), with death of ACh-producing neurons (Davies and Maloney, 1976; Whitehouse et al., 1986), and with the consequent disruption of cholinergic neurotransmission (Coyle et al., 1983; Fibiger, 1991). The resultant hypocholinergic condition is characterized by a relative excess of AChE. To define the contribution of cholinergic malfunction toward the AD phenotype, we have recently used the authentic promoter from the human *ACHE* gene in conjunction with the AChE-coding sequence to create transgenic mice expressing human AChE in CNS neurons. Manual use of the Morris water maze, revealed a progressively severe decline in the spatial learning and memory capabilities of these transgenic mice (Beeri et al., 1995). It was therefore of interest to carefully dissect the learning and memory impairments in AChE transgenic mice and examine in them which of the morphometric and/or biochemical correlates of AD can be causally associated with cholinergic malfunction.

Cortical neurons in normal aged humans may develop longer and more branched dendritic trees than either young adults or individuals with senile dementia (Buell and Coleman, 1981). Cognitive deficiencies are further associated with dysgenesis of dendritic spines, on which most cortical synapses reside (Purpura, 1974; Braak and Braak, 1985). We therefore wished to evaluate the state of dendrite arborizations and spine density in adult transgenic mice with excess brain AChE. Also, we explored the transport of choline, which is used by cholinergic neurons, both for reforming metabolized membrane phosphatidylcholine and for synthesizing the neurotransmitter acetylcholine (ACh). The levels of the high affinity Na^+-dependent choline transporter unique to these cells can be quantified using [^{3}H] hemicholinium-3 (Vickroy et al., 1984). The concentration of available choline is the rate limiting factor for ACh synthesis; when choline is in short supply, active cholinergic neurons were reported to sustain neurotransmission at the expense of membrane building (Wurtman, 1992). Indeed, cerebral cortical areas in AD brains exhibited marked decreases in choline acetyltransferase (ChAT) activity and

significant enhancement in [^{3}H] hemicholinium-3 binding. In the AD frontal cortex, transporter overexpression exceeded the level which is needed to compensate for the loss of synaptic terminals, persumably accelerating membrane turnover and neurodegeneration (Slotkin et al., 1994).

Experimental Results

In search for behavioral, neuroanatomical and metabolic characteristics of AD which may result from cholinergic malfunction, we employed transgenic mice which overexpresss AChE mRNA and active enzyme in brain neurons (Fig. 1). Mapping by *in situ* hybridization revealed similar distribution to transgenic and host AChE mRNA (Fig. 2). In a Morris water maze working memory paradigm, adult transgenic mice did not display the characteristic improvement found in control mice either between or within test days, and spent less time than control mice in the platform zone (Fig. 3). In 5 week-old transgenic mice, the basilar dendritic trees of layer V pyramidal neurons from the fronto-parietal cortex were essentially as developed as in age-matched controls (Table 1). However, branching totally ceased after this age, whereas in control adults it continued at least up to 7 months (Fig. 4). Therefore, dendritic arbors became smaller in adult transgenic mice than those of controls. Furthermore, the average number of spines was significantly lower on dendritic branches of 7 month-old, but not 5 week-old transgenics as compared with controls (Table 1). Binding of tritiated hemicholinium-3, a blocker of the high affinity choline uptake characteristic of active cholinergic terminals, was over 2-fold enhanced in the brain of transgenic mice (Fig. 5). In contrast, no differences were observed in the mRNA and ligand binding levels for several different subtypes of nicotinic and muscarinic acetylcholine receptors (Fig. 6). These findings suggest that 3 different hallmarks associated with Alzheimer's disease, namely, progressive cognitive failure, cessation of dendrite branching and spine formation and enhanced high affinity choline uptake are outcomes of cholinergic malfunction.

Table 1. Progressive deterioration of layer V pyramidal neurons in AChE-transgenic mice

	Tested parameters	5 week old mice		7 month old mice		Significance: C,T comparison	
		C	T	C	T	5 weeks	7 months
1	Golgi-stained neurons evaluated for dendrite branching (animal) [total]	9/(2) [18]	9/(2) [18]	9/(4) [36]	9/(4) [36]		
2	Cumulative total intersections /neuron (Sholl analysis, at 150 μm from soma)	123	118	126	109	$p \leq 0.23$	$p \leq 0.01$ (Gaussian approximation of Wilcoxin test)
3	Effectiveness of C,T pairing	0.9938		0.9969		$p \leq 0.0001$	$p \leq 0.0001$ (Spearman approximation)
4	stained neurons analyzed for dendritic spines/ (animal) and [total]	7/(2) [14]	7/(2) [14]	9/(4) [36]	9/(4) [36]		
5	Average number of spines / basilar branch / neuron (±SEM)	105.7 ±9.63	99.95 ±7.76	108.6 ±6.49	89.91 ±6.09	$p = 0.84$	$p = 0.04$ (unpaired t test)
6	difference between C,T means	5.71±12.37		18.65±8.90		$p = 0.22$	$p = 0.04$ (F test of variance)
7	variance comparison (Mann-Whitney U value)	87.50		444.0		$p = 0.65$	$p = 0.02$ (Mann-Whitney test, two-tailed P value)

1-3 Using coded slides, the basilar tree of the noted number of Golgi-stained neurons per brain in 2 or 4 animals per group (parentheses) were evaluated for branching, using Sholl analysis (method of concentric circles). Statistical analyses (specified under "significance") showed significant differences between the 7 month- but not 5 week-old controls and transgenics under highly significant pairing effectiveness.

4-7 Dendritic spines were counted along the entire dendritic branch of 3-5 branches per randomly selected 9 neurons for each brain. Both total and the average number of spines were significantly different between 7 month- but not 5 week-old transgenic (T) and control (C) mice.

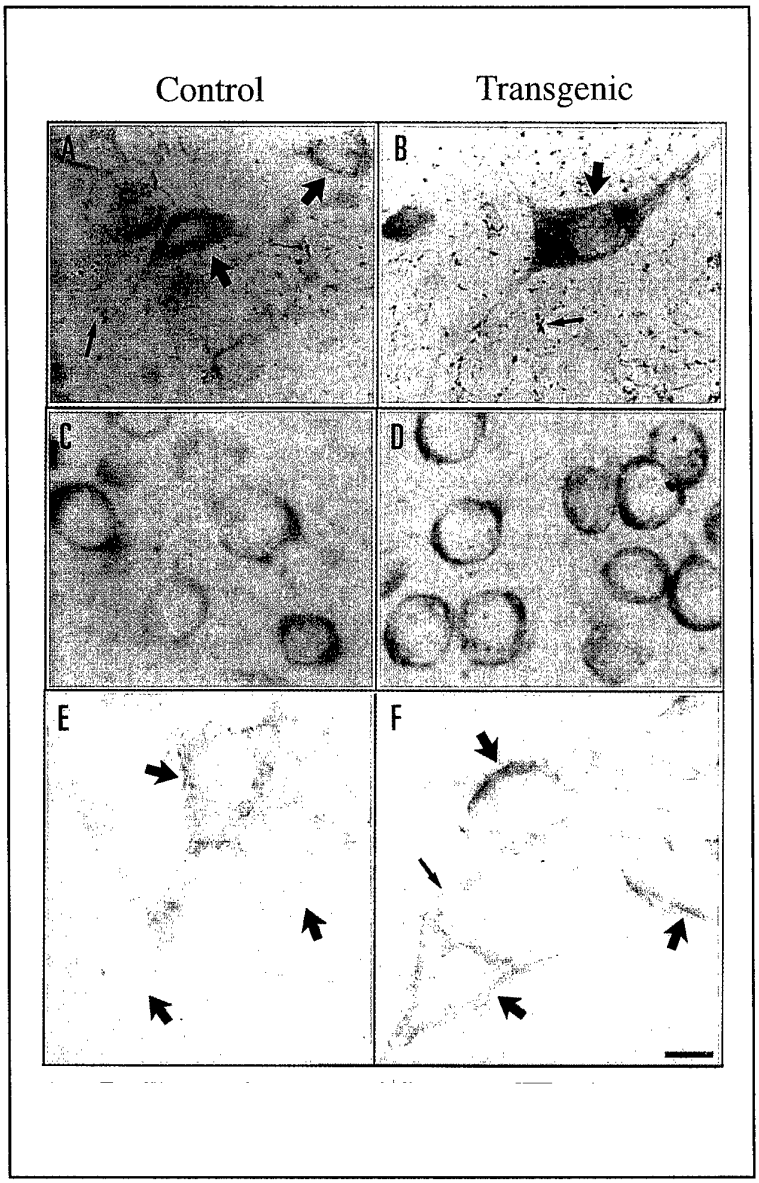

Fig. 1. AChE overexpression in neostriatal neurons. Upper panels: AChE mRNA. Presented are paraffin-embedded neostriatum (A,B) and cortical sections (C,D) from control (A,C) and transgenic (B,D) mice following *in situ* hybridization with a 5'-biotinylated AChE cRNA probe which detects both mouse and human ACHE mRNA. Lower panels: Active AChE. Presented are floating vibratome sections cytochemically stained for acetylthiocholine hydrolysis (E = control, F = transgenic). Because of the different treatments involved in these two procedures, the neurons appear somewhat shrunken in the paraffin -embedded sections. Judging by the heavier staining in neurons from transgenic mice as compared to controls, both cell bodies and apical processes of neostriatal neurons contain both the human mRNA and its human enzyme product. Size bar: 10 μm. Sites of heavy staining in neuronal processes are denoted by thin arrowheads and in cell bodies by thick arrowheads.

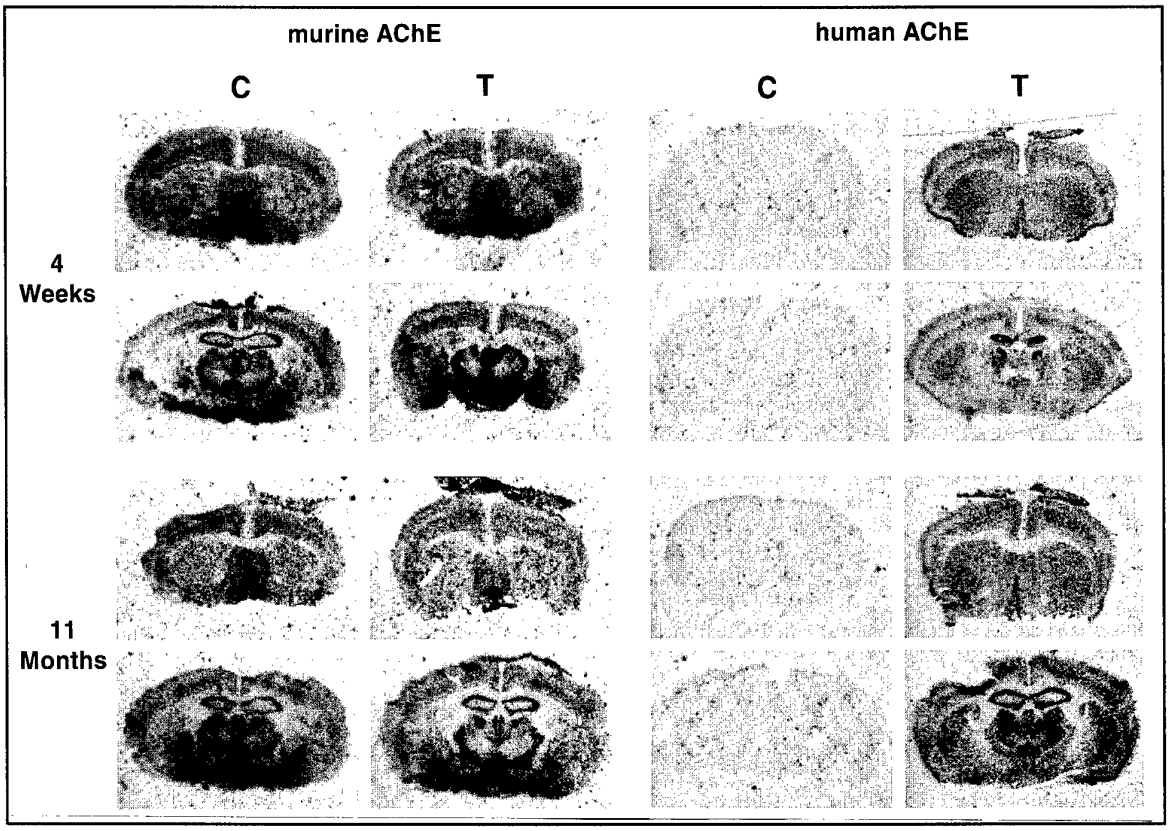

Fig. 2. Transgenic Human AChEmRNA is co-expressed with host mouse AChEmRNA. *In situ* hybridization of the murine and human AChE mRNA in control (C) and transgenic mice (T). Note the small dots in the striatum of the sections hybridized with the probe for the endogenous AChE which represent the striatal cholinergic inter

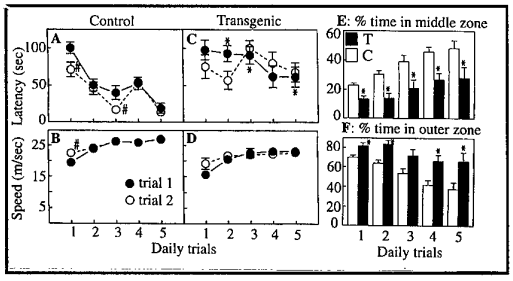

Fig. 3. Impaired performance of adult transgenic mice in a working memory procedure in the water maze. Improved mean (+/–SEM) latency to reach the platform in trial 1 in control (n=19, panel A) as compared with transgenic mice (n=11, panel C) indicate changes in reference memory. Improved performance in trial 2 vs. trial 1 indicate changes in working memory. Panels B,D present somewhat lower swimming speed in transgenic as compared to control mice. Panels E and F: Percent time spent in middle and outer concentric zones suggest impaired search strategy of transgenic mice. *, $p<0.05$ transgenic vs. control, #, $p<0.05$ trial 1 vs. trial 2.

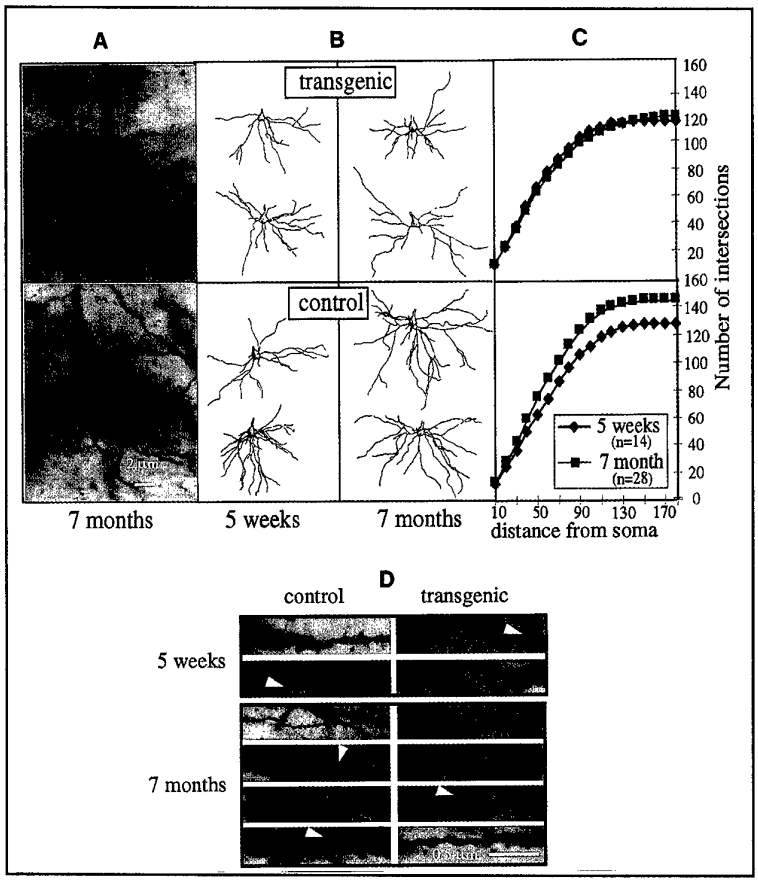

Fig. 4. Attenuated dendritic branching and spine loss in layer V pyramidal neurons from fronto-parietal cortex of transgenic mice. A. Shown are representative Golgi-stained preparations from 7 month-old brains of transgenic (top panel) and control (bottom panel) mice. B. Camera lucida tracings of the basilar tree of Golgi-stained pyramidal neurons from the fronto-parietal cortex of 5-week-old and 7 month-old transgenic and control brains. C. Shown are graphical presentations of data from Sholl analyses. Presented are numbers of dendritic branches intersecting with a series of concentric circles of increasing diameter as a function of their distance from the cell body. Numbers of intersections are expressed as a cumulative total. See text and Table 1 for details. D. Shown are representative high magnification photographs of dendritic branches from 5 week- and 7 month-old transgenic and control mice. Note the reduction in spines (arrowheads) on the transgenic dendrites.

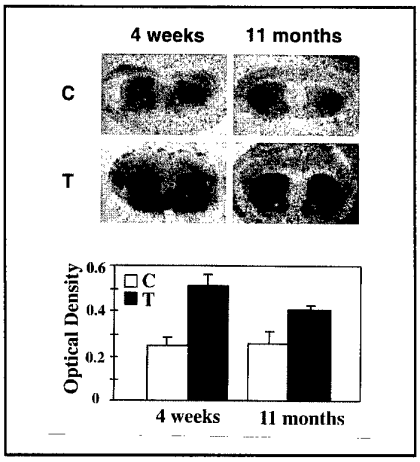

Fig. 5. Enhanced [^{3}H]-hemicholinium-3 binding in transgenic neostriatum. A. Autoradiography followed by image analysis. Increased binding of [^{3}H]-hemicholinium-3 to the neostriatum of 4 week (left)- and 12 month-old (right) of normal mice (top, C) as compared with transgenics (bottom, T). Presented are brain sections following 2 weeks exposure, indicating increased choline transport in these brain regions. B. Quantification of [^{3}H]-hemicholinium binding. Presented is one typical autoradiography experiment out of four, n=2 animals. For each animal, the image of two to six sections were digitized (at the neostriatum level, between level 21 and 30 of Franklin and Paxinos, 1997) and the mean gray value of the two hemistriatums were recorded. Data are expressed in absorbance (+/- SEM).

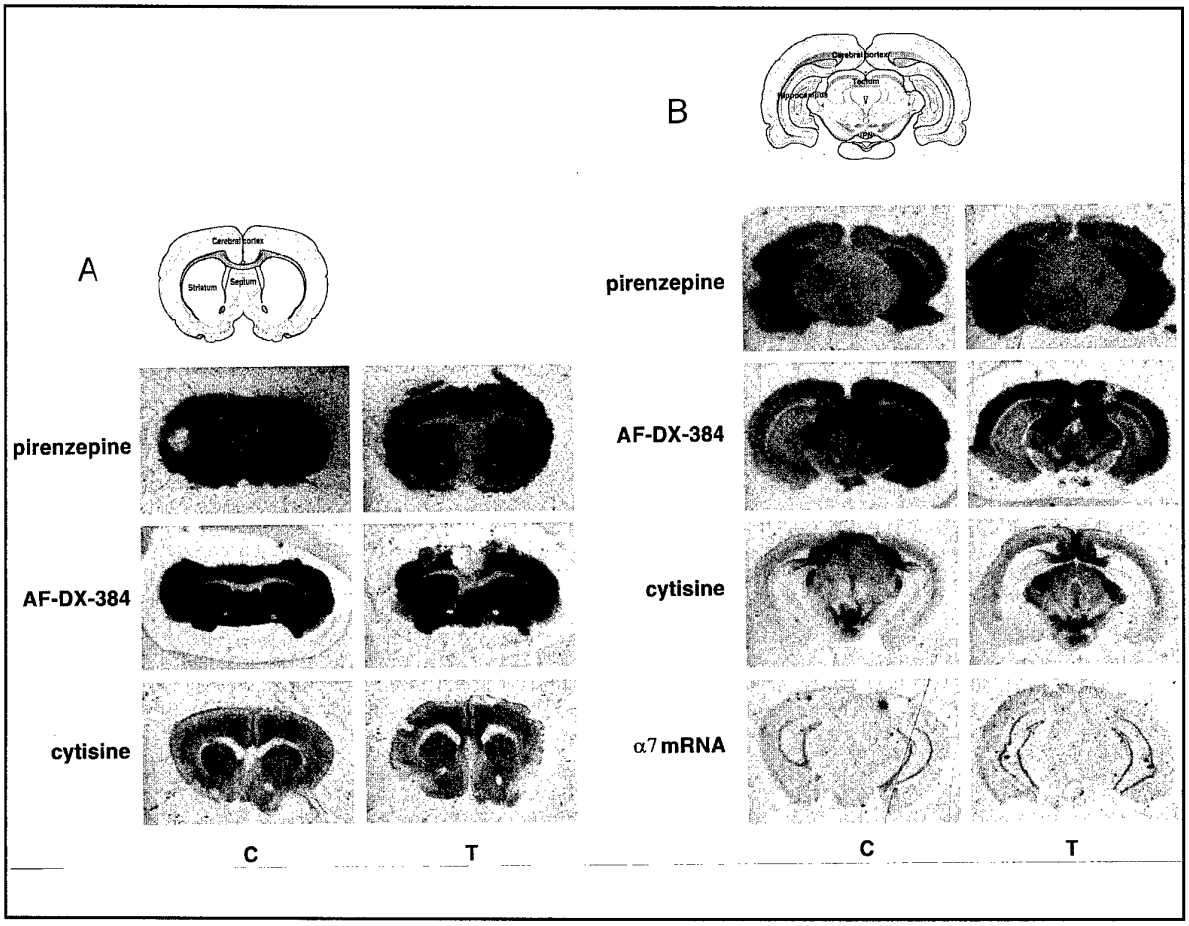

Fig. 6. Similar binding capacities to AChR subtypes in transgenic neostriatum. A. [^{3}H]-pirenzepine (M1 receptors), [^{3}H]-AF-DX-384 (M2 receptors) and [^{3}H]-cytisine (heteromeric nAChR) binding at the level of striatum of control (C) and transgenic (T) mice. Drawing: level 15 (Swanson, 1992). B. [^{3}H]-pirenzepine (M1 receptors), [^{3}H]-AF-DX-384 (M2 receptors) and [^{3}H]-cytisine (heteromeric nAChR) binding and *in situ* hybridization of nAChR α7 mRNA at the level of mesencephalon of control (C) mice and transgenic (T) mice. Drawing: level 39 (Swanson, 1992).

C. The increase of specific catalytic activity of AChE in response to phosphorylation

Introduction

Acetylcholinesterase (acetylcholine acetyl hydrolase, EC 3.1.1.7, AChE) is a key component of cholinergic brain synapses and neuromuscular junctions, in which it hydrolyzes the neurotransmitter acetylcholine (Taylor, 1990, Soreq & Zakut, 1993). In addition to terminating cholinergic neurotransmission, it may have non-catalytic function(s) in cellular development (Greenfield, 1984, Layer and Willbold, 1995; Small et al., 1995; Karpel et al., 1996). This may explain its presence on the surface of erythrocytes and in embryonic tissues (Massoulié et al., 1993). The central role of AChE in cholinergic neurotransmission is demonstrated by the fact that it is the target of a variety of toxic compounds, both natural and man-made. For example, several natural compounds inhibit the catalytic activity of cholinesterases including glycoalkaloids, which are found in solanaceous food plants such as potatoes (Neville et al., 1992), the snake venom protein inhibitor fasciculin (Bourne et al., 1995, Harel et al., 1995) and cyanobacterial toxins (Hyde and Carmichael, 1991). Chemical warfare agents (e. g., sarin and tabun) and organophosphate insecticides (e. g. malathion) also are designed to inhibit AChE (Taylor, 1990). In addition, AChE is a target of several pharmacological agents that are designed to enhance cholinergic neurotransmission in the treatment of disorders associated with cholinergic imbalance, such as Alzheimer's disease and myasthenia gravis (Schwarz et al., 1995; Loewenstein-Lichtenstein et al., 1996). The widespread presence of both natural and man-made anti-AChE compounds (Millard and Broomfield, 1995) raises the question if natural mechanisms exist that enable this enzyme to function under diverse conditions.

The crucial role of AChE in cholinergic neurotransmission implies that to be physiologically relevant, adjustments in its activity in response to fluctuating physiological conditions should occur within a very short time scale. This excludes regulation at the levels of gene expression, multimeric assembly and intracellular targeting, none of which offers a sufficiently rapid response. AChE is present in various glycosylated forms (Meflah et al., 1984), but the carbohydrate moiety does not contribute to catalytic activity (Fischer et al., 1993, Velan et al., 1993). Allosteric modulation and substrate inhibition of AChE have also been reported (Changeux, 1966, Barak et al., 1995), but no physiologically significant scheme for controlling AChE activity has been demonstrated. As phosphorylation is the most frequently seen post-translational mechanism of control of physiological processes, and since the human AChE amino acid sequence (Soreq and Zakut, 1993) reveals several consensus phosphorylation sites, we have investigated phosphorylation as a mechanism of control of AChE activity.

Experimental Results

We have found that the catalytic subunit of cAMP-dependent protein kinase (PKA) but not casein kinase II or protein kinase C phosphorylates recombinant human AChE *in vitro* (Fig. 1). This enhances acetylthiocholine hydrolysis up to 10-fold as compared to untreated AChE (Tables 1), while leaving unaffected the enzyme's affinity for this substrate and for various active and peripheral site inhibitors (Tables 2, 3). Alkaline phosphatase treatment enhanced the electrophoretic migration, under denaturing conditions, of part of the AChE proteins isolated from various mammalian sources and raised the isoelectric point of some of the treated AChE molecules (Fig. 2), indicating that a fraction of the AChE molecules are also phosphorylated *in vivo*. Enhancement of acetylthiocholine hydrolysis also occurred with *Torpedo* AChE, which has no consensus motif for PKA phosphorylation. Further, mutation of the single PKA site in human AChE (threonine 249) did not prevent this enhancement (Table 3), suggesting that in both cases it was due to phosphorylation at non-consensus sites (Fig. 3). *In vivo* suppression of the acetylcholine-hydrolyzing activity of AChE and consequent impairment in cholinergic neurotransmission occur under exposure

to both natural and pharmacological compounds, including organophosphate and carbamate insecticides and chemical warfare agents (Fig. 4). Phosphorylation of AChE may possibly offer a rapid feedback mechanism that can compensate for impairments in cholinergic neurotransmission, modulating the hydrolytic activity of this enzyme and enabling acetylcholine hydrolysis to proceed under such challenges.

Table 1. Effect of protein kinase A on the activity of cholinesterases from various sources[a]

	catalytic activity (μmol/min/ml)		+kinase - kinase	PKA consensus site
	- kinase	+ kinase		
AChE				
recombinant human, from 293 cells	8.3	76.9	9.3	+
recombinant human, from *E. coli*	0.3	2.4	8.0	+
human erythrocyte	3.2	12.8	4.0	+
human brain	4.5	11.3	2.5	+
Torpedo electroplax	4.2	17.7	4.2	-
COS cells transfected with normal E6-ACHEDNA	0.9	1.8	2.0	+
COS cells transfected with T249A E6-ACHEDNA	1.0	2.2	2.2	-
BuChE				
human serum	1.1	1.2	1.1	+

[a]The data represent one out of three reproducible experiments with standard deviations below 30%. For BuChE activity determinations, 5 mM butyrylthiocholine was used as a substrate. All enzyme preparations were highly purified except that for *Torpedo*, which was partially purified and for those for COS cells, which were tested in conditioned medium from transfected cells with no further purification. The presence (+) or absence (-) of a PKA phosphorylation consensus site on each of the examined sequences is noted.

Table 2. Kinetic constants of human acetylcholinesterase purified from embryonic kidney 293 cells.

	- kinase	+ kinase
Km (μM)	50	50
Ki values (μM)		
tacrine	0.007	0.006
fasciculin 02	0.0002	0.0003
BW284c51	0.3	0.3
IC_{50} (μM)		
physostigmine	0.01	0.01
echothiophate	0.01	0.01

Table 3. Abolition of the PKA consensus site does not modify AChE properties.

	E6-ACHEDNA-transfected[a]	T249A E6-ACHEDNA-transfected[b]
Ki values (mM)		
succinylcholine	290	290
dibucaine	720	730
BW284c51	0.007	0.007
tacrine	0.058	0.072
fasciculin 02	0.000,000,1	0.000,000,1
fasciculin 03	0.000,000,2	0.000,000,2
IC_{50} value (mM)		
pyridostigmine	0.50	0.55

[a]COS cells were transfected with E6-ACHEDNA and the biochemical properties of AChE secreted into the medium were determined as in Tables 1 and 2.

[b]Site-directed mutagenesis was employed to create the T249A mutant enzyme. Tests were similar to those for the non-mutated enzyme.

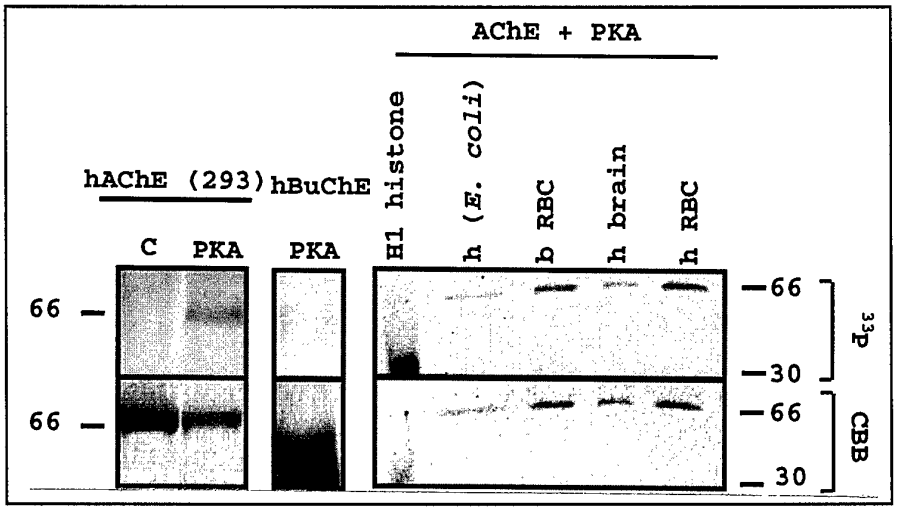

Fig. 1. *In vitro* phosphorylation of AChEs. Phosphorylation reactions were performed on 5 µg purified recombinant AChE expressed in 293 kidney cells (hAChE (293)), 2 µg purified recombinant AChE expressed in *E. coli* (h (E. coli)), 5, 3 and 5 µg of native AChE purified from human red blood cells (hRBC), human brain (hbrain) and bovine red blood cells (bRBC) respectively and 5 µg histone (H1). One fifth of each of the phosphorylation reactions, was separated by SDS-PAGE followed by either protein staining with Coomassie brilliant blue (CBB) or by 48 h autoradiography (^{33}P). An incubation without PKA served as a control (C). Numbers on both sides of the figure indicate molecular weight in kD.

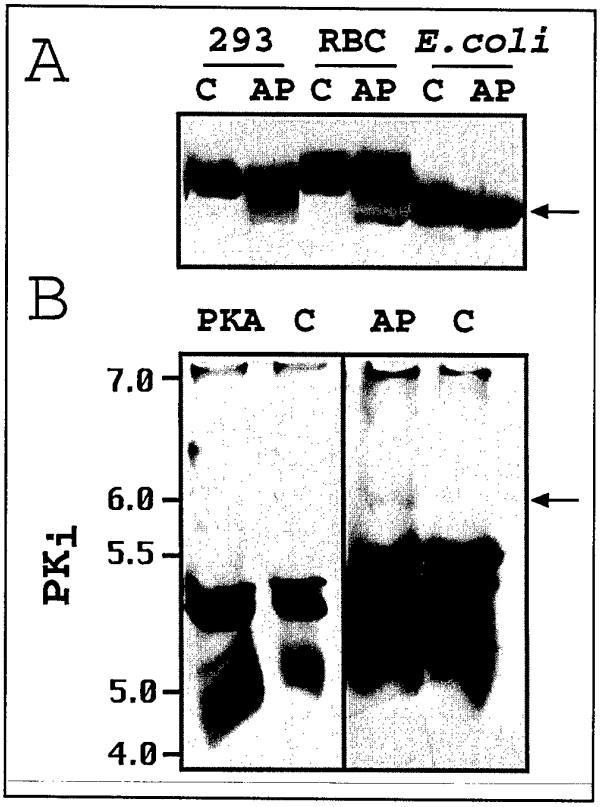

Fig. 2. Dephosphorylation of AChE modifies its electrophoretic and isoelectric properties. A. Alkaline phosphatase enhances the electrophoretic migration of AChE. Alkaline phosphatase (AP) treated and control untreated (C) recombinant human AChE from 293 cells (293, 3 μg), from human red blood cells (hRBC, 5 μg) or human AChE produced in *E. coli* (E. coli, 3 μg) were electrophoretically separated under denaturing conditions and immunochemically detected. The arrow indicates the position of that fraction of these proteins that migrated faster after dephosphorylation. B. Alkaline phosphatase induces the appearance of a novel AChE subtype with high isoelectric point. 3 μg hAChE (293) in a final volume of 20 μl was treated either with PKA or with AP and was subjected to isoelectric focusing gel electrophoresis followed by activity staining of the gels. Similarly treated AChEs served as a control (C). The arrow indicates an additional band at a higher isoelectric point, which could be observed only after AP treatment.

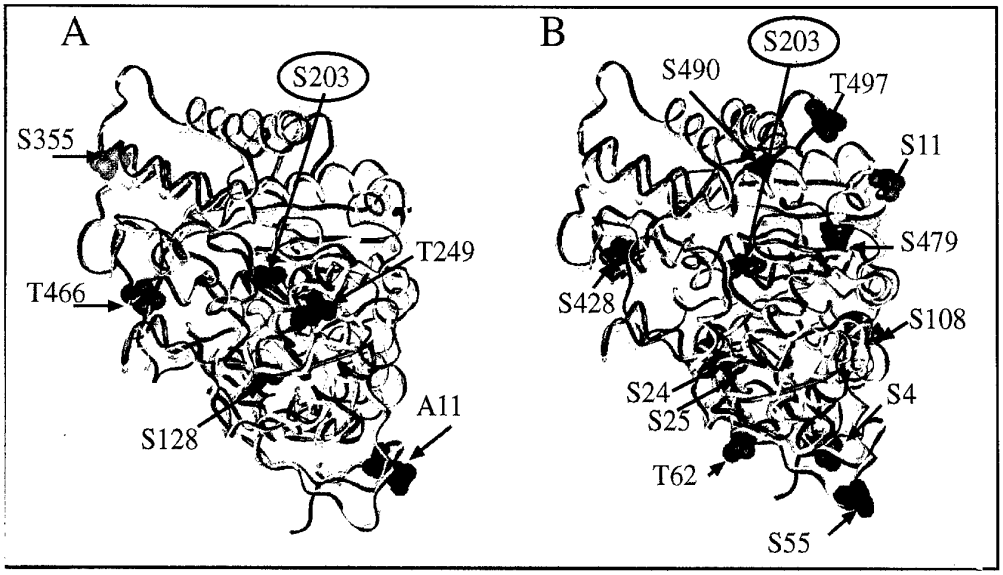

Fig. 3. Serine and threonine residues on the three dimensional models of AChE. A. Consensus motifs for various kinases. Superimposition of *Torpedo* (yellow) and mouse (magenta) AChEs according to their Ca atoms. Amino acid numbers are as in the human sequence. Active site serine (203) is displayed as a turquoise sphere, the PKA consensus site R/KXXT/S (beginning with arginine or lysine and ending with threonine or serine) threonine (249) in violet, the casein kinase II consensus sites S128, S355 and T466 in gray and the protein kinase C consensus site T11 (A11 in mouse) in green. B. Surface-exposed serine and threonine residues. Active site serine 203 is displayed as a turquoise sphere together with those serine and threonine residues which were calculated to be exposed at the surface of the *Torpedo* AChE protein.

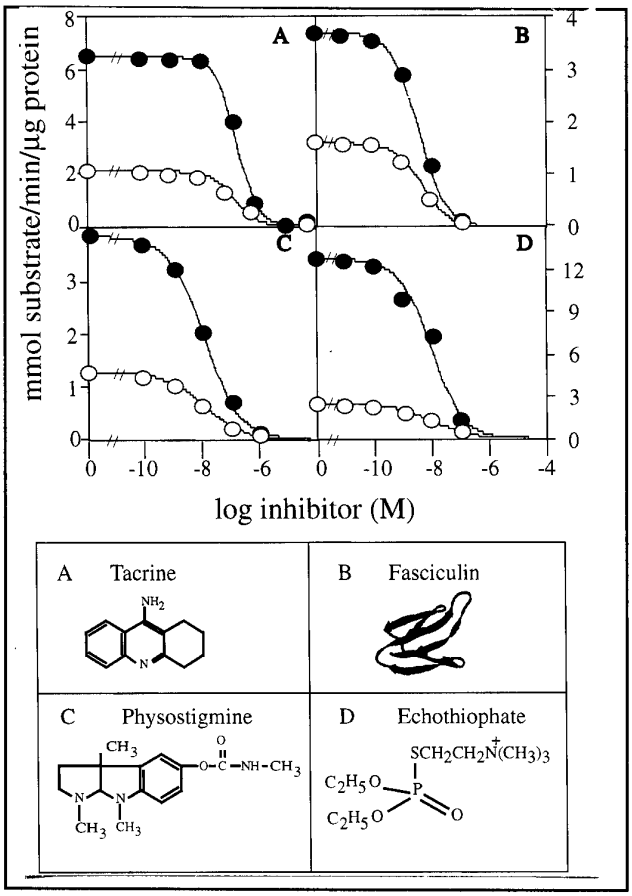

Fig. 4. PKA phosphorylation enhances AChE catalysis under exposure to various inhibitors. Human recombinant AChE purified from 293 cells was subjected to PKA phosphorylation with a PKA:AChE ratio adjusted in order to maintain AChE concentrations appropriate for inhibition measurements. Presented are enzyme activities in the presence of increasing concentrations of the noted inhibitors at 1 mM ATCh. Each curve is an average best-fit result of 2 experiments. The crystal structure of fasciculin is after Bourne et al. (1995). Filled circles, PKA-treated enzyme; empty circles, untreated enzyme.

D. The physiological basis of the paradoxical appearance of CNS symptoms in response to pyridostigmine, a peripherally acting AChE inhibitor

Introduction

Pyridostigmine, a carbamate AChE inhibitor, is routinely employed in the treatment of the autoimmune disease myasthenia gravis and was recommended by most western armies for use as pretreatment under threat of chemical warfare, because of its protective effect against organophosphate poisoning. Due to this drug's quaternary ammonium group, which prevents its penetration through the blood-brain barrier (BBB), the symptoms associated with its routine use reflect perturbations primarily in peripheral nervous system functions. Unexpectedly, under a similar regimen, pyridostigmine administration during the Gulf War resulted in an >3 fold increase in the frequency of reported central nervous system symptoms. This was not due do enhanced absorption (or decreased elimination) of the drug because the inhibition efficacy of serum BuChE was not altered. Since previous animal studies have shown stress-induced disruption of the BBB, an alternative possibility was that the stress situation associated with the battlefield allowed pyridostigmine penetration into the brain.

Experimental Results

We have found that following a forced swim protocol, shown previously to produce stress, an increase in BBB permeability reduces by >100 fold the pyridostigmine dose required to inhibit mouse brain AChE activity by 50% (Figs. 1,2). Under these conditions, peripherally administered pyridostigmine increased the brain levels of *c-fos* oncogene and AChE mRNAs. Moreover, *in vitro* exposure to pyridostigmine increased both electrical excitability and *c-fos* mRNA levels in brain slices (Fig. 3), demonstrating that the observed changes could be directly induced by pyridostigmine. These findings suggest that peripherally acting drugs administered under stress may reach the brain and affect centrally controlled functions.

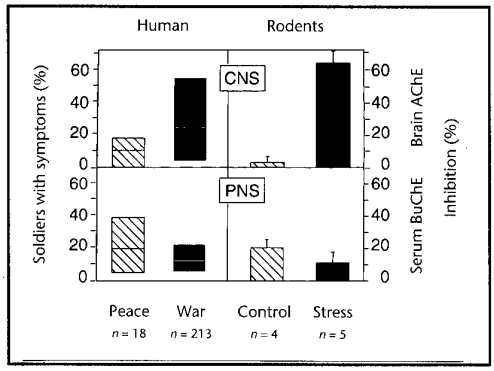

Fig. 1. Pyridostigmine effects in humans during peace and war and in non-stressed and stressed rodents. Left panels (humans). Results of a double blind, placebo-controlled study (extension of Glickson et al., 1991) (dashed bars, "peace"). Pyridostigmine (n=18) or placebo (n=17) were administered to healthy young male volunteers. Symptoms were reported at the end of the study. Presented are ranges (%) of soldiers reporting pyridostigmine-induced symptoms related to CNS (top) or PNS (bottom panel). During the Gulf War 213 male soldiers aged 18-22 years were questioned 24 hours after initiation of pyridostigmine treatment (filled bars). Mean values for human data are marked by horizontal lines across the relevant bars. Right panels (rodents). summary of measured brain AChE inhibition (top) and serum BuChE inhibition in mice (bottom) 10 min following injection of 0.1 mg/kg pyridostigmine in non-stressed (control, n=4), and stressed (n=5) mice. Percent inhibition ± standard deviation was calculated in comparison to the average activity calculated in non-injected, non-stressed (n=12) and stressed (n=6) animals.

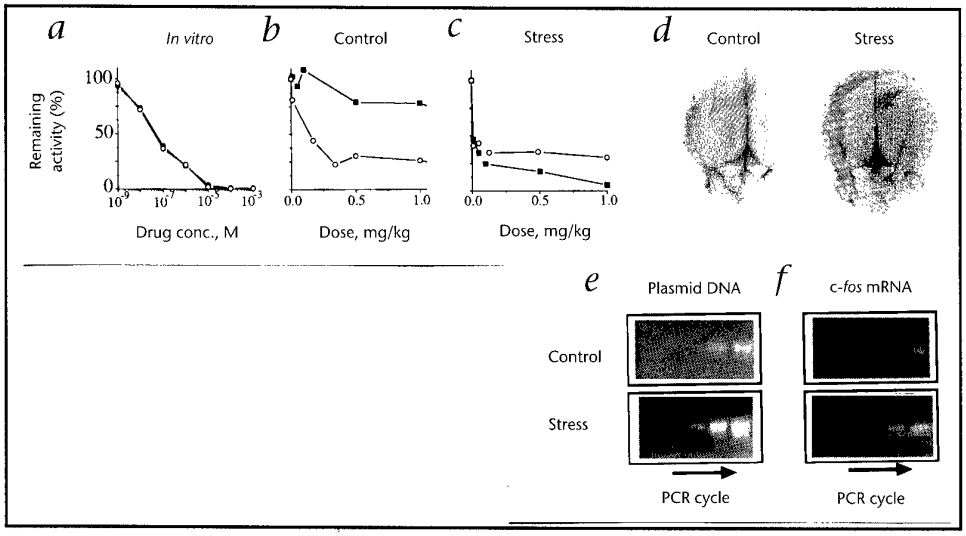

Fig. 2. Stress intensifies AChE inhibition by pyridostigmine due to increased brain penetration. A: AChE inhibition in brain homogenates. Acetylthiocholine hydrolysis was measured following addition of increasing concentrations of pyridostigmine (filled squares) or physostigmine (empty circles) to brain homogenates from control animals. Presented are percent remaining activities as compared with those of brain homogenates with no added drug. B: Inhibiting brain AChE activity by drug injection. Percent of normal specific cortical AChE activity was measured in brain homogenates prepared from non-stressed animals sacrificed 10 min following injection of the noted doses of physostigmine (n=9) or pyridostigmine (n=11). Presented are percent remaining activities as compared with those of brain homogenates from non-stressed, 0.9% NaCl injected animals (n=12). C: Pyridostigmine inhibition of brain AChE following stress. Swim forced test was followed 10 min later by injection of either 0.1 mg/kg pyridostigmine (n=8), or physostigmine (n=5). AChE activity measurements were as under B. Presented are percent remaining activities as compared with those of brain homogenates from similarly stressed, 0.9% NaCl injected animals (n=6). D: BBB permeability following stress. Shown are representative brains dissected from anaesthetized animals, 10 min following intracardial injection of Evan's blue. control: non-stressed animal, stress: 10 min. following stress session. E: Plasmid DNA penetration to the brain under stress. Control and stressed animals were injected *i.p.* with CMVACHE[8] plasmid. Proteinase K-treated brain homogenates were subjected to PCR amplification using a set of CMV-promoter forward primer and an ACHE reverse primer. PCR product samples were withdrawn every third cycle, which allows for 8-fold increases between samples. CMVACHE DNA was detected starting from cycle 21 in the brain of 4 out of 4 stressed animals. The PCR products from brain of control animals were considerably weaker and appeared only on cycle 24, indicating at least 8-fold less plasmid DNA in control brains as compared to stressed ones. In 2 out of 5 control animals no PCR product was detected. F: Kinetics of brain c-fos cDNA accumulation during RT-PCR amplification. Total RNA from mouse hippocampus was extracted using RNAclean (AGS, Heidelberg, Germany), its integrity verified by gel electrophoresis (evaluation of 2.0 ratio between 28 S and 18 S ribosomal RNA) and its quantity and purity from protein contamination evaluated by a A_{260}/A_{280} ratio of 1.8-2.0. *c-fos* cDNA was amplified following reverse transcription of equal amounts of total RNA samples from the brain of control or stressed animals. Kinetic follow-up of product accumulation was carried out as under E. The earlier appearance of amplified *c-fos* cDNA, 20 min following stress session as compared to control, indicates a significant increase in the amount of *c-fos* mRNA under stress.

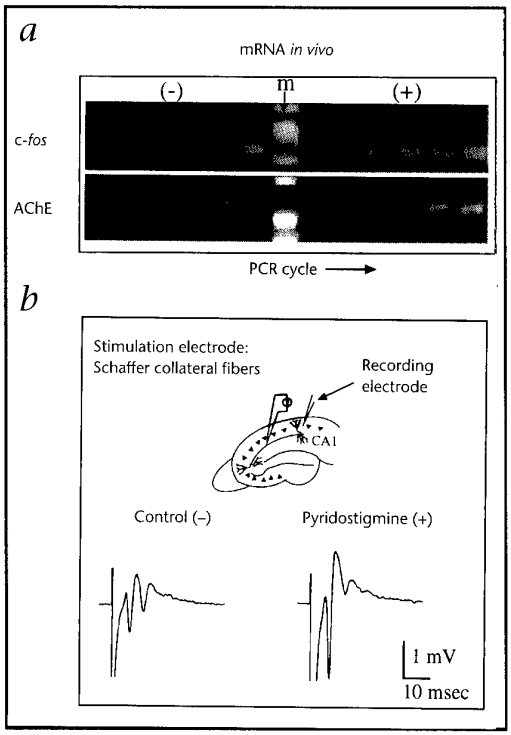

Fig. 3. Pyridostigmine enhances neuronal excitability and increases oncogene mRNA levels. A:. The kinetics of brain *c-fos* and AChE mRNA accumulation during RT-PCR amplification. RNA was extracted and reverse transcribed as under Fig. 1. The earlier appearance of the amplified PCR product 20 min. following injection of 2 mg/kg pyridostigmine (+) as compared to 0.9% NaCl (-) indicates an increase in the amount of *c-fos* (upper panel) and AChE mRNA (lower panel) under pyridostigmine exposure. B: Extracellular evoked potentials. Cortico-hippocampal slices (400 μm thick) were cut using a vibratome and were placed in a humidified holding chamber, continuously perfused with oxygenated (95% O_2, 5% CO_2) artificial cerebrospinal fluid (aCSF)[9]. Schaffer collateral fibers were stimulated with a bipolar tungsten stimulating electrode and extracellular evoked potentials were recorded in the cell-body layer of the CA1 area of the hippocampus. Single response to supramaximal stimulus intensity (1.5 times stimulus the intensity of which caused maximal response) is drawn before (-) and 30 min following (+) addition of pyridostigmine (1 mM) to the perfusing solution.

E. AS-ODN suppression of ACHE expression in cultured cells.

Introduction

Currently approved drugs for the treatment of Alzheimer's disease patients are designed to suppress the catalytic activity of the acetylcholine hydrolyzing enzyme acetylcholinesterase (acetylcholine acetylhydrolase, EC 3.1.1.7, AChE) (Knapp *et al.*, 1994). This is aimed to augment cholinergic neurotransmission, which is impaired in such patients due to a selective loss of cholinergic neurons. However, such inhibitors do not reduce the amount of the AChE protein. Also, there are recent reports of actions of AChE, unrelated to its catalytic activity, in process extension (Small *et al.*, 1995, Layer *et al.*; 1995, Jones *et al.*, 1995; Darboux *et al.*, 1996; Sternfeld *et al.*, 1997) and amyloid fibril formation (Inestrosa *et al.*, 1996). Therefore, in order to reduce levels of the protein itself, it is important to develop antisense oligodeoxynucleotides (AS-ODN) targeted against ACHEmRNA (Grifman *et al.*, 1997). By preventing the production of AChE, anti-ACHE ODNs would exert two functions; suppression of protein levels and reduction of enzyme activity. To achieve this goal, the AS-ODNs in question should be non-toxic, highly selective for the ACHE gene, operate in a sequence-dependent manner and exert their suppression activity on fully differentiated neurons.

The mammalian ACHE gene is transcribed and processed into 3 alternatively spliced mRNAs (Li *et al.*, 1990; Legay *et al.*, 1993; Karpel *et al.*, 1994). The mature transcript most abundant in brain is the one in which exon 4 is spliced to exon 6 (E6), whereas the isoform in which exon 4 is spliced to exon 5 (E5) is found mainly in cells of hematopoietic lineages. A third transcript, in which pseudointron 4 (I4) is not excised, was detected by means of RT-PCR (Karpel *et al.*, 1994, 1996) but its protein product has not yet been identified. We have previously shown that AS-ODNs can suppress ACHEmRNA levels in cultured primary hematopoietic cells (Soreq *et al.*, 1994), in bone marrow *in vivo* (Lev-Lehman *et al.*, 1994) and in cultured murine whole-brain primary neurons (Grifman *et al.*, 1997). However, these earlier studies did not include a methodical search for the most effective AS-ODN, were not performed in well-defined neurons and did not fully address the issue of neurotoxicity. Therefore, we have now designed 7 AS-ODNs which are directed against different sites along the various alternative mammalian ACHEmRNA chains. The capacity of these AS-ODNs to suppress AChE activity was tested in the rat neuroendocrine phaeochromocytoma cell line PC12 (Greene and Tischler, 1976). Several studies have used PC12 cells as an experimental model for AS-ODN-induced inhibition of gene expression (e.g.; Majocha *et al.*, 1994; Johannes *et al.*, 1994; Yamada *et al.*, 1996). Moreover, some of these studies were specifically aimed at suppression of expression of proteins which are altered in Alzheimer's disease patients, e.g. the microtubule-associated protein tau (Hanemaaijer and Ginzburg, 1991) and the amyloid plaque precursor protein (Majocha *et al.*, 1994). Nerve growth factor (NGF) treatment was shown, in several studies, to arrest the proliferation of PC12 cells, change their gene expression pattern (Lee et al., 1995) and induce their differentiation toward a cholinergic phenotype with increased AChE activity and neurite-like processes (Greene and Tischler, 1976; Tao-Chang *et al.*, 1995). Therefore, NGF-pre-treated PC12 cells may be expected to differ significantly from non-treated ones in their membrane properties, cytoarchitecture and levels of ACHEmRNA. Since such changes can potentially alter the effectiveness of AS-ODNs, we tested the series of AS-ACHE ODNs on PC12 cells before, during and after induction of differentiation by NGF. To evaluate the number of cells in our microtiter plate assay, we determined the content of free thiol groups in the cultured cell preparations and correlated this with cell count.

Our findings demonstrate limited susceptibility of non-differentiated PC12 cells to AS-ODN inhibition of ACHE gene expression as compared with up to 36% suppression of

AChE catalytic activity following 24 h incubation with no signs of neurotoxicity in NGF-treated PC12 cells. This model system therefore emerges as a viable alternative approach to the development of means for the simultaneous suppression of AChE activity and protein level in neurodegenerative diseases associated with a relative excess of AChE.

The only currently approved drugs for Alzheimer's disease (AD) are potent blockers of AChE activity. However, the above lines of evidence point to novel, non-catalytic morphogenic properties of AChE. This calls for the development of alternative approaches in which both AChE protein synthesis and enzymatic activity would be suppressed, such as the antisense" technology. To this end, we have begun to design synthetic 3'-phosphorothioated oligonucleotides (AS-ODNs) targeted towards AChEmRNA and to test their AChE suppression efficacy in the rat neuroendocrine pheochromocytoma cell line, PC12. This approach is outlined in Scheme 1. Several brain proteins have already been targeted by antisense oligonucleotides (Table 1).

Table 1. Recent brain-expressed targets of AS-ODN studies.

	protein product of target gene	modulated behavioral function	reference
1	corticotropin-releasing hormone	attenuation of social-defeat induced anxiety in rats	Sakai et al., 1994
2	*c-fos*	suppression of anxiety; generation of apomorphine- and amphetamine-induced behavior	Hooper et al., 1994; Molle et al., 1994; Dragunow et al, 1993
3	V1 vasopressin receptor	suppression of social discrimination ability and anxiety	Landgraf et al., 1995
4	5-HT6 receptor	enhanced cholinergic neuro-transmission; yawning, stretching	Bourson et al, 1995
5	galanin	reduced fat ingestion	Akabayashi et al, 1994
6	XCS-endorphin	suppressed response to novel environment	Spampinato et al., 1994
7	neuropeptide Y	suppression of appetite	Akabayashi et al, 1994
8	D2 dopamine receptor	suppression of cocaine response; suppression of quinpirole response	Silvia et al, 1994; Zhou et al., 1994

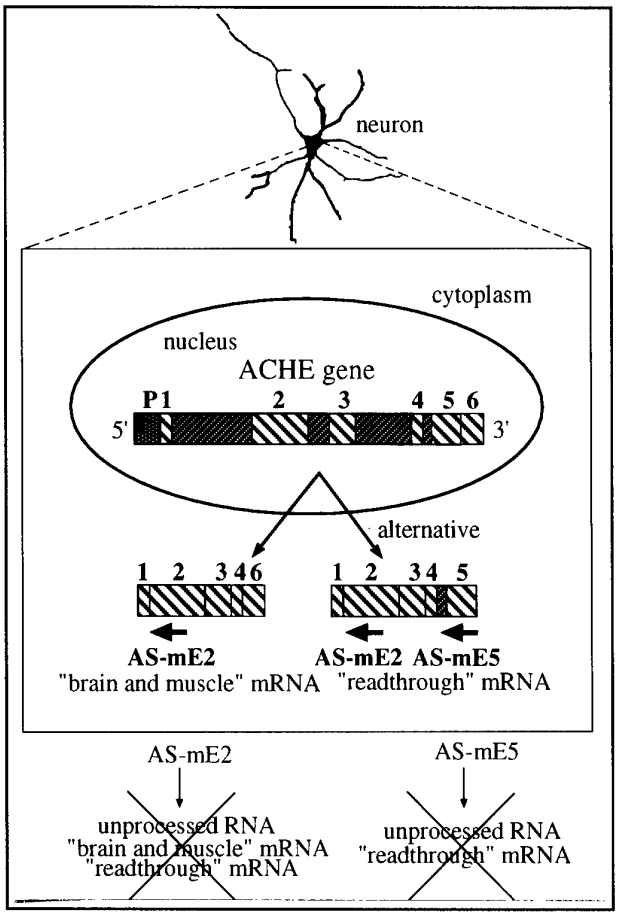

Scheme 1. Target sites for antisense oligonucleotide interactions with ACHEmRNA.

Conclusions

The long-term objective of our research is to understand the molecular and cellular mechanisms that govern those neurotransmission processes which involve the hydrolysis of ACh (cholinergic neurotransmission). Intricately concerted processes are known to mediate the coupling of short-term variations in cholinergic neurotransmission to corresponding long-term changes in motor, cognitive and autonomous functions. However, the pathways through which cholinergic inputs control neuronal and synaptic cytoarchitecture and determine changes in the functioning of downstream-regulated genes and complex vertebrate responses are as yet obscure. To address these issues, we have developed and used experimental tools which enable the modulation of cholinergic neurotransmission through targeted gain and loss of function of cholinesterases, the enzymes responsible for termination of cholinergic neurotransmission. This goal has been approached by steps, most of which have since been interwoven into an integrated research effort.

Transgenic overexpression of human AChE was initiated in developing *Xenopus* tadpoles, where the synaptic form of this enzyme enhanced the formation of neuromuscular junctions. 3'-Alternative spicing of AChEmRNA transcripts was subsequently shown to dictate synaptic and epidermal accumulation of specific AChE isoforms in microinjected *Xenopus laevis* tadpoles and to control neurite growth in cultured *Xenopus* motoneurons, the latter in a non-catalytic manner. Distinct domains within cholinesterase molecules were thus shown to contribute to their hydrolytic and growth-related properties. Delineation in the *Xenopus* system of an effective human promoter/ reporter construct enabled the subsequent creation of transgenic mice which express human AChE in their brain neurons. These mice suffered late-onset, progressive cognitive as well as neuromotor deterioration associated with changes in brain metabolism of key cholinergic elements, attenuated dendrite branching and massive synapse loss. These processes are strikingly reminiscent of those which occur in Alzheimer's disease, where the vulnerability of cholinergic neurons to inherited and/or environmental insults lead to late-onset deterioration of cholinergic functions, neuronal loss and cell death. However, similar symptoms have repeatedly been reported for individuals exposed to anti-cholinesterase drugs and poisons. That the same effect could result from both an increase in AChE expression and from inhibition of the enzyme, led us to initiate a search for feedback responses associated with exposure to anti-cholinesterases.

Early immediate transcriptional responses to anti-cholinesterases were unraveled in a search for the cause(s) of brain-associated symptoms reported by soldiers who had been treated prophylactically with the peripherally acting AChE inhibitor pyridostigmine. This study demonstrated efficient penetrance of numerous compounds through the blood-brain barrier, which we previously observed to be impenetrable to plasma constituents. Current continuation of this research direction reveals, *in vivo* and in cultured hippocampal brain slices, long lasting changes in cholinergic gene expression in response to acute stress, to anti-cholinesterase exposure. Such changes lead to massive neuronal AChE accumulation, creating essentially similar conditions to those previously engineered in the AChE-overexpressing transgenic mice, and providing a potential explanation for the strikingly similar neurological symptoms reported for Alzheimer's disease and insecticide poisoning patients. This, as well as the non-catalytic properties of AChE, called for the use of a molecular biology approach, to inhibition of the production of AChE, rather than to chemical blockade of its catalytic activity.

Antisense suppression of cholinesterase production was performed *ex vivo*, using phosphorothioated oligodeoxynucleotides capable of suppressing AChE activity in cultured mammalian neuroendocrine cells. The biomedical and environmental implications

of our research indicate that genomic polymorphisms in the coding and/or promoters of the *ACHE* and *BCHE* genes (and possibly additional loci) can modulate individual responses to anti-cholinesterases in a complex and yet not fully predictable manner, affecting the nervous system. Such polymorphisms can alter AChE gene expression and/or properties, affecting both short and long-term manifestations of cholinergic functions in a manner that may increase the risk for neurodegenerative disease due to either chemical or psychological insults. Our main goal in the near future will be to discern specific steps in the pathway leading to such outcome.

Abbreviations

ACh	acetylcholine
AChE	acetylcholinesterase
ACHE	acetylcholinesterase gene
AChR	acetylcholine receptor
AD	Alzheimer's disease
APP	amyloid protein precursor
AS-ODN	antisense oligodeoxynucleotide
ATCh	acetylthiocholine
BBB	blood-brain barrier
BCHE	butyrylcholinesterase gene
BuChE	butyrylcholinesterase
ChAT	choline acetyltransferase
CMV	cytomegalovirus
CNS	central nervous system
MEPP	miniature endplate potential
MuSK	muscarinic receptor tyrosine kinase
NGF	nerve growth factor
NMJ	neuromuscular junction
PCR	polymerase chain reaction
PKA	protein kinase A
RT-PCR	reverse transcriptase PCR
SEM	standard error of the mean

References

Aigner L., Arber, S., Kapfhammer, J.P., Laux, C.S., Botteri, F., Brenner, H-R, and Caroni, P. (1995) Overexpression of the neural growth-associated protein GAP-43 induces nerve sprouting in the adult nervous system of transgenic mice. Cell 83, 269-278.

Akabayashi, A., Wahlestedt, C., Alexander, J.T. and Leibowitz, S.I. (1994) Specific inhibition of endogenous neuropeptide synthesis in acruate nucleus by antisense oligonucleotides suppresses feeding behavior and insulin secretion. Molec. Brain Res. 21, 55-61.

Andres, C., Beeri, R., Friedman, A., Lev-Lehman, E., Henis, S., Timberg, R., Shani, M. and Soreq, H (1997) ACHE transgenic mice display embryonic modulations in spinal cord CHAT and neurxin Iβ gene expression followed by late-onset neuromotor deterioration. Proc Natl Acad Sci USA, 94, in press.

Anglister, L., Stiles J.R. and Salpeter, M.M. (1994) Acetylcholinesterase density and turnover number at frog neuromuscular junctions, with modeling of their role in synaptic function. Neuron 12, 783-794.

Barak, D., Ordentlich, A., Bromberg, A., Kronman , C., Marcus, D., Lazar, A., Ariel, N., Velan, B. and Shafferman, A. (1995) Allosteric modulation of acetylcholinesterase activity by peripheral ligands involves a conformational transition of the anionic subsite. Biochemistry 34, 15444-15452.

Bartus, R.T. and Uemura, Y. (1979) Physostigmine and recent memory: effects in young and aged non-human primates. Science 206, 1037-1089.

Beeri, R., Andres, C., Lev-Lehman, E., Timberg, R., Huberman, T., Shani, M. and Soreq, H. (1995) Transgenic expression of human acetylcholinesterase induces progressive cognitive deterioration in mice. Curr. Biol. 5, 1063-1071.

Beeri, R., LeNovere, N., Mervis, R., Huberman, T., Grauer, E., Changeux, J.P. and Soreq, H. (1997). Enhanced hemicholinium binding and attenuated dendrite branching in cognitively impaired ACHE-transgenic mice. J. Neurochem.

Ben Aziz-Aloya, R., Seidman, S., Timberg, R., Sternfeld, M., Zakut, H. and Soreq, H. (1993) Expression of a human acetylcholinesterase promoter-reporter construct in developing neuromuscular junctions of *Xenopus* embryos. Proc. Natl. Acad. Sci. 90, 2471-2475.

Bierer, L. M, Haroutunian, V., Gabriel, S., Knott, P. J., Carlin, L. S., Purohit, D. P., Perl, D. P., Schmeidler, J. Kanof, P. and Davis, K. L. (1995) Neurochemical correlates of dementia severity in AD: relative importance of the cholinergic deficits. J. Neurochem 64, 749-760.

Bourne, Y., Taylor, P. and Marchot, P. (1995) Acetylcholinesterase inhibition by fasciculin: crystal structure of the complex. Cell 83, 503-512.

Bourson, A., Borroni, E., Austin, R.H., Monsoma, F.J. Jr., and Sleight, A.J. (1995) Determination of the role of the 5-HT6 receptor in the rat brain: a study using antisense oligodnuceleotides. J. Pharmacol. Exp. Ther. 274, 174-180.

Braak, H. and Braak E. (1985) Golgi preparations as a tool in neuropathology with particular reference to investigations of the human telencephalic cortex. Progress in Neurobiol. 25, 366-368.

Millard, C.B. and Broomfield, C.A. (1995) Anticholinesterases: medical appilications of neurochemical principles. J. Neurochem. 64, 1909-1918.

Buell, S.J. and Coleman, P.D. (1981) Quantitative evidence for selective dendritic growth in normal human aging but not in senile dementia. Brain Res. 214, 23-41.

Burns, M.E. and Augustine, G.J. (1995) Synaptic structure and function: dynamic organization yields architectural precision. Cell, 83187-194.

Carbonetto, S. and Lindenbaum, M. (1995) The basement membrane at the neuromuscular junction: a synaptic mediatrix. Curr. Opin. Neurobiol. 5, 596-605.

Carraway, K.L. and Burden, S.J. (1995) Neuregulins and their receptors. Curr. Opin. Neurobiol. 5, 606-612.

Changeux, J-P. (1966) Responses of acetylcholinesterase from Torpedo marmorata to salts and curarizing drugs. Mol. Pharmacol. 2, 369-392.
Coyle, J.T., Price, D.L. and DeLong, M.R. (1983) Alzheimer's disease: a disorder of cortical cholinergic innervation. Science 219, 1186-1189.
Crawford, T.O. and Pardo, C.A. (1996) The neurobiology of childhood spinal muscular atrophy. Neurobiol. Disease 3, 97-110.
Darboux, I., Barthalay, Y., Piovant, M., and Hipeau Jacquotte, R. (1996). The structure-function relationships in Drosophila neurotactin show that cholinesterasic domains may have adhesive properties. EMBO J. 15, 4835-4843.
Davies, P. and Maloney, A.J.F. (1976) Selective loss of central cholinergic neurons in Alzheimer's disease. Lancet 2, 1403.
de La Escalera, S., Bockamp, E.O., Moya, F., Piovant, M. and Jimenez, F. (1990) Characterization and gene cloning of neurotactin, a Drosophila transmembrane protein related to acetylcholinesterase. EMBO J 9, 3593-3601.
Dechiarra, T.M., Bowen, D.C., Valenzuela, D.M., Simmons, M.V., Poueymirou, W.T., Thomas, S., Kinetz, E., Compton, D.L., Rojas, E., Park, J.S., Smith, C., DiStefano, P.S., Glass, D.J., Burden, S.J. and Yancopoulos, G.D. (1996) The receptor tyrosine kinase MuSK is required for neuromuscular junction formation in vivo. Cell 85, 501-512.
DeKosky, S.T. and Scheff, S. W. (1990) Synapse loss in frontal cortex biopsies in Alzheimer's disease: correlation with cognitive severity. Ann Neurol 27, 457-464.
Deuchar, E.M. (1966) *Biochemical Aspects of Amphibian Development.* Methuen and Co., Ltd. London.
Dragunow , M., Lawlor, P., Chiasson, B. and Robertson, H. (1993) *c-fos* antisense generates apomorphine and amphetamine-induced rotation. Neuroreport 5, 305-306.
Fibiger, H.C. (1991) Cholinergic mechanisms in learning, memory, and dementia: a review of recent evidence. Trends Neurosci 14, 220-223.
Fischer, M., Ittah, A., Liefer, I. and Gorecki, M. (1966) Expression and reconstitution of biologically active human acetylcholinesterase from *Escherichia coli.* Cell. Mol. Neurobiol. 13, 25-38.
Fischer, W., Gage, F.H. and Bjorklund, A. (1989) Degenerative changes in forebrain cholinergic nuclei correlate with cognitive impairments in aged rats. Eur. J. Neurosci. 1, 34-45.
Franklin, K.B.J. and Paxinos, G. (1997) *The Mouse Brain n Stereotaxic Coordinates.* Academic Press, San Diego.
Games, D., Adams, D., Alessandrini, R., Barbour, R., Berthelette, P., Blackwell, C., Carr, T., Clemens, J., Donaldson, T. and Gillespie, F. (1995) Alzheimer-type neuropathology in transgenic mice overexpressing V717F β-amyloid precursor protein. Nature 373, 523-527.
Gautam, M., Noakes, P.G., Mudd J., Nichol, M., Chu, G.C., Sanes, J.R. and Merlie (1995) Failure of post-synaptic specialization to develop at neuromuscular junctions of rapsyn-deficient mice. Nature 377, 232-236.
Gautam, M., Noakes, P.G., Moscoso, L., Rupp, F., Scheller, R.H., Merlie, J.P. and Sanes, J.R. (1996) Defective neuromuscular synaptogenesis in agrin-deficient mice. Cell 85, 525-535.
Glass, D.J., Bowen, D.C., Stitt, T.N., Radziejewski, C., Bruno, J., Ryan, T.E., Gies, D.R., Shah, S., Mattsson, K., Burden, S.J., DiStefano, P.S., Valenzuela, D.M., DeChiara, T.M. and Yancopoulos, G.D. (1996) Agrin acts via a MuSK receptor complex. Cell 85, 513-523.
Glickson, M. et al. (1991) The influence of pyridostigmine on human neuromuscular functions -studies in healthy human subjects. Fund. Appl. Toxicol. 16, 288-298.
Greene, L.A. and Tischler, A.S. (1976) Establishment of a noradrenergic clonal line of rat adrenal pheochromocytoma cells which respond to nerve growth factor. Proc. Natl. Acad. Sci. USA, 73, 2424-2428.

Greenfield, S. (1984) Acetylcholinesterase may have novel functions in the brain. Trends Neurosci. 7, 364-368.

Grifman, M., Lev-Lehman, E., Ginzberg, D., Eckstein, F., Zakut, H. and Soreq, H. (1997). Potential antisense oligonucleotide therapies for neurodegenerative diseases. In: *Concepts in Gene Therapy*, M. Strauss and J.A. Barranger, eds., Walter de Gruyter & Co., Berlin, 141-167.

Grinnell, A.D. (1995) Dynamics of nerve-muscle interaction in developing and mature neuromuscular junctions. Physiol. Rev. 75, 789-819.

Hall, Z.W. and Sanes, J.R. (1973) Synaptic structure and development: the neuromuscular junction. Cell 10, 99-121.

Hanemaaijer, R. and Ginzburg, I. (1991) Involvement of mature tau isoforms in the stabilization of neurites in PC12 cells. J. Neurosci. Res. 30, 163-171

Harel, M., Kleywegt, G.J., Ravelli, R.B., Silman I. and Sussman, J.L. (1995) Crystal structure of an acetylcholinesterase-fasciculin complex: interaction of a three-fingered toxin from snake venom with its target. Structure 3, 1355-1366.

Honer, W.G., Dickson, D.W., Gleeson, J. and Davies, P. (1992) Regional synaptic pathology in Alzheimer's disease. Neurobiol Aging 13, 375-382.

Hooper, M.L., Chiasson, B.J. and Robertson, H.A. (1994) Infusion into the brain of an anti-sense oligonucleotide to the immediate-early gene *c-fos* suppresses production of fos and produces a behavioral effect. Neurosci. 63, 917-924.

Hsiao, K.K., Borchelt, D.R., Olson, J., Johannsdottir, R., Kitt, C., Yunis, W., Xu, S., Eckman, C., Younkin, S., Price, D., Ladecola, C., Clark, B. and Carlson, G. (1995) Age related CNS disorder and early death in transgenic FVB/N mice overexpressing Alzheimer amyloid precursor proteins. Neuron 15, 1202-1218.

Hsiao, K., Chapman, P., Nilsen, S., Eckman, C., Harigaya, Y., Younkin, S., Yang, F. and Cole, G. (1996) Correlative memory deficits, Ab elevation and amyloid plaques in transgenic mice. Science 274, 99-102.

Hyde, E.G. and Carmichael, W.W. (1991) Anatoxin-a(s), a naturally occurring organophosphate, is an irreversible active site-directed inhibitor of acetylcholinesterase (EC 3.1.1.7) J. Biochem. Toxicol. 6, 195-201.

Ichtchenko, K., Hata, Y., Nguyen, T., Ullrich, B., Missler, M., Moomaw, C. and Sudhof, T.C. (1995) Neuroligin 1: a splice site-specific ligand for β-neurexins. Cell 81, 435-443.

Inestrosa, N.C., Alvarez, A., Perez, C.A., Moreno, R.D., Vicente, M., Linker, C., Casanueva, O.I., Soto, C. and Garrido, J. (1996) Acetylcholinesterase accelerates assembly of amyloid-beta-peptides into Alzheimer's fibrils: possible role of the peripheral site of the enzyme. Neuron 16, 881-891.

Jo, S.A., Zhu, X., Marchionni, M.A. and Burden, S.J. (1995) Neuregulins are concentrated at nerve-muscle synapses and activate ACh-receptor gene expression. Nature 373, 158-161.

Johannes, L., Lledo, P.M., Roa, M., Vincent, J.D., Henry, J.P. and Darchen, F. (1994) The GTPase Rab3a negatively controls calcium-dependent exocytosis in neuroendocrine cells. EMBO J. 13, 2029-2037.

Jones, S.A., Holmes, C., Budd, T.C. and Greenfield, S.A., (1995) The effect of acetylcholinesterase on outgrowth of dopaminergic neurons in organotypic slice culture of rat mid brain. Cell Tissue Res 279, 323-330.

Karpel, R., Ben Aziz-Aloya, R., Sternfeld, M., Ehrlich, G., Ginzberg, D., Tarroni, P., Clementi, F., Zakut, H. and Soreq, H. (1994) Expression of three alternative acetylcholinesterase messenger RNAs in human tumor cell lines of different tissue origins. Exp. Cell. Res. 210, 268-277.

Karpel, R., Sternfeld, M., Ginzberg, D., Guhl, E., Graessman, A. and Soreq, H. (1996) Overexpression of alternative human acetylcholinesterase forms modulates process extensions in cultured glioma cells. J Neurochem. 66, 114-123.

Knapp, M.J., Knopman, D.S., Solomon, P.R., Pendlebury, W.W., Davis, C.S. and Gracon, S.I. (1994) A 30-week randomized controlled trial of high-dose tacrine in patients with Alzheimer's disease. J. Am. Med. Assn. 271, 985-991.

LaFerla, F.M., Tinkle, B.T., Bieberich, C.J., Haudenschild, C.C. and Jay, G. (1995) The Alzheimer's Ab peptide induces neurodegeneration and apoptotic cell death in transgenic mice. Nature Genetics 9, 21-30.

Lambert, E.H. and Elmqvist, D. (1971) Quantal components of end plate potentials in the myasthenic syndrome. Ann. N.Y. Acad. Sci. 183, 183-199.

Landgraf , R. Gerstberger, R., Montkowski, A., Probst, J.C., Wotjak, C.T., Holsboer, F and Engelmann, M. (1995) V1 vassopressin receptor antisense oligodeoxynucleotide into septum reduces vasopressin binding, social discrimination abilities and anxiety-related behavior in rats. J. Neurosci. 15, 4250-4258.

Layer, P.G. and Willbold, E. (1995) Novel functions of cholinesterases in development, physiology and disease. Prog. Histochem. Cytochem. 29, 1-99.

Layer, P.G., Weikert, T. and Alber, R. (1993) Cholinesterases regulate neurite growth of chick nerve cells in vitro by means of a non-enzymatic mechanism. Cell Tissue Res 273, 219-226.

Lee, N.H., Weinstock, H.G., Kirkness, E.F., Earle-Huges, J.A., Fuldner, R.A., Marmaros, S., Glodek, A., Gocayne, J.D., Adams, M.D., Karlvage, A.R., Fraser, C.M. and Venter, C. (1995) Comparative expressed-sequence-tag analysis of differential gene expression profiles in PC-12 cells before and after nerve growth factor treatment. Proc. Natl., Acad. Sci. USA 92, 8303-8307.

Legay, C., Bon, S. and Massoulie, J. (1993) Expression of a cDNA encoding the glycolipid-anchored form of rat acetylcholinesterase. FEBS Lett. 315, 163-166.

Li, Y., Camp, S., Rachinsky, T.L., Getman, D. and Taylor, P (1991) Gene structure of mammalian acetylcholinesterase. Alternative exons dictate tissue-specific expression. J. Biol. Chem. 266, 23083-23090.

Loewenstein-Lichtenstein, Y., Glick, D., Gluzman, N., Sternfeld, M., Zakut, H. and Soreq, H. (1996) Overlapping drug interaction sites of human butyrylcholinesterase dissected by site-directed mutagenesis. Molec. Pharmacol. 50, 1423-1431.

Majocha, R.E., Agrawal, S., Tang, J.Y., Humke, E.W. and Marotta, C.A. (1994) Modulation of the PC12 cell response to nerve growth factor by antisense oligonucleotide to amyloid precursor protein. Cell. Mol. Neurobiol. 14, 425-437.

Massoulié, J., Pezzementi, L., Bon, S., Krejci, E. and Vallette, F.M. (1993) Molecular and cellular biology of cholinesterases. Prog. Neurobiol. 41, 31-91.

Masu, Y., Wolf, E., Holtmann, B. Sendtner, M., Gottfried, B. and Thoenen, H. (1993) Disruption of the CNTF gene results in motor neuron degeneration. Nature 365, 27-32.

Meflah, K., Bernard, S. and Massoulié, J. (1984) Interaction with lectins indicates differences in the carbohydrate composition of the membrane-enzymes acetylcholinesterase and 5'-nucleotidase in different cell types. Biochemie 66, 59-69.

Moller, C., Bing, O. and Heilig, M. (1994) *c-fos* expression in the amygdala: *in vivo* antisense modulation and role in anxiety. Cell. Molec. Neurobiol. 14, 414-423.

Moran, P.M., Higgins, L.S., Cordell, B. and Moser, P.C. (1995) Age related learning deficits in transgenic mice expressing the 751-amino acid isoform of human β-amyloid precursor protein. Proc. Natl. Acad. Sci. USA 92, 5341-5345.

Neville, L.F., Gnatt, A., Loewenstein, Y., Seidman, S., Ehrlich, G. and Soreq, H. (1992) Intramolecular relationships in cholinesterases revealed by oocyte expression of site-directed and natural variants of human BCHE. EMBO J. 11, 1641-1649.

Noakes, P.G., Gautam, M., Mudd, J., Sanes, J.R. and Merlie, J.P. (1995) Aberrant differentiation of neuromuscular junctions in mice lacking S-laminin/laminin b2. Nature 374, 258-262.

Nordberg, A., Adem, A., Hardy, J. and Winblad, B. (1988) Change in nicotinic receptor subtypes in temporal cortex of Alzheimer brain. Neurosci. Lett. 86:317-321.

organization yields architectural precision. Cell 83, 187-194.
Price, D.L., Sisodia, S.S. and Gandy, S.E. (1995) Amyloid β amyloidosis in Alzheimer's disease. Curr. Op. Neurobiol. 8, 268-274.
Purpura, D.P. (1974) Dendritic spine "dysgenesis" and mental retardation. Science 186, 1126-1128.
Robert, H. and Brown, G. Jr. (1995) Amyotrophic lateral sclerosis: recent insight from genetics and transgenic mice. Cell 80, 687-692.
Sakai, R. R., He, P. F., Yang, X. D., Ma, L. Y., Guo, Y. F., Reilly, J. J., Moga, C. N., and Fluharty, S. J. (1994). Intracerebroventricular administration of AT1 receptor antisense oligonucleotides inhibits the behavioral actions of angiotensin II. J. Neurochem. 62, 2053-2056.
Salpeter, M. (1967) Electron microscope radioautography as a quantitative tool in enzyme cytochemistry. I. The distribution of acetylcholinesterase at motor endplates of a vertebrate twitch muscle. J Cell Biol 32, 379-389.
Seidman, S., Ben Aziz-Aloya, R., Timberg, R., Loewenstein, Y., Velan, B., Shafferan, A., Liao, J., Norgaard-Pedersen, B., Brodbeck, U. and Soreq, H. (1994) Overexpressed monomeric human acetylcholinesterase induces subtle ultrastructural modifications in developing neuromuscular junctions of *Xenopus laevis* embryos. J Neurochem 62, 1670-1681.
Seidman, S., Sternfeld, M., Ben Aziz-Aloya, R., Timberg, R., Kaufer-Nachum, D. and Soreq, H. (1995) Synaptic and epidermal accumulation of human acetylcholinesterase are encoded by alternative 3'-terminal exons. Mol Cell Biol 15, 2993-3002.
Shillito, P., Vincent, A. and Newsom-Davis, J. (1993) Congenital myasthenic syndromes. Neuromuscul. Disord. 3, 183-190.
Silvia, C., King, G.R., Lee, T.H., Xue, Z.Y., Caron, M.G. and Ellinwood, E.H. (1994) Intranigral administration of D2 dopamine receptor antisense oligodeoxynucleotides establishes a role for nigrostriatal D2 autoreceptors in the motor actions of cocaine. Molec. Pharmacol. 46, 51-57.
Slotkin, T.A., Nameroff, C.B., Bissette, G. and Seidler, F.G. (1994) Overexpression of the high affinity choline transporter in cortical regions affected by Alzheimer's disease. J. Clin. Invest. 94, 696-702.
Small, D. H., Reed, G., Whitefield, B., and Nurcombe, V. (1995) Cholinergic regulation of neurite outgrowth from isolated chick sympathetic neurons in culture. J. Neurosci. 15,144-151.
Soreq, H. and Zakut, H. Human *Cholinesterases and Anticholinesterases*, Academic Press, San Diego, 1993, 300 pp.
Soreq, H., Patinkin, D., Lev-Lehman, E., Grifman, M., Ginzberg, D., Eckstein, F. and Zakut, H. (1994) Antisense oligonucleotide inhibition of acetylcholinesterase gene expression induces progenitor cell expansion and suppresses hematopoietic apoptosis *ex vivo*. Proc. Natl. Acad. Sci. USA 91, 7907-7911.
Spampinato, S., Canossa, M., Carboni, L, Campana, G., Leanza, G. and Ferri, S. (1994) Inhibition of proopiomelanocortin expression by an oligodeoxynucleotide complementary to β-endorphin mRNA Proc. Natl. Acad. Sci. USA 91, 8072-8076.
Sternfeld, M., Seidman, S., Beeri, R. and Soreq, H. (1997) Catalytic and non-catalytic acetylcholinesterase functions implied from transgenic ACHE expression in vertebrates. In: *Neurotransmitter Release and Uptake*, S. Pogun, ed.. (Springer-Verlag, Berlin), (in press).
Sussman, J. L., Harel, M., Frolow, F., Oefner, C., Goldman, A., Toker, L., and Silman, I. (1991). Atomic structure of acetylcholinesterase from Torpedo californica: a prototypic acetylcholine-binding protein. Science 253, 872-879.
Swanson, L.W. (1992) *Brain Maps: Structure of the Rat Brain*. Elsevier, Amsterdam.
Tao-Cheng, J. H., Dosemeci, A., Bressler, J. P., Brightman, M. W. and Simpson, D. L. (1995) Characterization of synaptic vesicles and related neuronal features in nerve

growth factor and ras oncogene differentiated PC12 cells. J. Neurosci. Res. 42, 323-334.

Taylor, P. Cholinergic agonists, Anticholinesterase agents. In: , A.G. Gilman, T.W. Rall, A.S. Nies and P. Taylor, P. (Eds), *Pharmacological Basis of Therapeutics*, Pergamon Press, New York, 1990, pp. 122-130, 131-149.

Terry, R.D., Masliah, E., Salmon, D.P., Butters, N., De Teresa, R., Hill, R. Hansen, L. A. and Katzman, R. (1992) Physical basis of cognitive alterations in Alzheimer's disease: synapse loss is the major correlate of cognitive impairment. Ann. Neurol. 30, 572-580.

Velan, B., Kronman, C., Ordentlich, A., Flashner, Y., Leitner, M., Cohen, S. and Shafferman, A. (1993) N-Glycosylation of human acetylcholinesterase: effects on activity, stability and biosynthesis. Biochem. J. 296, 649-656.

Vickroy, T., Roeske, W. and Yamamura, H. (1984) Sodium-dependent high-affinity binding of [^{3}H] hemicholinium-3 in the rat brain: a potentially selective marker for presynaptic cholinergic sites. Life Sci. 35, 2335-2343.

Whitehouse, P., Martino, A., Antuono, P., Lowenstein, P., Coyle, J., Price, D. and Kellar, K. (1986) Nicotinic acetylcholine binding sites in Alzheimer's disease. Brain Res. 371, 146-151.

Wurtman, R.J. (1992), Choline metabolism as a basis for the selective vulnerability of cholinergic neurons. Trends Neuorsci. 15, 117-122.

Yamada, H., Koizumi, S., Kimura, M. and Shimizu, N. (1989) Reduction Of FGF receptor levels in human tumor cells transfected with an antisense RNA expression vector. Exp. Cell Res. 184, 90-98.

Zhi, Q.X., Yi, F.H. and Xi, C.T. (1995) Huperzine A ameliorates the spatial working memory impairments induced by AF64A. Neuroreport 6, 2221-2224.

Zhou , L.W., Zhang, S.P., Quin, Z.H. and Weiss, B. (1994) *In vivo* administration of an oligodeoxynucleotide antisense to the D2 dopamine receptor messenger RNA inhibits D2 dopamine receptor-mediated behavior and the expression of the D2 dopamine receptors in mouse striatum. J. Pharmacol. Exp. Ther. 268, 1015-1023.

Theses submitted to The Hebrew University with US Army support

for Doctor of Philosophy

Efrat Lev-Lehman "Developmental role(s) of acetylcholinesterase revealed by multileveled modulations of *ACHE* gene expression", accepted 1997

Rachel Beeri-Leibson "Human AChE expression in transgenic mice: an approach to the molecular control of cholinergic responses", submitted 1997

for Master of Science

Nelly Gluzman "Site-direced mutagenesis approach to drug interactions of human cholinesterases", submitted 1997

Proc. Natl. Acad. Sci. USA
Vol. 94, pp. 8173–8178, July 1997
Neurobiology

Acetylcholinesterase-transgenic mice display embryonic modulations in spinal cord choline acetyltransferase and neurexin Iβ gene expression followed by late-onset neuromotor deterioration

(neuromuscular junction/motoneurons)

CHRISTIAN ANDRES*†‡, RACHEL BEERI*‡, ALON FRIEDMAN*, EFRAT LEV-LEHMAN*, SIVAN HENIS*, RINA TIMBERG*, MOSHE SHANI§, AND HERMONA SOREQ*¶

*Department of Biological Chemistry, The Hebrew University of Jerusalem, 91904 Israel; and §Department of Molecular Genetics, Agricultural Research Organization, The Volcani Center, Bet Dagan, 50250 Israel

Communicated by Roger D. Kornberg, Stanford University School of Medicine, Stanford, CA, May 9, 1997 (received for review March 12, 1997)

ABSTRACT **To explore the possibility that overproduction of neuronal acetylcholinesterase (AChE) confers changes in both cholinergic and morphogenic intercellular interactions, we studied developmental responses to neuronal AChE overexpression in motoneurons and neuromuscular junctions of AChE-transgenic mice. Perikarya of spinal cord motoneurons were consistently enlarged from embryonic through adult stages in AChE-transgenic mice. Atypical motoneuron development was accompanied by premature enhancement in the embryonic spinal cord expression of choline acetyltransferase mRNA, encoding the acetylcholine-synthesizing enzyme choline acetyltransferase. In contrast, the mRNA encoding for neurexin-Iβ, the heterophilic ligand of the AChE-homologous neuronal cell surface protein neuroligin, was drastically lower in embryonic transgenic spinal cord than in controls. Postnatal cessation of these dual transcriptional responses was followed by late-onset deterioration in neuromotor performance that was associated with gross aberrations in neuromuscular ultrastructure and with pronounced amyotrophy. These findings demonstrate embryonic feedback mechanisms to neuronal AChE overexpression that are attributable to both cholinergic and cell–cell interaction pathways, suggesting that embryonic neurexin Iβ expression is concerted *in vivo* with AChE levels and indicating that postnatal changes in neuronal AChE-associated proteins may be involved in late-onset neuromotor pathologies.**

Accumulated and compelling cell culture evidence increasingly points to noncatalytic morphogenic roles for acetylcholinesterase (AChE), the enzyme known for its function in terminating neurotransmission at cholinergic synapses by hydrolysis of acetylcholine (ACh) (1–3). At the *in vivo* milieu, we reported a morphogenic activity for overexpressed human AChE in developing amphibian neuromuscular junctions (NMJs) (4, 5). This activity was attributed primarily to modulations in synaptic acetylcholine levels and consequent changes in cholinergic neurotransmission. However, the high degree of sequence homology between AChE and a family of nervous system cell surface proteins suggests that AChE also might be involved in cell adhesion processes recruited during synaptogenesis and long-term synapse maintenance. Proteins participating in these processes include mammalian neuroligins (6, 7), *Drosophila* neurotactin (8), and gliotactin (9). Recently, a chimera in which the extracellular cholinesterase-like domain of neurotactin was replaced with the homologous domain from *Torpedo* AChE was reported to retain ligand-dependent cell-adhesive properties similar to the native molecule (10). This reinforced the notion that AChE may play a role in neuronal cell adhesion.

In mammals, the AChE-homologous neuroligins were identified as heterophilic ligands for a splice-site specific form of the synapse-enriched neuronal cell surface protein neurexin Iβ (11). Neurexins represent a family of three homologous genes (I, II, and III), giving rise to α and β forms that can undergo further alternative splicing to generate over 1,000 isoforms (12). Neurexins, as AChE, are expressed in postmitotic neurons of the embryonic nervous system, including spinal cord, before synaptogenesis (13). The wealth of alternative splicing patterns predicted for both the neurexins and the neuroligins, together with their spatio-temporally restricted expression patterns, have led to the suggestion that they could mediate an almost infinite number of highly specific cell-cell interactions in the nervous system (12, 13). This raises the possibility that AChE, by virtue of its homology to neuroligin, could play a role in neurexin-mediated cell-adhesion interactions. To explore this issue, we asked whether overexpression of AChE might feed back upon expression of neurexins *in vivo* and searched for potential correlations between AChE overexpression and changes in synapse development and maintenance. For this purpose, we chose to study the NMJ and its innervating motoneurons in transgenic mice expressing human AChE in brain and spinal cord (14). Our observations correlate neuronal overexpression of AChE with embryonic feedback mechanisms attributable to both cholinergic and noncholinergic pathways. They also suggest that postnatal changes in neuronal AChE and/or its associated proteins may play a role in late-onset neuromotor pathologies.

EXPERIMENTAL PROCEDURES

PCR Analyses. PCR was performed essentially as described previously (14) using species-specific primers assigned to nucleotides 1,522 (+) and 1,797 (−) in exons 3 and 4 of the human AChE cDNA, nucleotides 375 (+), 1,160 (−) in exons 2 and 3 of the mouse ACHE gene (15), nucleotides 83 (+), 646 (−) of the mouse choline acetyltransferase (CHAT) gene (16),

The publication costs of this article were defrayed in part by page charge payment. This article must therefore be hereby marked "*advertisement*" in accordance with 18 U.S.C. §1734 solely to indicate this fact.

Abbreviations: ACh, acetylcholine; AChE, acetylcholinesterase; ChAT, choline acetyltransferase; NMJ, neuromuscular junction; RT-PCR, reverse transcription–PCR.

†Present address: Laboratoire de Biochimie et de Biologie Moleculaire, Centre Hospitalier Régional Universitaire, INSERM U 316, 37044 Tours Cedex, France.
‡C.A. and R.B. contributed equally to this study.
¶To whom reprint requests should be addressed. e-mail: Soreq@shum.huji.ac.il.

nucleotides 822 (+), 996 (−) of the mouse β-actin gene (17), nucleotides 978 (+) and 1,113 (−) of the neurexin Iβ gene (12), and nucleotides 1,179 (+) and 1,450 (−) of the neurexin IIIβ gene (12). Resultant PCR products (276, 786, 564, 174, 136, and 272 bp, respectively) obtained from similar amounts of RNA were removed and analyzed on ethidium bromide-stained agarose gels.

High-Resolution *in Situ* Hybridization. Hybridization was done essentially as described (17) with the following modifications: Tissues were fixed in 4% paraformaldehyde/0.1% glutaraldehyde (2 hr) and washed at 4°C. Clearing in 6% H_2O_2 (1 hr) was followed by proteinase K (10 μg/ml, 15 min), glycine (2 mg/ml, 20 min), and refixation (4% paraformaldehyde/0.2% glutaraldehyde, 20 min), all in PBS/0.1% Tween-20. Hybridization buffer and washing solutions included 1% SDS. Hybridization was 16 hr at 52°C with 50-mer, 5′-biotinylated, 2-*O*-methyl cRNA probes (10 μg/ml) (Microsynth, Switzerland) directed to the following sequences: AChE mRNA: mouse exon 6, positions 1,932–1,981 (15); mouse exon 5, positions 249–199 (18); and mouse ChAT cRNA, positions 553–602 (16). Posthybridization washes were at 56°C.

Staining Procedures and Microscopy. Diaphragm muscles were fixed *in situ* with 4% paraformaldehyde/0.1% glutaraldehyde solution in PBS for 5 min at room temperature, dissected, refixed for 2 hr, and kept at 4°C in PBS until used. AChE activity staining was for 5 min at room temperature as previously described (14). Fifty-micrometer-thick, paraformaldehyde/glutaraldehyde-fixed spinal cord sections were stained for 30 min. Electron microscopy on 80-nm-thick sections and morphometric analyses were essentially as described (5). Student's *t* test was used to evaluate morphometric data.

AChE Activity Measurements. Acetylthiocholine hydrolysis levels were determined spectrophotometrically in the presence of 10^{-5} M of the selective butyrylcholinesterase inhibitor iso-OMPA (tetraisopropylpyrophosphoramide). Enzyme-antigen immunoassay was as described (5).

Electromyography. After dissection of the hindleg, a tungsten bipolar stimulating electrode was positioned on the trunk of the sciatic nerve and evoked muscle fiber potentials recorded by a microelectrode placed on the gastrocnemius muscle. The nerve was stimulated by brief (0.1 msec) stimuli at increasing intensities (<1 mA). Data were recorded through an AC-DC amplifier (A-M Systems, Everett, WA, model 1800), digitized on line, and analyzed using Pclamp 6.0 (Axon Instruments, Foster City, CA). Muscle temperature, maintained at 32 ± 1°C by a warming lamp, was continuously monitored. In each animal, about 10 different recordings were taken. Anesthesia was accomplished with intraperitoneal administration of Nembutal (60 mg/kg weight).

Grip Test. Mice were suspended by their forelegs on a 3-mm-thick horizontal rope 1 m above bench level. The time it took them to grip the rope with their hindlegs (escape latency) was measured three times at 1-min intervals for sex-matched mice with similar body weights. Unsuccessful trials and those that ended in animals falling off the rope were recorded as 10 sec.

RESULTS

Human AChE from Spinal Cord Motoneurons Reaches Transgenic Muscle. ACHE-transgenic mice carry, and express in their central nervous system (14), the synaptic form (5) of human AChE. Reverse transcription–PCR (RT-PCR) demonstrated expression of human AChE mRNA in spinal cord, but not in muscle (Fig. 1*A*) of ACHE-transgenic mice. High-resolution *in situ* hybridization using a biotinylated 2-O-methyl cRNA probe detected both mouse and human AChE mRNA transcripts throughout neuronal perikarya within the anterior horn of the spinal cord in both control and transgenic adult mice (Fig. 1 *B* and *C*). Large polygonal neurons with the characteristic features of α motoneurons as well as small round cells resembling γ motoneurons or interneurons, but not cells with glial morphology, were labeled (Fig. 1 *B* and *C*). Similar patterns of AChE mRNA labeling were observed in the cervical, lumbar, and dorsal regions of the spinal cord (data not shown). Cytochemical staining revealed AChE activity in neuronal processes within adult transgenic spinal cord, high above levels observed in controls (Fig. 1 *D* and *E*). Overexpression of AChE in spinal cord was confirmed by quantitative assays demonstrating approximately 25% higher activity in spinal cord extracts from transgenic animals. Using a human AChE-specific mAb (mAb 101–1) in an enzyme-antigen immunoassay, this difference was attributed to AChE of human origin evenly distributed between the salt and detergent-soluble fractions. In light of reports that motoneurons contribute to synaptic AChE at the amphibian NMJ (19) we considered the possibility that AChE of human origin might be present at the NMJ despite the apparent transcriptional silence of the human gene in muscle. In detergent muscle extracts, no significant difference in total AChE activity was observed between six control and seven transgenic adult mice (33.4 ± 6.9 vs. 35.9 ± 1.3 nmol/min per mg of protein, respectively). However, the binding of up to 6% of the total enzyme to mAb 101 indicated the presence of a minor fraction of human AChE in muscle (data not shown).

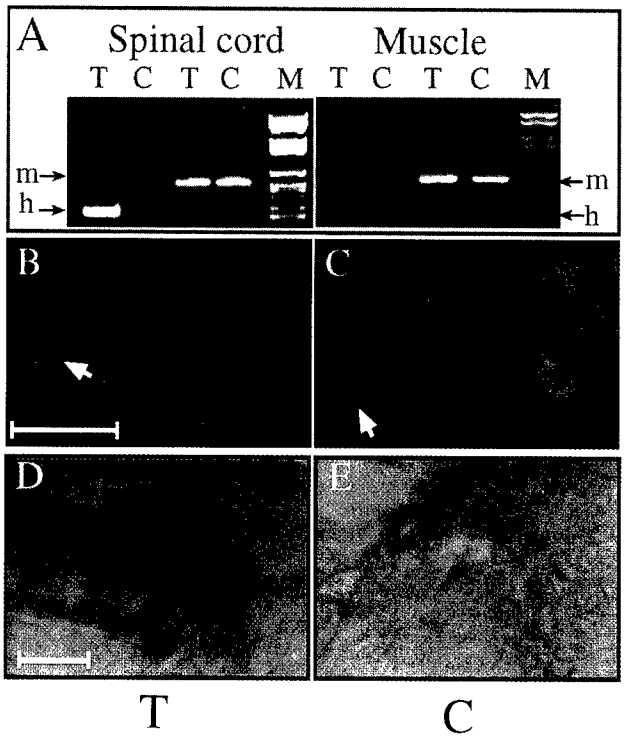

FIG. 1. Human AChE cDNA is expressed in spinal cord neurons but not muscle. (*A*) RT-PCR analyses. Primers specific for mouse (m) or human (h) AChE mRNA indicates expression of the transgene in transgenic (T) spinal cord, but not muscle. Control (C) mice express the endogenous mRNA in both tissues. (*B* and *C*) *In situ* hybridization. A probe detecting both mouse and human AChE mRNAs labeled neurons in 50-μm cervical spinal cord sections from both transgenic (*B*) and control (*C*) mice. Black arrows indicate large polygonal α motoneurons; white arrows indicate γ motoneurons and/or interneurons. ELF kit 6605 (Molecular Probes) diluted 1:250 was used for detection. (Size bar, 50 μm.) Note that labeling is restricted to cells with neuronal morphology. (*D* and *E*) Enzyme activity. Fixed sections from the anterior horn of lumbar spinal cord of transgenic (*D*) or control (*E*) mice were cytochemically stained for catalytically active AChE. Note the enhanced activity in nerve fibers and cell bodies from the transgenic spinal cord. (Size bar, 100 μm.)

Spinal Cord Neurons of Embryonic and Newborn Transgenic Mice Display Drastic Changes in ChAT and β-Neurexin

mRNAs. To search for potential changes in gene expression accompanying overexpression of AChE in spinal cord, we performed semiquantitative, kinetic RT-PCR. PCR signals reflected similar levels of human AChE mRNA in spinal cord of embryonic day 17 (E17), newborn, and 5-week-old mice (Fig. 2*A*). In contrast, mouse AChE mRNA was hardly detectable in the spinal cord before birth, but increased approximately 8-fold in newborn mice, and continued to increase in young adults, all in both groups (Fig. 2*A*). As excess AChE is expected to reduce the bioavailability of ACh and suppress cholinergic neurotransmission, we searched for potentially compensatory changes in expression of the ACh-synthesizing enzyme ChAT. RT-PCR demonstrated premature embryonic expression of ChAT mRNA at E17 in transgenic, but not control, spinal cord (Fig. 2*A*). In newborn mice, a smaller, but still apparent, enhancement in ChAT mRNA levels was observed in transgenic as compared with control mice. However, at 5 weeks transgenic and control mice displayed similar levels of this transcript. Actin mRNA levels, which served as a control for the integrity and amounts of mRNA in these preparations, remained unchanged throughout development (data not shown).

Transgenic, but not control, embryonic spinal cord neurons were intensively labeled in *in situ* hybridization with an AChE cRNA probe recognizing both human and mouse AChE mRNAs (Fig. 2*B*). In contrast, a probe selective for mouse AChE yielded fainter labeling and no significant difference between transgenic and control motoneurons (Fig. 2*B*). Significantly, a mouse ChAT cRNA probe prominently labeled motoneuron perikarya in transgenic, but not control, spinal cord (Fig. 2*B*). Thus, enhanced signals in both RT-PCR and *in situ* hybridization indicated augmented neuronal ChAT

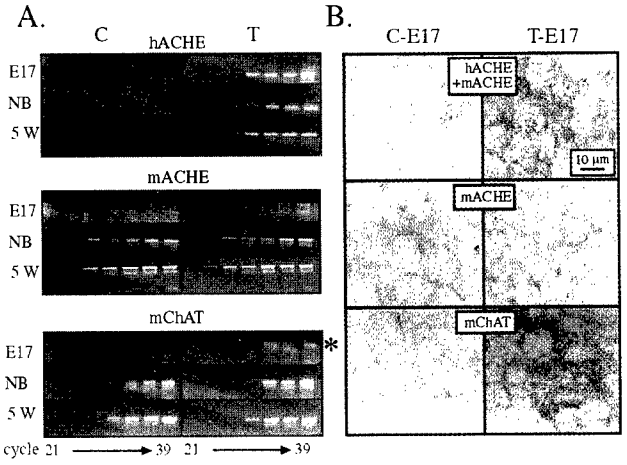

FIG. 2. Transgenic human AChE (hAChE) mRNA expression induces a transient embryonic enhancement in ChAT mRNA levels. (*A*) RT-PCR analyses. RNA extracted from spinal cord of control (C) and transgenic (T) mice at the noted ages was subjected to kinetic RT-PCR using primers for the noted mRNAs (see *Experimental Procedures*). Aliquots of amplified DNA representing human (h) or mouse (m) AChE or ChAT mRNAs were removed every third cycle from cycle 21, representing differences of *ca.* 8-fold between samples. Products were electrophoresed and stained with ethidium bromide. Note that hAChE mRNA is present only in transgenic mice, that endogenous AChE mRNA levels are similar in control and transgenic animals, and that while mChAT levels are undetectable in control E17 embryos, a prominent signal, marked by an asterisk, is observed in transgenic embryos. In postnatal mice, ChAT mRNA levels in transgenic and control spinal cord are indistinguishable. NB, newborn. (*B*) *In situ* hybridization. Seven-micrometer sections from the lumbar spinal cord of control (C) and transgenic (T) E17 embryos were subjected to *in situ* hybridization. Fast-red (Boehringer Mannheim) served for detection. Note the intense AChE and ChAT mRNA signals in transgenic cell bodies.

mRNA levels in transgenic mice. At subsequent ages, however, no such differences could be detected, pointing at the transient nature of this embryonic feedback response. In light of the considerable homologies between AChE and the neurexin β ligand neuroligin (7), we further looked for changes in the expression of neurexin β in spinal cord of transgenic mice. Both embryonic and newborn, but not 5-week-old, transgenic mice displayed drastically reduced levels of neurexin Iβ compared with controls (Fig. 3), suggesting that neurexin-neuroligin relationships would be altered in the transgenic spinal cord and indicating that the accessibility of AChE-like domains affects neurexin Iβ production. In contrast, neurexin IIIβ levels were barely detectable in either group at these ages and similar to each other at 5 weeks. Actin mRNA levels, as measured by RT-PCR, were identical in both groups at all ages.

Transgenic AChE Expression Induces Persistent Enlargement of Motoneurons. The total number and spatial distribution of motoneurons in transgenic spinal cord was essentially normal, suggesting that human AChE expression did not affect neuronal proliferation or migration and did not cause neuronal death. However, measurements of cell area revealed age-dependent changes in morphology among anterior horn neurons from transgenic as compared with control mice. Neuronal cell bodies in control embryos averaged 44.5 ± 15.8 μm^2 in size (mean ± SD) whereas transgenic neurons displayed areas of 51.5 ± 13.5 μm^2 (Fig. 4*A*) ($P < 0.05$, Student's *t* test). Postnatal maturation of spinal cord neurons was accompanied by dissociation into two distinct populations, one consisting of small neurons (25–150 μm^2) likely to be interneurons and γ motoneurons, and the other of large neurons (>150 μm^2) that includes the α motoneurons. There was no difference between postnatal control and transgenic spinal cord in either the number or the perikaryal area of the small neurons. Similarly, the fraction of neurons larger than 150 μm^2 was similar in transgenic and control mice (data not shown), suggesting normal lineage distribution of spinal cord motoneurons. Nevertheless, transgenic motoneurons were significantly enlarged relative to controls, with perikarya of 220 μm^2, as compared with 160 μm^2 ($P < 0.02$, Fig. 4*B*). The normal size and unmodified staining of nuclei suggested that the enlarged neurons were viable in both embryonic and adult spinal cord

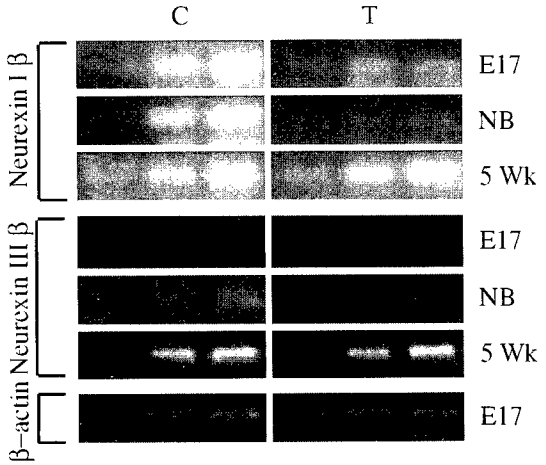

FIG. 3. Neurexin Iβ mRNA is dramatically suppressed in embryonic and newborn transgenic mice. Primers specific for neurexin Iβ and IIIβ mRNAs (see *Experimental Procedures*) were used in semiquantitative RT-PCR on spinal cord RNA from control (C) and transgenic (T) mice at the noted ages. Note the dramatic reduction in signal intensities for neurexin Iβ in embryonic (E17) and newborn (NB) transgenic mice compared with controls and to 5-week-old (5 Wk) mice. Primers for β-actin mRNA served to verify quantity and quality of RNA in each sample. Shown are PCR products sampled every third cycle (i.e., reflecting 8-fold differences) from cycle 21 for β-actin and cycle 24 for neurexins.

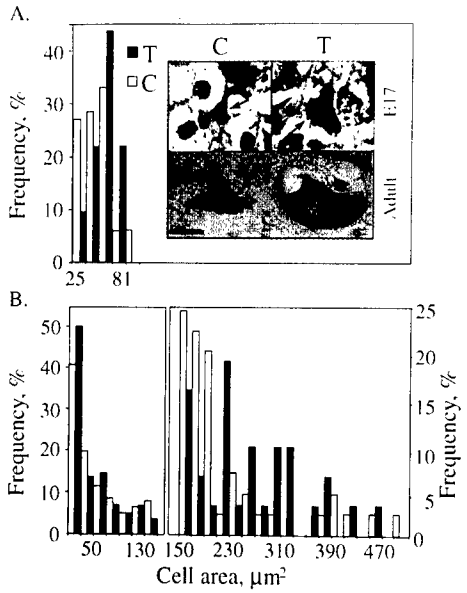

FIG. 4. AChE overexpression is associated with enlarged motoneuron perikarya. (*A*) Embryonic enlargement. Thoracic spinal cord sections from E17 transgenic (T) and control (C) mice were stained with cresyl violet, and the perikaryal areas in μm^2 of ventral horn cells measured. Presented are percent fractions of the total number of cresyl violet positive cells in each size group (67 control and 32 transgenic cells were measured). This analysis revealed overall enlargement of neurons in transgenic embryonic spinal cord ($P < 0.05$). (*Inset*) Representative cresyl violet-positive control (C) and transgenic (T) neurons from embryonic (E17) and 3-month-old (adult) mice are presented. Note that the enlarged neurons characteristic of transgenic animals maintain the normal polygonal morphology. (Size bar, 10 μm.) Arrows indicate motoneurons. (*B*) Adult enlargement. Separate size distributions for ventral horn neurons up to 150 μm^2 (*Left*) and larger than 150 μm^2 (*Right*) from adult mice are presented. Smaller cells (202 control and 186 transgenic cells), presumably interneurons and γ-motoneurons, showed similar perikaryal area distributions in transgenic and control animals. In contrast, the larger ventral horn cells, presumably α-motoneurons (44 control and 27 transgenic cells), preserved the embryonic trend of enlarged perikarya observed in transgenic animals ($P < 0.02$).

(Fig. 4*A*, *Inset*). We found no examples for such selective neuronal enlargement in neurodegenerative diseases.

AChE-Induced Progressive Impairments in Neuromuscular Function. Transgenic animals developed normally and acquired normal motor functions at the same ages as control mice. Adult transgenic mice walked normally, with track width and pace length similar to those of controls (not shown). Swimming speed of 4-month-old transgenic mice (21.4 ± 4.0 m/min) was only slightly slower than controls (25.0 ± 4.0 m/min) ($n = 10$). However, transgenic animals exhibited severely impaired performance in a rope grip test designed to test coordinated sensorimotor activity of the abdomen, back, and leg muscles (Fig. 5*A*). When hung on the rope, transgenic mice acquired a loose, weakened posture, and 4-month-old transgenic, but never control, mice fell off the rope altogether in 20% of 30 sessions with 10 animals. Weakness in the grip test was already evident as a >2-fold difference in escape latency ($P < 0.02$) at the age of 4 weeks, but worsened ($P < 0.01$) by 4 months of age.

Transgenic AChE Expression Leads to Electromyographic Abnormalities. The intensity of compound action potentials recorded on the surface of the sciatic nerve did not differ between control and transgenic adult mice. Nerve conduction velocity was normal, and no late potentials were detected, suggesting normal myelination and number of axons (data not shown). In addition, direct recording from the gastrocnemius muscle did not reveal spontaneous denervation activity. Nevertheless, evoked potentials recorded from the gastrocnemius muscle fibers in response to stimulation of the common trunk of the sciatic nerve disclosed three main abnormalities. In control animals, a small increase in stimulus intensity induced small and gradual increases in the amplitude of the muscle's compound action potential, so that supramaximal response amplitudes were up to 10-fold greater than the threshold response. In transgenic animals, parallel increases in stimulus intensity triggered considerably larger jumps in the amplitude of the action potentials. These observations indicated enlargement of functional motor units and an increased number of

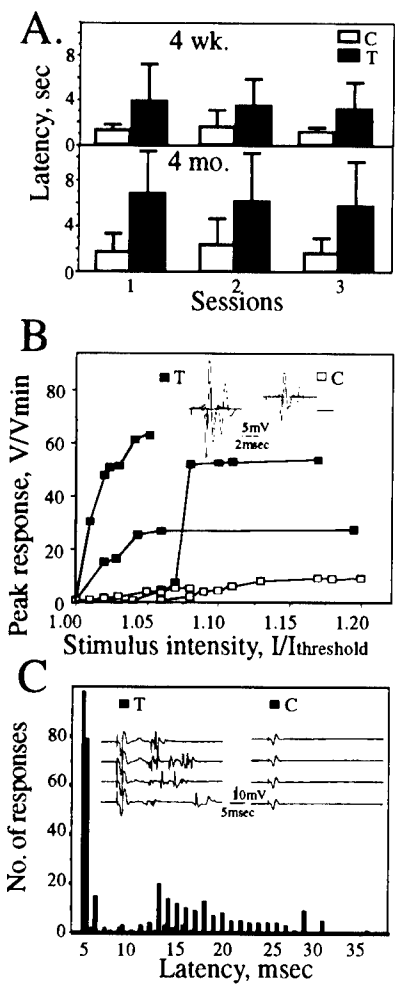

FIG. 5. Postnatal motor function impairments worsen with age. (*A*) Grip test performance. Groups of 5–10 mice at the ages of 4 weeks and 4 months [transgenic (T) and control (C)] were suspended with their forelegs on a 3-mm diameter rope and the time taken to securely grip the rope with their hindlegs was noted (latency) (see *Experimental Procedures*). Presented are escape latencies in seconds (average ± SD). Note the slower performance of transgenics as compared with controls at both age groups and the worsening of this phenotype with age. (*B*) Electromyographic profiles. Evoked muscle fiber potentials (V/Vmin) after sciatic nerve stimulation were recorded by a microelectrode placed on the surface of the gastrocnemius muscle in three transgenic (■) and three control (□) mice. (*Inset*) Superposition of responses evoked by increasing stimulus intensity up to 1.0 mA at 1 Hz as in the enclosed scale. Saturation of response occurred only at high stimulus intensities and required more stimuli in transgenics than in controls. Note that in the transgenic muscle several negative peaks were observed in response to a single stimulus. (*C*) Delayed repetitive firing of action potentials. After 100 supramaximal stimulations at 1 Hz, abnormal late potentials (filled bars) appeared in four transgenic animals for up to 40 msec poststimulation as compared with a few signals in four control animals (empty bars). Presented are numbers of response spikes as a function of latency time for 10 different measurements.

muscle fibers recruited by the stimulated axons (Fig. 5*B*). Moreover, muscle potentials in transgenic mice were of greater amplitude and duration than those in controls, with frequent multiwaved shapes (mainly three subpeaks) rarely seen in controls (Fig. 5 *B* and *C*). Finally, repetitive supramaximal stimulations at 1 Hz induced pathological late potentials (latency up to 40 msec), which appeared frequently in transgenic animals but very rarely in controls (Fig. 5*C*). In 2 of 4 cases, 3-Hz stimulations after tetanization by 300 stimulations at 30 Hz resulted in myasthenia-like decreases (>10%) in the intensity of responses in transgenic, but not in control animals (data not shown). These observations suggested disturbed neuromuscular communication in adult AChE-transgenic mice.

NMJs and Muscles of Transgenic Animals Undergo Dramatic Morphological Changes. Adult AChE-transgenic mice developed diaphragm motor endplates that were 60% larger, on average, than controls (Fig. 6*A*). Therefore, over half of the transgenic endplates examined, but only 10% of controls, were larger than 600 μm^2. In addition, transgenic endplates failed to display the complex boundaries found in control endplates, but acquired a simple ellipsoid aspect (Fig. 6*A*). Similar morphological changes also were found in hindleg quadriceps endplates and in anterior tibialis muscles (not shown).

NMJ ultrastructure in transgenic animals was highly variable. Although the mean length of postsynaptic membrane folds was similar among transgenics and controls (0.6 ± 0.05 $\mu m/\mu m$ synapse length), only 7 of 16 analyzed NMJs from transgenic mice as compared with 11 of 14 NMJs in control mice possessed average-length postsynaptic folds (Fig. 6*B*, *Top*). The remaining transgenic NMJs displayed either of two pathological features, both reported in NMJs of aged humans (20). One-fourth of the NMJs in transgenic mice as compared with 7% of control NMJs presented highly exaggerated, branched and densely packed postsynaptic folds, similar to those occurring in the Eaton–Lambert syndrome (21) (average of 0.87 ± 0.16 μm, Fig. 6*B*, *Middle*). The remaining third of the transgenic NMJs, but only 14% of control NMJs, possessed short, ablated postsynaptic folds (0.30 ± 0.07 μm, Fig. 6*B*, *Bottom*), which resembled those of myasthenia gravis patients (22).

Decreased muscle volume and atrophy of muscle fibers in adult transgenic animals were observed in 4-month-old mice. Electron microscopy subsequently indicated general loosening of intracellular structures in transgenic muscle fibers, but not in controls (Fig. 6*C*). Intracellular spaces were filled with large, structureless vacuoles. The distance between myofilaments and between myofibrils was enlarged. Triads of T tubules and terminal cisternae appeared to be dissociated, mitochondria were no longer aligned with I bands of the sarcolemma and were clearly swollen, with cristae no longer visible (Fig. 6*C*). No NMJ was observed in association with these wasted, damaged muscle regions.

DISCUSSION

We have observed that overexpression of AChE in spinal cord neurons of transgenic mice promotes a persistent, but enigmatic, enlargement of motoneuron perikarya and a severe, delayed-onset neuromotor pathology. The dual cholinergic and noncholinergic properties of AChE raise the possibility that either or both of these activities could be involved in mediating the morphologic transformation of motoneurons and the ultimate demise of NMJs and muscle fibers in adult mice. Enhanced levels of ChAT mRNA in motoneurons of transgenic embryos suggest the existence of a compensatory feedback loop that is sensitive to cholinergic inputs. As ChAT is responsible for synthesizing ACh, hyperactivation of ChAT gene expression in spinal cord motoneurons of transgenic embryos could increase available ACh and stabilize cholinergic circuitry under conditions of AChE overexpression. In contrast, suppressed levels of mRNA encoding the cell surface protein neurexin Iβ in spinal cord of embryonic and newborn mice should change neurexin-neuroligin interactions, possibly

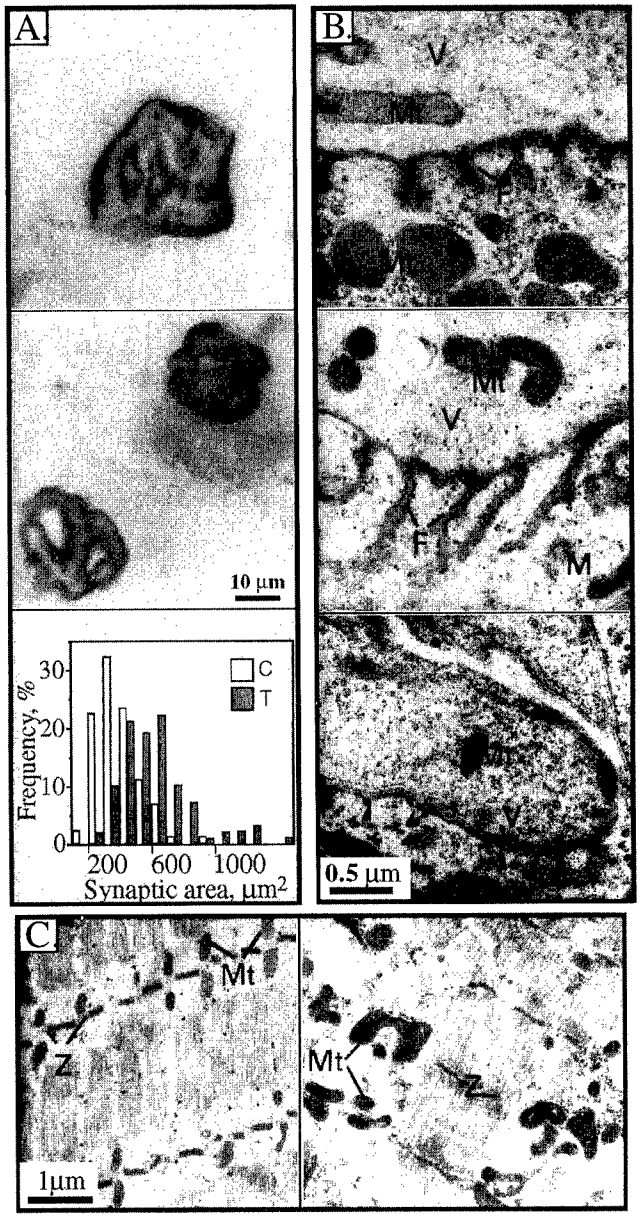

FIG. 6. Enlargement and shape modifications in diaphragm neuromuscular junctions of transgenic animals. (*A*) NMJ surface changes. Wholemount cytochemical staining of AChE activity was performed on fixed diaphragms from 4-month-old transgenic (*Top*) and control (*Middle*) animals. Transgenic NMJs displayed larger circumference and fading boundaries as compared with the complex, sharp contours in controls. Representative endplates from 12 control and transgenic mice. Similar results were obtained using methylene blue staining for total proteins (not shown). (*Bottom*) Stained areas in μm^2 for motor endplates illustrated above (for 90 control, 100 transgenic terminals) are presented as a frequency distribution plot. (*B*) Postsynaptic fold changes. Electron microscopy of 80-nm crosssections of terminal diaphragm zones reveals variable deformities in NMJ from transgenic mice. (*Top*) Normal NMJ. (*Middle*) Transgenic NMJ with exaggerated postsynaptic folds. (*Bottom*) Transgenic NMJ with short, undeveloped folds marked by arrowheads. V, vesicles; M, muscle; F, postsynaptic folds. (*C*) Muscle abnormalities. (*Left*) Longitudinal section from normal diaphragm muscle. Note the organization of mitochondria (Mt) at well-aligned Z bands (Z). (*Right*) Transgenic diaphragm muscle with fiber atrophy, loss of muscle fiber organization, and swelling of mitochondria at disrupted Z bands.

affecting both perikarya and synapse properties. This may tentatively hint at the activation of a feedback pathway that is responsive to the noncatalytic activities of AChE and attribute physiological significance to the homology between AChE and the neuroligin-related cell surface proteins, purported to be involved in cell adhesion and synaptogenic interactions in the nervous system. The postnatal normalization we observed in the levels of both ChAT and neurexin Iβ mRNAs implies a temporally restricted window during which motoneurons can recruit these two feedback loops. The delayed onset of neuromuscular pathologies, as compared with apparently normal embryonic development, thus may reflect the cumulative damage resulting from this irretrievable loss of neuronal transcriptional plasticity.

In light of a previous report that motoneurons contribute synaptic AChE to the amphibian NMJ (19), and assuming that NMJs represent less than 0.1% of the muscle surface (23), the 6% fraction of human enzyme we observed in extracts from muscle not itself expressing the transgene likely reflects a significant accumulation of motoneuron-derived transgenic enzyme in the synapse. This is not surprising as we previously noted that levels of synaptic AChE were elevated ≥ 5-fold in NMJs from *Xenopus* embryos overexpressing this same cDNA and in which the corresponding nerve terminals were stained for active enzyme (4, 5). Therefore, the disastrous long-term effects of overexpressed AChE could be tentatively attributed, to chronic disturbances in cholinergic neurotransmission. Impaired cholinergic transmission is indeed associated with several congenital and acquired amyotrophic diseases characterized by progressive, juvenile- or adult-onset neuromotor deterioration. Eaton–Lambert syndrome is associated with malfunctioning presynaptic calcium channels and suppressed ACh release (21), myasthenia gravis involves autoimmune suppression of muscle nicotinic acetylcholine receptors (22), and amyotrophic lateral sclerosis results from motoneuron death (24). However, while our findings demonstrate that a moderate, but stable, increase in motoneuron expression of AChE is sufficient to predispose mouse NMJs and muscle to late-onset progressive deterioration, it is not clear whether such deterioration is due to abnormal neuronal inputs, the presence of high levels of AChE in the synapse, or other reasons. Moreover, the severity of the neuromotor degenerative phenotype is difficult to explain solely in terms of cholinergic dysfunction. Rather, it likely represents the outcome of accumulated damage due to various secondary and tertiary changes in additional nerve and/or muscle components.

The morphogenic potency of AChE has now been well established in diverse cell culture models. A neurite outgrowth-promoting activity was demonstrated for AChE in various cultured chicken neurons and attributed to noncatalytic activities affecting cell adhesion properties (1, 2). In addition, our expression of various alternative human AChE cDNAs in glioma cells (25), as well as in *Xenopus* motoneurons (unpublished data) traced this activity to the synaptic form of the enzyme. The mechanism for noncatalytic AChE morphogenic activities is yet unknown. However, Darboux *et al.* (10) demonstrated that in addition to the primary sequence homologies between neurotactin and AChE, the esterase-like domain in *Drosophila* neurotactin likely shares a striking three-dimensional structural similarity with AChE and that this domain plays a prominent role in the protein's cell adhesion properties. In addition, the recently identified neuroligin family of mammalian neuronal cell surface molecules all contain an extracellular esterase-homologous domain sharing 35% homology with *Torpedo* AChE (7). That the overexpression of AChE in spinal cord neurons is associated with a specific suppression in the levels of neurexin Iβ mRNA during embryonic development is highly suggestive of a role for AChE in the neuroligin-neurexin paradigm of cell recognition events. If so, the spatiotemporally coordinated expression of AChE and neurexins in the embryonic spinal cord during normal development, together with the suppression of neurexin Iβ mRNA levels in ACHE-transgenic mice, could reflect a functional, rather than casual association. In that case, our findings would represent *in vivo* indications for a physiologically relevant interaction between AChE and a cell-surface molecule thought to be involved in neuronal development, synaptogenesis, and synapse maintenance.

We thank Drs. S. Seidman and C. Kalcheim (Jerusalem) for helpful discussions and Dr. B. Norgaard-Pedersen (Copenhagen) for antibodies. This work was supported by Grants 17-97-1-7007 from the U.S. Army Medical Research and Defense Command and the U.S.–Israel Binational Science Foundation (to H.S.). C.A. was a recipient of an Institut National de la Santé et de la Recherche Médicale (France) exchange fellowship with the Israel Ministry of Science and Arts. A.F. received a postdoctoral fellowship from the Smith Foundation for Psychobiology.

1. Small, D. H., Reed, G., Whitefield, B. & Nurcombe, V. (1995) *J. Neurosci.* **15,** 144–151.
2. Layer, P. G. & Willbold, E. (1995) *Prog. Histochem. Cytochem.* **29,** 1–99.
3. Jones, S. A., Holmes, C., Budd, T. C. & Greenfield, S. A. (1995) *Cell Tissue Res.* **279,** 323–330.
4. Shapira, M., Seidman, S., Sternfeld, M., Timberg, R., Kaufer, D., Patrick, J. & Soreq, H. (1994) *Proc. Natl. Acad. Sci. USA* **91,** 9072–9076.
5. Seidman, S., Sternfeld, M., Ben Aziz-Aloya, R., Timberg, R., Kaufer-Nachum, D. & Soreq, H. (1995) *Mol. Cell. Biol.* **14,** 459–473.
6. Ichtchenko, K., Hata, Y., Nguyen, T., Ullrich, B., Missler, M., Moomaw, C. & Sudhof, T. C. (1995) *Cell* **81,** 435–443.
7. Ichtchenko, K., Nguyen, T. & Sudhof, T. C. (1996) *J. Biol. Chem.* **271,** 2676–2682.
8. Barthalay, Y., Hipeau-Jacquotte, R., Escalera, S., Jimenez, F. & Piovant, M. (1990) *EMBO J.* **9,** 3603–3609.
9. Auld, V. J., Fetter, R. D., Broadie, K. & Goodman, C. S. (1995) *Cell* **81,** 757–767.
10. Darboux, I., Barthalay, Y., Piovant, M. & Hipeau-Jacquotte, R. (1996) *EMBO J.* **15,** 4835–4843.
11. Ushkaryov, Y. A., Petrendo, A. G., Geppert, M. & Sudhof, T. C. (1992) *Science* **257,** 50–56.
12. Ullrich, B., Ushkaryov, Y. A. & Sudhof, T. C. (1995) *Neuron* **14,** 497–507.
13. Puschell, A. W. & Betz, H. (1995) *J. Neurosci.* **15,** 2849–2856.
14. Beeri, R., Andres, C., Lev-Lehman, E., Timberg, R., Huberman, T., Shani, M. & Soreq, H. (1995) *Curr. Biol.* **5,** 1063–1071.
15. Rachinsky, T. L., Camp, S., Li, Y., Ekstrom, T. J., Newton, M. & Taylor, P. (1990) *Neuron* **5,** 317–327.
16. Misawa, H., Ishii, K. & Deguchi, T. (1992) *J. Biol. Chem.* **267,** 20392–20399.
17. Lev-Lehman, E., Deutch, V., Eldor, A. & Soreq, H. (1997) *Blood* **89,** 3644–3653.
18. Li, Y., Camp, S. & Taylor P. (1993) *J. Biol. Chem.* **268,** 5790–5795.
19. Anglister, L. (1991) *Cell Biol.* **115,** 755–764.
20. Wokke, L. H. J., Jennekens, F. G. I., van den Oord, C. J. M., Veldman, H., Smith, L. M. E. & Leppink, G. J. (1990) *J. Neurol. Sci.* **95,** 291–310.
21. Lambert, E. H. & Elmqvist, D. (1971) *Ann. N.Y. Acad. Sci.* **183,** 183–199.
22. Engel, A. G. & Santa, T. (1971) *Ann. N.Y. Acad. Sci.* **183,** 46–63.
23. Hall, Z. & Sanes, J. R. (1973) *Cell* **72,** 99–121.
24. Robert, H. & Brown, G., Jr. (1995) *Cell* **80,** 687–692.
25. Karpel, R., Sternfeld, M., Ginzberg, D., Guhl, E., Graessman, A. & Soreq, H. (1996) *J. Neurochem.* **66,** 114–123.

June 15, 1997

TRANSGENIC ACETYLCHOLINESTERASE INDUCES DETERIORATION OF MURINE NEUROMUSCULAR JUNCTIONS BUT LEAVES SPINAL CORD SYNAPSES INTACT

Christian Andres[1,2], Shlomo Seidman[1], Rachel Beeri[1], Rina Timberg[1] and Hermona Soreq[1,3]

[1]Department of Biological Chemistry, The Hebrew University of Jerusalem, 91904 Israel

[3]To whom correspondence should be addressed (Tel: 972 2 6585109, Fax: 972 2 6520258).

E-Mail: Soreq@shum.huji.ac.il

[2]Present Address: Laboratoire de Biochimie et de Biologie Moleculaire, INSERM U316, 37044 Tours Cedex, France.

Abstract

Acetylcholinesterase (AChE) produced by spinal cord motoneurons accumulates within axo-dendritic spinal cord synapses. It is also secreted from motoneuron cell bodies, through their axons, into the region of neuromuscular junctions, where it terminates cholinergic neurotransmission. Here we show that transgenic mice expressing human AChE in their spinal cord motoneurons display primarily normal axo-dendritic spinal cord cholinergic synapses in spite of the clear excess of transgenic over host AChE within these synapses. In contrast, a modest excess of AChE drastically affects the structure and long-term functioning of neuromuscular junctions in these mice, although they express human AChE in their spinal cord, but not muscle. Enlarged muscle endplates with either exaggerated or drastically shortened post-synaptic folds then lead to a progressive neuromotor decline and massive amyotrophy. These findings demonstrate that excess neuronal AChE may cause distinct effects on spinal cord and neuromuscular synapses, and attribute the late-onset neuromotor deterioration observed in AChE transgenic mice to neuromuscular junction abnormalities.

Abbreviations: AChE, acetylcholinesterase; ACh, acetylcholine; ATCh, acetylthiocholine; NMJ, neuromuscular junction.

Introduction

Mammalian synapses are continuously remodeled to adjust to growth and the demands of use (Burns and Augustine, 1995; Grinell, 1995). Various diseases of the central and peripheral nervous systems that are associated with postnatal or adult-onset, progressive deterioration reflect deficiencies in the remodeling processes of cholinergic synapses. Examples include Alzheimer's disease (AD) (Coyle et al., 1983), spinal muscular atrophy (Crawford and Pardo, 1996), Lambert-Eaton disease (Lambert and Elmqvist, 1971) and amyotrophic lateral sclerosis (Robert and Brown, 1995). A simple model to explain the delayed-onset of pathology in these degenerative conditions views the decline toward disease as a gradual accumulation of damage which results in pathology when it passes a threshold. In such a model, built-in margins of safety protect the system, and hence the organism, for a period of time that reflects the margins of safety. An alternative, or supplemental approach to understanding late-onset disease is to postulate the existence of mechanisms that adjust the levels of other proteins and assure normal function during embryonic, postnatal, and young adulthood periods, but which falter or fail during aging. In that case, the age of onset will depend on the limits of adjustment and on the functional integrity of the cellular and molecular mechanisms which regulate feedback pathways. To distinguish between these possibilities and to search for putative age-limited adjustment mechanisms, animal models with late-onset nervous system defects are required.

Imbalanced cholinergic neurotransmission can be induced in animal models by acetylcholinesterase (AChE) over-production. Changes in synaptic AChE density, in particular, are predicted to modulate synaptic levels of acetylcholine (ACh) as well as postsynaptic miniature endplate potentials (mepps, Anglister et al., 1994). Transient overexpression of AChE indeed exerts a morphogenic effect on the development of neuromuscular junctions (NMJ) in AChE-transgenic *Xenopus* embryos (Seidman et al. 1995). The morphogenic effects of overexpressed AChE were attributed, at least in part, to subtle alterations in cholinergic neurotransmission. However, while the overall normal development of AChE-transgenic tadpoles suggested that developing NMJs can tolerate some deviation from normal cholinergic activity, the short time course of those experiments (3-5 days) precluded an investigation into the long-term effects of deregulated AChE expression on neuromuscular integrity and function. To this end, AChE-transgenic mice provide an intriguing model in which the effects of chronic AChE excesses can be examined in depth.

Transgenic overexpression of acetylcholinesterase (AChE) in cholinergic brain neurons of transgenic mice promotes late-onset progressive impairments in learning and memory (Beeri et al., 1995, Beeri et al., 1997) as well as in neuromotor functioning (Andres et al., 1997). The

cognitive defects observed in these mice could potentially reflect a cholinergic deficit which is caused by excessive hydrolysis of ACh and a consequent cholinergic hypofunction. In this sense, the adult-onset loss-of-function observed in AChE transgenic mice can serve as a model for the loss of cholinergic faculties observed in Alzheimer's disease (AD) patients (Coyle et al., 1983). However, the neuromotor deficiency in these AChE-overexpressing transgenic mice was preceded by changes in the expression of both choline acetyl transferase and neurexin Iβ, reflecting feedback processes affecting non-cholinergic functions in addition to the cholinergic ones (Andres et al., 1997). This, in turn, predicted changes in the properties and/or cytoarchitecture of specific synapses that were associated with the delayed onset of AChE-promoted neurodeterioration in these transgenic mice. To define which synapses were thus affected, we have undertaken a comparative ultrastructure analysis of neuromuscular junction (NMJ) and cholinergic spinal cord axo-dendritic synapses in the AChE-transgenic mice.

Formation of NMJs differs from that of inter-neuronal synpases in that it involves the differentiation of precisely defined domains on the surface of muscle fibers (Hall and Sanes, 1993; Carbonetto and Lindenbaum, 1995). Mammalian NMJ formation depends on several important neuron-derived proteins including agrin, which stimulates the formation of subneural clusters of ACh receptors (AChR) and AChE (reviewed by Grinnell, 1995 and Gautam et al., 1996) and neuregulin, which promotes the expression of several of the AChR subunit genes (Jo et al., 1995; Carraway and Burden, 1995). Experimental elimination of either of these proteins drastically reduces or abolishes NMJ formation during embryogenesis and results in prenatal or perinatal death (Gautam et al., 1996, Glass et al., 1996). Global interference with NMJ formation has also been achieved experimentally by genomic disruption or overexpression of other key NMJ proteins, CNTF (Masu et al., 1993), laminin β2, (Noakes et al., 1995), GAP-43 (Aigner et al., 1995), rapsyn (Gautam et al., 1995), and MuSK (Dechiarra et al., 1996). However, the early onset and severity of the neuromuscular defects obtained in knock-out studies precludes investigation into the role of these molecules in the long-term maintenance of synaptic ultrastructure and function during adulthood.

AChE-transgenic mice express a modest excess of human AChE in spinal cord but not muscle (Beeri et al., 1995; Andres et al., 1997). We now report that the ultrastructure of spinal cord cholinergic synapses is largely retained in spite of this excess, unlike NMJs of AChE transgenic mice which undergo dramatic cytoarchitectural changes. AChE-transgenic mice thus can be used for dissecting the molecular and cellular chains of events which lead from AChE excess toward postnatal neuromuscular pathology. Moreover, they can be employed to differentiate between effects of impaired cholinergic neurotransmission and those due to modified cell-cell interactions. Therefore, they may establish a valid paradigm for approaching delayed-

onset human diseases of environmental and/or multigenic origin that are associated with AChE overproduction.

Experimental Procedures

Tissue preparation and subcellular fractionation: AChE transgenic and control FVB/N mice (2-3 months old) were sacrificed by cervical dislocation and tissues were rapidly dissected, frozen in liquid nitrogen and kept at -70°C until use. Tissues were homogenized using a Potter Elvehiem homogenizer and extracts were successively prepared in 9 vol/weight of low salt, detergent or high salt solutions (low salt solution: 0.02 M Tris HCl, pH 7.5, 0.05 M NaCl; detergent solution: 0.01 Na phosphate buffer, pH 7.4, 1% Triton X-100 (w/w); high salt solution: 0.01 Na phosphate buffer, pH 7.4, 1 M NaCl), all with 2 mM EDTA, 5 μg/ml leupeptin and 10 μg/ml aprotinin. Homogenates were centrifuged in a Beckman TL100.2 rotor at 400,000g for 10 min. The supernatants of each solution contained the low salt-soluble, detergent-soluble and high salt-soluble fractions of AChE, respectively.

Determination of cholinesterase specific activities and protein concentrations: Cholinesterase activities were measured according to Ellman et al. (1961) in 96 well Nunc (Roskilde, Denmark) plates, in a final volume of 200 μl. Incubations of 20 min in solutions containing either BW 284 C 51 (1,5-bis(4-allyldimethyl-ammoniumphenyl)pentan-3-one-dibromide) at 10^{-5} M or iso-OMPA (isopropylpyrophosphoramide) at 10^{-4} M were used to inhibit AChE and butyrylhcholinesterase (BuChE) activities, respectively. Activities are expressed in nmol of acetylthiocholine (AcSCh) hydrolyzed/min/mg protein. Protein concentrations were determined by the method of Bradford (1976), using bovine serum albumin (BSA) as standard.

Sucrose gradient centrifugation: Ten ml linear sucrose gradients (4-20% w/w) were prepared in 0.01 M Tris-HCl buffer, pH 7.4, 1 M NaCl, 1 mM EGTA and 1% Triton X-100. AChE containing solutions (200-250μl) were deposited on the top of the gradients with 20 μl of catalase as a sedimentation marker (11.4 S). Centrifugation was performed in a Beckman SW 41 rotor at 37,000g for 17 h. After centrifugation, gradients were fractionated and cholinesterase activities measured. Catalase (11.45) was localized by determining absorption at 405 nm.

Binding to antibodies: Anti-AChE monoclonal antibodies (AC 101.1, Seidman et al., 1995) raised against bovine brain AChE and which recognize human but not mouse AChE (Liao et al., 1992) were bound overnight at 4 °C to 96-well Nunc Maxisorb plates (5 μg/ml antibody in 100 μl/well of 0.1 M Na bicarbonate buffer, pH 9.6). Non-specific binding sites were blocked by 1 h incubation in 3% BSA in phosphate-buffered saline containing 0.05% Tween 20 (PBS-T) at 37°C. Coated plates were kept at 4°C with PBS-T until use. Tissue extracts (20 μl, prepared as described above) or sucrose gradient fractions were then added for overnight incubation at 4 °C

with 80 µl of PBS-T. Wells were washed 3 times with PBS-T and bound AChE activity was assayed as above.

Staining procedures: For structural NMJ analyses, diaphragm muscles from mice sacrificed by cervical dislocation were fixed *in situ* by repeated (5 min, room temp.) application of fresh 4% paraformaldehyde, 0.1% glutaraldehyde solution in PBS. Fixed diaphragm was then dissected, refixed for 2 h and kept at 4 °C in PBS until used for cytochemical AChE staining (Beeri et al., 1995). When staining with 0.1% methylene blue, tissues were similarly handled. Diaphragm regions rich in NMJs were dissected into rectangles of about 3 x 5 mm, immobilized on glass slides and photographed in a Zeiss Axioplan microscope at 200-fold magnification. Sections of cervical spinal cord (50 µm, paraformaldehyde-glutaraldehyde fixed) were stained for 30 min and thiocholine precipitates observed by electron microscopy in 80 nm cut stained sections (Seidman et al., 1995). Control experiments on sections from transgenic spinal cord, with no ATCh verified that these electron-dense deposits were indeed reaction products of *in situ* AChE catalysis-mediated hydrolysis of the substrate. Morphometric measurements were performed as detailed previously (Seidman et al., 1995) using the Sigma Scan program (Jandel, Hamburg, Germany).

Results

Axo-dendritic cholinergic spinal cord synapses display subtle changes under excess AChE accumulation: Cytochemical staining for AChE activity, of axo-dendritic cholinergic synapses in the ventral horn of the spinal cord, revealed that synaptic areas occupied by electron dense AChE reaction products (Table I and Fig. 1) were 7-fold larger in transgenic as compared with control spinal cord sections, indicating synaptic accumulation of transgene-derived enzyme. Presynaptic areas occupied by vesicles were smaller in transgenic synapses than in control terminals, whereas vesicle density was higher in transgenic synapses as compared with controls (Table I). However, neither of these differences was statistically significant. Also, transgenic and control synapses exhibited generally similar axon diameters, pre-synaptic lengths and numbers of adjacent mitochondria (Table I and data not shown). Thus, increased synaptic AChE only changed morphometric parameters of cholinergic axo-dendritic synapses in a subtle manner.

Globular human AChE tetramers are found in muscle and spinal cord: Human ACHEmRNA is produced in spinal cord, but not muscle of adult ACHE transgenic mice (Andres et al., 1997). This finding corroborates previous analyses which demonstrated expression of the transgene, including 596 bp of the native human ACHE promoter, in the central nervous system but not in peripheral target organs (Beeri et al., 1995). To characterize the biochemical properties of transgenic AChE, we subjected detergent-soluble spinal cord and muscle extracts to sucrose density centrifugation. AChE activity in spinal cord extracts from transgenic animals, 255 nmol ATCh hydrolyzed/min/mg protein, was ca. 25% higher than that of control animals. This difference could be attributed to AChE of human origin. The transgenic enzyme was evenly distributed between the low salt-soluble and the detergent-soluble fractions (data not shown). No hAChEmRNA was found in muscle, and no significant increment was observed in total muscle AChE activities (33.4 ± 6.9 nmol/min/mg protein in 6 control animals, vs 35.9 ± 1.3 in 7 transgenics). However, 6% of total muscle AChE activity was contributed by the transgene as it reacted with human-specific antibodies (Fig. 2; Seidman et al., 1995).

Linear sucrose gradient centrifugation followed by measurement of AChE activities revealed that the detergent-soluble AChE in the spinal cord consisted mainly of globular tetramers (G_4), with minor fractions of monomers (G_1) and dimers (G_2). The G_4 enzyme peak in the spinal cord of transgenic mice, 18% of which was of human origin, was considerably higher than in controls (Fig. 2A,B). Unlike the spinal cord, detergent-soluble AChE in muscle extracts from control animals was composed of approximately equal parts of globular monomers and tetramers ($G_1 = G_4$), whereas the G_4:G_1 ratio was 2-fold higher in transgenics (Fig. 2C,D). This excess of AChE tetramers could reflect transport from spinal cord motoneurons. There were only negligible quantities of multimeric asymfmetric forms of AChE in the transgenic muscle: within

the high salt fraction, less than 5% of AChE activity sedimenting as A12 multimers were bound to AC101.1 antibodies. Whereas muscle is known to contribute the collagen-tailed synaptic AChE forms which are soluble in high salt solution (Massoulié et al., 1993), our present findings therefore suggest that a significant fraction of the detergent-soluble globular AChE tetramers in mammalian in a muscle may be of neuronal origin, similar to the situation in amphibia (Anglister, 1991). They further support the notion that exercise-induced increases in muscle G_4 AChE. may be mediated in part by motoneuron transcriptional response (Sveistrup et al., 1995).

Motor Endplates of transgenic animals undergo dramatic morphological changes: Diaphragm endplates from AChE transgenic mice were 60% larger, on average, than controls (Table II). Over half of transgenic but only 10% of control endplates were larger than 600 μm^2. This increase reflected general structural changes, as it was observed both with the non-specific dye methylene blue and followng cytochemical staining for active AChE (Table II). Moreover, 82% of 161 transgenic endplates failed to display the classical "pretzel" boundaries (Lyons and Slater, 1991) found in 82% of 172 control endplates (for 4 animals in each case). Rather, transgenic endplates acquired a simple elipsoid aspect (Andres et al., 1997). Also, muscle fiber diameters were 15% larger in transgenics compared to controls ($p< 0.005$, Student's t test) (Table II). Similar morphological changes were also found in hindleg quadriceps and anterior tibialis endplates (not shown).

Electron microscope analyses of diaphragm NMJs: Morphometric analyses revealed highly variable NMJ ultrastructure in transgenic animals. Similar to the tendency observed in spinal cord neurons, the density of pre-synaptic vesicles was significantly higher in transgenic as compared with control NMJs (Table II). Also, although the mean length of post-synaptic folds per μm synapse was identical between the two groups, the variability in this parameter was considerably higher in transgenics. Only 7 out of 16 analyzed NMJs in transgenic mice, as compared with 11 out of 14 NMJs in control mice, possessed average length post-synaptic folds (0.6 ± 0.05 μm/μm synapse length, Table II). Other transgenic NMJs displayed either of two pathological patterns, both reported in NMJs of aged humans (Wokke et al., 1990). One fourth of the NMJs in transgenic mice as compared with only 7% of analyzed control NMJs presented highly exaggerated, branched and densely packed post-synaptic folds, similar to those which occur in the Lambert-Eaton syndrome (Lambert and Elmqvist, 1971) (average of 0.87 ± 0.16 μm). Another third of transgenic NMJs, but only 14% of control NMJs possessed short, ablated post-synaptic folds (0.30 ± 0.07 μm) which resembled those of myasthenia gravis patients (Engel and Santa, 1971). The changes in NMJ morphology that we observed in hAChE-transgenic mice imply modulations in the input of cholinergic signals from motoneurons into muscle, the ultimate target of the motor system.

Discussion

Excess human AChE, capable of inducing late-onset cognitive and neuromotor deficiencies, accumulates in transgenic mice in both axo-dendritic spinal cord cholinergic synapses and NMJs. While the morphology of AChE-overexpressing spinal cord synapses remained largely unchanged, NMJs were drastically altered by the transgenic protein. The early appearance of nicotinic AChR and AChE clusters on the muscle surface during myogenesis, their aggregation at presumptive NMJ sites, and the acquisition of ACh sensitivity by muscles prior to NMJ formation suggests that cholinergic neurotransmission plays a role in NMJ biogenesis. The spontaneous release of ACh by outgrowing motoneurons as they encroach upon the muscle fibers (Grinell, 1995) and the observation that ACh may exert trophic effects on neurite outgrowth (Zheng et al., 1994) further strengthens the hypothesis that cholinergic signaling plays a formative role in the establishment and maintenance of neuromuscular connectivity. Our observations of delayed neuromotor pathology in AChE transgenic mice (Andres et al., 1997) suggest that developing NMJs may display a greater capacity to adjust to cholinergic imbalances than the mature adult function.

Spinal cord cholinergic synapses appear resistant to hAChE overexpression: Spinal cord AChE activities in the transgenic mice were increased by 25% over control activities. However, cytochemical staining of axo-dendritic cholinergic synapses in the transgenic spinal cord revealed up to 7-fold higher AChE activities as compared to control synapses. This is close to the excess observed in NMJs of transiently transgenic *Xenopus* tadpoles which express the same ACHE transgene (Ben Aziz et al., 1993, Shapira et al., 1994, Seidman et al., 1995), suggesting an upper limit for AChE excess which is compatible with development of synaptic infrastructure. Interestingly, characteristic morphometric parameters of spinal cord synapses such as axon diameter, pre-synaptic length, total vesicle number and mitochondria density remained largely unchanged, by excess AChE. Although the space occupied by pre-synaptic vesicles was slightly reduced and vesicle density reciprocally increased, neither of these changes was statistically significant. This indicates that unlike disruption of β2-laminin (Noakes et al., 1995), altered AChE levels did not prevent pre-synaptic release. Moreover, the difference between the changes observed in spinal cord synapses and NMJs demonstrated that the latter are much more sensitive to the long-term effects of AChE excess than spinal cord synapses.

Transgenic model to neuromotor deterioration: Several late-onset amyotrophic diseases are associated with disturbed cholinergic transmission and progressive neuromotor deterioration in the adult. For example, the Lambert-Eaton syndrome is associated with malfunctioning presynaptic calcium channels (Lambert and Elmqvist, 1971) and suppressed ACh release; whereas myasthenia gravis involves autoimmune suppression of muscle nicotinic AChRs (Engel and Santa,

1971), and amyotrophic lateral sclerosis results from motoneuron death (Robert and Brown, 1995). While each of these syndromes can be traced to a single molecular origin, their long term outcomes clearly reflect accumulated damage due to secondary and tertiary changes in additional nerve and/or muscle components. Our present findings demonstrate that AChE excess *per se* may induce neuromotor deficiencies associated with NMJ malformation, without changing the structure of spinal synapses.

Theoretical calculations based on synaptic configurations of adult frog and lizard NMJs (Anglister et al., 1994) predicted that increasing synaptic AChE concentration by up to 2-fold should carry minimal consequences for miniature endplate potentials. However, long-term effects of excess AChE, insufficient feedback responses to the excessive ACh hydrolysis or non-catalytic activities of AChE (Sternfeld et al., 1997) were not considered in that model. The clearly abnormal phenotypes which we observe are associated with considerably larger AChE excesses in the synaptic microenvironment. Thus, our findings demonstrate that a moderate increase in the motoneuron expression of AChE is sufficient to alter not only NMJ modes of development, but also carries implications for its long-term function and structure. The increased vesicle density in NMJs of adult transgenic mice may reflect enhanced pre-synaptic release, which aleviates some of the AChE overexpression. That this adjustment is insufficient, is clear from the progressive muscle deterioration which occurs in these mice.

Mouse and *Xenopus* NMJs respond similarly to transgenic hAChE expression: Transgenic mice displayed generally normal motor behavior so long as no special muscle efforts were required of them (Andres et al., 1997). This suggests that basal level NMJ function was sustained, unlike what was observed when β2-laminin was changed (Hall and Sanes, 1993). Nevertheless, transgenic spinal cord AChE promoted muscle deterioration in adult animals, even though this transgene was not expressed in muscle. The reported lack of AChE in the basal lamina of malfunctioning agrin knock-out mice (Gautam et al., 1996) suggests that the post-synaptic accumulation of AChE occurs secondarily to AChR clustering, which is subject to motoneuron control. Considering the fact that NMJs represent less than 0.1% of the muscle surface (Hall and Sanes, 1993), the 6% muscle enzyme of human origin reflects a significant accumulation of the motoneuron-derived transgenic enzyme in the synaptic microenvironment. Yet, neuromotor deterioration occurred only after the cessation of neuronal transcriptional changes (Andres et al., 1997). This suggests that these changes alternated, in early development, the transgene-induced cholinergic imbalance.

In both mouse and *Xenopus* NMJs, hAChE overexpression increased the size of transgenic NMJs in a manner dependent on pre-synaptic expression of the human transgene (Shapira et al., 1994 and the present report). That hAChE-expressing NMJ areas were enlarged to the same

extent in these two evolutionarily distant species supports the hypothesis that AChE functions as a morphogenic factor in vertebrate NMJs, and may reflect a limit of the degree to which viable NMJs may be enlarged. Exaggeration of post-synaptic folds also occurs in the Lambert-Eaton syndrome (Lambert and Elmqvist, 1971), where the functioning of pre-synaptic Ca^{++} channels is impaired and hence ACh secretion and post-synaptic receptor activation are decreased. Enhanced ACh hydrolysis due to excess AChE production likely decreases activation of ACh receptors in at least some of the nerve terminals of our transgenic mice. The yet more severe phenotype of degenerated post-synaptic folds appears in NMJs of myasthenia gravis patients, where post-synaptic ACh receptors deteriorate due to autoantibodies (Engel and Santa, 1971). It therefore appears that both phenotypes reflect primarily changes in the synaptic activity of ACh in our mice.

AChE overexpression may gradually change NMJ properties: Unlike brain synapses, NMJs are not protected from the environment by the blood-brain barrier. Therefore, these special synapses are frequently subject to insults by various endogenous and exogenous toxic compounds such as drugs (i.e. succinylcholine), poisons (i.e. agricultural insecticides) and constituents of the circulation (i.e. antibodies) that impair their cholinergic balance (see Schwarz et al., 1995 for a recent review). Increases in ACh release were recently reported in bungarotoxin-treated rats, which developed myasthenia gravis symptoms (Plomp et al., 1995). One possible explanation for that could involve enhanced choline acetyl transferase (ChAT) production, which operates as a primary feedback mechanism also under the cholinergic hypofunction in embryonic AChE transgenic mice (Andres et al., 1997). However, the capacity for this compensation in the transgenic mice declines with age. In the absence of excess ChAT, overexpressed AChE would reduce ACh levels in the synaptic cleft of transgenic NMJs and limit the activation of post-synaptic receptors. The outcome would parallel the Lambert-Eaton syndrome, with limited ACh release due to malfunctioning pre-synaptic Ca^{++} channels. This postulates the appearance of seemingly functional NMJs with increased density of pre-synaptic vesicles and prolonged, exaggerated and over-branched post-synaptic folds. Yet more drastic reductions in ACh levels may inactivate post-synaptic ACh receptors, parallel to the autoimmune blockade of such receptors in myasthenia gravis. This may explain our finding of degenerate NMJs, with characteristically small post-synaptic folds and diffuse ablated structures. Finally, muscle fiber denervation should elicit reinnervation, motor unit enlargement and NMJs loss, all of which were seen in ACHE transgenic mice (Andres et al., 1997). We have no way of concluding whether a single synapse can first acquire one of these structural phenotypes, then the second and finally disappear altogether. However, the progressive worsening of muscle functioning in these mice suggests that this may be the case.

Non-catalytic properties of AChE may affect NMJ abnormalities:

Accumulating evidence suggests non-catalytic activities for AChE, especially in cell-cell interactions (Layer et al., 1995, Small et al., 1995, Sternfeld et al., 1997). It is conceivable that such properties, apart from the cholinergic imbalance induced by AChE overexpression, may affect specific synapses in different manners. Additional animal models (for example, mice expressing genetically inactivated AChE) will be needed to explore this possibility.

Acknowledgements

We thank Dr. B. Norgaard-Pedersen (Copenhagen) for antibodies and Dr. D. Glick (Jerusalem) for critically reviewing this manuscript. This work was supported by USARMRDC grant 17-97-1-7007 and Ester/Medica Neurosciences (Tel Aviv and Boston). C. A. was a recipient of an INSERM (France)-NCRD exchange fellowship with the Israel Ministry of Science and Arts.

References

Aigner L., Arber, S., Kapfhammer, J.P., Laux, C.S., Botteri, F., Brenner, H-R, and Caroni, P. (1995) - Overexpression of the neural growth-associated protein GAP-43 induces nerve sprouting in the adult nervous system of transgenic mice. *Cell* **83**:269-278.

Andres, C., Beeri, R., Friedman, A., Lev-Lehman, E., Henis, S., Timber, R., Shani, M. and Soreq, H. (1997). ACHE transgenic mice display embryonic modulations in spinal cord CHAT and neurexin Iβ gene expression followed by late-onset neuromotor deterioration. *Proc. Natl. Acad. Sci.* USA, **94**, in press.

Anglister, L. (1991) - Acetylcholinesterase from the motor terminal accumulates in the synaptic basal lamina of the myofiber. *Cell Biol.* **115**: 755-764.

Anglister, L., Stiles J.R. and Salpeter M.M. (1994) - Acetylcholinesterase density and turnover number at frog neuromuscular junctions, with modeling of their role in synaptic function. *Neuron* **12**:783-794.

Ben-Aziz-Aloya, R., Seidman, S., Timberg, R., Sternfeld, M., Zakut, H. and Soreq, H. (1993) - Expression of a human acetylcholinesterase promoter-reporter construct in developing neuromuscular junctions of *Xenopus* embryos. *Proc. Natl. Acad. Sci.* USA **90**:2471-2475.

Beeri, R., Andres, C., Lev-Lehman, E., Timberg, R., Huberman, T., Shani, M. and Soreq, H. (1995) - Transgenic expression of human acetylcholinesterase induces progressive cognitive deterioration in mice. *Curr. Biol.* **5**:1063-1071.

Beeri, R., LeNovere, N., Mervis, R., Huberman, T., Grauer, E., Changeux, J.P. and Soreq, H. (1997). Enhanced hemicholinium binding and attenuated dendrite branching in cognitively impaired ACHE-transgenic mice. Submitted.

Bradford, M.M. (1976) - A rapid and sensitive method for the quantitation of microgram quantities of proteins utilizing the principle of protein dye binding. *Anal Biochem* **72**:248-254.

Burns, M.E. and Augustine, G.J. (1995) - Synaptic structure and function: Dynamic organization yields architectural precision. *Cell* **83**:187-194.

Carbonetto, S. and Lindenbaum, M. (1995) - The basement membrane at the neuromuscular junction: a synaptic mediatrix. *Curr. Opin. Neurobiol.* **5**:596-605.

Carraway, K.L. and Burden, S.J. (1995) - Neuregulins and their receptors. *Curr. Opin. Neurobiol.* **5**:606-612.

Coyle, J.T., Price, D.L. and DeLong, M.R. (1983) - Alzheimer's disease: a disorder of cortical cholinergic innervation. *Science* **219**:1186-1189.

Crawford, T.O. and Pardo, C.A. (1996) - The neurobiology of childhood spinal muscular atrophy. *Neurobiol. of Disease* **3**, 97-110.

Dechiarra, T.M., Bowen, D.C., Valenzuela, D.M., Simmons, M.V., Poueymirou, W.T., Thomas, S., Kinetz, E., Compton, D.L., Rojas, E., Park, J.S., Smith, C., DiStefano, P.S., Glass, D.J., Burden, S.J. and Yancopoulos, G.D. (1996) - The receptor tyrosine kinase MuSK is required for neuromuscular junction formation *in vivo*. *Cell* **85**:501-512.

Ellman, G.L., Courtney, D., Andres V. Jr. and Featherstone RM (1961) - A new and rapid colorimetric determination of acetylcholinestease activity. *Biochem. Pharmacol.* **7**:88-95.

Engel, A. G. and Santa, T. (1971) - Histometric analysis of the ultrastructure of the neuromuscular junction in myasthenia gravis and in the myasthenic syndrome. Ann. N. Y. *Acad. Sci.*, **183**:46-63.

Gautam, M., Noakes, P.G., Mudd J., Nichol, M., Chu, G.C., Sanes, J.R. and Merlie (1995) - Failure of post-synaptic specialization to develop at neuromuscular junctions of rapsyn-deficient mice. *Nature* **377**:232-236.

Gautam, M., Noakes, P.G., Moscoso, L., Rupp, F., Scheller, R.H., Merlie, J.P. and Sanes, J.R. (1996) Defective neuromuscular synaptogenesis in agrin-deficient mice. *Cell* **85:** 525-535.

Glass, D.J., Bowen, D.C., Stitt, T.N., Radziejewski, C., Bruno, J., Ryan, T.E., Gies, D.R., Shah, S., Mattsson, K., Burden, S.J., DiStefano, P.S., Valenzuela, D.M., DeChiara, T.M. and Yancopoulos, G.D. (1996) - Agrin acts via a MuSK receptor complex. *Cell* **85:**513-523.

Grinnell, A.D. (1995) Dynamics of nerve-muscle interaction in developing and mature neuromuscular junctions. *Physiol. Rev.* **75**, 789-819.

Hall, Z.W. and Sanes, J.R. (1993) - Synaptic structure and development: the neuromuscular junction. *Cell* **10**:99-121.

Jo, S.A., Zhu, X., Marchionni, M.A. and Burden, S.J. (1995) - Neuregulins are concentrated at nerve-muscle synapses and activate ACh-receptor gene expression. *Nature* **373**:158-161.

Lambert, E.H. and Elmqvist, D. (1971) - Quantal components of end plate potentials in the myasthenic syndrome. Ann. N.Y. *Acad. Sci.* 183-199.

Liao, J., Mortensen, V., Norgaard-Pedersen, B., Koch, C. and Brodbeck, U. (1992) - Monoclonal antibodies against brain acetylcholinesterase which recognize the subunit bearing the hydrophobic anchor. *Eur. J. Biochem.* 215:*333-340.*

Lyons, P.R. and Slater, C.R. (1991) - Structure and function of the neuromuscular junction in young and adult mdx mice. *J. Neurocytol* **20:**969-981.

Massoulié, J., Pezzementi, L., Bon, S., Krejci, E. and Vallette, F.M. (1993) - Molecular and cellular biology of cholinesterases. *Prog. Neurobiol.* **41**:31-91.

Masu, Y., Wolf, E., Holtmann, B. Sendtner, M., Gottfried, B. and Thoenen, H. (1993) - Disruption of the CNTF gene results in motor neuron degeneration. *Nature* **365**:27-32.

Noakes, P. G., Gautam, M., Mudd, J., Sanes, J. R. and Merlie, J. P. (1995) - Aberrant differentiation of neuromuscular junctions in mice lacking S-laminin/laminin β2. *Nature* **374**: 258-262.

Plomp, J.J., Van-Kempen, G.T., De-Baets, M.B. Graus, Y.M., Kuks, J.B. and Molenaar, P.C. (1995) - Acetylcholine release in myasthenia gravis: regulation at single end-plate level. *Ann-Neurol* **37**:627-36.

Robert, H. and Brown, G. Jr. (1995) - Amyotrophic lateral sclerosis: recent insight from genetics and transgenic mice. *Cell* **80**:687-692.

Schwarz, M., Loewenstein-Lichtenstein, Y., Glick, D., Liao, J., Norgaard-Pedersen, B. and Soreq, H. (1995) - Successive organophosphate inhibition and oxime reactivation reveals distinct responses of recombinant human cholinesterase variants. *Molec. Brain Res.* **31:** 101-110.

Seidman, S., Sternfeld, M., Ben Aziz-Aloya, R., Timberg, R., Kaufer-Nachum, D. and Soreq, H. (1995) - Synaptic and epidermal accumulations of human acetylcholinesterase are encoded by alternative 3'-terminal exons. *Mol Cell Biol.* **14**: 459-473.

Shapira, M., Seidman, S., Sternfeld, M., Timberg, R., Kaufer, D., Patrick, J. and Soreq, H. (1994) - Transgenic engineering of neuromuscular junctions in *Xenopus laevis* embryos transiently overexpressing key cholinergic proteins. *Proc. Natl. Acad. Sci.* USA **91**:9072-9076.

Sternfeld, Meira, Ming, Guo-li, Song, Hong-jun, Sela, Keren, Soreq, Hermona and Poo, Mu-ming (1997). Acetylcholinesterase exerts a C-terminus specific, non-catalytic nerve growth promoting activity.

Sveistrup, H., Chan, R.Y., Jasmin, B.J., (1995) - Chronic enhancement of neuromuscular activity increases acetylcholinesterase gene expression in skeletal muscle. *Am. J. Physiol.* **269**:856-862.

Wokke, L.H.J., Jennekens, F.G.I., van den Oord, C.J.M., Veldman, H., Smith, L.M.E. and Leppink, G.J. (1990) - Morphological changes in the human end plate with age. *J. Neurol. Sci.* **95**:291-310.

Zheng, J. Q., Felder, M., Connor, J. A. and Poo, M-m. (1994) - Turning of nerve growth cones induced by neurotransmitters. *Nature* **368**: 140-144.

Tables and Figures

Table 1: Morphometric parameters of hAChE-expressing spinal cord synapses

Morphometric parameters were derived from photographs taken using light or electron microscopy as detailed under Experimental Procedures for the numbers of axo-dendritic cholinergic synapses from the anterior spinal cord of at least 5 adult control and transgenic mice. Statistical significance (Student's t test) is noted wherever relevant.

Table 2: Morphometric parameters of hAChE-expressing neuromuscular junctions

Morphometric parameters were determined as detailed in Table I for the numbers noted of NMJs, analysed folds or muscle fibers from the diaphragm muscle of control and transgenic mice.

Figure 1: AChE overexpression in axo-dendritic synapses from anterior spinal cord of transgenic mice. Electron micrographs of three representative synapses from transgenic and control (C) mice are presented. Acetylthiocholine hydrolysis products representing sites of AChE accumulation appear as dark crystals, (add arrowheads) particularly conspicuous in the synaptic cleft between axons (A) and dendrites (D). Size bar equals 1 μm.

Figure 2: Transgenic human AChE is found in spinal cord and muscle homogenates. Detergent-soluble homogenates of spinal cord and muscle were fractionated by sucrose gradient centrifugation and AChE activity determined in each fraction prior to (line) or after binding to a specific anti-human AChE monoclonal antibody (shaded area) (Seidman et al., 1995). Note the different activity scales for spinal cord (left) and muscle (right hand side). Arrows denote sedimentation of an internal marker, bovine catalase (11.4 S). Activity peaks reflecting globular monomers, dimers and tetramers are labeled G1, G2 and G4, respectively. Fractions drawn from the top of each tube represented by fraction No. 1.

TABLE I: Morphometric parameters of hAChE-expressing anterior spinal cord axo-dendritic synapses

Parameter	Control	Transgenic	
AChE stained area, μm^2	0.05 ± 0.04 (43)	0.34 ± 0.90 (47)	P<0.03
area occupied by vesicles, μm^2	0.47 ± 0.3 (37)	0.39 ± 0.29 (44)	n.s.
No. of vesicles/μ^2	95.8 ± 33.9 (16)	107.9 ± 27.9 (16)	n.s.
axon minimal diameter, μm	0.93 ± 0.34 (40)	0.74 ± 0.28 (44)	n.s.
axonic mitochondria area, μm^2	0.23 ± 0.13 (37)	0.19 ± 0.1 (31)	n.s
dendrite minimal diameter, μm	2.44 ± 2.3 (20)	1.61 ± 0.9 (15)	n.s.
dendritic mitochondria area, μm	0.52 ± 0.52 (19)	0.35 ± 0.21 (13)	n.s.

TABLE II: Morphometric parameters of hAChE-expressing cholinergic synapses expressing neuromuscular junctions

Parameter	Control	Transgenic	
AChE stained area, μm^2	398 ± 136.4 (90)	625.6 ± 227.7 100)	P<0.001
Methylene blue stained area, μm^2	301 ± 92.1 (38)	723.7 ± 495.3 (33)	P< 0.001
Mean length of post-synaptic folds/μm NMJ	0.56 ± 0.12 (14)	0.65 ± 0.37 (16)	n.s.
No. of vesicles/μm^2	122.5 ± 30.7 (12)	161.4 ± 41.8 (9)	P< 0.02
Muscle fiber diameter, μm	30.8 ± 7.45 (69)	35.6 ± 5.17 (7.5)	n.s.

c\soreq\group\andres\docs\tabl0905

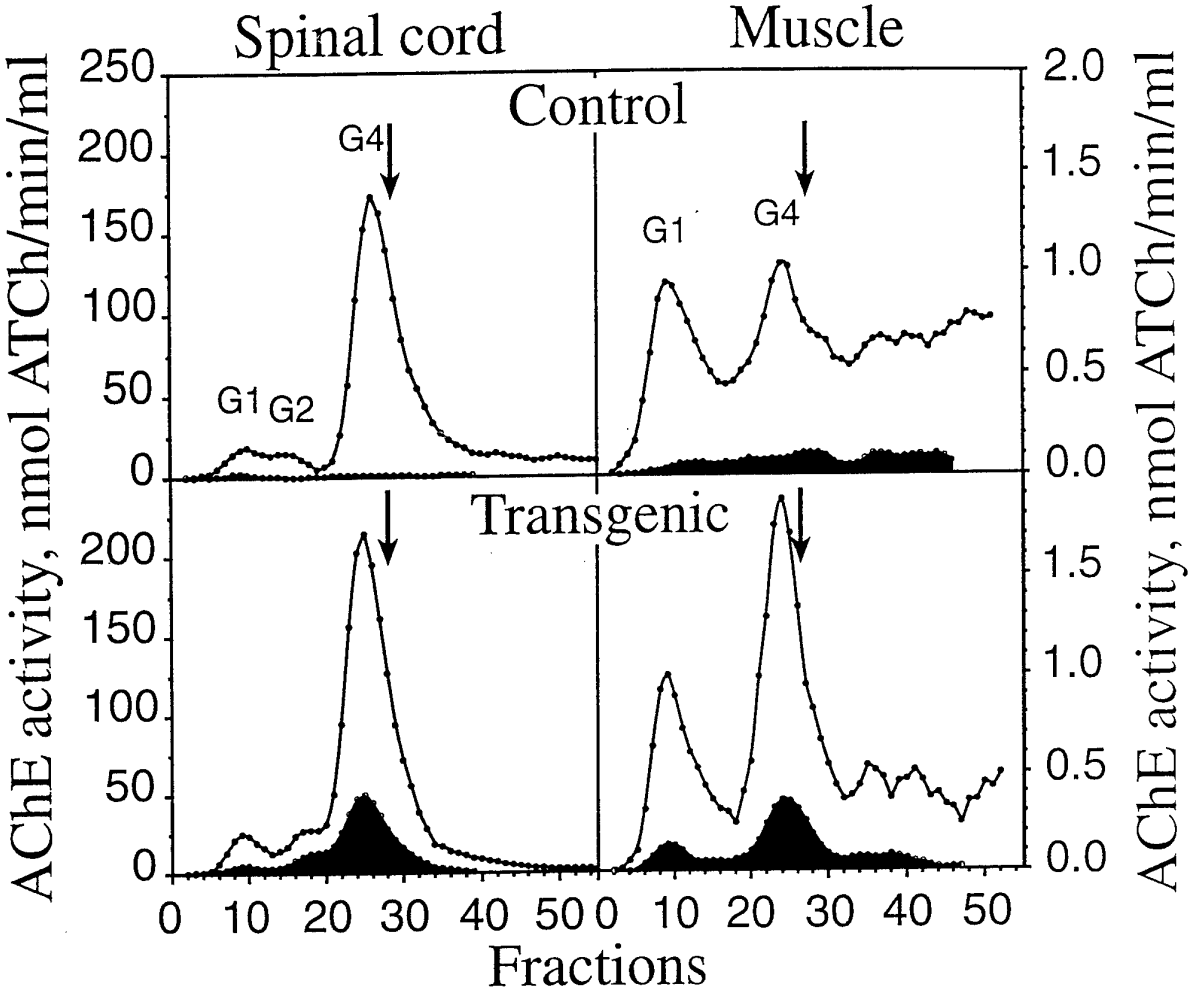
Spinal cord
Muscle
Control
Transgenic
G1
G2
G4
G1
G4
AChE activity, nmol ATCh/min/ml
AChE activity, nmol ATCh/min/ml
Fractions
0
50
100
150
200
250
0.0
0.5
1.0
1.5
2.0
0 10 20 30 40 50

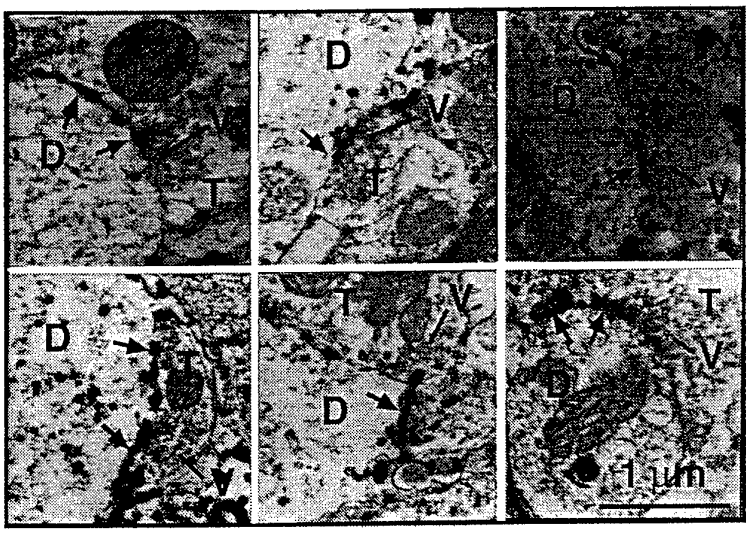

control

transgenic

[redacted]al of Neurochemistry
Lippincott-Raven Publishers, Philadelphia

Enhanced Hemicholinium Binding and Attenuated Dendrite Branching in Cognitively Impaired Acetylcholinesterase-Transgenic Mice

R. Beeri, *N. Le Novère, †R. Mervis, T. Huberman, ‡E. Grauer, *J. P. Changeux, and H. Soreq

*Department of Biological Chemistry, Life Sciences Institute, Hebrew University of Jerusalem, Jerusalem; ‡Department of Pharmacology, Israel Institute for Biological Research, Ness-Ziona, Israel; *Molecular Neurobiology Laboratory, Biotechnologies Department, Pasteur Institute, Paris, France; and †Neuro-Cognitive Research Laboratories, Columbus, Ohio, U.S.A.*

Abstract: In a search for behavioral, neuroanatomical, and metabolic characteristics of Alzheimer's disease that may result from cholinergic malfunction, we used transgenic mice overexpressing acetylcholinesterase (AChE) mRNA and active enzyme in brain neurons. Mapping by in situ hybridization revealed that transgenic and host AChE mRNAs were distributed similarly. In a Morris water maze working memory paradigm, adult transgenic mice did not display the characteristic improvement found in control mice either between or within test days and spent less time than control mice in the platform zone. In 5-week-old transgenic mice, the basilar dendritic trees of layer 5 pyramidal neurons from the frontoparietal cortex were essentially as developed as in age-matched controls. However, branching totally ceased after this age, whereas in control adults it continued up to at least 7 months. Therefore, dendritic arbors became smaller in adult transgenic mice than those of controls. Furthermore, the average number of spines was significantly lower on dendritic branches of 7-month-old but not 5-week-old transgenics as compared with controls. Binding of tritiated hemicholinium-3, a blocker of the high-affinity choline uptake characteristic of active cholinergic terminals, was over twofold enhanced in the brain of transgenic mice. In contrast, no differences were observed in the mRNA and ligand binding levels of several different subtypes of nicotinic and muscarinic acetylcholine receptors. These findings suggest that three different hallmarks associated with Alzheimer's disease—namely, progressive cognitive failure, cessation of dendrite branching and spine formation, and enhanced high-affinity choline uptake—are outcomes of cholinergic malfunction. **Key Words:** Acetylcholinesterase—Alzheimer's disease—Choline uptake—Dendritic fields—Spines—Memory deficit.
J. Neurochem. **69,** 2441–2451 (1997).

Animal models for studying late-onset disorders associated with cholinergic deterioration and most notably Alzheimer's disease (AD) should display progressive deterioration of memory and learning, as well as senile plaques and neurofibrillary tangles (Price et al., 1995), a hypofunctional cholinergic system (Bierer et al., 1995), and breakdown in cortical circuitry related to cell and synaptic loss (Davies and Maloney, 1976; DeKosky and Scheff, 1990; Honer et al., 1992; Terry et al., 1992). Aged, cognitively impaired animal models displayed the expected behavioral, neuroanatomical, and/or neurochemical changes in their cholinergic system (Bartus and Uemura, 1979). Several physical or pharmacological modulations also resulted in loss of cholinergic synapses and impaired memory (Fischer et al., 1989; Zhi et al., 1995). Subsequently transgenic amyloid precursor protein mouse models (Games et al., 1995; Hsiao et al., 1995, 1996; LaFerla et al., 1995; Moran et al., 1995) demonstrated development of amyloid β protein deposits, neuritic plaques, synaptic loss, and late-onset spatial memory deficits. However, in AD, amyloid plaques and tangles are particularly concentrated in brain regions where cholinergic circuits operate (Coyle et al., 1983). Also, synaptic loss but not the presence of amyloid plaques or neurofibrillary tangles could be convincingly correlated with cognitive impairment in AD (Terry et al., 1992). Yet, correlation between high levels of β-amyloid deposits and progressive severity of the cognitive defect was only shown in some of the above transgenic models (Hsiao et al., 1996). Therefore, it remained unresolved

Received April 23, 1997; revised manuscript received June 19, 1997; accepted July 9, 1997.

Address correspondence and reprint requests to Dr. H. Soreq at Department of Biological Chemistry, Life Sciences Institute, Hebrew University of Jerusalem, Jerusalem 91904, Israel.

Abbreviations used: ACh, acetylcholine; AChE, acetylcholinesterase; AChR, acetylcholine receptor; AD, Alzheimer's disease; ChAT, choline acetyltransferase; MGV, mean gray value; OD, optical density; RT-PCR, reverse transcription-polymerase chain reaction.

whether the learning deficits in these mice were caused by or only correlated with increased brain amyloid β peptide levels and amyloid depositions.

In AD, structural changes in brain cholinergic synapses (DeKosky and Scheff, 1990) are associated with loss of neuronal nicotinic binding sites (Nordberg et al., 1988), with death of acetylcholine (ACh)-producing neurons (Davies and Maloney, 1976; Whitehouse et al., 1986), and with the consequent disruption of cholinergic neurotransmission (Coyle et al., 1983; Fibiger, 1991). The resultant hypocholinergic condition is characterized by a relative excess of the ACh-hydrolyzing enzyme acetylcholinesterase (AChE). To define the contribution of cholinergic malfunction toward the AD phenotype, we have recently used the authentic promoter from the human ACHE gene in conjunction with the AChE-coding sequence to create transgenic mice expressing human AChE in CNS neurons. Manual use of the Morris water maze revealed a progressively severe decline in the spatial learning and memory capabilities of these transgenic mice (Beeri et al., 1995). It was therefore of interest to dissect carefully the learning and memory impairments in AChE-transgenic mice and examine in them which of the morphometric and/or biochemical correlates of AD can be causally associated with cholinergic malfunction.

Cortical neurons in normal aged humans may develop longer and more branched dendritic trees than those in either young adults or individuals with senile dementia (Buell and Coleman, 1981). Cognitive deficiencies are further associated with dysgenesis of dendritic spines, on which most cortical synapses reside (Purpura, 1974; Braak and Braak, 1985). We therefore wished to evaluate the state of dendrite arborizations and spine density in adult transgenic mice with excess brain AChE. Also, we explored the transport of choline, which is used by cholinergic neurons, both for reforming metabolized membrane phosphatidylcholine and for synthesizing the neurotransmitter ACh. The levels of the high-affinity Na^+-dependent choline transporter unique to these cells can be quantified using [^{3}H]hemicholinium-3 (Vickroy et al., 1984). The concentration of available choline is the rate-limiting factor for ACh synthesis: When choline is in short supply, active cholinergic neurons were reported to sustain neurotransmission at the expense of membrane building (Wurtman, 1992). Indeed, cerebral cortical areas in AD brains exhibited marked decreases in choline acetyltransferase (ChAT) activity and significant enhancement in [^{3}H]hemicholinium-3 binding. In the AD frontal cortex, transporter overexpression exceeded the level that is needed to compensate for the loss of synaptic terminals, presumably accelerating membrane turnover and neurodegeneration (Slotkin et al., 1994).

In the search for behavioral, morphological, and molecular correlates common to AD and the AChE-transgenic mice we used video imaging to assess carefully the memory impairment in these mice. We further examined in them the dendritic branching and spine density in cortical neurons, the mRNA and protein levels of ACh receptors (AChRs), and the levels of [^{3}H]hemicholinium-3 binding. Our findings demonstrate complex cognitive failure, attenuated dendrite branching, decreased spine density, and imbalanced choline metabolism in AChE-transgenic mice, with all of these phenomena being attributed to AChE excess and the associated cholinergic malfunction.

MATERIALS AND METHODS

Mice

FVB/N mice carrying human AChE cDNA under the control of 586 bp of the authentic human AChE promoter were constructed and identified as described (Beeri et al., 1995; Andres et al., 1997). Age- and sex-matched wild-type FVB/N mice served as controls.

In situ hybridizations

For radioactive in situ hybridization, cryostat-cut brain sections were hybridized with 45-mer oligodeoxynucleotides end-labeled with [α-^{33}P]dATP (Boehringer-Mannheim, Germany), according to the manufacturer's recommendations. Prehybridization, hybridization, and washings were as described elsewhere (Le Novère et al., 1996). The probes used were targeted toward rat nicotinic AChR subunits α3, 4, 5, and 7 and β2, 3, and 4. Discriminative probes of AChE were as follows: human ACHE, 5′-GACACCAG-CACAGTCCTGTCGGCCTGTACCAAGAAGCGGCCA-TCG-3′; mouse ACHE, 5′-GATACCAACACAGCTCCC-TCAACCTGGGCCAGGAAACGGCCGTCA-3′. Genbank accession numbers for the sequences targeted by these probes are L31621, M15681, J05231, M85273, L31622, J04636, J05232, M55040, and X56518, respectively. These sequences can be electronically retrieved at Le Novère and Changeux (1995).

High-resolution nonradioactive in situ hybridization with 2-*O*-methyl biotinylated mouse AChE cRNA (exon 6), streptavidin–alkaline phosphatase conjugate, and fast red substrate was performed on 5-μm-thick paraffin brain sections as detailed elsewhere (Andres et al., 1997). Three sections from different brain levels of three individual mice (control and transgenic) were used.

Morris water maze test

Mice were tested in a circular black pool, 140 cm in diameter and 50 cm high, filled to the height of 24 cm with water (at ~23°C). The pool was divided by imaginary lines into four quadrants of equal size and three concentric zones. A black painted platform was placed in the center of a quadrant (in the middle zone) of the pool with its top surface (12 × 12 cm) located <1 cm below water level. The pool was placed in the center of a well-lit room with ample cues that were kept constant throughout the testing period. The performance of the mice was monitored by a video tracking system (HVS IMAGE; Ormond Crescent, Hampton, U.K.), thus enabling detailed analysis of the swimming pattern.

Path length, latency to reach the platform, and swimming speed were simultaneously recorded, as well as the percentage of time spent in each quadrant and zone. Mice were tested in two successive trials (2 h apart) per day. Each trial began by placing the mouse on the platform for 30 s, after

which it was placed in the water in the appropriate location and allowed to swim and find the platform for a maximum of 2 min. Within each pair of daily trials, the platform location and the starting point were the same, but both locations were changed each day. Improvement within each pair of trials was indicative of intact working memory, whereas improvement over days was indicative of intact reference memory (Morris, 1984). Data were statistically analyzed by a three-way ANOVA (groups × days × trials, with repeated measures on the last two factors) performed separately on each of the recorded parameters. *F* test for simple effects was used for post hoc analysis.

Golgi staining, Sholl analysis, and spine detection

Brain sections after fixation with 10% formalin in phosphate-buffered saline were stained with the rapid Golgi technique as detailed elsewhere (Valverde, 1976). Sholl analysis quantifies the number of intersections of the dendritic branches at 10-μm intervals with a series of enlarging circles with the origin placed at the center of the soma in each neuron (Sholl, 1953). All visible flanking denditic spines were counted along the basilar branches of the layer V pyramids, using a Zeiss Axio plan microscope with a 63× long-working distance objective, a 2.0 intermediate Optivar magnifier lens, and a 10× eyepiece (final magnification, ×1,260).

Reverse transcription-polymerase chain reaction (RT-PCR)

Brains were removed from homozygous transgenic mice and control mice after cervical dislocation. RNA extraction and semiquantitative RT-PCR amplifications were performed as detailed elsewhere (Andres et al., 1997) with 65°C as the annealing temperature. PCR primers were designed at nucleotides 375 (+) and 1,160 (−) of the mouse AChE gene, 83 (+) and 646 (−) of the mouse ChAT gene, 212 (+) and 660 (−) of the rat synaptophysin gene, 371 (+) and 840 (−) of the human cardiac L-type calcium channel α1 subunit gene, 130 (+) and 519 (−) of the mouse M1 muscarinic AChR gene, and 181 (+) and 600 (−) of the rat neuronal nicotinic AChR α4 subunit gene. Genbank accession numbers for these are X56518, D12487, X06177, L29536, and M15681, respectively. Resultant PCR products obtained from similar amounts of RNA were removed at intervals of three PCR cycles and electrophoresed on agarose gels.

Ligand binding experiments

Binding experiments were performed in triplicate fresh 14-μm-thick cryostat-cut brain sections on gelatin-coated slides from five brain levels and two to four individual brains from each age group.

Muscarinic agonists. Sections were preincubated for 15 min in 120 m*M* NaCl, 1.2 m*M* KH_2PO_4, 5.6 m*M* glucose, 25 m*M* $NaHCO_3$, 2.5 m*M* $CaCl_2$, and 4.7 m*M* KCl, pH 7.4. Incubation was for 60 min at room temperature in the same buffer, in the presence of 10 n*M* [*N-methyl*-^{3}H]pirenzepine (NEN) for M1 receptors or [2,3-*dipropylamino*-^{3}H]AF-DX 384 (NEN) for M2 receptors. Sections were washed three times for 4 min each at 4°C with 50 m*M* Tris-HCl (pH 7.4) and were exposed for 2 weeks to tritium-sensitive Hyperfilm (Amersham, U.K.).

Nicotinic agonists. α-Bungarotoxin: Sections were incubated for 30 min at room temperature in 50 m*M* Tris-HCl and 1 mg/ml bovine serum albumin and 120 min in the presence of 1.4 n*M* [^{125}I-Tyr^{54}]α-bungarotoxin (NEN). Washing was six times for 30 min at 4°C with 50 m*M* Tris, pH 7.4. Exposure was for 2 days. Nicotine: Sections were incubated for 30 min at room temperature in 50 m*M* Tris (pH 7.4), 8 m*M* $CaCl_2$, and 4 n*M* [^{3}H]nicotine (Amersham, U.K.), followed by two washes of 2 min in ice-cold 50 m*M* Tris and one brief wash with ice-cold water and exposure for 60 days. Cytisine: Sections were incubated for 30 min at room temperature in 50 m*M* Tris (pH 7.4) and 2 n*M* [^{3}H]cytisine (NEN). Washes and exposure were as for nicotine. Epibatidine: Sections were incubated for 30 min at room temperature in 50 m*M* Tris (pH 7.4) and 0.2 n*M* [^{3}H]epibatidine (NEN). Washes and exposure were as for nicotine. Hemicholinium: Sections were incubated for 60 min in 33 m*M* NaCl and 50 m*M* Tris-HCl in the presence of 15 n*M* [*methyl*-^{3}H]hemicholinium-3 diacetate salt (NET-884; Du Pont NEN) at 4°C, followed by six washes of 1 min each with 50 m*M* Tris buffer at 4°C and exposure for 2 weeks.

Binding was quantified with Densitometria, a package of image analysis developed by one of us (N.L.N.), with a high-resolution Hammamatsu CCD camera and an Imaging Technology acquisition card. For each animal, several images from the same area were digitalized. On each section the mean gray value (MGV) of the structures and of the corpus callosum (taken as the background) were recorded. Optical density (OD) was computed for each value as $OD = \ln (MGV_{background}/MGV_{total})$.

RESULTS

Transgenic AChE accumulates in perikarya and processes of neostriatal cholinergic neurons

Neurons from different regions in brain sections from FVB/N transgenic mice carrying the human ACHE gene (Beeri et al., 1995) and control sex- and age-matched nontransgenic FVB/N mice were analyzed for AChE mRNA and enzyme activity. Radioactive in situ hybridization using a human-specific oligodeoxynucleotide probe and a matching mouse-specific probe (Fig. 1) revealed expression of the transgene in the same brain regions where endogenous murine AChE mRNA is expressed. This corresponded to the maps derived for AChE mRNA distribution in rat brain (Hammond et al., 1994). High-resolution in situ hybridization was performed with a 2-*O*-methylated, 5′-biotinylated AChE cRNA probe and subsequent decoration by streptavidin–alkaline phosphatase conjugates and corresponding enzyme staining (Fig. 2A–D). Intensified labeling was observed in both perikarya and apical processes of cholinergic brain neostriatal neurons of transgenic mice (Fig. 2B) as compared with controls (Fig. 2A). In the parietal cortex, excess staining was concentrated in perikarya (compare Fig. 1C and D). Cytochemical staining further revealed higher AChE activity in transgenic neostriatal cell bodies and processes (Fig. 2F) than in neostriatal neurons of control mice (Fig. 2E). AChE expression levels showed no age-related differences (data not shown), suggesting that cholinergic neurons in AChE-transgenic mice are continuously subject to the insult involved in hypocholinergic functioning.

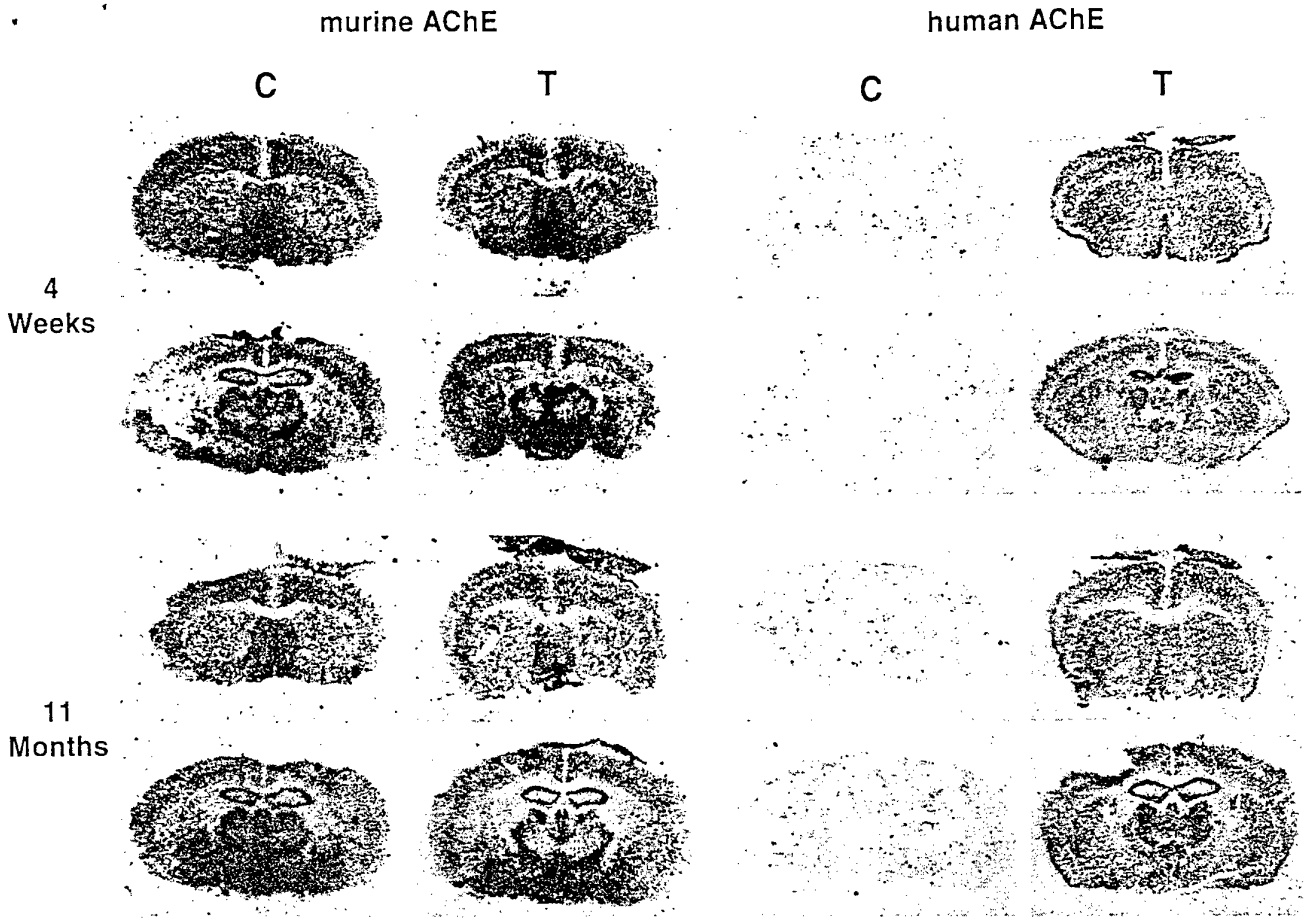

FIG. 1. Transgenic human AChE mRNA is coexpressed with host mouse AChE mRNA, shown by in situ hybridization of the murine and human AChE mRNA in control (C) and transgenic (T) mice. Note the small dots in the striatum of the sections hybridized with the probe for the endogenous AChE, which represent the striatal cholinergic interneurons.

Impaired performance in the Morris water maze

To dissect the progressive cognitive impairment that was initially identified in these mice by manual follow-up of the Morris water maze (Beeri et al., 1995), 5-month-old AChE-transgenic (n = 11) and control (n = 19) mice were compared in the Morris water maze by video imaging and dedicated software. Control mice showed a gradual decrease in the mean latency to reach the platform over days, indicating intact reference memory (Fig. 3A). In contrast, transgenic mice failed to show improvement over time (group × days effect, $F_{4,108} = 5.92$, $p < 0.001$), which suggests impaired reference memory (Fig. 3C). In addition, control mice showed a mild improvement in the overall performance of the second trial as compared with the first one within the same day (this limited improvement may result from the long delay between the two trials). Transgenic mice showed no such improvement within the daily trials (group × trials effect, $F_{1,27} = 4.14$, $p = 0.05$), suggesting an impaired working memory (Fig. 3A and C). Transgenic mice were further significantly different from control mice in their mean swimming speed (group main effect, $F_{1,27} = 17.7$, $p < 0.001$; Fig. 3B and D). Because this speed difference between the groups remained constant throughout the test period, it cannot account for the increased difference in latency performance between the two groups, which developed over time. Rather, this physical parameter probably reflects the progressive neuromotor decline displayed by these mice (Andres et al., 1997).

Control animals showed improved search strategy seen as an increase in the time spent in the concentric middle zone, where the platform was located (Fig. 3E). No such increase was seen in the group of transgenic mice (Fig. 3E; group main effect, $F_{1,27} = 20.7$, $p < 0.001$), which showed a significant tendency to remain near the pool wall, i.e., thigmotaxis (Fig. 3F; group main effect, $F_{1,27} = 9.67$, $p < 0.001$). The thigmotaxis may reflect higher sensitivity to stress. Combined effects of memory impairment and increased sensitivity to stress were also demonstrated in the cholinergically impaired WKY rat strain (Grauer and Kapon, 1993).

Attenuated dendritic branching and reduced spine numbers in midaged human promoter AChE-transgenic mice

Assessment of dendritic branching of Golgi-impregnated cortical neurons was carried out in 7-month-old and 5-week-old transgenics and age-matched controls

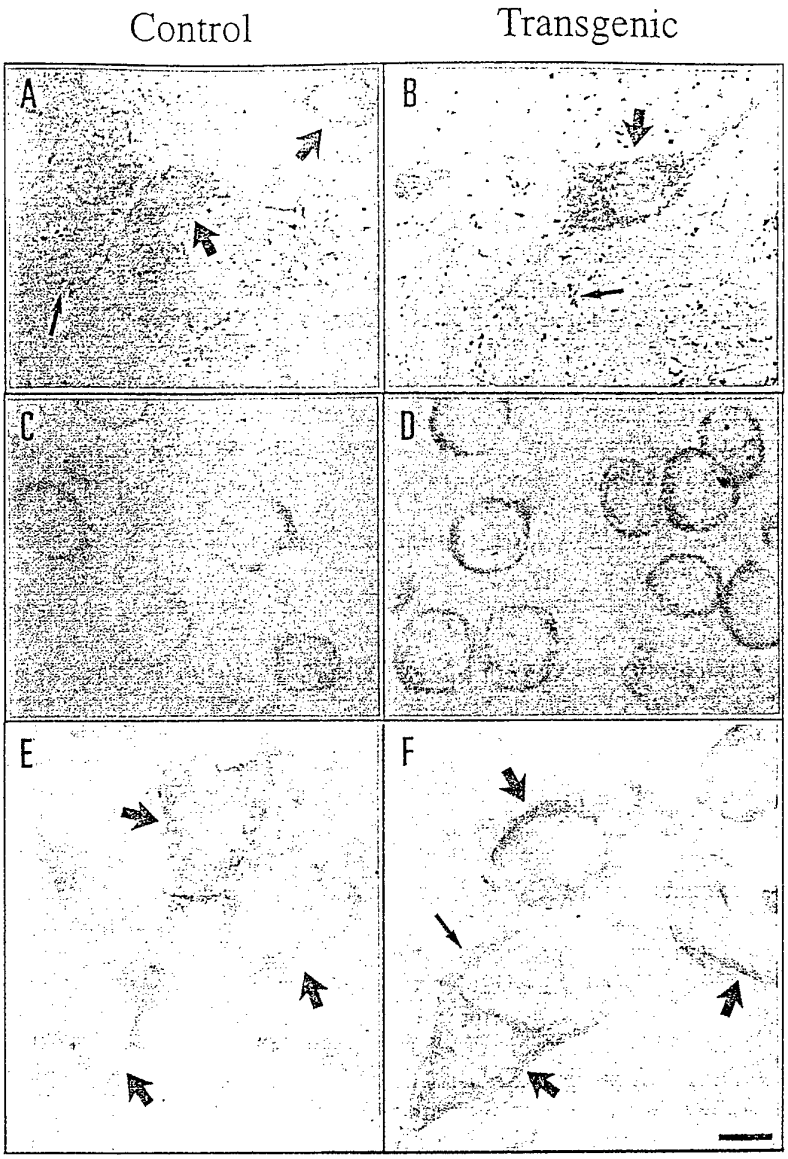

FIG. 2. AChE overexpression in neostriatal neurons. **Upper and middle panels:** AChE mRNA. Presented are paraffin-embedded neostriatum (**A** and **B**) and cortex sections (**C** and **D**) from control (A and C) and transgenic (B and D) mice following in situ hybridization with a 5′-biotinylated AChE cRNA probe detecting both mouse and human AChE mRNA. **Lower panels:** Active AChE. Presented are floating Vibratome-cut sections cytochemically stained for acetylthiocholine hydrolysis from (**E**) control and (**F**) transgenic mice. Because of the different treatments involved in these two procedures, the neurons appear somewhat shrunken in the paraffin-embedded sections. Judging by the heavier staining in neurons from transgenic mice as compared with controls, both cell bodies and apical processes of neostriatal neurons contain both the human mRNA and its human enzyme product. Sites of heavy staining are denoted in neuronal processes by thin arrowheads and in cell bodies by thick arrowheads. Bar = 10 μm.

(four animals per group). Figure 4A presents examples of such Golgi staining. Camera lucida drawings of the basilar tree of nine randomly selected layer V pyramidal cells from the frontoparietal cortex of each group (see examples in Fig. 4B) were further evaluated by Sholl analysis. The dendritic arbors in 7-month-old control brains were slightly larger than those of 5-week-old controls ($p \leq 0.6$), whereas dendritic arbors of transgenic neocortical pyramidal neurons were smaller in 7-month-old animals ($p \leq 0.060$) than in 5-week-old ones. The combined effects of the upward age-related small shift in the controls and greater downward shift in the transgenics resulted in significant differences between dendritic domains of neurons from the 7-month-old transgenic and control mice ($n = 36$; $p \leq 0.011$ using a Gaussian approximation; Fig. 4C and Table 1). AChE overexpression therefore had a detrimental effect on maintenance of the dendritic arbor. The onset of this effect coincided with the onset of the progressive cognitive failure in these transgenic mice (Beeri et al., 1995), suggesting a causal relationship between these two AD-characteristic phenomena (Buell and Coleman, 1981; Katzman, 1986).

Dendritic spines of the basilar tree, which represent the loci for the vast majority of all synaptic input to the neuron, were counted along the entire dendritic branch (from the terminal tips to first-order branches) of three to five branches per randomly selected seven neurons per brain. As seen in Table 1, in comparison with age-matched controls the 5-week-old transgenic mice showed no significant differences in the average number of spines per basilar tree. In contrast, neurons from the 7-month-old cognitively impaired transgenic mice had significantly fewer spines ($p \leq 0.040$) in comparison with those from 7-month-old controls (Table 1). By 7 months, the number of spines in control mice increased by 10% from that of 5 weeks, whereas in transgenics it decreased by 15% (Table 1). This led to a highly significant difference in the total number of dendritic spines per cell ($p \leq 0.0055$ by unpaired

t test). Figure 4D presents examples for the reduced spine number in adult but not young transgenic neurons.

No apparent adjustment in cholinergic receptors

Reduction in levels of nicotinic AChRs has been reported in AD (Whitehouse et al., 1986; Nordberg et al., 1988; Perry et al., 1995). Therefore, we examined in AChE-transgenic mice the protein and mRNA levels of several AChR subtypes. Also, we considered other potential levels for up-regulating receptor binding capacities, e.g., translation efficiency, protein stability, and allosteric modulation of binding properties (Heidmann and Changeux, 1978). To this end, the binding levels of different nicotinic and muscarinic agonists were examined in frozen coronary brain sections from transgenic and control mice.

Levels of mRNA for neuronal nicotinic AChR $\alpha 3-5$, $\alpha 7$, and $\beta 2-4$ subunits were examined by in situ hybridization to coronary brain sections from several brain regions of 4-week-, 5-month-, and 11-month-old transgenic and control mice. Hybridization signals revealed no apparent difference in signal localization and intensity between control and transgenic mice of all ages (Fig. 5 and data not shown). In addition, semiquantitative RT-PCR analyses revealed similar levels of the mRNAs for nicotinic AChR $\alpha 4$ and M1 muscarinic AChR mRNAs in control and transgenic brains (data not shown). Binding levels of [*N-methyl*-^{3}H]pirenzepine and [2,3-*dipropylamino*-^{3}H]AF-DX 384 reflected M1 and M2 muscarinic AChRs, respectively. Binding of ^{125}I-α-bungarotoxin revealed the $\alpha 7$-containing nicotinic AChR, and [^{3}H]nicotine, [^{3}H]-cytisine, and [^{3}H]epibatidine detected $\alpha 2-6$, $\beta 2-4$-containing nicotinic AChRs. All remained unchanged in both young and old transgenic mouse brains as compared with controls (Fig. 5 and data not shown).

Although the methods we used to assess receptor production and binding capacities would probably overlook minor modifications, these analyses gave clear indication for the lack of major changes in the transcription and/or stability of the mRNA for several nicotinic AChRs and muscarinic AChR subunits as well as in their corresponding protein products. That most of the nicotinic AChR and muscarinic AChR subunits were present in the AChE-transgenic brain in normal levels and binding capacities and the presence of unmodified levels of neuronal nicotinic receptor subunits in $\beta 2$ nicotinic AChR knockout mice (Picciotto et al., 1995) therefore supports the notion that the transcriptional and/or posttranscriptional control of AChR production is not associated with cholinergic imbalance processes in the mammalian brain.

Enhanced levels of high-affinity choline transporter in transgenic mouse brain

We examined whether changes occurred in choline uptake by incubating coronal brain sections with [^{3}H]-hemicholinium-3, the effective blocker of the high-affinity Na^+-dependent choline transporter (Vickroy et al., 1984). The autoradiographic distribution of [^{3}H]hemicholinium-3 binding sites correlated with the distribution of classical presynaptic markers of the cholinergic system and was associated with the presence of cholinergic terminals. High-density binding sites were found in striatum, amygdala, and interpeduncular nucleus, and labeling density was much lower in the cortex and hippocampus (Forloni and Angeretti, 1992; data not shown). Twofold higher levels of hemicholinium binding were found in the neostriatum of young (4-week-old) and midaged (11-month-old) transgenics as compared with control mice (Fig. 6). It is interesting that the enhancement of hemicholinium binding to frontal cortex sections from Alzheimer's brains was also twofold (Slotkin et al., 1994). Similar enhancement in hemicholinium binding was also found in the cholinoceptive interpeduncular nucleus of transgenic mice but not in their hippocampus (data not shown). In contrast, semiquantitative RT-PCR revealed no difference in the mRNA levels between control and transgenic brain for the ACh-synthesizing enzyme ChAT, the vesicular protein synaptophysin that serves as general synaptic marker (Leube et al., 1987), and L-type Ca^{2+} channel α subunit (data not shown). This was so at both the ages of 4–5 weeks and 11–12 months, which excludes the possibility of late-onset changes. Therefore, hemicholinium binding was selectively enhanced in both cholinergic and cholinoceptive brain regions of AChE-overexpressing mice, where a high density of binding sites was reported in normal brain (Forloni and Angeretti, 1992).

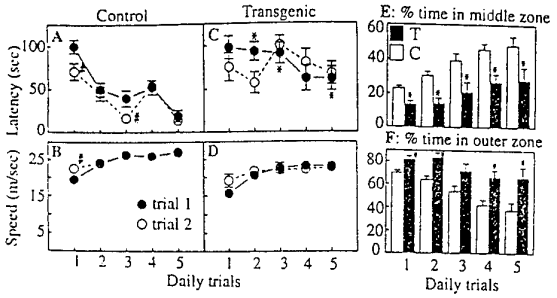

FIG. 3. Impaired performance of adult transgenic mice in a working memory procedure in the water maze. Improved mean ± SEM (bars) latency to reach the platform in trial 1 in control (n = 19; **A**) as compared with transgenic (n = 11; **C**) mice indicates changes in reference memory. Improved performance in trial 2 versus trial 1 indicates changes in working memory. **B** and **D**: Somewhat lower swimming speed occurs in transgenic as compared with control mice. **E** and **F**: Percent time spent in middle and outer concentric zones suggests an impaired search strategy of transgenic mice. $^*p < 0.05$ for transgenic versus control; $^\#p < 0.05$ trial 1 versus trial 2. See text for detailed statistical analysis.

DISCUSSION

Transgenic mice overexpressing AChE in their brain neurons suffer complex impairments in learning and memory, late-onset attenuation of dendrite branching

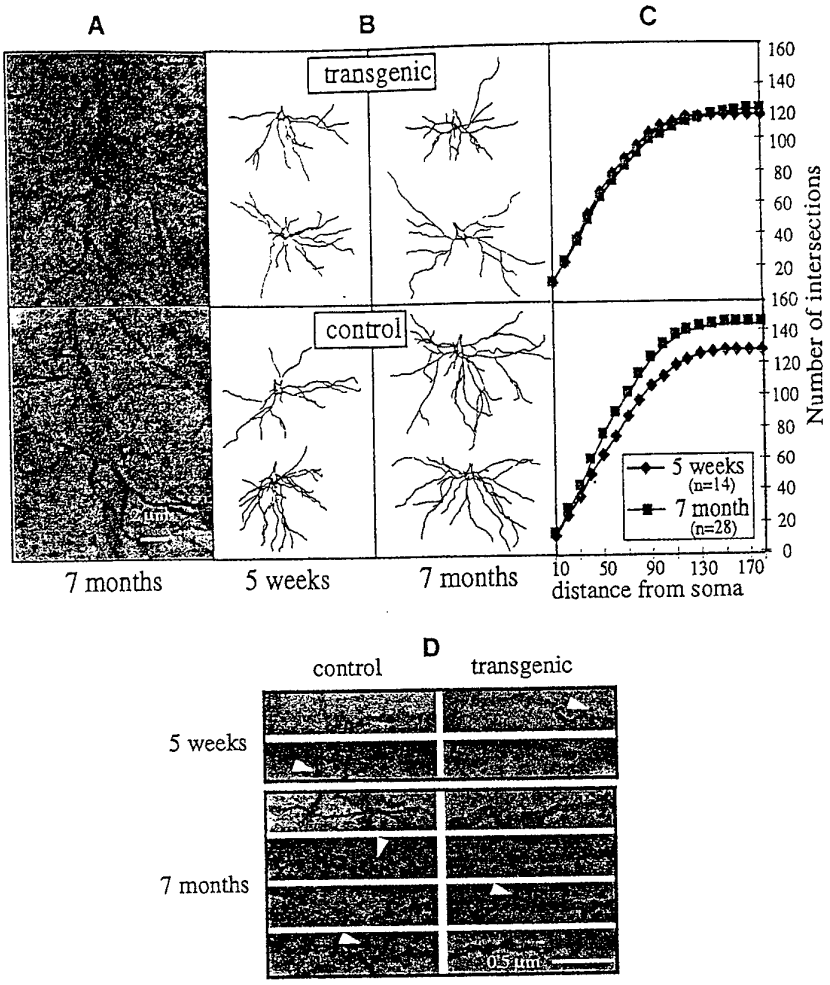

FIG. 4. Attenuated dendritic branching and spine loss in layer 5 pyramidal neurons from the frontoparietal cortex of transgenic mice. **A:** Representative Golgi-stained preparations from brains of transgenic (**top panel**) and control (**bottom panel**) 7-month-old mice. **B:** Camera lucida tracings of the basilar tree of Golgi-stained pyramidal neurons from the frontoparietal cortex of 5-week- and 7-month-old transgenic and control brains. **C:** Graphical presentations of data from Sholl analyses. Shown are numbers of dendritic branches intersecting with a series of concentric circles of increasing distance from the cell body. Numbers of intersections are expressed as a cumulative total. See text and Table 1 for details. **D:** Representative high-magnification photographs of dendritic branches from 5-week- and 7-month-old transgenic and control mice. Note the reduction in spines (arrowheads) on the transgenic dendrites.

in pyramidal neurons within the frontoparietal cortex, and enhanced binding capacity of the high-affinity Na^+-dependent choline transporter in the neostriatum. Young mice, at the age of 4–5 weeks, exhibit less severe depletions than older adult animals, at the age of 7–11 months, representing a progressive, complex cognitive decline which these mice undergo. This supports the notion that these phenotypic sequelae are related to the cholinergic deficit also in AD patients.

Complex memory impairments

The impairment in both working and reference memory in AChE-transgenic mice is more severe and complex compared with other models with cholinergic deficits. Apolipoprotein E-deficient mice, which revealed reduced ChAT activities and impaired hypothermic responses to the cholinergic agonist oxotremorine, suffered impairments in working but not reference memory (Gordon et al., 1995). Working but not reference memory is selectively vulnerable to central cholinergic blockade as well as to medial septal and hippocampal lesions (Gordon et al., 1995). One recent model in which reference memory was impaired was based on overexpression of the mutant 695-amino-acid isoform of β-amyloid precursor protein (Hsiao et al., 1996). However, the performance of mutant β-amyloid-expressing mice improved in the Morris water maze even at the age of 10 months, unlike our mice, which totally failed to improve performance at as early as 5 months of age. The authentic overexpression of AChE in cholinergic neurons (Beeri et al., 1995; Andres et al., 1997; present study) may explain the severity of these cognitive phenotypes. Also, AChE-transgenic mice revealed a significant tendency to thigmotaxis, similar to rats administered scopolamine (Hodges, 1996). As habituation to stress improved water maze performance of old rats, which tend to exhibit thigmotaxis (Mabry et al., 1996), our results may indicate that AChE overexpression and/or the resultant cholinergic imbalance creates higher sensitivity to stress conditions.

Attenuated dendritic branching and loss of spines in cortical neurons

Loss of synapses and neurons has repeatedly been demonstrated to correlate with the degree of cognitive impairment in AD (DeKosky and Scheff, 1990). In the adult nervous system, continuous changes in the size and shape of the dendritic tree involve dendritic retraction and elongation, formation of new branches,

TABLE 1. *Progressive deterioration of layer V pyramidal neurons in AChE-transgenic mice*

Tested parameters	5-week-old mice		7-month-old mice		Significance of C, T comparison	
	C	T	C	T	5 weeks	7 months
1. No. of Golgi-stained neurons evaluated for dendrite branching (animal) [total]	9/(2) [18]	9/(2) [18]	9/(4) [36]	9/(4) [36]		
2. Cumulative total intersections/ neuron (Sholl analysis, at 150 μm from soma)	123	118	126	109	$p \leq 0.2323^a$	$p \leq 0.0113^a$
3. Effectiveness of C, T pairing	0.9938		0.9969		$p \leq 0.0001^b$	$p \leq 0.0001^b$
4. No. of stained neurons analyzed for dendritic spines/(animal) [total]	7/(2) [14]	7/(2) [14]	9/(4) [36]	9/(4) [36]		
5. Average no. of spines/basilar branch/neuron (mean ± SEM)	105.7 ± 9.63	99.95 ± 7.76	108.6 ± 6.49	89.91 ± 6.09	$p = 0.8378^c$	$p = 0.0398^c$
6. Difference between C, T means	5.71 ± 12.37		18.65 ± 8.90		$p = 0.2238^d$	$p = 0.03552^d$
7. Variance comparison (Mann–Whitney U value)	87.50		444.0		$p = 0.6459^e$	$p = 0.0220^e$

For parameters 1–3, using coded slides, the basilar tree of the noted no. of Golgi-stained neurons per brain in two or four animals per group (parentheses) was evaluated for branching, using Sholl analysis (method of concentric circles). Statistical analyses (specified under "significance") showed significant differences between the 7-month-old but not 5-week-old control (C) and transgenic (T) mice under highly significant pairing effectiveness. For parameters 4–7, dendritic spines were counted along the entire dendritic branch of three to five branches per randomly selected nine neurons for each brain. Both total and the average no. of spines were significantly different between 7-month-old but not 5-week-old T and C mice.

[a]Gaussian approximation of Wilcoxon test.
[b]Spearman approximation.
[c]Unpaired t test.
[d]F test of variance.
[e]Mann–Whitney test, two-tailed p value.

and creation of new synapses between them. Moreover, dendritic arborization is enhanced in the normal adult brain, under conditions of increased functional requirements (Buell and Coleman, 1981). Basilar dendritic arbors of frontal cortical neurons in aged rats are significantly larger than those of young adult rats (Wellman and Sengelaub, 1995), which is likely a compensatory response to the death of other cortical neurons (Coleman and Flood, 1987). All of these changes in dendritic arbors were apparently stopped in the brain of adult AChE-transgenic mice, accompanied by loss of dendritic spines.

Dendritic organization is primarily determined by extrinsic factors mediated through communication between dendrites of neighboring cells, the activity of afferent neuronal connections or chemotrophic factors, and intrinsic neuronal properties affecting the response to all these stimuli (Arendt et al., 1995). Lesions of the nucleus basalis magnocellularis do not significantly affect dendritic morphology in young adult rats, but cortical neurons in middle-aged and aged rats showed a marked reduction in dendritic arbors following such lesions (Wellman and Sengelaub, 1995). Quantitative studies also revealed shorter and less branched dendrites in neurons from some cortical regions of humans with senile dementia compared with normal aged individuals (Buell and Coleman, 1981). Newly formed dendrites have also been reported, but only in neurons that exhibited reduced appearance of dendritic arbors on the remaining dendrites (Ferrer et al., 1990). Dendritic growth and neuronal and spine loss can hence be regarded as bidirectional processes that occur simultaneously but result in opposite effects on the total of the dendritic network as an attempt of repair following neuronal and synapse deterioration or as primary pathological events leading to neuronal degeneration.

The late-onset attenuation of dendritic material in AChE-transgenic mice would logically represent the anatomical correlate of the progressive age-related behavioral impairments. The concomitant loss of dendritic spines may suggest that the transgenic mice at midage have impaired compensation capabilities of dendritic trees and synapses under conditions of cholinergic imbalance. The cognitive decline under dysfunction of the cholinergic system in normal elderly individuals has also been associated with age-related dendritic attenuation (McEntee and Crook, 1992; Gallagher and Colombo, 1995). In light of the rapidly increasing percentage of elderly in the population, treatment of such "normal" age-associated memory impairments should be considered as a cost-effective public health measure to delay more serious degeneration. The AChE-transgenic model may thus prove to be of particular value toward the development of therapeutic pharmaceutical strategies to attenuate (halt or

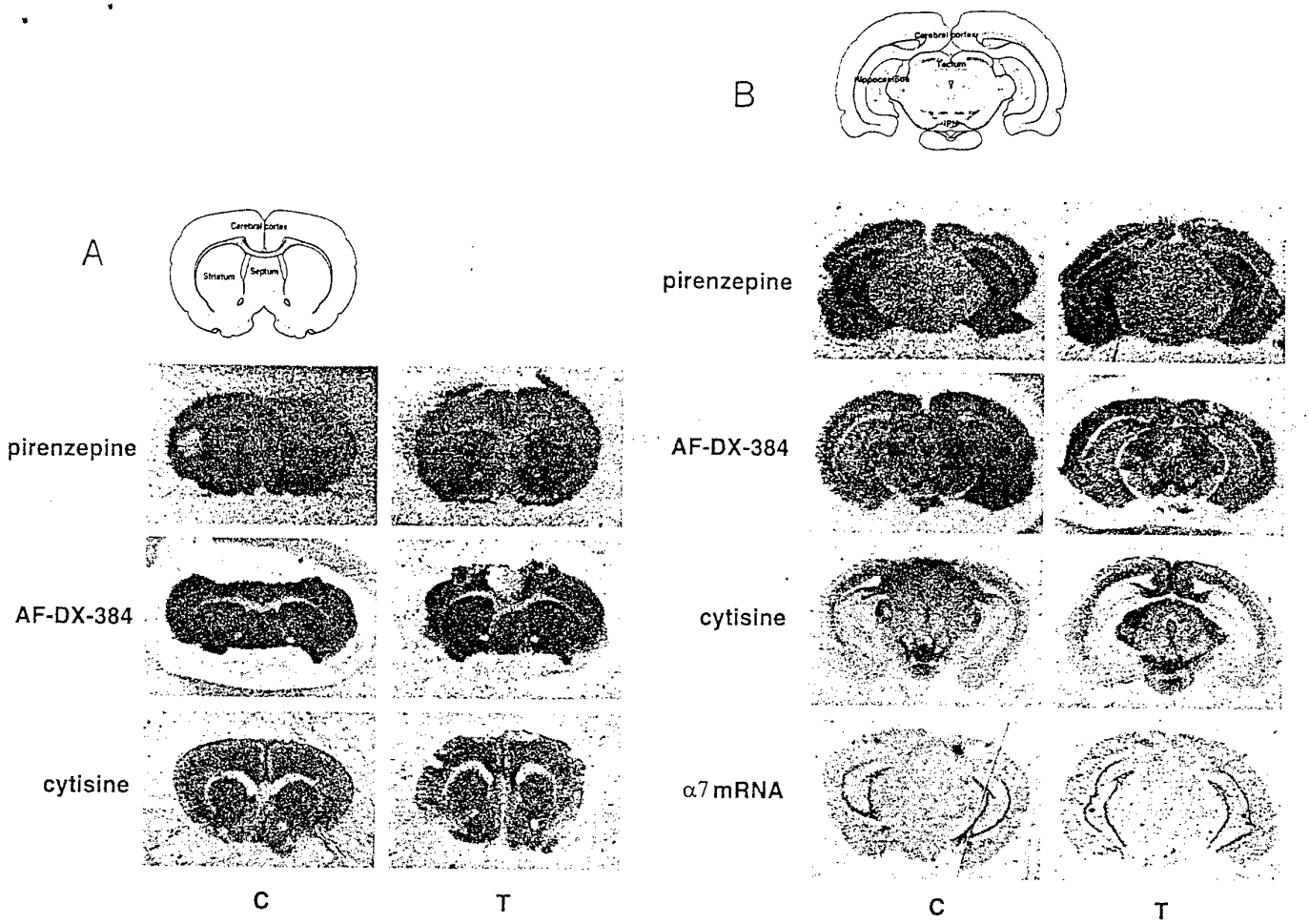

FIG. 5. Similar binding capacities to AChR subtypes in transgenic neostriatum. **A:** [^{3}H]Pirenzepine (M1 receptors), [^{3}H]AF-DX-384 (M2 receptors), and [^{3}H]cytisine (heteromeric nicotinic AChR) binding at the level of striatum of control (C) and transgenic (T) mice. The drawing is of level 15 (Swanson, 1992). **B:** [^{3}H]Pirenzepine (M1 receptors), [^{3}H]AF-DX-384 (M2 receptors), and [^{3}H]cytisine (heteromeric nicotinic AChR) binding and in situ hybridization of nicotinic AChR α7 mRNA at the level of the mesencephalon of C mice and T mice. The drawing is of level 39 (Swanson, 1992).

even reverse) this mild to moderate nonpathological cognitive decline.

Normal levels of AChR mRNAs and proteins

The expression levels and properties of AChR subtypes and several other synaptic proteins were normal in AChE-transgenic mice, as revealed by in situ hybridization, RT-PCR, and ligand binding experiments. Also, up to the age of 12 months there was no sign of cell death in their brains. The functional deficits that we observed previously in the capacity of these transgenic mice to respond to muscarinic and nicotinic drugs (Beeri et al., 1995; Andres et al., 1996) suggest that some modifications in receptor functioning in vivo did take place. In view of the similar expression and binding patterns of AChRs, the receptor loss in AD can tentatively be related to the reduced dendritic branching and spine formation rather than to production deficiences. This explains the relative resistance of AChE-transgenic mice as compared with control animals to the hypothermic effects of muscarinic and nicotinic agonists (Beeri et al., 1995; Andres et al., 1996), yet raises doubts as to the value of such agonists for treating AD patients with behavioral cholinergic deficits.

Regional enhancement in [^{3}H]hemicholinium-3 binding

Although ChAT mRNA levels remained unchanged in the transgenic brain, the rate-limiting step in ACh synthesis is choline reuptake into neuronal terminals (Wurtman, 1992). Forloni and Angeretti (1992) showed a >50% decrease in number of hemicholinium-3 binding sites in the striatum of aged rats. Using tissue from rapid autopsy, Slotkin et al. (1994) showed that choline uptake and [^{3}H]hemicholinium-3 binding are elevated in cortical regions but not the putamen of Alzheimer's patients, indicating that the rise in binding was specifically associated with regions undergoing cholinergic degeneration. The increase in hemicholinium-3 binding to the striatum of AChE-transgenic mice compared with controls suggests elevated choline uptake and ACh synthesis, as a compensatory reaction to ACh deficits. The twofold enhancement in hemi-

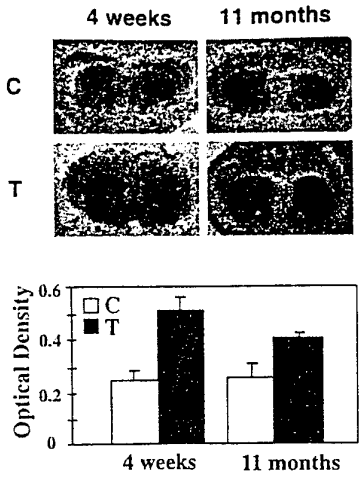

FIG. 6. Enhanced [^{3}H]hemicholinium-3 binding in transgenic neostriata. **A:** Autoradiography followed by image analysis. Binding was increased of [^{3}H]hemicholinium-3 to the neostriatum of 4-week- (**left**) and 12-month-old (**right**) normal mice (**top**; C) as compared with transgenics (**bottom**; T). Presented are brain sections following 2 weeks of exposure, indicating increased choline transport in these brain regions. **B:** Quantification of [^{3}H]-hemicholinium binding. Presented is one typical autoradiography experiment of four (n = 2 animals). For each animal, the images of two to six sections were digitized [at the neostriatum level, between level 21 and 30 of Franklin and Paxinos (1997)], and the MGV of the two hemistriata was recorded. See Materials and Methods for calculations. Data are expressed as mean ± SEM (bars) OD values.

cholinium binding was seen both in 4–5-week-old transgenic mice and in 11–12-month-old ones and could have contributed to imbalanced membrane metabolism, which may perhaps explain the attenuation in dendrite branching.

In conclusion, attenuated dendritic branching, reduced spine formation, impaired working and reference memory, and enhanced choline transport emerged in our work as primary neuroanatomical, behavioral, and metabolic correlates of pathological conditions that involve AChE overexpression and/or cholinergic imbalance. Therefore, AChE-transgenic mice should be most useful for exploring the mechanisms leading to these correlates. Moreover, the observed mechanisms for potential structural and metabolic compensation can shed new light on the late-onset, progressive nature of diseases associated with cholinergic imbalance. The observed progressive cognitive and motor deterioration in transgenic mice expressing human AChE in CNS (Beeri et al., 1995; Andres et al., 1996, 1997) could hence indicate the failure of control mechanism(s) to maintain this balance beyond a certain age.

Acknowledgment: This work was supported by USARMRDC grant 17-97-1-7007 and by Ester/Medica Neurosciences (to H.S.). R.B. was the recipient of an EMBO and an ENN short-term fellowships for the work in J.P.C.'s laboratory.

REFERENCES

Andres C., Beeri R., Huberman T., Shani M., and Soreq H. (1996) Cholinergic drug resistance and impaired spatial learning in transgenic mice overexpressing human brain acetylcholinesterase. *Prog. Brain Res.* **109,** 265–272.

Andres C., Beeri R., Friedman A., Lev-Lehman E., Henis S., Timberg R., Shani M., and Soreq H. (1997) ACHE transgenic mice display embryonic modulations in spinal cord CHAT and neurexin Iβ gene expression followed by late-onset neuromotor deterioration. *Proc. Natl. Acad. Sci. USA* **94,** 8173–8178.

Arendt T., Marcova L., Bigl V., and Bruckner M. K. (1995) Dendritic reorganisation in the basal forebrain under degenerative conditions and its defects in Alzheimer's disease. I. Dendritic organisation of the normal human basal forebrain. *J. Comp. Neurol.* **151,** 169–188.

Bartus R. T. and Uemura Y. (1979) Physostigmine and recent memory: effects in young and aged non-human primates. *Science* **206,** 1037–1089.

Beeri R., Andres C., Lev-Lehman E., Timberg R., Huberman T., Shani M., and Soreq H. (1995) Transgenic expression of human acetylcholinesterase induces progressive cognitive deterioration in mice. *Curr. Biol.* **5,** 1063–1071.

Bierer L. M., Haroutunian V., Gabriel S., Knott P. J., Carlin L. S., Purohit D. P., Perl D. P., Schmeidler J., Kanof P., and Davis K. L. (1995) Neurochemical correlates of dementia severity in Alzheimer's disease: relative importance of the cholinergic deficits. *J. Neurochem.* **64,** 749–760.

Braak H. and Braak E. (1985) Golgi preparations as a tool in neuropathology with particular reference to investigations of the human telencephalic cortex. *Prog. Neurobiol.* **25,** 366–368.

Buell S. J. and Coleman P. D. (1981) Quantitative evidence for selective dendritic growth in normal human aging but not in senile dementia. *Brain Res.* **214,** 23–41.

Coleman P. D. and Flood D. G. (1987) Neuron numbers and dendritic extent in normal aging and Alzheimer's disease. *Neurobiol. Aging* **8,** 521–545.

Coyle J. T., Price D. L., and DeLong M. R. (1983) Alzheimer's disease: a disorder of cortical cholinergic disruption. *Science* **219,** 1186–1189.

Davies P. and Maloney A. J. F. (1976) Selective loss of central cholinergic neurons in Alzheimer's disease. *Lancet* **2,** 1403.

DeKosky S. T. and Scheff S. W. (1990) Synapse loss in frontal cortex biopsies in Alzheimer's disease: correlation with cognitive severity. *Ann. Neurol.* **27,** 457–464.

Ferrer I. N., Guionnet F. C., and Tunon T. (1990) Neuronal alterations in patients with dementia: a Golgi study on biopsy samples. *Neurosci. Lett.* **144,** 11–16.

Fibiger H. C. (1991) Cholinergic mechanisms in learning, memory, and dementia: a review of recent evidence. *Trends Neurosci.* **14,** 220–223.

Fischer W., Gage F. H., and Bjorklund A. (1989) Degenerative changes in forebrain cholinergic nuclei correlate with cognitive impairments in aged rats. *Eur. J. Neurosci.* **1,** 34–45.

Forloni G. and Angeretti N. (1992) Decreased [^{3}H]hemicholinium binding to high-affinity choline uptake sites in aged rat brain. *Brain Res.* **570,** 354–357.

Franklin K. B. J. and Paxinos G. (1997) *The Mouse Brain in Stereotaxic Coordinates.* Academic Press, San Diego.

Gallagher M. and Colombo P. J. (1995) Aging: the cholinergic hypothesis of cognitive decline. *Curr. Opin. Neurobiol.* **5,** 161–168.

Games D., Adams D., Alessandrini R., Barbour R., Berthelette P., Blackwell C., Carr T., Clemens J., Donaldson T., and Gillespie F. (1995) Alzheimer-type neuropathology in transgenic mice overexpressing V717F β-amyloid precursor protein. *Nature* **373,** 523–527.

Gordon I., Grauer E., Genis I., Sehayek E., and Michaelson D. M. (1995) Memory deficits and cholinergic impairments in apolipoprotein E-deficient mice. *Neurosci. Lett.* **199,** 1–4.

Grauer E. and Kapon Y. (1993) Wistar–Kyoto rats in the Morris

water maze: impaired working memory and hyper-reactivity to stress. *Behav. Brain Res.* **59,** 147–151.

Hammond P., Rao R., Koenigsberger C., and Brimijoin S. (1994) Regional variation in expression of acetylcholinesterase mRNA in adult rat brain analyzed by in situ hybridization. *Proc. Natl. Acad. Sci. USA* **91,** 10933–10937.

Imann T. and Changeux J. P. (1978) Structural and functional properties of the acetylcholine receptor protein in its purified and membrane bound states. *Annu. Rev. Biochem.* **47,** 317–357.

Hodges H. (1966) Maze procedures: the radial-arm and the water maze compared. *Cognitive Brain Res.* **3,** 167–181.

Honer W. G., Dickson D. W., Gleeson J., and Davies P. (1992) Regional synaptic pathology in Alzheimer's disease. *Neurobiol. Aging* **13,** 375–382.

Hsiao K. K., Borchelt D. R., Olson J., Johannsdottir R., Kitt C., Yunis W., Xu S., Eckman C., Younkin S., Price D., Iadecola C., Clark B., and Carlson G. (1995) Age related CNS disorder and early death in transgenic FVB/N mice overexpressing Alzheimer amyloid precursor proteins. *Neuron* **15,** 1202–1218.

Hsiao K., Chapman P., Nilsen S., Eckman C., Harigaya Y., Younkin S., Yang F., and Cole G. (1996) Correlative memory deficits, $A\beta$ elevation and amyloid plaques in transgenic mice. *Science* **274,** 99–102.

Katzman R. (1986) Alzheimer's disease. *N. Engl. J. Med.* **314,** 964–973.

LaFerla F. M., Tinkle B. T., Bieberich C. J., Haudenschild C. C., and Jay G. (1995) The Alzheimer's $A\beta$ peptide induces neurodegeneration and apoptotic cell death in transgenic mice. *Nature Genet.* **9,** 21–30.

Le Novère N. and Changeux J. P. (1995) Ligand Gated Ion Channel Subunit Database. http://www.pasteur.fr/units/neubiomol/LGIC.html.

Le Novère N., Zoli M., and Changeux J. P. (1996) Neuronal nicotinic receptor $\alpha 6$ subunit mRNA is selectively concentrated in catecholaminergic nuclei of the rat brain. *Eur. J. Neurosci.* **8,** 2428–2439.

Leube R. E., Kaiser P., Seiter A., Zimbelmann R., Franke W. W., Rehm H., Knaus P., Prior P., Betz H., Reinke H., Beyreuther K., and Wiedenmann B. (1987) Synaptophysin: molecular organization and mRNA expression as determined from cloned cDNA. *EMBO J.* **6,** 3261–3268.

Mabry T. R., McCarty R., Gold P. E., and Foster T. C. (1996) Age and stress history effects on spatial performance in the swim task in Fischer-344 rats. *Neurobiol. Learn. Mem.* **66,** 1–10.

McEntee W. J. and Crook T. H. (1992) Cholinergic function in the aged brain: implications for treatment of memory impairments associated with ageing. *Behav. Pharmacol.* **3,** 327–336.

Moran P. M., Higgins L. S., Cordell B., and Moser P. C. (1995) Age related learning deficits in transgenic mice expressing the 751-amino acid isoform of human β-amyloid precursor protein. *Proc. Natl. Acad. Sci. USA* **92,** 5341–5345.

Morris R. (1984) Development of a water-maze procedure for studying spatial learning in the rat. *J. Neurosci. Methods* **11,** 47–60.

Nordberg A., Adem A., Hardy J., and Winblad B. (1988) Change in nicotinic receptor subtypes in temporal cortex of Alzheimer brain. *Neurosci. Lett.* **86,** 317–321.

Perry E., Morris C., Court J., Cheng A., Fairbairn A., McKeith I., Ieving D., Brown A., and Perry R. (1995) Alteration in nicotine binding sites in Parkinson's disease, Lewy body dementia and Alzheimer's disease: possible index of early neuropathology. *Neuroscience* **64,** 385–395.

Picciotto M. R., Zoli M., Lena C., Bessis A., Lallemand Y., Le Novère N., Vincent P., Pich E. M., Brulet P., and Changeux J. P. (1995) Abnormal avoidance learning in mice lacking functional high-affinity nicotine receptor in the brain. *Nature* **374,** 65–67.

Price D. L., Sisodia S. S., and Gandy S. E. (1995) Amyloid β amyloidosis in Alzheimer's disease. *Curr. Opin. Neurobiol.* **8,** 268–274.

Purpura D. P. (1974) Dendritic spine "dysgenesis" and mental retardation. *Science* **186,** 1126–1128.

Seidman S., Sternfeld M., Ben Aziz-Aloya R., Timberg R., Kaufer-Nachum D., and Soreq H. (1995) Synaptic and epidermal accumulations of human acetylcholinesterase are encoded by alternative 3′-terminal exons. *Mol. Cell. Biol.* **15,** 2993–3002.

Sholl D. A. (1953) Dendritic organization in the neurons of the visual and motor cortices of the cat. *J. Anat.* **87,** 387–406.

Slotkin T. A., Nemeroff C. B., Bissette G., and Seidler F. G. (1994) Overexpression of the high affinity choline transporter in cortical regions affected by Alzheimer's disease. *J. Clin. Invest.* **94,** 696–702.

Swanson L. W. (1992) *Brain Maps: Structure of the Rat Brain.* Elsevier, Amsterdam.

Terry R. D., Masliah E., Salmon D. P., Butters N., De Teresa R., Hill R., Hansen L. A., and Katzman R. (1992) Physical basis of cognitive alterations in Alzheimer's disease: synapse loss is the major correlate of cognitive impairment. *Ann. Neurol.* **30,** 572–580.

Valverde F. (1976) Aspects of cortical organization related to the geometry of neurons with intra-cortical axons. *J. Neurocytol.* **5,** 509–529.

Vickroy T., Roeske W., and Yamamura H. (1984) Sodium-dependent high-affinity binding of [^{3}H]hemicholinium-3 in the rat brain: a potentially selective marker for presynaptic cholinergic sites. *Life Sci.* **35,** 2335–2343.

Wellman C. L. and Sengelaub D. R. (1995) Alterations in dendritic morphology of frontal cortical neurons after basal forebrain lesions in adult and aged rats. *Brain Res.* **669,** 48–58.

Whitehouse P., Martino A., Antuono P., Lowenstein P., Coyle J., Price D., and Kellar K. (1986) Nicotinic acetylcholine binding sites in Alzheimer's disease. *Brain Res.* **371,** 146–151.

Wurtman R. J. (1992) Choline metabolism as a basis for the selective vulnerability of cholinergic neurons. *Trends Neurosci.* **15,** 117–122.

Zhi Q. X., Yi F. H., and Xi C. T. (1995) Huperzine A ameliorates the spatial working memory impairments induced by AF64A. *Neuroreport* **6,** 2221–2224.

Pyridostigmine brain penetration under stress enhances neuronal excitability and induces early immediate transcriptional response

ALON FRIEDMAN[1,2], DANIELA KAUFER[1], JOSHUA SHEMER[2,3], ISRAEL HENDLER[2,3], HERMONA SOREQ[1] & ILAN TUR-KASPA[2,3]

[1]*Department of Biological Chemistry, the Life Sciences Institute, the Hebrew University, Jerusalem 91904, Israel*
[2]*Medical Corps, Israel Defense Forces, P.O. Box 02419, Israel*
[3]*Sheba Medical Center, Sackler School of Medicine, Tel-Aviv University, Tel-Hashomer 52621, Israel*
The views expressed are those of the authors and are not to be construed as official policy of the Medical Corps, Israel Defense Forces.
Correspondence should be addressed to A.F.

Pyridostigmine, a carbamate acetylcholinesterase (AChE) inhibitor, is routinely employed in the treatment of the autoimmune disease myasthenia gravis[1]. Pyridostigmine is also recommended by most Western armies for use as pretreatment under threat of chemical warfare, because of its protective effect against organophosphate poisoning[2,3]. Because of this drug's quaternary ammonium group, which prevents its penetration through the blood–brain barrier, the symptoms associated with its routine use primarily reflect perturbations in peripheral nervous system functions[1,4]. Unexpectedly, under a similar regimen, pyridostigmine administration during the Persian Gulf War resulted in a greater than threefold increase in the frequency of reported central nervous system symptoms[5]. This increase was not due to enhanced absorption (or decreased elimination) of the drug, because the inhibition efficacy of serum butyrylcholinesterase was not modified[5]. Because previous animal studies have shown stress-induced disruption of the blood–brain barrier[6], an alternative possibility was that the stress situation associated with war allowed pyridostigmine penetration into the brain. Here we report that after mice were subjected to a forced swim protocol (shown previously to simulate stress[7]), an increase in blood–brain barrier permeability reduced the pyridostigmine dose required to inhibit mouse brain AChE activity by 50% to less than 1/100th of the usual dose. Under these conditions, peripherally administered pyridostigmine increased the brain levels of c-*fos* oncogene and AChE mRNAs. Moreover, *in vitro* exposure to pyridostigmine increased both electrical excitability and c-*fos* mRNA levels in brain slices, demonstrating that the observed changes could be directly induced by pyridostigmine. These findings suggest that peripherally acting drugs administered under stress may reach the brain and affect centrally controlled functions.

Pyridostigmine and physostigmine displayed similar efficacy in inhibiting acetylcholinesterase (AChE) activity when added to brain homogenates (Fig. 1*a*). Also, they were similarly effective in reducing serum butyrylcholinesterase (BuChE) activity when injected intraperitoneally (i.p.) into nonstressed mice (16.7% ± 6.9% and 22.6% ± 5.4% reduction from normal levels, respectively, 10 minutes after injection of 0.1 mg pyridostigmine or physostigmine per kg body weight into three animals in each group). However, brain AChE activity in homogenates prepared from nonstressed mice was considerably less inhibited by the injected pyridostigmine than by physostigmine (Fig. 1*b*). Thus, pyridostigmine doses previously proven to be protective against organophosphates (0.1–0.5 mg/kg, 15–30% inhibition of serum BuChE activity)[2,3] did not reduce brain AChE levels, whereas similar doses of physostigmine inhibited more than 50% of brain AChE activity (Fig. 1*b*). In contrast, AChE activity, measured in homogenates from the cerebral cortex of drug-injected stressed mice, was reduced by 0.1 mg/kg of either pyridostigmine or physostigmine to less then 50% of normal level (Fig. 1*c*). The stress treatment therefore reduced the pyridostigmine dose required to inhibit 50% of brain AChE from 1.50 to 0.01 mg/kg. This coincided with a >10-fold increase in brain penetration of either the albumin-binding dye Evan's blue (Fig. 1*d*) or AChE plasmid DNA including the cytomegalovirus (CMV) promoter[8] (Fig. 1*e*) under stress. Because the pyridostigmine doses that inhibited cortical AChE activity in nonstressed mice (>1 mg/kg) were reported to perturb central nervous system (CNS) functions in primates[9], we examined its effect on mRNA levels of the c-*fos* oncogene, an indirect marker for enhanced neuronal excitability[7], by reverse transcription followed by PCR amplification (RT-PCR). Earlier appearance of PCR product, reflecting a more than 100-fold increase in brain c-*fos* mRNA level, was evident in stressed as compared with control animals (Fig. 1*f*), in line with previous reports[7]. A similar increase in c-*fos* mRNA was observed in nonstressed animals as soon as 10 minutes following i.p. injection of 2 mg/kg pyridostigmine (95% inhibition of cortical AChE) (Fig. 2*a*, *top*). To explore the direct effect of pyridostigmine on cholinergic brain circuits, we performed electrophysiological and molecular neurobiology analyses on brain slices maintained *in vitro*[10]. Direct application of 1 mM pyridostigmine to hippocampal slices reduced AChE activity within 30 minutes with similar efficacy to that observed *in vivo* at a dose of 2 mg/kg and induced a parallel 100-fold increase in c-*fos* mRNA levels. Control tests with primers for synaptophysin mRNA revealed no change either *in vivo* or in brain slices,

demonstrating the selectivity of the above responses (data not shown). Moreover, the earlier appearance of AChE mRNA product under pyridostigmine administration (Fig. 2*a*, *bottom*) reflects an association between c-*fos* levels and the transcriptional control of key cholinergic proteins. Electrophysiological recordings in such slices revealed a pyridostigmine-induced increase in the amplitude and rate of rise of evoked population spikes in the CA1 area of the hippocampus, in response to stimulation of the Schaffer collaterals (Fig. 2*b*). This enhancement in summated neuronal activity demonstrated directly the increased excitability of the local circuit following pyridostigmine application.

Results from double-blind human studies testing pyridostigmine effects on 35 young healthy volunteers (in "peacetime," ref. 11, and unpublished data) as compared with those observed in 213 soldiers treated during the Gulf War (extension of ref. 5) resemble our current rodent data. In both human studies each individual was asked to report on a questionnaire, responding yes or no, regarding symptoms related to the drug. During peacetime, in agreement with previous reports[1,4], documented symptoms were mainly related to peripheral nervous system (PNS) functions (symptoms included abdominal pain, diarrhea, frequent urination, increased salivation, rhinorrhea and excess sweating) with an average of 18.8% (range 5.5–38.9%), whereas only 8.3% (range 0–16.6%) of participants reported symptoms related to CNS functions (headaches, insomnia, drowsiness, nervousness, difficulties in focusing attention and impaired calculation capacities) (Fig. 3, dashed bars). In contrast, extension of the reported study performed during the Gulf War[5], revealed that 23.6% (range 6.2–53.4%) of the 213 soldiers reported CNS symptoms, whereas only 11.4% (range 6.1–20.4%) reported PNS symptoms (Fig. 3, filled bars). In parallel, in control mice injected with 0.1 mg/kg pyridostigmine, serum BuChE activity was inhibited similarly to that measured in humans during peacetime (18.8 ± 3.5% in humans and 20.4 ± 5.5% in mice). Under these conditions, no inhibition of mouse brain AChE was measured (see also Fig. 1*b*). Injection of similar doses of pyridostigmine into stressed mice caused a significant inhibition of brain AChE, with a tendency toward limitation of BuChE inhibition (Fig. 3). Thus, PNS effects were relatively suppressed and CNS effects enhanced, probably because of either the restraint stress in mice or the psychological stress associated with war in humans.

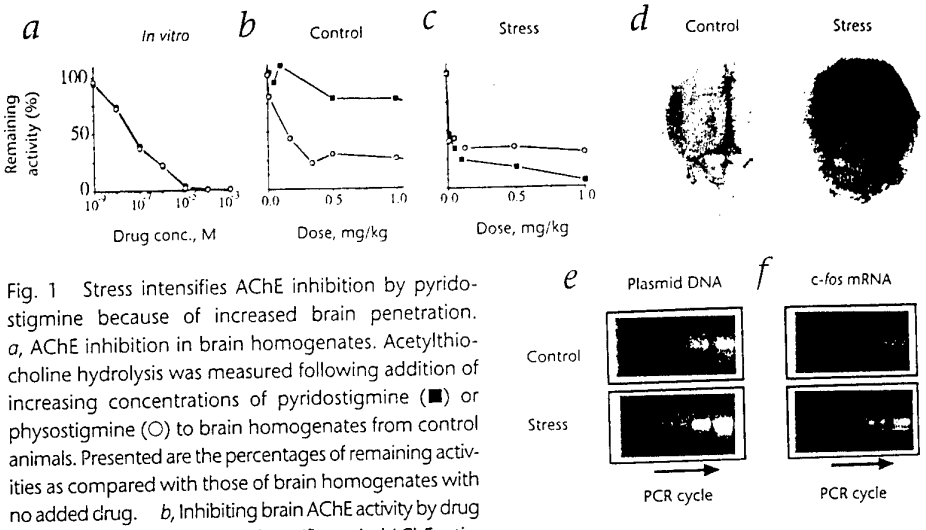

Fig. 1 Stress intensifies AChE inhibition by pyridostigmine because of increased brain penetration. *a*, AChE inhibition in brain homogenates. Acetylthiocholine hydrolysis was measured following addition of increasing concentrations of pyridostigmine (■) or physostigmine (○) to brain homogenates from control animals. Presented are the percentages of remaining activities as compared with those of brain homogenates with no added drug. *b*, Inhibiting brain AChE activity by drug injection. Percentage of normal specific cortical AChE activity was measured in brain homogenates prepared from nonstressed animals killed 10 min after i.p. injection of the noted doses of physostigmine ($n = 9$) or pyridostigmine ($n = 11$). Presented are the percentages of remaining activities as compared with those of brain homogenates from nonstressed, 0.9% NaCl-injected animals ($n = 12$). *c*, Pyridostigmine inhibition of brain AChE following stress. A forced swim test was followed 10 min later by injection of either 0.1 mg/kg pyridostigmine ($n = 8$), or physostigmine ($n = 5$). AChE activity measurements were as described in *b*. Presented are the percentages of remaining activities as compared with those of brain homogenates from similarly stressed, 0.9%-NaCl-injected animals ($n = 6$). *d*, Blood–brain barrier permeability following stress. Shown are representative brains dissected from anaesthetized animals, 10 min after intracardial injection of Evan's blue. The controls were nonstressed animals; dye was injected into stressed animals 10 min after the stressful session. *e*, Plasmid DNA penetration to the brain under stress. Control and stressed animals were injected i.p. with CMV AChE (ref. 8) plasmid. Proteinase K-treated brain homogenates were subjected to PCR amplification using a set of CMV-promoter forward primer and an AChE reverse primer. PCR product samples were withdrawn every third cycle, which allows for eightfold increases between samples. CMV AChE DNA was detected starting from cycle 21 in the brain of four out of four stressed animals. The PCR products from brain of control animals were considerably weaker and appeared only on cycle 24, indicating at least eightfold less plasmid DNA in control brains as compared with stressed ones. In two out of five control animals, no PCR product was detected. *f*, Kinetics of brain c-*fos* cDNA accumulation during RT-PCR amplification. Total RNA from mouse hippocampus was extracted using RNAclean (AGS, Heidelberg, Germany), its integrity verified by gel electrophoresis (evaluation of 2.0 ratio between 28S and 18S ribosomal RNA) and its quantity and purity from protein contamination evaluated by absorbance measures, the A_{260}/A_{280} ratio of 1.8 up to 2.0. c-*fos* cDNA was amplified following reverse transcription of equal amounts of total RNA samples from the brain of control or stressed animals. Kinetic follow-up of product accumulation was carried out as described in *e*. The earlier appearance of amplified c-*fos* cDNA, 20 min following stress session as compared with control, indicates a significant increase in the amount of c-*fos* mRNA under stress.

Our findings demonstrate significant correlation between stress and pyridostigmine-induced CNS effects. We confirmed the accepted notion that treating nonstressed mice with prophylactic doses of pyridostigmine does not inhibit CNS AChE, corresponding to unaffected CNS functions in nonstressed primates[9] or humans during peacetime[4]. Yet, similar treatment under stress conditions (in mice) was associated with increased brain penetration, significant inhibition of brain AChE activity, increased neuronal excitability and oncogene activation. This increase in c-*fos* mRNA levels may explain the induction of AChE transcription by the presence of a c-*fos* binding site in the mammalian AChE promoter[8,12]. It is of interest that we found that serum BuChE inhibition is suppressed under stress in a way similar to that seen in the PNS-related symptoms caused by pyridostigmine. The stress-

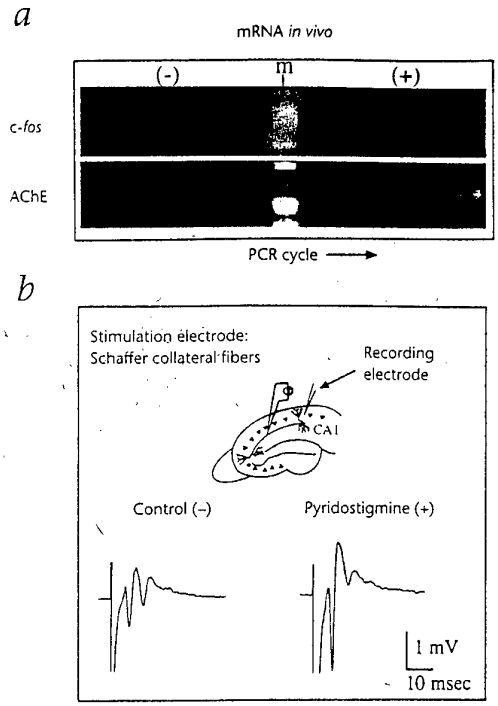

Fig. 2 Pyridostigmine enhances neuronal excitability and increases oncogene mRNA levels. *a*, The kinetics of brain c-*fos* and AChE mRNA accumulation during RT-PCR amplification. RNA was extracted and reverse-transcribed as described in Fig. 1. The earlier appearance of the amplified PCR product 20 min after injection of 2 mg/kg pyridostigmine (+) as compared with 0.9% NaCl (–) indicates an increase in the amount of c-*fos* (*top*) and AChE mRNA (*bottom*) under pyridostigmine exposure. *b*, Extracellular evoked potentials. Cortico-hippocampal slices (400 μm thick) were cut using a vibratome (Vibroslice, Campden Instruments, Loughborough, UK) and were placed in a humidified holding chamber, continuously perfused with oxygenated (95% O_2, 5% CO_2) artificial cerebrospinal fluid (aCSF)[9]. Schaffer collateral fibers were stimulated with a bipolar tungsten stimulating electrode, and extracellular evoked potentials were recorded in the cell-body layer of the CA1 area of the hippocampus. Single response to supramaximal stimulus intensity (1.5 times stimulus the intensity of which caused maximal response) is drawn before (–) and 30 min after (+) addition of pyridostigmine (1 mM) to the perfusing solution.

induced suppression in PNS effects reported by soldiers during wartime as compared with those reported by volunteers tested during peacetime could be due to enhanced drug scavenging in peripheral tissues, for example, by adrenaline induction of the cytochrome P-450 scavenging system[13]. Alternatively, or in addition, drug concentration in the periphery could be reduced because of the dilution effect caused by the stress-induced brain penetrance. Hormonal changes have been known to disrupt the integrity of the intricate microglial connections blocking access of large molecules to the brain[14], which may explain at least some of the observed changes under stress treatment. However, it is conceivable that AChE inhibition has an additive effect (in addition to these hormonal effects on microglial connections) thus increasing blood–brain barrier permeability. Further studies will be required to reveal whether AChE is expressed in microglia and to examine their potential response to its inhibition.

In view of the reports of blood–brain barrier disruption in Alzheimer's disease[15], our current data may explain the effects of low doses of pyridostigmine, which affected electroencephalograph (EEG) patterns, attention and short-term memory in Alzheimer's disease patients[16], as well as reports of myasthenic patients who developed, under routine pyridostigmine doses, CNS symptoms that regressed following withdrawal of the drug[17]. Susceptibility to CNS symptoms may particularly be expected when free drug levels are increased in the circulation because of reduced capacities for drug scavenging, for example, in carriers of the "atypical" *BCHE* gene mutation[18]. Other potential reasons for such CNS effects include liver malfunctioning, which is known to reduce BuChE levels in the circulation[19]. Individuals subjected to drugs of abuse (that is, cocaine) should also be vulnerable to cholinesterase inhibitors, as BuChE is the major cocaine scavenger in human blood[20].

That increased neuronal excitability and c-*fos* mRNA levels were observed following application of pyridostigmine both *in vivo* and in hippocampal slices maintained *in vitro* suggests that this can be the direct outcome of pyridostigmine access to the brain. The early immediate transcriptional response following pyridostigmine application can be attributed to AChE inhibition, increasing acetylcholine levels, subsequent massive activation of muscarinic receptors[21] and corresponding induction of signal transduction processes. As central cholinergic neurotransmission systems are normally involved in stress responses[22], access of pyridostigmine to the brain can be expected to add yet more "stress-like" symptoms to those associated with the war situation. That some of the associated stress effects[22] parallel those reported during the Gulf War[5] further strengthens this hypothesis.

Although this study describes acute, short-term effects induced by pyridostigmine under stress, it does not yet address the intricate long-term consequences reported by Gulf War veterans[23]. However, the transcriptional responses observed in our study predict the induction of secondary and tertiary processes with unknown consequences, depending on complex and variable elements. For example, the observed pyridostigmine-induced enhancement of the capacity to produce AChE reflects a potential selective feedback mechanism that would diminish cholinergic overactivation. If this is a general mechanism, the CNS symptoms attributed to pyridostigmine may shed new light on previously unforeseen complications attributable to various peripherally acting drugs. The enhanced capacity of systematically administered plasmid DNA to reach the brain under stress may further explain the vulnerability of stressed animals to CNS viral infections[24]. Further understanding of the mechanisms underlying these alterations in blood–brain barrier permeability might have far-reaching clinical implications with regard to delivery of drugs or gene therapy agents to the brain. Hence, our study predicts that compounds considered to be limited to the periphery may become centrally active under stress conditions.

Methods

Stress induction. Stress was induced in adult FVB/N mice by two 4-min forced swim sessions with a 4-min rest interval[7]. Ten minutes following stress, animals were injected i.p. with 0.9% NaCl (control), pyridostigmine (Research Biochemical International, Natick, Massachusetts) or physostigmine (Sigma) at the noted doses. Animals were decapitated 10 min after injection, trunk blood was collected[7], and the cerebral cortex was quickly dissected and homogenized in solution D (10 mM Tris-HCl, pH 7.4, 1M NaCl, 1% Triton X-100, 1 mM EDTA, 1:10 wt/vol)[25].

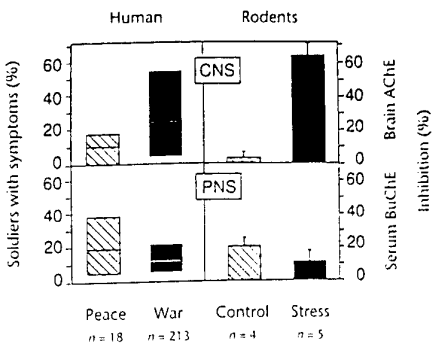

Fig. 3 Pyridostigmine effects in humans during peace and war and in nonstressed and stressed rodents. *left* (humans), Results of a double-blind, placebo-controlled study (extension of ref. 10) (dashed bars, "peacetime"). Pyridostigmine (n = 18) or placebo (n = 17) were administered to healthy young male volunteers. Symptoms were reported at the end of the study. Presented are ranges (%) of soldiers reporting pyridostigmine-induced symptoms related to CNS (*top*) or PNS (*bottom*). During the Gulf War 213 male soldiers aged 18–22 years were questioned, 24 hours after initiation of pyridostigmine treatment[3] (filled bars). Mean values for human data are marked by horizontal lines across the relevant bars. *right* (rodents), Summary of measured brain AChE inhibition (top) and serum BuChE inhibition in mice (bottom) 10 minutes following injection of 0.1 mg/kg pyridostigmine in nonstressed (control, n = 4), and stressed (n = 5) mice. Percent inhibition (standard deviation was calculated in comparison with the average activity calculated in noninjected, not stressed (n = 12) and stressed (n = 6) animals.

AChE activity measurements. Acetylthiocholine (ATCh) hydrolysis levels were determined spectrophotometrically in nanomoles ATCh per minute per milligram brain protein, as previously described[26]. BuChE activity in serum was measured using butyrylthiocholine (BTCh) as substrate. In both cases, selective inhibitors were employed to suppress nonspecific hydrolysis[25].

Determination of blood–brain barrier permeability. *Evan's blue.* Anesthetized animals (Nembutal, 60 mg/kg) were injected intracardially with 0.1 ml of 2% of the albumin-binding dye Evan's blue in 0.9% NaCl. Following perfusion with 0.9% NaCl, brains were removed and homogenized, and dye concentration was determined spectrophotometrically[27]. *Plasmid DNA.* CMV-driven AChE plasmid DNA (ref. 8, 100 µg, ca. 6 kb) in 0.1 ml of 0.9% of NaCl was injected i.p. into control or stressed animals. Animals were killed 20 min after injection; trunk blood and brain were collected; and plasmid DNA was detected by kinetic follow-up of PCR amplification in tissue homogenates treated with proteinase K (100 µg/ml, overnight incubation, 65 °C).

Reverse transcriptase-PCR. Brain c-*fos* cDNA was amplified by RT-PCR using as primers 1604(+): 5'–TCTTATTCCGTTCCCTTCGGATTCTCCGTT–3' and 2306(–): 5'–TCTTATTCCGTTCCCTTCGGATTCTCCGTT–3'. Brain AChE cDNA was amplified using as primers 375(+): 5'–AGACTGCCTGTATCTTAATGTGTGGACACC–3' and 1160(–): 5'–CGGCTGATGAGAGATTCATTGTCTTTGCTG–3'. Numbers denote nucleotide positions in the GenBank c-*fos* sequence (accession no. V00727) or in the mouse AChE cDNA sequence[28], respectively. Samples of each reaction mixture (10 µl) were removed every third cycle from 18 to 39, separated by electrophoresis and stained with ethidium bromide[26].

Electrophysiological recordings. Extracellular potentials were recorded in hippocampal slices maintained *in vitro*[10]. Schaffer collateral fibers were stimulated with a bipolar tungsten stimulating electrode. Recording glass microelectrodes were located in the CA1 area.

Acknowledgments

We thank Z. Selinger, J. Yarom (Jerusalem) and E. Lev (I.D.F.) for helpful discussions and for help with experiments, and D. Darom for expert photography. Supported in part by the US Army Medical Research and Development Command (to H.S.), and by a research grant from the Charles E. Smith Laboratory for collaborative research, the National Institute for Psychobiology in Israel (to A.F. & H.S.).

RECEIVED 4 SEPTEMBER; ACCEPTED 17 OCTOBER 1996

1. Taylor, P. Cholinergic agonists. *and* Anticholinesterase agents. in *The Pharmacological Basis of Therapeutics*, 8th edn. (eds. Gilman, A.G., Rall, T.W., Nies, A.S. & Taylor, P.) 122–130, 131–147 (Pergamon, New York, 1990).
2. Deyi, X., Linxiu, W. & Shuqiu, P. The inhibition and protection of cholinesterase by physostigmine and pyridostigmine against soman poisoning *in vivo*. *Fundam. Appl. Toxicol.* 1, 217–221 (1981).
3. Diruhumber, P., French, M.C., Green, D.M., Leadbeater, L. & Stratton, J.A. The protection of primates against soman poisoning by pretreatment with pyridostigmine. *J. Pharmacol.* 31, 295–299 (1979).
4. Borland, R.G., Breman, D.H. & Nicholson, A.N. Studies on the possible central and peripheral effects in man of a cholinesterase inhibitor (pyridostigmine). *Hum. Toxicol.* 4, 293–300 (1985).
5. Sharabi, Y. *et al.* Survey of symptoms following intake of pyridostigmine during the Persian Gulf War. *Isr. J. Med. Sci.* 27, 656–658 (1991).
6. Sharma, H.S., Cervos-Navarro, J. & Dey, P.K. Increased blood–brain barrier permeability following acute short-term swimming exercise in conscious normotensive young rats. *Neurosci. Res.* 10, 211–221 (1991).
7. Melia, K.M., Ryabinin, A.E., Schroeder, R., Bloom, F.E. & Wilson, M.C. Induction and habituation of immediate early gene expression in rat brain by acute and repeated restraint stress. *J. Neurosci.* 14, 5929–5938 (1994).
8. Ben Aziz-Aloya, R. *et al.* Expression of a human acetylcholinesterase promoter-reporter construct in developing neuromuscular junctions of *Xenopus* embryos. *Proc. Natl. Acad. Sci. USA* 90, 2471–2475 (1993).
9. Blick, D.W. *et al.* Acute behavioral toxicity of pyridostigmine or soman in primates. *Toxicol. Appl. Pharmacol.* 126, 311–318 (1994).
10. Friedman, A. & Gutnick, M.J. Intracellular calcium and control of burst generation in neurons of guinea-pig neocortex *in-vitro*. *Eur. J. Neurosci.* 1, 374–381 (1989).
11. Glickson, M. *et al.* The influence of pyridostigmine on human neuromuscular functions — studies in healthy human subjects. *Fundam. Appl. Toxicol.* 16, 288–298 (1991).
12. Ekstrom, T.J., Klump, W.M., Getman, D., Karin, M. & Taylor, P. Promoter elements and transcriptional regulation of the acetylcholinesterase gene. *DNA Cell Biol.* 12, 63–72 (1993).
13. Ehrhart-Bornstein, M. *et al.* Adrenaline stimulates cholesterol side-chain cleavage cytochrome P450 mRNA accumulation in bovine adrenocortical cells. *J. Endocrinol.* 131, 5–8 (1991).
14. Brust, P. Blood–brain-barrier transport under different physiological and pathophysiological circumstances including ischemia. *Exp. Pathol.* 42, 213–219 (1991).
15. Harik, S.I. & Kalaria, R.N. Blood-brain-barrier abnormalities in Alzheimer's disease. *Ann. N. Y. Acad. Sci.* 640, 47–52 (1991).
16. Agnoli, A., Martucci, N., Manna, V., Conti, L. & Fioravanti, M. Effect of cholinergic and anticholinergic drugs on short term memory in Alzheimer's dementia: A neuropsychological and computerized electroencephalographic study. *Clin. Neuropharmacol.* 6, 311–323 (1983).
17. Iwasaki, Y., Wakata, N. & Sinoshita, M. Parkinsonism induced by pyridostigmine. *Acta Neurol. Scand.* 78, 236 (1988).
18. Loewenstein-Lichtenstein, Y. *et al.* Genetic predisposition to adverse consequences of anti-cholinesterases in 'atypical' BCHE carriers. *Nature Med.* 1, 1082–1085 (1995).
19. Whittaker, M. Cholinesterases. *Monogr. Hum. Genet.* 65–85 (1986).
20. Schwarz, M., Glick, D., Loewenstein, Y. & Soreq, H. Engineering of human cholinesterases explains and predicts diverse consequences of administration of various drugs and poisons. *Pharmacol. Ther.* 67, 283–321 (1995).
21. Brown, D.A. Slow cholinergic excitation - a mechanism for increasing neuronal excitability. *Trends Neurosci.* 6, 302–306 (1983).
22. McEwen, B.S. & Sapolsky, R.M. Stress and cognitive function. *Curr. Opin. Neurobiol.* 5, 205–216 (1995).
23. Gavaghan, H. NIH panel rejects Persian Gulf syndrome. *Nature* 369, 8 (1994).
24. Ben-Nathan, D., Lustig, S. & Danenberg, H.D. Stress-induced neuroinvasiveness of a neurovirulent noninvasive Sindbis virus in cold or isolation subjected mice. *Life Sci.* 48, 1493–1500 (1991).
25. Neville, L.F., Gnatt, A., Padan, R., Seidman, S. & Soreq, H. Anionic site interactions in human butyrylcholinesterase disrupted by two single point mutations. *J. Biol. Chem.* 265, 20735–20738 (1990).
26. Seidman, S. *et al.* Synaptic and epidermal accumulations of human acetylcholinesterase are encoded by alternative 3'-terminal exons. Mol. Cell. Biol. 15, 2993–3002 (1995).
27. Uyama, O. *et al.* Quantitative evaluation of vascular permeability in the gerbil brain after transient ischemia using Evans blue fluorescence. *J. Cerebral Blood Flow Metab.* 8, 282–284 (1988).
28. Rachinsky, T.L. *et al.* Molecular cloning of mouse acetylcholinesterase: Tissue distribution of alternatively spliced mRNA species. *Neuron* 5, 317–327 (1990).

Reprinted from

MOLECULAR BRAIN RESEARCH

Molecular Brain Research 51 (1997) 179–187

Research report

In vitro phosphorylation of acetylcholinesterase at non-consensus protein kinase A sites enhances the rate of acetylcholine hydrolysis

Mirta Grifman [a], Ayelet Arbel [a], Dalia Ginzberg [a], David Glick [a], Sharona Elgavish [a,b], Boaz Shaanan [a,b], Hermona Soreq [a,*]

[a] *Department of Biological Chemistry, Institute of Life Sciences, Hebrew University of Jerusalem, Jerusalem 91904, Israel*
[b] *Wolfson Center for Applied Structural Biology, Institute of Life Sciences, Hebrew University of Jerusalem, Jerusalem 91904, Israel*

ELSEVIER

SCOPE AND PURPOSE

MOLECULAR BRAIN RESEARCH is a special section of **Brain Research** which provides a medium for prompt publication of studies on molecular mechanisms of neuronal, synaptic and related processes that underlie the structure and function of the brain. Emphasis is placed on the molecular biology of fundamental neural operations relevant to the integrative of the nervous system.

TYPES OF PAPERS

1. **Interactive Reports** are papers describing original, high quality, fundamental research in any area of Neuroscience. These will first appear electronically on the WWW (**http:/www.elsevier.com/locate/bres** or **http://www.elsevier.nl/locate/bres**) and published soon after in the relevant section of *Brain Research*. The on-line version may include additional data sets, 3-D/confocal images, animations, etc., and be linked to relevant on-line databases. Comments from readers may be appended later in a linked ***Discussion Forum*** at the discretion of an appointed Moderator.

2. **Research Reports** reporting results of original fundamental research in any branch in the brain sciences. It is expected that these papers will be published about six months after acceptance.

3. **Short Communications** reporting on research which has progressed to the stage when it is considered that the results should be made known quickly to other workers in the field. The maximum length allowed will be 1500 words or equivalent space in tables and illustrations. It is expected that Short Communications will be published about three months after acceptance.

4. **Protocols:** full-length protocols in any area of Neuroscience, to be published in the journal section *Brain Research Protocols*. Updates on published protocols submitted by the authors thereof, describing new developments which are of sufficient interest to the neuroscience community, but which do not warrant a completely new submission, will be published as **Protocol Updates**. The maximum length allowed will be 1500 words or equivalent space in tables and illustrations. Comments on published Protocols describing useful hints and "tricks" related to any aspect of the Protocol, such as timing, equipment, chemicals, troubleshooting, etc., will be published in the on-line version of the journal as linked **Technical Tips** at the discretion of the Editor.

SUBMISSION OF MANUSCRIPTS

Submission of a paper to ***Molecular Brain Research*** is understood to imply that it deals with original material not previously published (except in abstract form), and that it is not being considered for publication elsewhere. Manuscripts submitted under multiple authorship are reviewed on the assumption that all listed authors concur with the submission and that a copy of the final manuscript has been approved by all authors and tacitly or explicitly by the responsible authorities in the laboratories where the work was carried out. If accepted, the article shall not be published elsewhere in the same form, in either the same or another language, without the consent of the Editors and Publisher. The Publisher and Editor regret that they are unable to return copies of submitted articles except in the case of rejected articles, where only one set of manuscript plus figures will be returned to the author.

Manuscripts in English should be organised according to the ***Brain Research*** *Guidelines for the Submission of Manuscripts* and sent to the appropriate address shown below. Authors should state clearly the section of the journal for which the article/Interactive Report should be considered.

Research Reports & Short Communications:
Professor D.P. Purpura
Brain Research, Office of the Dean
Albert Einstein College of Medicine
Jack and Pearl Resnick Campus
1300 Morris Park Avenue
Bronx, NY 10461, USA
Tel.: (1) (718) 430-2387
Fax: (1) (718) 430-8980
E-mail: brain@aecom.yu.edu

Interactive Reports:
Professor F.E. Bloom
Brain Research Interactive
Dept. of Neuropharmacology
The Scripps Research Institute
10666 N. Torrey Pines Road
La Jolla, CA 92037, USA
Fax: (1) (619) 784-8851
E-mail: smart@scripps.edu
Website: http://smart.scripps.edu

Protocols & Protocol Updates:
Dr. Floris G. Wouterlood
Department of Anatomy
Faculty of Medicine
Free University
van der Boechorststraat 7
1081 BT Amsterdam
The Netherlands
Fax: (31) (20) 444-8054
E-mail: fg.wouterlood.anat@med.vu.nl

Correspondence regarding ***accepted*** *manuscripts relating to proofs, publication and reprints should be sent to:*
Brain Research, Elsevier Science B.V., P.O. Box 2759, 1000 CT Amsterdam, The Netherlands. Tel. (31) (20) 485-3474; Fax: (31) (20) 485-3271; E-mail: a.prukar@elsevier.nl.

EDITORIAL BOARD

GUIDELINES FOR THE SUBMISSION OF MANUSCRIPTS

These can be found in the "front matter" of the last issue of each volume of the journal.
The preferred medium for *final* submission is on disk with accompanying manuscript (see "Electronic manuscripts").

Offprint

Concepts in Gene Therapy

Editors
Michael Strauss · John A. Barranger

Walter de Gruyter · Berlin · New York 1997

9. Potential Antisense Oligonucleotide Therapies for Neurodegenerative Diseases

Mirta Grifman, Efrat Lev-Lehman, Dalia Ginzberg, Fritz Eckstein, Haim Zakut and Hermona Soreq

9.1 Introduction

For the first time in the history of neuropharmacological research, it is possible to design short synthetic strands of DNA as effectors of neuromodulatory events or phenomena. Antisense oligodeoxynucleotides (AS-ODNs) are short DNA strands often protected by chemical modification from nucleolytic degradation. They are aimed at suppression of the expression of a target gene or genes or prevention of the enhancement in its expression in cases where such enhancement takes place. They operate by creating stable hybrids with their target sequences in a highly specific and highly selective manner. Once such hybrids are formed, they may remain as such (which temporarily prevents translation) or degrade (which destroys the target mRNA altogether). The well-defined requirements for hybridization (i.e. complementarity and length of the interacting sequences, ionic strength and pH conditions) provide a preliminary option for simple design of such AS-ODN drugs with a high probability that they will efficiently hybridize with their mRNA targets.

Antisense technology lies somewhere between gene and conventional therapies. Like conventional drugs, it involves the administration of a synthetic compound (in this case, an oligodeoxyribonucleotide or an analog thereof; for a chain of 20 nucleotides, this implies a molecular weight of ca. 6,000 g/mol). Also, it is intended to prevent the functioning of a particular protein, similarly to most conventional drugs, and it may be used for short or long periods and can cause transient or long-term side effects like many such drugs. This further means that the development of antisense drugs depends on criteria similar to those familiar for conventional drugs: the effective dose should be as low as possible, the therapeutic window as wide as possible, delivery should be simple and convenient, drug stability high and adverse responses minimal. However, antisense drugs are based on gene sequences and aimed

at interaction with such sequences, rather than at binding to particular protein(s). Their capacity to prevent the functioning of the protein products of their target genes is hence indirect. Unlike gene therapy protocols, they must be administered repeatedly; however, their specificity is expected to be far higher than that of protein blockers, thanks to the basic parameters characterizing the hybridization reaction between oligonucleotide chains and the target mRNA. Also, since they interact with mRNAs and not proteins, the number of target molecules they should encounter in a cell is inevitably smaller than the number of molecules to be blocked by protein inhibitors. Therefore, the effective dose of antisense drugs can be lower than that of protein inhibitors. In contrast, the mode of AS-ODNs delivery poses considerable difficulties, and chemical modification(s) are a necessary prerequisite for improving the rather poor stability of unprotected DNA chains. At the same time, administration of an AS-ODN is far simpler than gene therapy and can therefore be available to larger numbers of patients. Lastly, little is yet known about side effects and ways to avoid them.

In vivo suppression of gene expression with AS-ODNs has been demonstrated in various vertebrates including ducks, rats, mice, and pigs by targeting mRNAs encoding diverse proteins such as MYC, cdk2, RAS and NF-κB (1, 2). Direct intracerebroventricular (ICV) administration of AS-ODNs has been shown in several cases to elicit specific mRNA reduction in the brain of rats, resulting in detectable behavioral changes (3, 4, 5, see details below). These experiments prompted intensive research efforts directed toward developing the potential of antisense-based therapies for various diseases of the nervous system and several antisense "drugs" directed toward mRNA transcripts expressed in brain have already reached clinical trials (1, 2). In the following, we discuss the accumulated experience with neurochemically-relevant examples of this concept.

At the chemical level, antisense oligodeoxynucleotides (AS-ODNs) are designed to operate by sequence-specific binding to preselected RNA targets. The underlying physical-chemical principle for such drug-target interaction is hydrogen bonding between the pharmacologic agent and heterocyclic base moieties in its RNA target (6), which conceptually derives from the synthesis of analogs of nucleic acids as model polymer systems (7). These analogs contain the heterocyclic bases of nucleic acids but differ from the natural polymer in the connecting backbone. As an example, polymers derived from 1-vinyl uracil and 1-vinyl adenine were shown to display inhibitory activity against RNA viruses (8). These and other types of synthetic analogs of nucleic acids were described by Halford and Jones nearly 30 years ago as future drugs. The authors argued that as nuclease-resistant uncharged compounds, these analogs might be taken up by cells more readily than unmodified charged oligonucleotides, and would therefore interfere with the function of mRNA in biological systems. A yet more important aspect of these analogs was their longevity. This was first demonstrated for interferon induction by modified double stranded RNA (9). Nuclease-resistant phosphorothioate RNA was then presented as a potentially more effective inducer of interferon by virtue of its longer half-life *in vivo*. This pharma-

cological advantage has been used since then for blocking various viral sequences (see, for example,10, 11, 12). The same concept is currently being exploited in the design of possible antisense drugs for different uses, including neuropharmacology.

Like all drugs, AS-ODNs should be tested for their dose and time dependence. Thanks to their special mode of functioning through hybridization, they would operate only in those cells expressing their target mRNA transcripts. This leaves their vulnerability to nuclease destruction as a major deficit hampering the development of AS-ODNs into practical drugs, which leads us into the concept of their phosphorothioate modification.

9.2 The Concept of Phosphorothioate Modifications

While the principle of antisense mechanisms has been verified with unmodified oligomers, their therapeutic applications require stabilization for improved half-life. Several types of chemical modification were attempted for this purpose over the years (for reviews, see 1, 2, 13). Of these, the phosphorothioate protection of internucleotide bonds is the one used most frequently.

Phosphorothioate modification of oligodeoxynucleotides has been in existence now for 30 years. It involves the substitution of a non-bridging oxygen atom in normal phosphate backbones in ODNs with a sulfur atom (14, 15, 16). Phosphorothioate oligomers are water soluble, easy to produce by automated procedures and resistant to enzymatic breakdown. Interestingly, cells take up phosphorothioate oligonucleotides more easily than was originally thought. This occurs not only by passive diffusion across the cell membrane but by endocytosis as well.

Once the synthesis of phosphorothioated nucleotides and oligonucleotides was demonstrated, researchers proceeded to demonstrate the use of such oligonucleotides to improve resistance of cells to viral infection in culture (9) and *in vivo* (17). By the mid-1970s, novel solution synthesis methods were exploited to obtain a 13-mer oligodeoxyribonucleotide complementary to a portion of a reiterated terminal sequence in Rous sarcoma virus (RSV). This enabled Zamecnik and Stephenson (18) to assess the influence of such an oligonucleotide on the course of cellular infection by RSV. The researchers also investigated the use of 3' and 5' terminal protection, via source derivatization, as a means of preventing antisense oligomer degradation by exonucleases. This strategy is now widely emulated, using different types of nucleic acid modifications.

Highly efficient, yet uncomplicated automated systems for protein sequencing (19) and oligonucleotide synthesis (20, 21) became widely available at the beginning of the 1980s as part of the advent of genetic engineering and biotechnology. Simple-to-use automated DNA sequencing was successfully marketed in 1987. At about the same time, automated synthetic chemistries and product purification protocols for

phosphorothioate oligonucleotide analogs were commercialized. This made available to investigators interested in the antisense approach the necessary technology to more readily conduct their experimental programs.

The main potential value of phosphorothioate oligonucleotides as neurochemically active drugs lies in the specificity of the hybridization reaction. The repertoire of proteins that are expressed in the brain is far higher than in any other tissue, and many of these proteins share sequence homologies with other proteins. This leads to non-specific interactions of numerous drugs with proteins that resemble their intended target. In contrast, once phosphorothioate antisense oligonucleotides are actively taken up by cells, they find their target mRNA chains and selectively associate with them to form highly specific RNA:DNA double-strands. Phosphorothioated oligonucleotides further increase, within these cells, the activity of a particular ribonuclease – RNaseH – which selectively destroys the double stranded RNA chains. Therefore, the nuclease resistance of phosphorothioate AS-ODNs, their functional specificity and their capacity to lead to destruction of their target mRNA make this approach advantageous over the use of protein inhibitors to block expression of protein products of single genes. This would particularly be the case when these protein products, but not nucleotide sequences, resemble homologous molecules.

Three questions which are often asked with regard to the use of AS-ODNs refer to the optimal length of AS-ODNs, to the preferred concentration of such compounds and to the choice of the location of these AS-ODNs within their target mRNA sequence. A recent study (22), demonstrated that AS-ODN-mediated inhibition is strongly dependent on polymer length and concentration but almost independent of location of the target sequence along the mRNA chain. The study employed microinjection into *Xenopus* oocytes of the mRNA for α-amino-3-hydroxy-5-methyl-4-isoxasole propionate receptor and was based on electrophysiological measurement of remaining receptors. The authors compared phosphorothioate AS-ODNs with unmodified, phosphodiester polymers. The choice of a functionally active AS-ODN should hence be an essential initial phase in each study which involves this technology. In both cases they observed length dependence, with half-maximal inhibition decreasing from 9.9 nucleotides for non-protected AS-ODNs to 7.6 for the phosphorothioated ones. Phosphorothioate and phosphodiester AS-ODNs of 12 and 15 nucleotides, respectively, sufficed to block 95% of their target mRNA. However, phosphorothioate protection reduced the AS-ODN concentration needed for half-maximal inhibition from 18 ng/μl to as low as 0.19 ng/μl for 12-mer oligos. This 100-fold difference may make an analytically useful compound into an economically sensible drug, which emphasizes the value of phosphorothioate protection for AS-ODN drug design. Octamer AS-ODNs dispersed throughout the target mRNA, from the initiator AUG to the 3'-untranslated region, reduced by 70% the level of the tested mRNA (22). It should be noted, however, that this is one specific case; with regard to other genes, certain sites on the mRNA may make better targets than others. In another study, 18 different AS-ODNs were designed against various domains in a specific mRNA sequence, but only 3 of those were satisfactorily effective (23). The

Tab. 9.1 Historical milestones in the development of phosphorothioate antisense technology

	Milestone	Example References
1	Synthesis of phosphorothioated nucleotides	14
2	Synthesis of nuclease-resistant nucleic acid analogs	7
3	Induction of interferon *in vitro* and *in vivo* by modified double stranded RNA	9, 17
4	Demonstration of inhibitory activity against RNA viruses	8
5	Suppression of Rous sarcoma virus infection by a 13-mer AS-ODN	18
6	Automation of protein sequencing	19
7	Automation of oligonucleotide synthesis	20, 21
8	Pharmacokinetics and toxicology studies of phosphorothioate AS-ODNs	24
9	Demonstration of sequence-independent protein binding activity of AS-ODNs	24, 79

choice of a functionally active AS-ODN should hence be an essential initial phase in each study which involves this technology.

When administered to live animals, phosphorothioate oligonucleotides were argued to be unevenly distributed in different tissues and organs, with kidney, liver and bone marrow being their main targets (24). At least part of their effects in these tissues may be due to AS-ODN-protein interactions, particularly with nuclear proteins in young, proliferating bone marrow cells (25). Consequently, their main toxicological outcome is paucity of blood platelets, thrombocytopenia (24). However, it is quite clear that what disadvantages the phosphorothioates have or might have are far outweighted by the advantages that this particular modification offers as compared to the potential use of unmodified AS-ODNs or of those carrying other modifications. This is clearly seen by the fact that almost all publications in the antisense field employ this particular modification (for reviews see 1, 2, 26). This development sheds new light on the phosphorothioate invention, the importance of which could not be fully imagined beforehand, and which transported the antisense technology from a basic biomedical science tool to a pharmacological approach of potentially great clinical value. Table 9.1 presents some key historical milestones for the development of phosphorothioate antisense technology.

9.3 False Positive and False Negative Outcome of AS-ODNs

Like many other therapeutic protocols, the use of AS-ODNs may lead to a false positive or a false negative outcome. False positive results will be obtained when the

functioning of the target protein is suppressed through mechanisms other than AS-ODN-mRNA hybridization. For example, the host cells may respond to the mere presence of the AS-ODN agent by suppressing production of many proteins, including the intended one. This may imply that the target protein belongs to a susceptible subgroup of gene products whose expression is vulnerable to external stimuli. Alternatively, the selected AS-ODN may exert its effect through non-sequence dependent competition with endogenous host genes or mimic bacterial or viral motifs and therefore elicit responses characteristic of attacks by such entities. Stein and Krieg refer to such false positives in their recent editorial (27). They point out that a positive drug effect is what drug developers aim for; however, such false positives may become a dangerous precedence for subsequent development of other drugs using the antisense principle.

A false negative outcome of AS-ODNs may be yet more frustrating than a false positive, as in this case the AS-ODN agent totally fails to suppress the functioning of the protein translated from its target mRNA. This may happen if the protein in question is very stable, if it is present in the cell in high levels or when total RNA transcription is enhanced as a reaction to the treatment. Worse, yet, it is possible to predict that the suppression effect of certain AS-ODNs will last only very briefly, as it will immediately elicit a selective feedback response leading to increase in the level of its target mRNA. Finally, complex combinations of all of the above possibilities may further obscure the picture, preventing evaluation of the mechanism(s) of response. Also, AS-ODNs targeted to consensus domains in genes that belong to large families may interact with a certain region in many genes (for example, the sequence encoding the membrane spanning domain in a specific family of receptors). Suppression of several receptors may in this case, be wrongly interpreted as general toxicity when in fact it represents a true antisense mechanism, albeit to many sequences.

All this does not preclude the antisense approach, neither does it imply that in using this new technology one encounters more difficulties than when developing conventional drugs. It is conceivable that *any* drug causes complex feedback responses and that false positives and negatives appear for numerous reasons in *any* case of rational drug design. However, as approval of new drugs for human use is increasingly more difficult, one should be aware of the pitfalls that lie ahead, even more so when the drug involved is based on human genome data.

9.4 Drug Delivery

The obvious difficulty in delivery of AS-ODN drugs to the brain stimulated considerable efforts toward solving this problem, and several innovative approaches have been developed which improve the penetration of AS-ODNs into the brain and the targeting of such molecules to specific brain regions. At the mechanical level, high-flow microinfusion at a constant flow rate of 3 µl/min into the gray matter distributes

macromolecules into an area with a 1.5 cm radius within 12 hr. (28). This may ascertain that the delivered AS-ODN will be distributed throughout a certain nucleus in the human brain. The concentration of delivered material is rather uniform, which is important for preventing toxicity. A totally different delivery approach involves the use of the avidin-biotin conjugation reaction for improved protection of AS-ODNs against serum nuclease degradation (29). According to this concept the AS-ODN agents are monobiotinylated at their 3'-end. When reacted with avidin, they form tight, nuclease-resistant complexes with 6-fold improved stability over non-conjugated ODNs. A major concern regarding this approach is that the tight complex may prevent the subsequent uptake of these well-protected agents into cells. This additional difficulty may be solved by the use of liposomes for AS-ODN delivery (30). While these phospholipid vesicles were mainly introduced into the field to treat tumors, they may be of value also for delivery into the brain (31). A method which combines the lipophilic advantage of liposomes with the efficiency of direct conjugation is based on chemical conjugation of cholesteryl moieties to the AS-ODN agent (32). When conjugated to the 5'end of a phosphorothioate AS-ODN, the elimination half-life of these agents is shortened (from 55 to 23 hr). The cholesteryl oligonucleotides suppress their target mRNAs in a sequence-specific manner in spite of their reduced bioavailability. However, they are hepatotoxic at concentrations above 1 mg/kg.

The main obstacle for AS-ODN transport into the brain is the blood brain barrier (BBB). This capillary endothelial wall may be penetrated by ICV drug infusion or hyperosmotic treatment (i.e. using mannitol), by using liposomes or by coupling the transported agent to a transport peptide that is known to enter the brain by absorptive or receptor-mediated transcytosis. For example, a monoclonal antibody to the transferrin receptor operates as an efficient BBB transporter (31, 33). When injected intravenously, it concentrates the coupled agent in brain (5-fold over plasma concentration) within 5 hr. The coupling may be chemical or biological (i.e. through avidin-biotin connection). In this case as well, the question arises to what extent such complexes will disintegrate once they reach the inner side of the BBB and enter their target neurons. However, the method certainly increases BBB penetration. Brain oligonucleotide uptake was recently shown to be improved by this method to the extent that 0.1% of the injected dose reach brain within 60 min following intravenous injection (comparable to the brain uptake of morphine) (34).

9.5 Antisense Modulation of Behavioral Phenotypes in Mammals

While several AS-ODN drugs are currently being tested in clinical trials, none of them is yet designed for treating neurodegenerative disease, probably due to the complex and yet unraveled mechanisms underlying the development of such diseases

which has prevented the identification of an appropriate target mRNA. However, ample research is being performed which tackles the issue of modulating behavioral phenotypes in mammals, an inevitable phase preceding serious development of rationally designed drugs.

Over the past few years, AS-ODNs were employed for *in vivo* modulation of diverse behavioral phenotypes. Several of those were aimed at preventing anxiety. AS-ODNs which suppress the levels of corticotropin-releasing hormone when ICV infused at three 30 μg doses 12 hr apart, were shown to attenuate social defeat-induced anxiety in rats (4). Direct injection of c-fos AS-ODNs into the amygdala suppressed the c-fos expression induced by anxiety and functioned similarly to antianxiety drugs (35, 36). Infusion of AS-ODNs directed against the V1 vasopressin receptor gene into the septum suppressed social discrimination abilities and anxiety-related behavior in rats (37). Other AS-ODNs had more general effects. An increase in cholinergic neurotransmission occurred in rats injected with AS-ODNs to the 5-ht6 receptor gene; this was accompanied by a phenotype of yawning, stretching and chewing which could be antagonized by atropine in a dose-dependent manner (38). Injection of AS-ODNs targeted at galanin mRNA into the paraventricular nucleus reduced fat ingestion and body weight gain (39), demonstrating a definite function for this intriguing peptide in the mammalian brain. A less direct effect was demonstrated by inhibition of proopiomelanocortin expression. An AS-ODN against β-endorphin mRNA (40) reduced adrenocortiocotropin (ACTH) and β-endorphin concentrations in corticotrophic cell cultures, while not affecting the cellular levels of irrelevant proteins or cell viability and proliferation. When microinfused into the rat hypothalamic arcuate nucleus, this AS-ODN reduced ACTH and β-endorphin levels and suppressed the grooming behavior characteristic of exposure to a novel environment.

Another behaviorally important neuropeptide produced in the arcuate nucleus, neuropeptide Y, controls feeding behavior. Direct anti-neuropeptide Y AS-ODN injection to the arcuate nucleus at daily intervals reduced neuropeptide Y levels by 40% in the arcuate nucleus but not in adjacent nuclei, and suppressed appetite (39). While this finding demonstrates clearly that the effect of this AS-ODN was highly specific, it also indicates the drug distribution problem which may be associated with the use of AS-ODN to suppress expression of genes normally expressed in the brain.

The antisense approach has also been used to explore the behavioral patterns caused by drugs of abuse. One target of such AS-ODNs was the D2 dopamine receptor, thought to control certain behavioral responses to cocaine, particularly the characteristic walking in close circles. Unilateral administration to the rat substantia nigra of AS-ODNs to the mRNA translated into this receptor suppressed the cocaine rotational response of the treated rats while reducing the D2 receptor in the substantia nigra (41) by 40%. This *in vivo* effect was, however, more limited than that observed with the same AS-ODN in cultured retinoblastoma cells, where 1 μM of the AS-ODN suppressed D2 dopamine receptor levels by 57% within 3 days. This study thus sheds light on a problem particular to the use of AS-ODNs in the brain: there is a limited accessibility to nerve cells *in vivo*, even under the cumbersome

approach of ICV administration. In another experiment, c-fos AS-ODNs generated apomorphine and amphetamine-induced rotation. To this end, sodium pentobarbital-anaesthesized rats were injected ipsilaterally with an AS-ODN against c-fos and contralaterally with a "sense" ODN into the striatum. When treated 10 hr later with an amphetamine or apomorphine, these rats showed drug-induced rotation toward the AS-ODN-treated side (42). Also, c-fos and Jun-B levels were reduced in striatal neurons at the AS-ODN treated hemisphere, suggesting that the c-fos AS-ODN suppressed the drug-induced behavioral phenotype (43).

The selectivity of behavioral phenotypes associated with the D2 dopamine receptor was examined by *in vivo* administration of a D2 AS-ODN into the striatum of mice with unilateral lesions induced by 6-hydroxydopamine (44). When challenged by acute injections of various agents that cause D2-associated contralateral rotational behavior (i.e. quinpirole) these mice did not rotate. In contrast, injections of the muscarinic cholinergic receptor agonist oxotremorine induced rotational behavior both in control mice and in those treated with the D2 receptor AS-ODN. The reduction in quinpirole-induced rotational behavior was related to the amount and length of time the D2 AS-ODN was given. The effect was visible after 1 day of treatment and almost completely disappeared by 6 days. Yet the effect was reversible within 2 days after cessation of treatment. It was also associated with significant and selective reduction in D2 receptor mRNA within the striatum, suggesting a genuine antisense mechanism. Table 9.2 presents these recent examples for behavioural functions modulated by AS-ODNs.

9.6 AS-ODNs and Human Neuropathology

When considering the use of antisense drugs for treating nervous system diseases, several special arguments should be kept in mind.

First, brain neurons are terminally differentiated cells for which there will be no replacement. This implies that special care should be taken to minimize both sequence-dependent and sequence-independent cytotoxicity of AS-ODNs. Also, the lifetime of a neuron by far exceeds that of cells in other tissues. Therefore, it may be much more difficult to change properties of a neuron than, for example, those of a tumor cell. However, once modified, the affected neuron will survive and not proliferate.

Second, the intricate networks connecting brain neurons predict that suppression of the level of particular mRNA transcripts or their protein products in a particular brain region may affect totally different brain regions due to complex and not-yet-understood signal transduction mechanisms. Another outcome of neuronal complexity is that the feedback responses to AS-ODN-induced changes can hardly be predicted. Therefore, the establishment of AS-ODN therapies for nervous system diseases necessitates careful pre-clinical studies in both cultured neurons and animal models. This, however highlights yet one more difficulty, that of species specificity.

Tab. 9.2 Recent Brain-expressed Targets in AS-ODN Studies

	Protein product of target gene	Modulated behavioral Function	References
1	Corticotropin-releasing hormone	attenuation of social-defeat induced anxiety in rats	4
2	c-fos	suppression of anxiety; generation of apomorphine and amphetamine-induced behavior	35, 36, 42
3	V1 vasopressin receptor	suppression of social discrimination ability and anxiety	37
4	5-ht6 receptor	enhanced cholinergic neurotransmission, yawning, stretching	38
5	galanin	reduced fat ingestion	39
6	XCS-endorphin	suppressed response to novel environment	40
7	neuropeptide Y	suppression of appetite	39
8	D2 dopamine receptor	suppression of cocaine response; suppression of quinpirole response	41, 44

Primate experiments are excluded from many studies because of economic concerns, yet the rodent brain differs from the human in many different aspects. Also, several human diseases of major importance (i.e. Alzheimer's disease, multi-infarct dementia) do not occur in rodents. Finally, due to species-specific differences in codon usage, AS-ODNs studied in rodents may differ from those to be developed later as drugs for human use. This adds to the risk involved in subsequent clinical studies.

Once these conceptual arguments have been met, technical difficulties emerge. As stated above, delivery of AS-ODN drugs to the brain is far more complex than to any other tissue or organ. Drug pharmacokinetics in the brain should also be more complex than in any other tissue, as the rate of removal of AS-ODNs from particular subsets of neurons might depend on transient parameters such as electrophysiological firing rate, synaptic plasticity and circadian rhythm. Yet one more difficulty is late diagnosis: many nervous system diseases are diagnosed in advanced stages, when most of the relevant neurons have already died and the mode of functioning of the remaining ones has been drastically altered from that characteristic of the normal state. Therefore, the ultimate levels of the target mRNA transcripts will be highly variable between patients and with disease progression; however, in most cases it is extremely difficult to define the disease stage, as diagnosis is generally based on subjective criteria and because most nervous system diseases limit the caretaker's capacity to evaluate the patient's mental state. All this is well illustrated for Alzheimer's disease, as is presented in the following.

9.7 The Challenges of Alzheimer's disease

Recent studies unraveled several genes whose protein products are abnormally expressed in the demented brain. However, the primary cause(s) of Alzheimer's disease are not yet known, which complicates the choice of target genes and/or proteins whose functions should be blocked for attenuating the progress of this neurodegenerative disease. One clear fact is that cholinergic neurotransmission is perturbed in the Alzheimer's disease brain. This has been the basis for past and present therapies and it is on this fact that our current report is focused. This, in turn, requires a short introduction.

The Cholinegic Hypothesis

Acetylcholine (ACh) is the agent which mediates neurotransmission in cholinergic brain synapses. Impaired cholinergic neurotransmission may result from pathological or pharmacological insults that alter the balanced interaction between ACh and its receptors (45). Alzheimer's disease (AD) is characterized by a selective loss of ACh-producing neurons (46). The cholinergic hypothesis of AD proposes that loss of cholinergic neurons leads to an ACh deficit which is correlated with progressive degeneration of central cholinergic systems and the accompanying deterioration of cognitive function characteristic of AD patients (46, 47, 48). About 5-10% of cases are genetically determined, but even within this group, there are at least four classes, associated with four different chromosomes. The great majority of AD cases do not have an obvious hereditary component, but most cases of whatever origin, are characterized by microscopic abnormalities in brain tissue, called plaques and tangles. These structures have been for pathologists, the diagnostic feature of AD, and much effort has gone into characterizing the constituent protein, β-amyloid, abnormalities of which lead to the plaques and tangles. The concept that cholinergic imbalance may be etiologically associated with the impaired cognitive performance in AD was supported by studies in aging rats (49 and references therein) and recently strengthened by the finding that transgenic mice which overexpress the enzyme that hydrolyzes ACh, acetylcholinesterase (AChE) in brain neurons display progressive deterioration in spatial learning and memory (50). Altogether, these findings support the notion that an approach aimed at redressing the cholinergic imbalance, e.g. suppression of AChE levels, should be therapeutically beneficial for treating AD patients.

The Pharmacological Approach

A widely accepted approach to the retardation of the AD-related decline of cognitive functions has been to reverse the ACh deficit with cholinesterase inhibitors (48). Normally, AChE serves to restrict duration of the post-synaptic response by hydrolyzing ACh to acetate and choline. In the well-studied vertebrate neuromuscular junction (NMJ), AChE inhibitors have proven effective in prolonging miniature endplate potentials, presumably by extending the lifetime of ACh released into the synap-

tic cleft and thereby increasing the number of receptor-transmitter interactions (45). Tacrine (THA, tetrahydroamino-acridine, Cognex®) – the first FDA-approved AD drug – is a potent AChE inhibitor which relieves cognitive symptoms in 30-50% of mildly to moderately affected AD patients (51, 52). Unfortunately, anti-AChE therapies for AD, including tacrine, are associated with exacerbated cholinergic deficits, hematopoietic irregularities, and hepatotoxicity in some patients (48, 53). Therapeutic response and hypersensitivity to these drug regimens are likely attributable to individually variable interactions of AChE inhibitors with other proteins, especially the homologous, but genetically diverse, serum enzyme butyrylcholinesterase (BuChE;54). Thus, a more selective approach for AD is called for.

A Molecular Biology Approach

When searching for appropriate target genes, the suppression of which could be advantageous for treating AD patients, one remembers the tangle structures that characterize the pathophysiology of this disease. The tangles are composed of disarranged microtubules with abnormally high phosphorylation levels of the microtubule-associated protein tau. When transfected with tau DNA, pheochromocytoma PC12 cells responded to nerve growth factor by extending neurites more effectively than control cells; when transfected with anti-tau DNA, these cells failed to extend neurites in response to nerve growth factor treatment (55). In principle, anti-tau AS-ODNs might hence suppress formation of the tangle structures. Other important hallmarks of AD pathology are the plaque structures which contain precipitated amyloid peptides. When PC12 cells were treated with AS-ODNs to suppress amyloid peptide production, they lost the ability to respond to nerve growth factor by extending neurites (56). However, if nerve growth factor treatment preceded the addition of AS-ODNs, the oligonucleotides had no effect. This study therefore implies that AS-ODN treatment for suppressing amyloid peptide production should be initiated prior to plaque formation, a major difficulty under today's conditions when no prognosis or early diagnosis is available.

Another intriguing property of AD plaques is that they stain positively for AChE activity. AChE has a morphogenic activity in transfected glial cells (57), transiently transgenic *Xenopus* embryos (58) and transgenic mice (59). This suggests that the value of anti-AChE therapies could, at least in part, be related to suppression of this morphogenic activity and hence of plaque growth. Here again, a molecular biology approach may be of benefit. This and the long-recognized low selectivity of anti-AChE inhibitors prompted the search for alternative strategies to block AChE activity *in vivo*. Taking advantage of the divergent nucleotide sequences of the genes which encode AChE and BuChE, we developed the technology for selective inhibition of AChE expression in living cells by use of partially phosphorothioated AS-ODNs (15, 25) targeted against AChEmRNA (60, 61). Thanks to the precise and specific interaction of such AS-ODNs with their mRNA target, we hoped that they would efficiently block biosynthesis of AChE via RNaseH-mediated destruction of the message, or by steric interference with RNA splicing or translation (1). In light of their high speci-

ficity and low-dose biological effects, AS-ODNs targeted against AChEmRNA can potentially offer a promising new alternative strategy to cholinomimetic treatment of AD, which require evaluation in cultured neurons as well as in an appropriate mammalian model prior to the initiation of clinical trials. Therefore, and because this is the AS-ODN study with which we are most familiar, we chose to present it in more detail.

9.8 Human Cholinesterase Genes as Potential Targets for Antisense Therapy

Cholinesterases (ChEs) are the enzymes which terminate each nerve impulse by hydrolyzing ACh. There are two distinct ChE genes in all vertebrates. The two human genes, ACHE and BCHE, were cloned, mapped to specific chromosomal sites and expressed in transgenic organisms (reviewed by 62, 63). Interestingly, these two genes are very different in their base composition and nucleotide sequence. This ensures that antisense agents targeted to the RNA product of AChE will not interact with the RNA product of BCHE. The selectivity of AS-ODN agents therefore favors, in this gene family, the antisense approach. In contrast, most inhibitors targeted to one of the ChE proteins, like carbamates and organophosphates, will also interact with the other, since these proteins are 50% identical and >85% homologous (reviewed by 64). As the BCHE gene is frequently subject to mutation, the level and properties of its protein product are highly variable. This situation further complicates the use of ChE inhibitors (54), yet should not interfere with the action and specificity of AS-ODNs targeted at ChE genes.

An important consideration when designing a drug is that its function will not perturb basic biological properties other than that for which it is intended. For example, for neurochemical uses of antisense drugs to suppress the expression of ChEs, one needs to assure sustained neuromuscular communication by selecting AS-ODN doses which will sufficiently inhibit these enzymes in the brain but will not reduce their levels in NMJs that essential amount required for breathing and other motor functions. Furthermore, the use of anti-ChEs in AD is based on the assumption that AChE is primarily involved in the termination of cholinergic neurotransmission. However, as is the case with many other proteins, the biological role of ChEs may include additional functions. For example, accumulating evidence suggests that AChE is also involved in the regulation of nervous system development. To this end, it was shown using several experimental approaches that expression of AChE during the early stages of brain development correlates closely with the major phase of neurite outgrowth (65, 66). When overexpressed in transgenic *Xenopus* tadpoles, the brain and muscle form of the enzyme accumulates in NMJs and enhances their development (58, 67). In the C6 glioma cell line, transfected ACHE DNA induces cytomorphological alterations that lead to process extensions (57). Moreover, it was recently shown that AChE stimulates neurite outgrowth from cultured chick neurons

in a manner unrelated to its catalytic activity (68, 69). Therefore, AS-ODNs targeted to the ACHE gene can be expected to affect both neurochemical and morphogenic effects.

There are at least three options for alternative splicing of ACHEmRNA transcripts, with distinct tissue distribution for each of these mRNA subtypes (57, 70) and, possibly, different biological functions. Therefore, one would like to distinguish between ACHEmRNA subtypes involved in specific function(s) and target AS-ODNs toward those domains in the AChEmRNA chain which are required for the function to be perturbed, without interfering with other functions of the AChE protein. To this end, we decided to examine the antisense approach for inhibiting AChE expression in primary murine neuronal cultures. It should be emphasized in this context, that the neuropathological hallmark of AD, the plaque structure, includes abnormally grown processes that cytochemically stain for AChE activity. Therefore, in this case we were interested in suppressing the morphogenic activity of AChE in addition to suppressing some of its catalytic capacity. It so happened that this preclinical study combined several aspects of AS-ODN studies in the use of *in vivo* and *ex vivo* systems and required several different techniques for analyzing the outcome of AS-ODN administration. In the following, we describe these experiments with some details referring to the methods employed and the interpretation of the results.

9.9 Effects of Antisense Oligonucleotides Targeted to Primary Neuron mRNAs

Important considerations in the design of an AS-ODN approach for use with neurons is the uptake mechanism of the AS-ODNs and their potential capacity to block expression of their target genes. The uptake of AS-ODNs directed against neuronal ACh receptors was studied in cultured chick primary neurons (71). Fifteen-mer AS-ODNs added to the culture medium were taken up into the cell bodies in a temperature-dependent, saturable manner (up to 20 μM). Monomeric nucleotides (AMP, ATP) competed effectively with this active uptake process in a manner reminiscent of the endocytosis of AS-ODNs described in non-neuronal cells. The efficiency of uptake depended on the age of the embryos from which neurons were removed but not on the number of days that these neurons were maintained *in vitro*. The functioning of neuronal nicotinic ACh receptors was effectively blocked in these neurons by suppressing expression of the α3 subunits of these receptors (by 80-90%). Electrophysiological analyses demonstrated abnormal properties of remaining receptors, suggesting aberrant assembly of other receptor subunits. This study paved the way for further manipulations of mammalian brain neurons.

Primary Neuron ACHE Antisense Studies

To study the involvement of AChE in mammalian neurite outgrowth and differentiation, we added synthetic 20-mer 3'-terminally phosphorothioated AS-ODNs

complementary to two alternative exons in the ACHE gene, to primary neuronal cultures from 14 day-old embryonic (E14) mouse whole brain. Cells grown for 24 hr in serum-free medium on serum-coated dishes were treated with these AS-ODNs or with a control oligonucleotide with the inverted base sequence. Both antisense treatments but not the inverse oligodeoxynucleotide induced the appearance of multilayered cell aggregates and suppressed neurite outgrowth (72). The effect appeared earlier with increasing doses of the AS-ODNs, indicating dose dependence. These oligonucleotide-induced phenotypic changes suggested AChE involvement in neuronal growth and differentiation and supported the development of AS-AChE oligomers as potential drugs to replace mechanism-based AChE inhibitors for AD therapy.

The methodology involved was quite straightforward. Primary mouse neuronal cultures were prepared from embryonic (E14) mouse (Balb/C) whole brains (73). Brains were removed and cells mechanically dissociated and plated in serum-free medium ($2.5X10^6$ cells/ml) in 24-well (1 ml per well) culture dishes coated successively with poly-L-ornithine and culture medium containing 10% fetal calf serum. Cultures grown for 24 hr at 37°C, 5% CO_2 were treated with synthetic 20-mer 3'-terminally phosphorothioated oligonucleotides (25) complementary to either the consensus ACHE exon 2, common to all of the alternative forms of ACHEmRNA (AS-mE2) or the alternative 3' exon 5 (AS-mE5). The inverse sequence of AS-mE2 (inv-mE2) was used as a control. After 24 hr growth, cells were cytochemically examined to determine the remaining levels of ChEs under each treatment as correlated with the morphogenic changes caused by the oligodeoxynucleotide treatments. Figure 9.1 presents the positions of these AS-ODNs along the ACHE gene.

Alternative AS-ODNs with Common Effects

Several parameters may be used to assess the effectiveness of AS-ODN experiments and deduce which was the mechanism(s) through which they exerted their effects. It is commonly assumed that when more than one AS-ODN agent targeted against a certain mRNA species cause similar biological effects, it is likely that it occurred through an antisense mechanism. In the case of the ACHE gene, we had the option to design AS-ODNs against common and alternative regions in the ACHEmRNA transcripts. Common outcome in terms of biological effect would imply that a single function was suppressed whereas different results for each AS-ODN could distinguish between the yet undefined functions of these alternative transcripts.

The mouse ACHE gene which includes 6 exons and 4 introns, gives rise to two alternative mRNAs in mouse primary neuronal cultures:

a) brain and muscle ACHE mRNA which includes exons 1-4 and 6,
b) "readthrough" ACHE mRNA which includes exons 1-4, continued by pseudointron 4, which in certain tissues operates as an exon (70), and exon 5.

AS-mE2 and AS-mE5 were designed to hybridize with specific domains in exon 2 and exon 5, respectively. Therefore AS-mE2 could potentially lead to destruction

of both ACHE mRNAs, whereas AS-mE5 could interact with only the readthrough mRNA or with the complete, yet unprocessed, transcript. Cells grown and treated for 24 hr with 0.5 μM of either AS-mE2, AS-mE5 or inv-mE2, were first stained with May-Grunwald and Giemsa stains, following with visible microscopy was performed with a Zeiss inverted microscope.

Untreated and inv-mE2 treated cells formed monolayers of single neurons with thin extensions. This important control experiment demonstrated that the inverse sequence, with identical base composition but no target, was not cytotoxic. Cells treated with either AS-mE2 or AS-mE5 were re-organized in multicellular, multilayered aggregates connected by a few thick processes. Moreover, the initiation time of the antisense ACHE morphogenic effect was dose-dependent. Thus, cell cultures treated with increasing concentrations (0.1-5.0 μM) of AS-mE2 were monitored for 5 days and the day on which aggregation was first observed was noted. At the highest concentration of oligonucleotide (5.0 μM), cytotoxicity was observed, cells detached from the dishes and died. However, cells treated with 0.1-0.5 μM AS-ODN were morphologically affected but remained viable.

The mouse ACHE gene, controled by the promoter, P, includes 6 exons (light cross-hatching) and 4 introns (dark cross-hatching), and gives rise to two alternative mRNAs in mouse primary neuronal cultures: "brain an muscle" ACHEmRNA includes exons 1-4 and 6, and "readthrough" ACHEmRNA includes exons 1-4, pseudointron 4 (which in certain tissues operates as an exon) and exon 5. The antisense oligonucleotides AS-mE2 and AS-mE5 were designed to hybridize with specific sequences in exons 2 and 5, respectively. Therefore, AS-mE2 can potentially lead to destruction of unprocessed mRNA and both alternatively spliced mRNAs, whereas AS-mE5 can interact only with unprocessed mRNA and the "readthrough" form.

The viability issue is of major concern when vulnerable nerve cells are to be treated with a potentially cytotoxic agent, and viability tests should probably be included in any preclinical study with AS-ODNs. In our particular case, the viability of neuronal primary cultures which displayed the cytomorphological effect following 24 hr growth in the presence of 0.5 μM AS-mE2 was assayed using a viability/cytotoxicity kit. To this end, we exploited the fact that enzymatic conversion by ubiquitous esterases in viable cells of the permeable, non-fluorescent dye calcein generates an intensely fluorescent green form of the dye. This product is retained within viable cells, producing the green fluorescence (with emission wavelength of about 530 nm). A second dye, ethidium homodimer, was used to identify dead cells, since it penetrates only damaged membranes. In the cell it binds to nucleic acids, producing a bright red fluorescence (>600 nm). Fluorescence microscopy was performed with a Zeiss Axioplan microscope equipped with X40 Achroplan lens, suitable for photographying viable cells under medium, a HC100 camera and a FITC/Texas red 485/578 double excitation filter, at magnification X400. This test proved that the aggregated cells in AS-mE2 treated cultures remained viable.

To demonstrate that the antisense treatement reduces ChE activities in these primary neuronal cultures, neuronal cell cultures were treated for 24 hr with no oligonu-

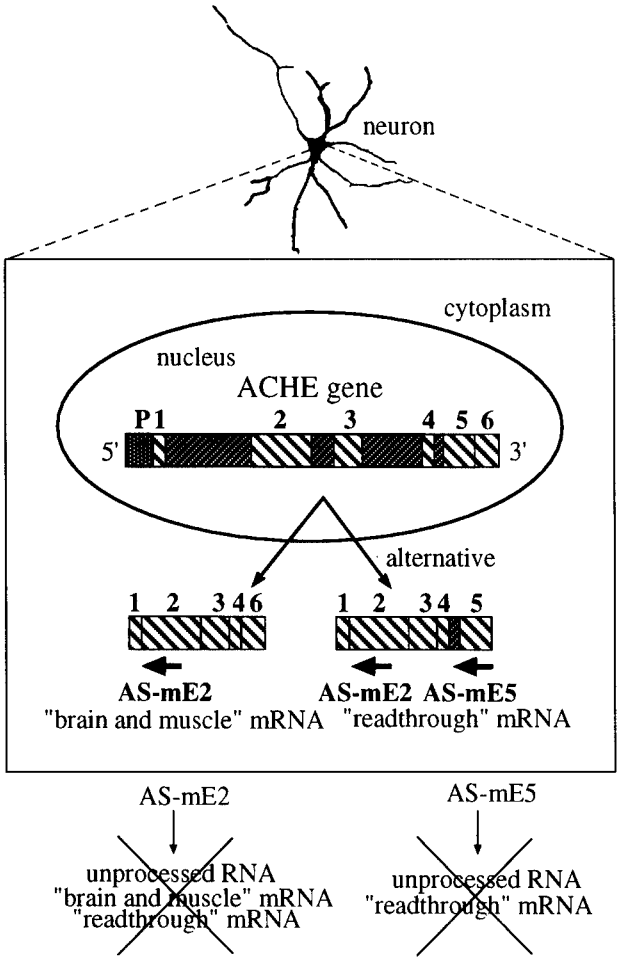

Fig. 9.1: Target sites for antisense oloigonucleotide interactions with ACHEmRNA.

cleotide, or with 0.5 μM of the noted oligomers (AS-mE2 or Inv-mE2). Cells were then stained for AChE activity overnight at 4°C with no prior fixation (59). Stained cells in 20 different microscope fields for each preparation (magnification X1000), were classified by the intensity of staining. Each field contained aproximately 250 neurons. Stained neurons (approxinmately 0.5-5% of total) included:

(1) light brown-stained cells
(2) more intensely stained cells, particularly around the cell body
(3) very intensely, dark brown stained cells, with stain reaching into neuronal extensions.

Within all classes, staining was considerably lower in AS-mE2 treated cells but not in those treated with Inv-mE2, suggesting an antisense mechanism (72).

The antisense suppression of AChE activity was further visualized by electron microscopy. For this purpose, neuronal cell cultures were treated for 24 hr with no oligonucleotide, or with 0.5 μM of the noted oligomers (AS-mE2 or Inv-mE2). Cells were then fixed for 30 min in 4% paraformaldehyde, lightly stained for AChE activity for 4 hr at room temperature and analyzed by transmission electron microscopy as detailed elsewhere (58). Crystals formed by non-enzymatic reaction initiated by the thiocholine product of AChE action on acetylthiocholine appeared in control neurons, but not in neurons treated with AS-mE2. This analysis thus demonstrated the efficacy of the employed AS-ODNs as well as their selectivity. A word of caution is in order. We do not understand the mechanism that connects AChE inhibition to prevention of neurite outgrowth. Antisense suppression of the metabolically unrelated enzyme 5'-nucleotidase also prevents neurite outgrowth (74). Both AChE and 5'-nucleotidase are ectopic enzymes in these cells, and the common effect may be to change, in an unknown manner, the surfaces of the cells. Therefore, the morphogenic changes observed in primary neurons with suppressed AChE activity suggested that suppressing this enzyme's activity may exert morphogenic changes also in other tissues in which AChE is produced, for example in hematopoietic cells. To search for the potential side effects of oligonucleotides for suppression of AChE production in such sites, we employed the antisense approach also to hematopoietic cells and tissues.

9.10 *In vitro* and *in vivo* Tests for Potential Side Effects

In addition to brain neurons and muscle cells, bone marrow cells (red blood cells, lymphocytes, platelet progenitors) from all known vertebrates express ChEs. This raises the concern for side effects of the proposed antisense therapy due to AChE inhibition in hematopoietic cells. Indeed, injection of mice with carbamate ChE inhibitors, alters proliferation of megakaryocytes (platelet progenitors) in rodents (reviewed by 62). In addition, farmers using organophosphorous anti-ChEs as insecticides are at an increased risk of development of leukemia (75). We therefore investigated the therapeutic safety margins of AS-ODNs targeted to the ACHE gene or to the closely related BCHE gene. In previous studies, we found that 25% of leukemic patients carry cholinesterase genes with abnormal copy numbers and structures (76, 77). Altogether, this implied that interference with the expression of blood cell AChE and/or BuChE is associated with enhanced bone marrow proliferation. BuChE is quantitatively more important in the blood (75% of total blood ChEs). Therefore, we considered that the bone marrow damage caused by chemical anti-ChEs could have occurred due to AChE and/or BuChE inhibition. To identify the highest concentration of oligonucleotides which will be therapeutically safe, we have further studied the expression of BuChE in the bone marrow of patients with somatically mutated, aberrantly expressed and amplified ACHE and BCHE genes. This phenomenon is

associated with very low platelet counts and abnormal development of megakaryocytes (76), the platelet progenitors from which platelets are formed. We therefore attempted to mimic interference with BCHE gene expression, using phosphorothioated AS-ODNs.

Non Sequence-Dependent Interactions

When 5 μM of a fullly phosphorothioated antisense agent intended to block BCHE gene expression (AS-BCHE) was added to murine bone marrow cells grown in culture in the presence of the cytokine interleukin 3 (IL-3), megakaryocyte progenitor development was severely inhibited (78). When incubated with bone marrow cells, radioactively labeled phosphorthioated oligonucleotides bound to yet unidentified nuclear protein(s) in small, dividing cells. Incubation of bone marrow cellular proteins with these agents also resulted in protein labeling (25). However, this proved to be unrelated to the nucleotide sequence of the employed oligonucleotides – a non-specific interaction which could explain part of the interference with *ex vivo* bone marrow proliferation that was previously observed for AS-BCHE in its totally phosphorothioated form (25). Recent findings (79) strengthen this assumption and attribute part of the megakaryocytopoietic suppression observed with our AS-ODNs as well as with oligomers targeted to other genes and to AS-ODN-protein interactions.

Suppression of platelet production may lead to severe thrombocytopenia, a dangerous toxicological outcome of several other AS-ODNs. For example, this is the main danger involved in rel A antisense therapy, aimed at suppression of production of the P65 subunit of the NFκB transcription factor in tumor cells (24). This phenomenon could have resulted from the antisense effect itself (because developing promegakaryocytes depends on NFκB for their maturation). Alternatively, or additionally, it could reflect binding to and inhibition of essential nuclear proteins in promegakaryocytes, a confirmed property of phosphorothioate ODNs. To prevent, or at least minimize this protein interaction and its consequent cytotoxicity, the following observations were taken into consideration when designing anti-BCHE ODNs:

(1) Phosphorothioate protection is important for RNaseH induction and oligonucleotide stabilization.
(2) This protection may also be cytotoxic and induce part or all of the observed interference with cell development.
(3) Since RNA destruction is primarily initiated at the 3'-end, it can be blocked effectively by interfering with this activity at that end alone.
(4) Blocking only three 3'-terminal phosphorothioates is sufficient to protect the AS-ODN. This partially protected oligomer should be less toxic than, yet equally effective as the fully-blocked oligomer.

Based on these arguments, phosphorothioate protection of AS-BCHE was limited to the three 3'-terminal internucleotidic bonds. When administered in similar doses, thus partially protected AS-ODN reduced production of platetlet progenitors as ef-

ficiently as their fully protected counterparts (25). However, when incubated with bone marrow proteins, they displayed no binding. Also, their addition to cultures apparently did not interfere with the functioning of genes other than those targeted, and no non-specific reduction in cell proliferation could be observed when irrelevant oligomers were tested. Altogether, this technological improvement demonstrated that antisense inhibition of BCHE mRNA (80) would indeed cause hematopoietic side effects, if used at 5 μM concentrations. To test the validity of this assumption, we moved on to combine cell culture studies with *in vivo* studies.

9.11 Comparative Studies with AS-ODNs for Genes with Closely Related Functions

When mice were injected with sufficient AS-ODNs to achieve a concentration of 5 μM of the oligomer in body fluids blocking BCHE gene expression (AS-BCHE), their platelet progenitors revealed reduced levels of BCHEmRNA (as tested by *in situ* hybridization). This indicated that specific RNA destruction occurred. At the same time, an unrelated gene (i.e. β-actin) remained fully expressed, as tested by reverse transcription followed by PCR amplification (RT-PCR), reflecting low toxicity of these antisense agents. When bone marrow cells from the injected mice were cultured, megakaryocyte colony development was severely inhibited (40% reduction). *In vitro* megakaryocytopoietic cultures incubated with AS-BCHE further displayed a sharp shift in differentiation, from predominantly megakaryocyte to myeloid lineages (81). Thus suppression of BuChE production can cause thrombocytopenia *and* increase myeloid cell counts, two hematopoietic effects which indeed were reported in Alzheimer's disease patients under tacrine treatment (82).

The AS-BCHE studies may be regarded as a necessary precaution, aimed at explaining hematopoietic complications in patients treated with chemical anti-ChEs of relatively limited selectivity. However, the drug(s) we aim to develop is(are) AS-ACHE. Therefore, our goal was to test ACHE AS-ODNs for their effects on hematopoietic development. Intraperitoneal injection of AS-ACHE to block expression of AChE resulted in much more dramatic changes than those observed with AS-BCHE. A single injection of 5 μg/g body weight yielding 5 μM AS-ODN in body fluids, caused drastic reductions in the fractions of bone marrow erythrocytes and lymphocytes at 12 days post-treatment, as well as reciprocal increases in myeloid cells, changes which were almost totally reversed by day 20 (61). The possibility of transcriptional feedback could not be excluded. Moreover, since *in vivo* it is virtually impossible to determine absolute numbers of bone marrow cells, we could not conclude whether erythroid development had been inhibited, if myeloid cell proliferation had been enhanced, or both. To answer these questions, we administered such AS-ACHE oligocnucleotides *ex vivo*, in primary cultures of murine bone marrow cells.

Bone marrow cell cultures have several advantages over *in vivo* analytical studies of antisense effects.

(1) They reveal the absolute number of proliferating stem cells present at plating time, each of which develops into a colony, whereas the other terminally differentiated cells die in culture (essentially, as they would *in vivo* as well). Therefore, they yield important information on the effect of the tested AS-ODNs on hematopoiesis in general.
(2) They are subject to convenient modulation by cytokines. In the presence of interleukin-3 IL-3, both platelet progenitors and myeloid cells will develop, but with added erythropoietin, erythroid cells will develop as well. This enables differential cell counts and examination of the dependence of cell composition on AS-ODN effects and growth factors.
(3) Apart from their importance for evaluation of the safety of AD drugs, the *ex vivo* cultures are a clinically important model system for progenitor cells produced for transplantation. This increasingly popular procedure is currently used for treatment of cancer patients following drastic chemotherapy or irradiation.

When added to erythropoietic cell cultures, 15 μM AS-ACHE caused a dose-dependent increase in colony and cell counts and increased the fraction of myeloid cells at the expense of erythroid cells and megakaryocytes (60). This implies that thrombocytopenia and increased myeloid cell counts can occur under AS-ACHE treatment as well, especially at high concentrations. With IL-3 alone, AS-ACHE decreased colony counts but not cell numbers, and diverted up to 50% of the cells into erythroblasts (which could not develop further for the lack of erythropoietin). Additional tests revealed transient early reduction in ACHEmRNA, followed by 10-fold increase by day 4 post-treatment. This could reflect an antisense mechanism which elicits a feedback response replacing the missing ACHEmRNA molecules and more, and calls for prolonged exposure to AS-ODNs in any therapeutic regimen.

A general change in the pattern of mRNA transcripts demonstrated by using the approach of Differential PCR display (60) supported the possibility of a feedback response. A 10-fold increase in DNA yield and prevention of the DNA fragmentation (83) which appeared in non-treated cultures confirmed the increased cell counts, and the generally healthier appearance of cells under AS-ACHE treatement (fewer vacuoles, larger nuclei, smoother cell surface) strengthened this assumption. As mentioned above, AS-BCHE did not cause such changes, it only reduced the number of megakaryocytes at the expense of meyloid cells (80). Comparison of the effects of AS-ACHE to those of AS-BCHE in erythropoietic cultures thus revealed the wider scope and dominant nature of AS-ACHE over erythroid and megakaryocyte development. However, since all of these effects occurred only at AS-ODN concentrations higher than 5 μM, the hematopoietic studies also confirmed that AS-ACHE should be therapeutically safe at the concentrations effective in neurons (0.1-0.5 μM). While this leaves open the question of body fluids concentration required to reach the desired levels of AS-ODNs in the brain, the safety margin does seem reassuring.

9.12 Discussion

We have presented the design and application of antisense techniques for the treatment of Alzheimer's disease, which illustrates many of the advantages inherent in this approach. We have also been at pains to elaborate on complications we encountered because they may be generally instructive. To sum up the principle concepts we tried to present, several major questions are raised when an antisense drug is to be considered for therapeutic use:

(1) Can it produce the desired biological effect?
(2) Can it reduce the level of the corresponding protein product for prolonged periods?
(3) Does it suppress the level of targeted mRNA?
(4) Does this effect appear both in cultured cells and *in vivo*?
(5) Is the tissue specificity of the relevant AS-ODN sufficient to exclude dangerous side effects?

We have addressed these questions by covering recent publications in the field of molecular brain research and by describing our own research using antisense drugs for the cholinesterase genes. Yet more specifically, we designed two AS-ODNs targeted to the ACHE gene. AS-ACHE ODNs suppressed neurite extension from cultured primary neurons in a dose-dependent manner, suggesting that they might attenuate AD plaque development; they suppressed the level of the AChE protein, although mRNA studies suggested feedback responses that modulate ACHEmRNA levels; and their functions(s) *in vivo* resembled their effects in cultured cells. Also, the sensitivity of neurons to AS-ACHE ODNs exceeded by 50-fold that of hematopoietic cells, providing a potentially safe therapeutic window. While many questions remain to be solved before AS-ACHE ODNs reach clinical trials, their use seems promising.

To test for potential side effects of the proposed drugs, we employed hematopoietic cell cultures. Our findings in these cultures, and in subsequent *in vivo* experiments confirm the suggestion of others of a regulatory role of the ChEs in bone marrow development. The accumulated evidence suggests that AS-ACHE apparently blocks the production of the multi-potential progenitors of both erythroid and megakaryocyte cells. Under such conditions, cultured bone marrow cells can only proliferate or develop into myeloid cells, which indeed they do. This explains complications associated with the use of conventional anti-AChE drugs and emphasizes the advantages of AS-ACHE ODNs as substitutes.

The hypothesis that emerges from the above experiments is that ChEs possibly participate in directing proliferating stem cells toward a differentiated state that eventually will terminate in programmed death. When their expression is blocked, hematopoietic proliferation may be perturbed. The range of AS-ODNs found useful in primary neurons from mice (0.1 to 0.5 μM) will be a starting point for their eval-

uation in primate pre-clinical trials, to test for efficacy while avoiding hematopoetic side effects. In addition, important implications arise for bone marrow transplantations, since this *ex vivo* procedure includes a phase of cell culture very much like the *in vitro* culture technique detailed above. It would be extremely helpful to amplify the number of proliferating stem cells prior to their reintroduction into the patient – thus shortening considerably the hospitalization time and improving the patient's condition while reducing the volume of cells to be injected. The complication involved in the use of AS-ACHE for neurochemical purposes may thus become a benefit for bone marrow uses.

If reproduced in humans, our procedure further offers the opportunity to improve the proliferative state of bone marrow in patients following chemotherapy or irradiation for any pathology, not only hematopoietic in nature. In addition, this same fact explains certain hematopoietic side effects reported in AD patients under anti-ChE therapy. Special care should therefore be taken to reduce the concentration of AS-ACHE drugs to minimum, to avoid such dangerous side effects.

A general concern as regards to the use of AS-ODNs in brain refers to the impermeability of the BBB, potentially posing a delivery problem. However, the blood brain barrier is known to be disrupted in AD patients (84); the delivery of AS-ACHE can thus be effected with simple i.v. injections. The main remaining difficulty, one which pertains to all other AS-ODN protocols, is that of the feedback response to be expected and its possible long-term effects.

In addition to the value of this therapeutic approach, the studies discussed bear intriguing basic research implications. ChEs are known to be expressed during embryonic development of many other cell types that undergo terminal differentiation (i.e., muscle and bone cells). It would be fascinating to discover whether in those tissues as well, these interesting enzymes are involved in controlling the shift from proliferation to differentiation. Thus, we may expect further basic science spin-offs as antisense technology is developed for clinical use.

Measured in terms of publications and emergence of biotechnology-based new enterprises, the interest and activity in antisense phosphorothioate drugs has grown rapidly during the past 5 years, and has directed much attention to synthesis of oligonucleotide analogs (79, 2). Important, but as yet unresolved issues in antisense technology deal with elucidating the mechanisms of antisense-agent uptake by cells. In addition, refining and understanding of antisense-agent pharmacokinetics and cellular distribution are required. For each drug to be developed, toxicology and efficacy must be evaluated. In addition, the mechanism of action of such drugs is of primary importance, as recent evidence indicates that many of the biomedically-active AS-ODNs operate through protein binding and not necessarily by the antisense mechanism (27). These and many other parameters will determine the future of antisense-based chemotherapies. However, the status of this technology as an innovation of pharmacotherapeutics has already been gained.

Acknowledgements

We thank Dr. D. Patinkin and Ms. R. Timberg (Jerusalem) for their contribution toward these studies, and Drs. D. Glick and S. Seidman for critical evaluation of this manuscript. This research was supported, in part, by the United States Army Medical Research and Development Command (contract DAMD 1797-1-7007, to H.S. and H.Z.), the German Israeli Fund (to H.S. and F.E.), the Israel Ministry of Health (to H.S. and H.Z.) and the E.W.H. Trust, London (to H.Z.).

References

1. Wagner, R. W. (1994). Gene inhibition using antisense oligodeoxynucleotides. Nature *372*, 333-335.
2. Strauss, M. (1996). Antisense Molecules and Ribozymes: Medical Applications. Antisense Technology (in press).
3. McCarthy, M. M., Masters, D. B., Rimvall, K., Schwartz-Giblin, S., and Pfaff, D. W. (1994). Intracerebral administration of antisense deoxynucleotides to GAD65 and GAD67 mRNAs modulate reproductive behavior in the female rat. Brain Res. *636*, 209-220.
4. Skutella, T., Probst, J. C., Jirikowski, G. F., Holsboer, F., and Spanagel, R. (1994). Ventral tegmental area (VTA) injection of tyrosine hydroxylase phosphorothioate antisense oligonucleotide suppresses operant behavior in rats. Neurosci. Lett. *167*, 55-58.
5. Sakai, R. R., He, P. F., Yang, L. Y., Ma, Y. F. Guo, J. J., Reilly, C. N., and Fluharty, S. J. (1994). Intracerebroventicular administration of AT1 receptor antisense oligonucleotides inhibits the behavioral actions of angiotensin II. J. Neurochem. *62*, 2053-2056.
6. Maurizot, J. C., Brahms, J., and Eckstein, F. (1969). Forces involved in the conformational stability of nucleic acids. Nature *222*, 559-561.
7. Halford, M. H. and Jones, A. S. (1968). Synthetic analogues of polynucleotides. Nature *217*, 638-640.
8. Pitha, P. M., Teich, N. M., Lowy, D. R., and Pitha, J. (1973). Inhibition of murine leukemia virus replication by poly (vinyluracil) and poly (vinyladenine). Proc. Natl. Acad. Sci. USA *70*, 1204-1208.
9. De Clercq, E., Eckstein, F., and Merigan, T.C. (1969). Interferon induction increased through chemical modification of a synthetic polyribonucleotide. Science *165*, 1137-1139.
10. Zamecnik, P. C., Goodchild, J., Taguchi, Y., and Sarin P. S. (1986). Inhibition of replication and expression of human T-cell lymphotropic virus type III in cultured cells by exogenous synthetic oligonucleotides complementary to viral RNA. Proc. Natl. Acad. Sci. USA *83*, 4143-4146.
11. Matsukura, M., Shinozuka, K., Zon, G., Mitsuya, R. M., Cohen, J. S., and Broder S. (1987). Phosphorothioate analogs of oligodeoxynucleotide inhibitors of replication and effects on human immunodeficiency virus. Proc. Natl. Acad. Sci. USA *84*, 7706-7710.
12. Agrawal, S., Goodchild, J. Civeira, M. P. Thornton, A. H., Sarin, P. S., and Zamecnik P. C. (1988). Oligodeoxphosphoroamidates and phosphorothioates as inhibitors of human immunodeficiency virus. Proc. Natl. Acad. Sci. USA *85*, 7079-7083.
13. Stein, C. A. and Cheng, Y. C. (1993). Antisense oligonucleotides as therapeutic agents – Is the bullet really magical? Science *261*, 1004-1012.
14. Eckstein, F. (1966). Nucleoside phosphorothioates. J. Am. Chem. Soc. *88*, 4292-4294.
15. Eckstein, F. (1985). Nucleoside phosphorothioates. Annu. Rev. Biochem. *54*, 367-402.
16. Eckstein, F. and Gish, G. (1989). Phosphothioates in molecular biology. Trends Biochem. Sci. *14*, 97-100.
17. De Clercq, E., Eckstein, F., Sternbach, H., and Merigan, T.C. (1970). The antiviral activity of thiophosphate-substituted polyribonucleotides *in vitro* and *in vivo*. Virology *42*, 421-428.
18. Zamecnik, P. C. and Stephenson, M. L. (1978). Inhibition of Rous sarcoma virus replication and cell transformation by a specific oligodeoxynucleotide. Proc. Natl. Acad. Sci. USA *75*, 280-284.
19. Hewick, R. M., Hunkapiller, M. W., Hood, L. E., and Dreyer, W.J. (1981). A gas-liquid solid phase peptide and protein sequenator. J. Biol. Chem. *256*, 7990-7997.

20. Caruthers, M. H. (1985). Gene synthesis machines: DNA chemistry and its uses. Science *230*, 281-285.
21. Alvarado-Urbina, G., Sathe, B. M., Liu, W.-C., Gillen, M. F., Duck, P. D., Bender, R., and Ogilvie, K. K. (1981). Automated synthesis of gene fragments. Science *214*, 270-274.
22. Fakler, B., Herlitze, S., Amthor, B., Zenner, H. P., and Ruppersberg, J. P. (1994). Short antisense oligonucleotide-mediated inhibition is strongly dependent on oligo length and concentration but almost independent of location of the target sequence. J. Biol. Chem. *269*, 16187-16194.
23. Bennett, C. F., Condon, T. P., Grimm, S., Chan, H., and Chiang, M. V. (1994). Inhibition of endothelial cell adhesion molecule expression with antisense oligonucleotides. J. Immunol. *152*, 3530-3540.
24. Sarmiento, U. M., Perez, J. R., Becker, J. M., and Narayan, R. (1994). *In vivo* toxicological effects of rel A antisense phosphorothioates in CD-1 mice. Antisense Res. Develop. *4*, 99-107.
25. Ehrlich, G., Patinkin, D., Ginzberg, D., Zakut, H., Eckstein, F., and Soreq, H. (1994). Use of partially phosphorothioated "Antisense" oligodeoxynucleotides for sequence-dependent modulation of hematopoiesis. Antisense Res. Develop. *4*, 173-183.
26. Stein, C. A. and Narayanan, R. (1994). Antisense oligodeoxynucleotides. Curr. Opin. Oncol. *6*, 587-594.
27. Stein, C. A. and Krieg, A. M. (1995). Problems of interpretation of data derived from *in vitro* and *in vivo* use of antisense oligodeoxynucleotides. Antisense Res. Develop. *4*, 67-69.
28. Morrison, P. F., Laske, D. W., Bobo, H., Oldfield, E. H., Dedrick, R. L. (1994). High-flow microinfusion: tissue penetration and pharmacodynamics. Am. J. Physiol. *266*, R292-305.
29. Boado, R. J. and Pardridge, W. M. (1992). Complete protection of antisense oligonucleotides against serum nuclease degradation by an avidin-biotin system. Bioconjug. Chem. *3*, 519-523.
30. Juliano, R. L. and Akhtar, S. (1992). Liposomes as a drug delivery system for antisense oligonucleotides. Antisense Res. Develop *2*, 165-176.
31. Pardridge, W. M. (1992). Recent development in peptide drug delivery to the brain. Pharmacol. Toxicol. *71*, 3-10.
32. Desjardins, J., Mata, J., Brown, T., Graham, D., Zon, G., and Iversen, P. (1995). Cholesteryl-conjugated phosphorothioate oligodeoxynucleotides modulate CYP2B1 expression *in vivo*. J. Drug Target *2*, 477-85.
33. Pardridge, W. M. (1994). Vector-mediated delivery of a polyamide ("peptide") nucleic acid analogue through the blood-brain barrier *in vivo*. Trends Biotechnol. *12*, 239-245.
34. Pardridge, W. M., Boado, R. J., and Kang, Y. S. (1995). Vector-mediated delivery of a polyamide ("peptide") nucelic acid analogue through the blood-brain barrier *in vivo*. Proc. Natl. Acad. Sci., USA. *92*, 5592-5596.
35. Hooper, M. L., Chiasson, B. J., and Robertson, H. A. (1994). Infusion into the brain of an antisense oligonucleotide to the immediate-early gene c-fos suppresses production of fos and produces a behavioral effect. Neurosci. *63*, 917-924.
36. Moller, C., Bing, O., and Heilig, M. (1994). c-fos expression in the amygdala: *in* vivo antisense modulation and role in anxiety. Cell. Molec. Neurobiol. *14*, 415-423.
37. Landgraf, R., Gerstberger, R., Montkowski, A., Probst, J.C., Wotjak, C.T., Holsboer, F., and Engelmann, M. (1995). V1 vasopressin receptor antisense oligodeoxynucleotide into septum reduces vasopressin binding, social discrimination abilities and anxiety-related behavior in rats. J. Neurosci. *15*, 4250-4258.
38. Bourson, A., Borroni, E., Austin, R. H., Monsma, F. J. Jr; and Sleight, A. J. (1995). Determination of the role of the 5-ht6 receptor in the rat brain: a study using antisense oligonucleotides. J. Pharmacol. Exp. Ther. *274*, 173-180.
39. Akabayashi, A., Wahlestedt, C., Alexander, J. T., and Leibowitz, S. F. (1994). Specific inhibition of endogenous neuropeptide Y synthesis in arcuate nucleus by antisense oligonucleotides suppresses feeding behavior and insulin secretion. Molec. Brain Res. *21*, 55-61.
40. Spampinato, S., Canossa, M., Carboni, L., Campana, G., Leanza, G., and Ferri, S. (1994). Inhibition of proopiomelanocortin expression by an oligodeoxynucleotide complementary to beta -endorphin mRNA. Proc. Natl. Acad. Sci. USA. *91*, 8072-8076.
41. Silvia, C. P., King, G. R., Lee, T. H., Xue, Z. Y., Caron, M. G., and Ellinwood, E. H. (1994). Intranigral administration of D2 dopamine receptor antisense oligodeoxynucleotides establishes a role for nigrostriatal D2 autoreceptors in the motor actions of cocaine. Molec. Pharmacol. *46*, 51-57.
42. Dragunow M., Lawlor, P., Chiasson, B., and Robertson, H. (1993). c-fos antisense generates apomorphine and amphetamine-induced rotation. Neuroreport *5*, 305-306.

43. Sommer, N., Melms, A., Weller, M., and Dichgans, J. (1993). Ocular myasthenia gravis. A critical review of clinical and pathological aspects. Doc. Opthalmol. *84*, 309-333.
44. Zhou, L. W., Zhang, S. P., Quin, Z. H., and Weiss, B. (1994). *In vivo* administration of an oligodeoxynucleotide antisense to the D2 dopamine receptor messenger RNA inhibits D2 dopamine receptor-mediated behavior and the expression of D2 dopamine receptors in mouse striatum. J. Pharmacol. Exp. Ther. *268*, 1015-1023.
45. Katz, B. and Miledi, R. (1973). The binding of acetylcholine to receptors and its removal from the synaptic cleft. J. Physiol. Lond. *231*, 549-574.
46. Coyle, J. T., Price, D. L., and DeLong, M. R. (1983). Alzheimer's disease: a disorder of cortical cholinergic innervation. Science *219*, 1184-1189.
47. Katzman, R. (1986). Alzheimer's disease. New Eng. J. Med. *314*, 964-973.
48. Davis, R. E., Emmerling, M. R., Jaen, J. C., Moos, W. H., and Spiegel, K. (1993). Therapeutic intervention in dementia. Crit. Rev. Neurobiol. *7*, 41-83.
49. Kadar, T., Silbermann, M., Weissman, B. A., and Levy, A. (1990). Age-related changes in the cholinergic components within the central nervous system II. Working memory impairement and its relation to hippocampal muscarinic receptors. Mech. Aging Develop. *55*, 139-149.
50. Beeri, R. Andres, C., Lev-Lehman, E., Timberg, R., Huberman, T., Shani, M., and Soreq, H. (1995). Transgenic expression of human acetylcholinesterase induces progressive cognitive deterioration in mice. Curr. Biol. *5*, 1063-1071.
51. Crimson, M. L. (1994). Tacrine: first drug approved for Alzheimer's disease. Ann. Pharmacother. *28*, 744-751.
52. Wagstaff, A. J. and McTavish, Y. (1994). Tacrine. A review of its pharmacodynamic and pharmacokinetic properties, and therapeutic efficacy in Alzheimer's disease. Drugs Aging *4*, 510-540.
53. Knapp, M. J., K, D. S., Solomon, P. R., Pendlebury, W. W., Davis, C. S., and Gracon, S. I. (1994). A 30-week randomized controlled trial of high-dose tacrine in patients with Alzheimer's disease. JAMA *271*, 985-991.
54. Loewenstein-Lichtenstein, Y., Schwarz, M., Glick, D., Norgaard-Pedersen, B., Zakut, H., and Soreq, H. (1995). Genetic predisposition to adverse consequences of anticholinesterases in 'atypical' BCHE carriers. Nature Med. *1*, 1082-1085.
55. Esmaeli-Azad, B., McCarty, J. H., and Feinstein, S. C. (1994). Sense and antisense transfection analysis of tau function: tau influences net microtubule assembly, neurite outgrowth and neuritic stability. J. Cell Sci. *107*, 869-879.
56. Majocha, R. E., Agrawal, S., Tang, J. Y., Humke, E. W., and Marotta, C. A. (1994). Modulation of the PC12 cell response to nerve growth factor by antisense oligonucleotide to amyloid precursor protein. Cell. Mol. Neurobiol. *14*, 425-437.
57. Karpel, R., Sternfeld, M., Ginzberg, D., Guhl, E., Graessman, A., and Soreq H. (1996). Overexpression of alternative human acetylcholinesterase forms modulates extensions in cultured glioma cells. J. Neurochem. *66*, 114-123.
58. Seidman, S., Sternfeld, M., Ben Aziz-Aloya, R., Timberg, R., Kaufer, D., and Soreq, H. (1995). Synaptic versus epidermal accumulation of human acetylcholinesterase is encoded by alternative 3'-terminal exons. Molec. Cell Biol. *14*, 459-473.
59. Andres, C., Beeri, R., Huberman, T., Shani, M., and Soreq, H. (1996). Cholinergic drug resistance and impaired spatial learning in transgenic mice overexpressing human brain acetylcholinesterase. K. Loffelholz, Ed. Prog. Brain. Res. 109, pp. 265-272.
60. Soreq, H., Patinkin, D., Lev-Lehman, E., Ginzberg, D., Grifman, M., Eckstein, F., and Zakut, H. (1994). Antisense oligonucleotide inhibition of acetylcholinesterase gene expression induces progenitor cell expansion and suppresses hematopoietic apoptosis *ex vivo*. Proc. Natl. Acad. Sci USA. *91*, 7907-7911.
61. Lev-Lehman, E., Ginzberg, D., Hornreich, G., Ehrlich, G. Meshorer, A., Eckstein, F., Soreq, H., and Zakut, H. (1994). Antisense inhibition of acetylcholinesterase gene expression causes transient hematopoietic alterations *in vivo*. Gene Therapy *1*, 127-135.
62. Soreq, H. and Zakut, H. (1993). Human Cholinesterases and Anticholinesterases. San Diego Academic Press.
63. Massoulie, J., Pezzementi, L., Bon, S., Krejci, E., and Vallette, F. M. (1994). Molecular and cellular biology of the cholinesterases. Prog. Neurobiol. *41*, 31-91.

64. Schwarz, M., Glick, D., Loewenstein, Y., and Soreq, H. (1995). Engineering of human cholinesterases explains and predicts diverse consequences of administration of various drugs and poisons. Pharmac. Ther. *67*, 283-322.
65. Layer, P. G., Weikert, T., and Willbold, E. (1992). Chicken retinospheroids as developmental and pharmacological *in vitro* models: acetylcholinesterase is regulated by its own and by butyrylcholinesterase activity. Cell Tissue Res. *268*, 409-418.
66. Catalono, S. M., Robertson, R. T., and Killackey, H. P. (1991). Early ingrowth of thalamocortical afferents to the neocortex of the prenatal Rat. Proc. Natl. Acad. Sci. USA *88*, 299-3003.
67. Shapira, M., Seidman, S., Sternfeld, M., Timberg, R., Kaufer, D., Patrick, J. W., and Soreq, H. (1994). Transgenic engineering of neuromuscular junctions in *Xenopus laevis* embryos transiently overexpressing key cholinergic proteins. Proc. Natl. Acad. Sci. USA *91*, 9072-9076.
68. Layer, P. G., Weikert, T., and Alber, R. (1993). Cholinesterases regulate neurite growth of chick nerve cells *in vitro* by means of a non-enzymatic mechanism. Cell Tissue Res. *273*, 219-226.
69. Small, D. H., Reed, G., Whitefield, B., and Nurcombe, V. (1995). Cholinergic regulation of neurite outgrowth from isolated chick sympathetic neurons in culture. J. Neurosci. *15*, 144-151.
70. Karpel, R., Ben Aziz-Aloya R., Sternfeld, M., Ehrlich, G., Ginzberg, D., Tarroni, P., Clementi, F., Zakut, H., and Soreq, H. (1994). Expression of three alternative acetylcholinesterase messenger RNAs in human tumor cell lines of different tissue origins. Exp. Cell Res. *210*, 268-277.
71. Yu, C., Brussaard, A. B., Yang, X., Listerud, M., and Role L.W. (1993). Uptake of antisense oligonucleotides and functional block of acetylcholine receptor subunit expression in primary embryonic neurons. Dev. Genet. *14*, 296-304.
72. Grifman, M., Ginzburg, D., and Soreq, H. (1995). Impairment of neurite extension and apoptosis-dependent DNA fragmentation in primary neuronal cell cultures administered with an ACHE antisense oligonucleotide. J. Neurochem. *65 (Suppl.)*, 82.
73. Weiss, S., Pin, J. P., Sebben, M., Kemp, D.E., Sladeczek, F., Gabrion, J., and Bockaert, J. (1986). Synaptogenesis of cultured striatal neurons in serum free medium: a morphological and biochemical study. Proc. Natl. Acad. Sci. USA *83*, 2238-2242.
74. Zimmermann, H., Heilbronn, A., Braun, N., Carstensen, C., Kegel, B., and Maienschein, V. (1995). Extracellular metabolism of nucleotides in the nervous system. J. Neurochem. *65 (Suppl.)*, 210.
75. Brown, L. M., Blair, A., Gibson, R., Everett, G. D., Cantor, K. P., Shuman, L. M., Burmeister, L. F. Van Lier, S. F., and Dick, F. (1990). Pesticide exposures and other agricultural risk factors for leukemia among men in Iowa and Minnesota. Cancer Res. *50*, 6585-6591.
76. Lapidot-Lifson, Y., Prody, C. A., Ginzberg, D., Meytes, D., Zakut, H., and Soreq, H. (1989). Co amplification of human acetylcholinesterase and butyrylcholinesterase genes in blood cells: Correlation with various leukemias and abnormal megakaryocytopoiesis. Proc. Natl. Acad. Sci. USA *86*, 4715-4719.
77. Zakut, H., Lapidot-Lifson, Y., Beeri, R., Ballin A., and Soreq, H. (1992). *In vivo* gene amplification in non-cancerous cells: Cholinesterase genes and oncogenes amplify in thrombocytopenia associated with lupus erythematosus. Mut. Res. *276*, 275-284.
78. Patinkin, D., Seidman, S., Eckstein, F., Benseler, F., Zakut, H., and Soreq, H. (1990). Manipulations of cholinesterase gene expression modulate murine megakaryocytopoiesis *in vitro*. Molec. Cell Biol. *10*, 6046-6050.
79. Wagner, R. (1995). Toward a broad-based antisense technology. Antisense Res. Develop. *5*, 113-144.
80. Soreq, H., Lev-Lehman, E., Patinkin, D., Grifman, M., Ehrlich, G., Ginzberg, D., Eckstein, F., and Zakut, H. (1995). Antisense oligonucleotides suppressing expression of cholinesterase genes modulate hematopoiesis *in vivo* and *ex vivo*. In: Enzymes of the Cholinesterase Family, D. M. Quinn, A. S. Balasubramanian, B. P. Doctor and P.Taylor, eds. New York: Plenum Press, 1-6.
81. Patinkin, D., Lev-Lehman, E., Zakut, H., Eckstein F., and Soreq, H. (1994). Antisense inhibition of butyrylcholinesterase gene expression predicts adverse hematopoietic consequences to cholinesterase inhibitors. Cell. Molec. Neurobiol. *14*, 459-473.
82. Winker, M.A. (1994). Tacrine for Alzheimer's disease, which patent, what dose? JAMA *271*, 1023-1024.
83. Gavrieli, Y., Sherman, Y., and Ben-Sasson S. (1992). Identification of programmed cll deeath *in situ* via specific labeling of nuclear DNA fragmentation. J. Cell Biol. *119*, 493-501.
84. Harik, S. I. and Kalaria, R. N. (1991). Blood-brain barrier abnormalities in Alzheimer's disease. Ann. N.Y. Acad. Sci. *640*, 47-52.

Converting and typesetting by: Knipp Medien und Kommunikation, Dortmund. – Printing: Karl Gerike GmbH, Berlin. – Binding: Heinz Stein, Berlin. – Cover Design: Hansbernd Lindemann, Berlin.
Printed in Germany.

ELSEVIER

Molecular Brain Research 51 (1997) 179–187

MOLECULAR BRAIN RESEARCH

Research report

In vitro phosphorylation of acetylcholinesterase at non-consensus protein kinase A sites enhances the rate of acetylcholine hydrolysis

Mirta Grifman [a], Ayelet Arbel [a], Dalia Ginzberg [a], David Glick [a], Sharona Elgavish [a,b], Boaz Shaanan [a,b], Hermona Soreq [a,*]

[a] *Department of Biological Chemistry, Institute of Life Sciences, Hebrew University of Jerusalem, Jerusalem 91904, Israel*
[b] *Wolfson Center for Applied Structural Biology, Institute of Life Sciences, Hebrew University of Jerusalem, Jerusalem 91904, Israel*

Accepted 8 July 1997

Abstract

Here, we report that the catalytic subunit of cAMP-dependent protein kinase (PKA) but not casein kinase II or protein kinase C phosphorylates recombinant human acetylcholinesterase (AChE) in vitro. This enhances acetylthiocholine hydrolysis up to 10-fold as compared to untreated AChE, while leaving unaffected the enzyme's affinity for this substrate and for various active and peripheral site inhibitors. Alkaline phosphatase treatment enhanced the electrophoretic migration, under denaturing conditions, of part of the AChE proteins isolated from various mammalian sources and raised the isoelectric point of some of the treated AChE molecules, indicating that part of the AChE molecules are also phosphorylated in vivo. Enhancement of acetylthiocholine hydrolysis also occurred with *Torpedo* AChE, which has no consensus motif for PKA phosphorylation. Further, mutating the single PKA site in human AChE (threonine-249) did not prevent this enhancement, suggesting that in both cases it was due to phosphorylation at non-consensus sites. In vivo suppression of the acetylcholine hydrolyzing activity of AChE and consequent impairment in cholinergic neurotransmission occur under exposure to both natural and pharmacological compounds, including organophosphate and carbamate insecticides and chemical warfare agents. Phosphorylation of AChE may possibly offer a rapid feedback mechanism that can compensate for impairments in cholinergic neurotransmission, modulating the hydrolytic activity of this enzyme and enabling acetylcholine hydrolysis to proceed under such challenges. © 1997 Elsevier Science B.V.

Keywords: Acetylcholinesterase; Neurotransmission; cAMP-dependent protein kinase A; Non-consensus phosphorylation site; Protein phosphorylation

1. Introduction

Acetylcholinesterase (acetylcholine acetyl hydrolase, EC 3.1.1.7; AChE) is a key component of cholinergic brain synapses and neuromuscular junctions, in which it hydrolyzes the neurotransmitter acetylcholine [44,46]. In addition to terminating cholinergic neurotransmission, it may have non-catalytic function(s) in cellular development [3,8,18,22,41]. This may explain its presence on the surface of erythrocytes and in embryonic tissues [25]. The central role of AChE in cholinergic neurotransmission is demonstrated by the fact that it is the target of a variety of toxic compounds, both natural and man-made. For example, several natural compounds inhibit the catalytic activity of cholinesterases including glycoalkaloids, which are found in solanaceous food plants such as potatoes [31], the snake venom protein inhibitor fasciculin [5,10] and cyanobacterial toxins [14]. Chemical warfare agents (e.g. sarin and tabun) and organophosphate insecticides (e.g. malathion) also are designed to inhibit AChE [46]. In addition, AChE is a target of several pharmacological agents that are designed to enhance cholinergic neurotransmission in the treatment of disorders associated with cholinergic imbalance, such as Alzheimer's disease and myasthenia gravis [24,37]. The widespread presence of both natural and man-made anti-AChE compounds [27] raises the question if natural mechanisms exist that enable this enzyme to function under diverse conditions.

The crucial role of AChE in cholinergic neurotransmission implies that to be physiologically relevant, adjustments in its activity in response to fluctuating physiological conditions should occur within a very short time scale. This excludes regulation at the levels of gene expression, multimeric assembly and intracellular targeting,

* Corresponding author. Fax: +972 (2) 652-0258; E-mail: soreq@shum.huji.ac.il

0169-328X/97/$17.00
PII S0169-328X(97)00246-5

none of which offers a sufficiently rapid response. AChE is present in various glycosylated forms [26], but the carbohydrate moiety does not contribute to catalytic activity [7,49]. Allosteric modulation and substrate inhibition of AChE have also been reported [1,6], but no physiologically significant scheme for controlling AChE activity has been demonstrated. As phosphorylation is the most frequently seen post-translational mechanism of control of physiological processes, and since the human AChE amino-acid sequence [44] reveals several consensus phosphorylation sites, we have investigated phosphorylation as a mechanism of control of AChE activity.

2. Materials and methods

2.1. Computer analyses

The MOTIF program (version 8, Genetics Computer Group, University of Wisconsin, Madison, WI) was used to identify consensus phosphorylation motifs. The amino-acid sequence numbers of human and *Torpedo* AChE sequences correspond to the m55040 and x05497 GenBank Accession Numbers, respectively. The three-dimensional structure of AChE [45] was plotted using the Insight II program (Biosym Technologies) on a Silicon Graphics computer (Indigo R4000). Surface residues were identified according to the proportion of exposed surface as compared to the relative exposure level of the same residue in Gly-X-Gly peptides [28].

2.2. Materials

Purified recombinant human AChE preparations were gifts of Drs. A. Shafferman, Ness Ziona (293 cells preparations) and A. Fischer, Ness Ziona (*E. coli* preparations). AChE, purified from human erythrocytes and brain and from bovine erythrocytes as well as monoclonal antibodies to human AChE [39] were gifts from U. Brodbeck (Bern, Switzerland). H1 histone was a Boehringer (Mannheim, Germany) product. Echothiophate, pyridostigmine bromide and fasciculin were products of Ayerst Laboratories (Montreal, Canada), Research Biochemicals International (Natick, MA) and Alomone (Jerusalem, Israel), respectively. All other reagents were purchased from Sigma (St. Louis, MO). All anti-cholinesterases were dissolved in double-distilled water and kept at −20°C as 100-fold concentrated stock solutions or were added directly to reaction mixtures.

2.3. Cell lines and transfections

COS-1 monkey kidney cells (a gift of Y. Gruenbaum, Jerusalem) were grown in Dulbecco's modified Eagle's medium (DMEM) containing 10% fetal calf serum (FCS) at 37°C, 5% CO_2, in a humidified chamber. COS-1 cells were transfected using Lipofectamine (Gibco-BRL, Bethesda, MD) according to the manufacturer's instructions and were incubated in DMEM containing 2% FCS for 3 days, at which stage medium was collected for AChE enzymatic analyses [43].

2.4. In vitro phosphorylation / dephosphorylation

Proteins were phosphorylated by 30 min incubation at 30°C in 18 mM Mg acetate, 25 mM MES, pH 6.8, 50 mM EDTA, 0.2 mM ATP (Boehringer), 1 μCi [γ-^{33}P]ATP (1000–3000 Ci/mmol, Amersham Life Sciences, Aylesbury, UK) and 25 casein units of cAMP-dependent protein kinase catalytic subunit (Promega, Madison, WI) in a final volume of 50 μl. For the enzymatic analysis of phosphorylated AChE, 100 casein units were used. To inhibit phosphorylation, 20 μg of cAMP-dependent protein kinase peptide inhibitor (Promega) were added to the phosphorylation reaction mixture. For dephosphorylation, AChEs were incubated for 60 min at 37°C in 50 mM Tris-HCl, pH 8.5, 0.1 mM EDTA with 20 U calf intestine alkaline phosphatase (Boehringer) in a final volume of 20 μl. λ-Phosphatase (New England Biolabs, Beverly, MA) and protein phosphatase 1 (Boehringer) were also used according to manufacturers' instructions.

2.5. Gel electrophoresis

SDS-PAGE was performed according to Laemmli [21] using 8% polyacrylamide gels. For immunochemical detection, proteins from SDS gels were electroblotted onto nitrocellulose membranes (Schleicher and Schuell, Dassel, Germany) in a semi-dry-blot system as described [11]. After transfer, membranes were washed in 20 mM Na phosphate, pH 7.4, 144 mM NaCl, 0.1% (v/v) Tween-20, at room temp. for 1 h, blocked in 5% (w/v) dried skim milk, then rinsed and incubated with anti-human AChE monoclonal antibodies 132-2 and 132-3 at 6 μg/ml each for 1 h. After 3 washes, as above, membranes were incubated for 1 h with a 1:4000 dilution of a sheep anti-mouse Ig, horseradish peroxidase linked F(ab$'_2$) fragment (Amersham). Chemiluminescent detection was performed with Amersham's ECL kit as instructed.

Proteins were separated according to their isoelectric points on native polyacrylamide-ampholyte gels, pH 4–6, as described [4]. Gels were pre-focused for 30 min at 100 mV and then run for an additional 2.5 h at 100 mV. After separation, gels were stained overnight for cholinesterase activity as detailed [18] using 0.5 mM acetylthiocholine (ATCh).

Colorimetric determination of cholinesterase activities was performed as described elsewhere, using 1 mM ATCh [31]. For K_m determination, ATCh in the range of 0.01–10 mM was used. Effects of inhibitors were determined over a concentration range of at least 5 orders of magnitude. Pre-incubations of the inhibitor with the enzyme for 20

min preceded the addition of substrate and activity measurements. K_i values for reversible inhibitors were calculated from experimental IC_{50} values according to the equation $K_i = IC_{50}/(1 + S/K_m)$, were S was the ATCh concentration, 1 mM.

2.6. PCR mutagenesis

T249A E6-ACHEDNA was produced from the CMV-E6 plasmid [18] by PCR mutagenesis as described [12], using the following primers: hACHEmut987 (+): 5′-CAGGGCCGCGCAGCTGGCCCAC-3′; hACHEmut 1008 (−): 5′-GTGGGCCAGCTGCGCGGCCCTG-3′; hACHE 823 (+): 5′-GGTGACCCGACATCAGTGACGCTGTT-3′; hACHE1855 (−): 5′-GGAAGCGGTTCCAGAAGGCGCAGGC-3′, where the underlined base denotes the mutation, the primer numbering corresponds to the human ACHE sequence and (+) or (−) is the upstream or downstream orientation, respectively. The PCR program was 1 min at 94°C (first cycle for 15 min), 1 min at 68°C and 1 min at 72°C (last cycle for 5 min). The amplified end product was restricted with *Not*I and *Sph*I (New England Biolabs) and exchanged with the corresponding wild-type fragment. The accuracy of the T249A substitution was verified by automated sequencing (Applied Biosystems 377).

3. Results

3.1. AChE carries consensus phosphorylation sites

The human AChE amino-acid sequence was searched for consensus phosphorylation sites with the aid of the three-dimensional models of the closely homologous *Torpedo* [45] and mouse [5] AChEs. This enabled the selection of serine or threonine residues at the surface of the protein, which are susceptible to enzyme phosphorylation, both in *Torpedo* and mammalian AChE. Five such sites were found in human AChE: for casein kinase II (S128, S355 and T466), protein kinase C (T11, A11 in mouse) and protein kinase A (T249), where numbers correspond to the human AChE sequence (Fig. 1A). Eleven more serine and threonine residues were found on the protein surface of *Torpedo* AChE, however, none of those was part of a known consensus motif for phosphorylation by any recognized kinase (Fig. 1B).

3.2. AChE can be phosphorylated in vitro

To determine which of the kinases identified in this search is in practice capable of phosphorylating human AChE, we used commercially available kinases and the highly purified human recombinant AChE produced in transfected 293 cells [48]. Casein kinase II and protein

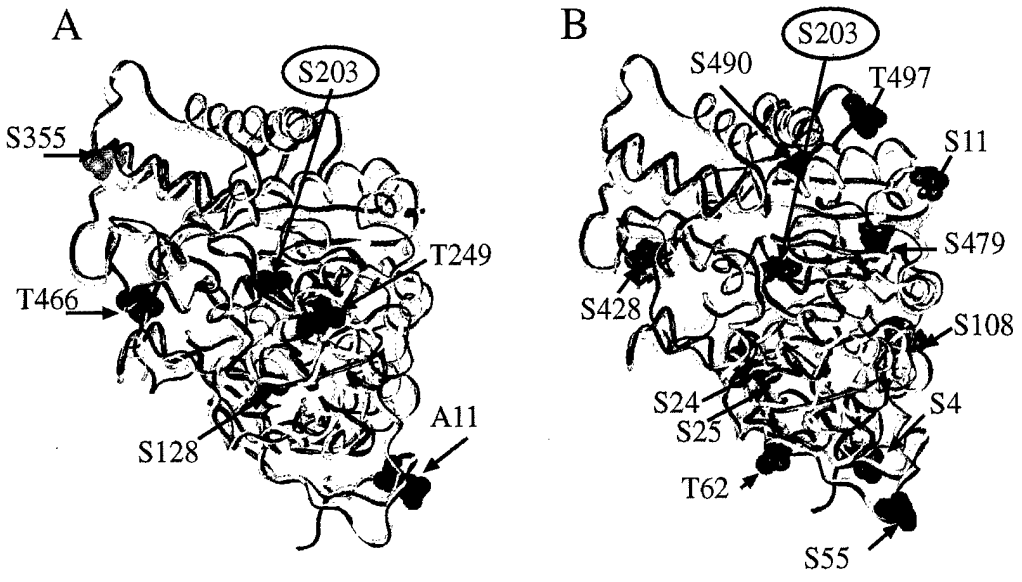

Fig. 1. Serine and threonine residues on the three-dimensional models of AChE. A: consensus motifs for various kinases: superimposition of *Torpedo* (yellow) and mouse (magenta) AChEs according to their Cα atoms. Amino-acid numbers are as in the human sequence. Active site serine (203) is displayed as a turquoise sphere, the PKA consensus site R/KXXT/S (beginning with arginine or lysine and ending with threonine or serine) threonine-249 in violet, the casein kinase II consensus sites S128, S355 and T466 in gray and the protein kinase C consensus site T11 (A11 in mouse) in green. B: surface-exposed serine and threonine residues: active site serine 203 is displayed as a turquoise sphere together with those serine and threonine residues which were calculated to be exposed at the surface of the *Torpedo* AChE protein (see Section 2).

kinase C were both incapable of phosphorylating AChE in vitro. In contrast, protein kinase A (PKA) efficiently induced the incorporation of ^{33}P from labeled ATP into AChE. Moreover, this kinase also phosphorylated recombinant human AChE produced in *E. coli*, human AChE isolated from brain or blood sources and bovine erythrocyte AChE, all with apparently similar efficiency (Fig. 2). Control incubation with kinase in the absence of ATP failed to phosphorylate AChE. The intensity of kinase labeling of human and bovine AChE was lower than that obtained under the same conditions with H1 histone, suggesting a relatively limited availability of AChE amino-acid residues susceptible to phosphorylation. PKA completely failed to phosphorylate the closely related enzyme human butyrylcholinesterase (BuChE), even though it includes a consensus PKA site (Fig. 2).

3.3. Ex vivo AChE may be partially phosphorylated

When treated with alkaline phosphatase (AP), electrophoretically separated under denaturing conditions and subjected to immunodetection, a small fraction of purified AChEs from different mammalian sources migrated faster than the non-treated enzyme (Fig. 3A). This indicated that certain portions of each of these AChE preparations had been phosphorylated in vivo, that these enzyme molecules retained their phosphorylation throughout the purification process and that at least some of the phosphate groups associated with AChE in vivo could be removed in vitro by AP. This, in turn predicted that the AP treatment should reduce some of the negative charges associated with the treated enzyme molecules. To test this prediction, we performed isoelectric focusing under non-denaturing conditions followed by activity staining of the AP-treated recombinant enzyme. Interestingly, a new faint band representing a novel AChE subtype appeared on the isoelectric focusing gel. This enzyme displayed an isoelectric point of 5.9, higher than any of the isoelectric subtypes of the untreated enzyme (Fig. 3B). Its activity represented $< 3\%$ of the total staining, a far smaller portion than that part of the immunochemically detected AP-treated enzyme which migrated faster in SDS-PAGE (cf. Fig. 3A and Fig. 3B), suggesting that the AP-dephosphorylated molecules are less active than others in this preparation.

The AP-insensitive AChE molecules could either be non-phosphorylated or phosphorylated yet modified post-translationally in a way preventing the action of AP. However, PKA phosphorylation did not create new immunochemically detectable protein bands following electrophoresis under denaturing conditions (not shown). Furthermore, PKA treatment of hAChE followed by isoelectric focusing and activity staining revealed only activity bands that had existed in the untreated control enzyme preparation (Fig. 3B), in agreement with the results observed by immunochemical detection. These experiments indicate that native AChE purified from red blood cells and recombinant AChE expressed in 293 cells are at least partially phosphorylated and that most of these phosphate residues cannot be removed by AP. Neither λ-phosphatase nor protein phosphatase-1 had any effect on the electrophoretic migration of AChE.

3.4. AChE phosphorylation enhances hydrolytic activity

PKA phosphorylation increased by up to 10-fold the rate of ATCh hydrolysis by the recombinant human enzyme from either *E. coli* or transfected cells. This also

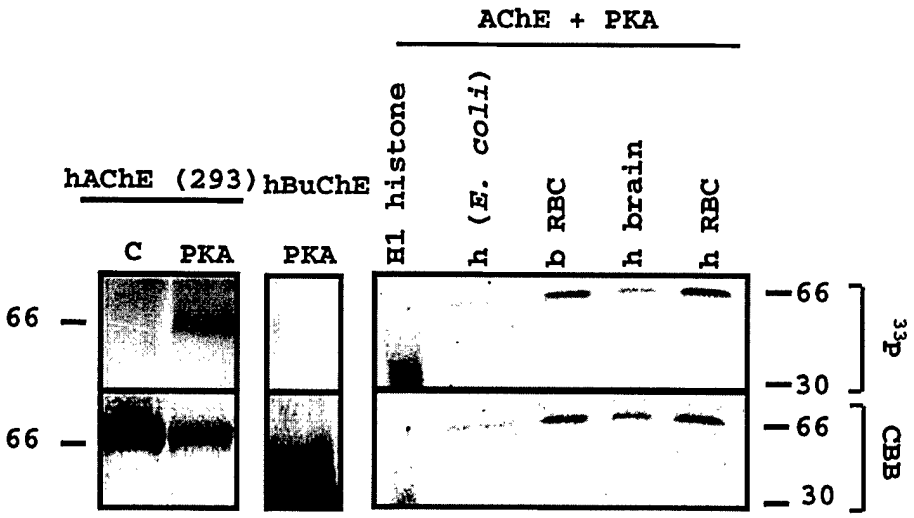

Fig. 2. In vitro phosphorylation of AChEs. Phosphorylation reactions were performed on 5 μg purified recombinant AChE expressed in 293 kidney cells (hAChE (293)), 2 μg purified recombinant AChE expressed in *E. coli* (h (*E. coli*)), 5, 3 and 5 μg of native AChE purified from human red blood cells (hRBC), human brain (hbrain) and bovine red blood cells (bRBC), 0.2 mU hBuChE, respectively, and 5 μg histone (H1). One-fifth of each of the phosphorylation reactions, was separated by SDS-PAGE followed by either protein staining with Coomassie brilliant blue (CBB) or by 48 h autoradiography (^{33}P). An incubation without PKA served as a control (C). Numbers on both sides of the figure indicate molecular mass in kDa.

Table 1
Effect of protein kinase A on the activity of cholinesterases from various sources [a]

	Catalytic (μmol/min/ml)		Activity	PKA consensus site
	− Kinase	+ Kinase	+ Kinase/ − Kinase	
AChE				
Recombinant human, from 293 cells	8.3	76.9	9.3	+
Recombinant human, from *E. coli*	0.3	2.4	8.0	+
Human erythrocyte	3.2	12.8	4.0	+
Human brain	4.5	11.3	2.5	+
Torpedo electroplax	4.2	17.7	4.2	−
COS cells transfected with normal E6-ACHEDNA	0.9	1.8	2.0	+
COS cells transfected with T249A E6-ACHEDNA	1.0	2.2	2.2	−
BuChE				
Human serum	1.1	1.2	1.1	+

[a] The data represent one out of three reproducible experiments with standard deviations below 30%. For BuChE activity determinations, 5 mM butyrylthiocholine was used as a substrate. All enzyme preparations were highly purified except that for *Torpedo* which was partially purified and for those for COS cells which were tested in conditioned medium from transfected cells with no further purification. The presence (+) or absence (−) of a PKA phosphorylation consensus site on each of the examined sequences is noted.

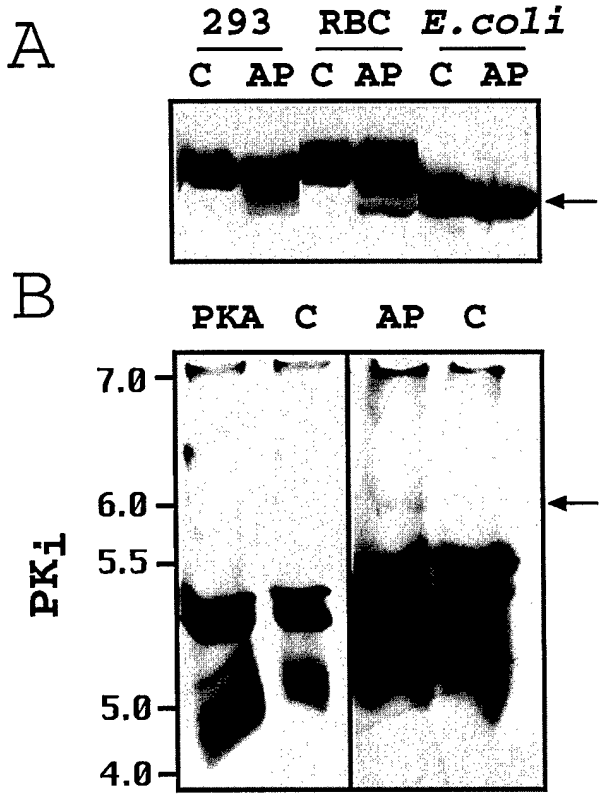

Fig. 3. Dephosphorylation of AChE modifies its electrophoretic and isoelectric properties. A: alkaline phosphatase enhances the electrophoretic migration of AChE. Alkaline phosphatase (AP) treated and control untreated (C) recombinant human AChE from 293 cells (293, 3 μg), from human red blood cells (RBC, 5 μg) or human AChE produced in *E. coli* (*E. coli*, 3 μg) were electrophoretically separated under denaturing conditions and immunochemically detected. The arrow indicates the position of that fraction of these proteins that migrated faster after dephosphorylation. B: alkaline phosphatase induces the appearance of a novel AChE subtype with high isoelectric point. 3 μg hAChE (293) in a final volume of 20 μl was treated either with PKA or with AP and was subjected to isoelectric focusing gel electrophoresis followed by activity staining of the gels. Similarly treated AChEs served as a control (C). The arrow indicates an additional band at a higher isoelectric point which could only be observed after AP treatment.

occurred, although to a more limited extent, with AChE purified from human brain or erythrocytes or *Torpedo* electroplax (Table 1). This latter increment was rather surprising as *Torpedo* AChE lacks the consensus T249 PKA site. Yet, the role of PKA was further demonstrated by the fact that activation of AChE by PKA was inhibited by 40% in the presence of the highly specific PKA inhibitor, PKI.

In contrast, PKA had no effect on butyrylthiocholine hydrolysis by human serum BuChE, although this enzyme does carry the PKA consensus motif (Table 1). Thus, incorporation of ^{33}P and the enhancement in ATCh hydrolysis were clearly associated with each other.

Unlike the catalytic rate, the K_m for ATCh of the treated AChE preparations remained unaffected, at 0.05 mM. Moreover, IC_{50} and K_i values for several cholinesterase inhibitors targeted either to the active or the peripheral site [37] were also unmodified. These included the carbamate physostigmine, the organophosphate echothiophate, the Alzheimer's disease drug tetrahydroamino acridine (tacrine, Cognex™), the selective AChE inhibitor BW284c51, which acts both at the active and the periph-

Table 2
Kinetic constants of human acetylcholinesterase purified from embryonic kidney 293 cells [a]

	− Kinase	+ Kinase
K_m (μM)	50	50
K_i values (μM)		
Tacrine	0.007	0.006
Fasciculin 02	0.0002	0.0003
BW284c51	0.3	0.3
IC_{50} (μM)		
Physostigmine	0.01	0.01
Echothiophate	0.01	0.01

[a] Kinetic constants of recombinant AChE purified from 293 cells with no further treatment (−kinase) or treated with PKA (+kinase) were determined as detailed in Section 2.

Table 3
Abolition of the PKA consensus site does not modify AChE properties

	E6-ACHEDNA-transfected [a]	T249A E6-ACHEDNA-transfected [b]
K_i values (μM)		
Succinylcholine	290	290
Dibucaine	720	730
BW284c51	0.007	0.007
Tacrine	0.058	0.072
Fasciculin 02	0.0000001	0.0000001
Fasciculin 03	0.0000002	0.0000002
IC_{50} value (μM)		
Pyridostigmine	0.50	0.55

[a] COS cells were transfected with E6-ACHEDNA as detailed in Section 2 and the biochemical properties of AChE secreted into the medium were determined as in Tables 1 and 2.
[b] Site-directed mutagenesis was employed to create the T249A mutant enzyme. Tests were similar to those for the non-mutated enzyme.

eral site and the snake venom protein inhibitor fasciculin (Table 2).

To test the potential of AChE phosphorylation to enhance acetylcholine hydrolysis under exposure to various AChE inhibitors, we subjected identical amounts of recombinant human AChE produced in transfected 293 cells to PKA phosphorylation in vitro and then to increasing concentrations of several inhibitors. PKA-phosphorylated human AChE was as sensitive as the untreated enzyme to inhibition by tacrine (Fig. 4A). However, at therapeutic tacrine concentrations of 2×10^{-8} M [17,19], phosphorylated AChE displayed considerably higher activities than the control enzyme (Fig. 4A). A parallel difference in remaining enzyme activity was observed in the presence of 10^{-10} to 10^{-8} M physostigmine (Fig. 4B), 10^{-11} to 10^{-8} M fasciculin (Fig. 4C), which blocks the entrance to the active site of AChE [5] and 10^{-11} to 10^{-8} M echothiophate (Fig. 4D). Thus, PKA phosphorylation can potentially serve to compensate for suppression of AChE activity by a wide range of concentrations of various inhibitors.

3.5. Evidence for phosphorylation at non-consensus sites

The only consensus site for PKA phosphorylation in the human AChE sequence is T249 (see Fig. 1A) and it is conserved in all of the mammalian AChEs [25], but not in *Torpedo*. Nevertheless, PKA was able to enhance the catalytic activity of *Torpedo* AChE (Table 1). This in turn, suggested that PKA phosphorylation might occur also at non-consensus sites in all of the examined AChE preparations, including those of human origin. In that case, substitution of T249 in the human enzyme should not prevent the capacity of PKA to increase its catalytic activity. To test this hypothesis, we employed site-directed mutagenesis to substitute threonine-249, which resides on the protein surface close to the entrance to the active site gorge, by alanine. Non-purified T249A hAChE secreted from transfected COS cells hydrolyzed ATCh at a normal rate

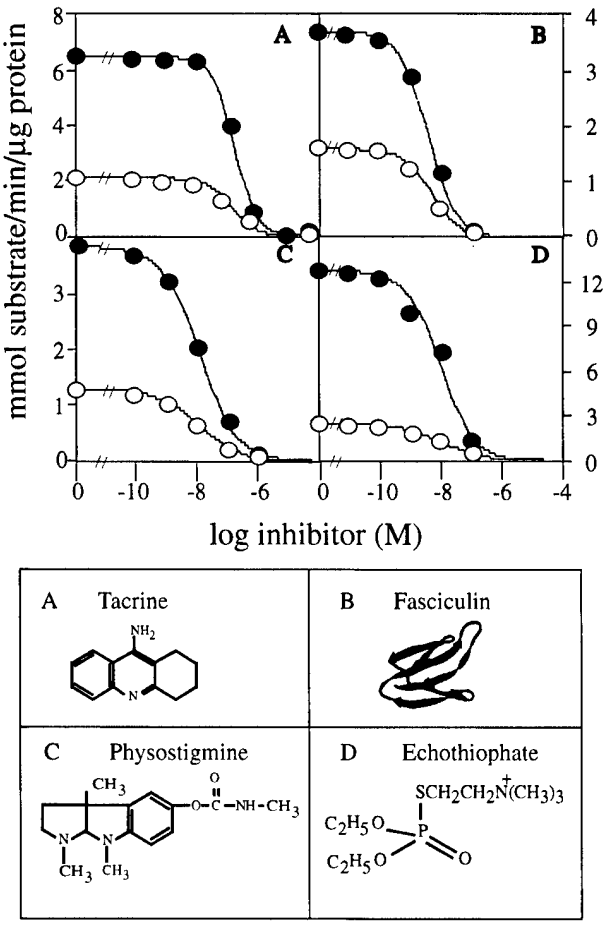

Fig. 4. PKA phosphorylation enhances AChE catalysis under exposure to various inhibitors. Human recombinant AChE purified from 293 cells was subjected to PKA phosphorylation as in Section 2, except that the PKA:AChE ratio was lower in order to maintain AChE concentrations appropriate for inhibition measurements. Presented are enzyme activities in the presence of increasing concentrations of the noted inhibitors at 1 mM ATCh. Each curve is an average best-fit result of 2 experiments. The crystal structure of fasciculin is after [5]. Filled circles, PKA-treated enzyme; empty circles, untreated enzyme. Effects of the inhibitors indicated in the lower panels are shown in the upper panels.

and was 2-fold activated by PKA, an efficiency similar to that observed for its non-mutated counterpart (Table 1). Moreover, the mutant unpurified enzyme displayed a similar K_m to that of its normal counterpart and maintained unmodified IC_{50} and K_i values for several cholinesterase inhibitors (Table 3). We conclude that PKA phosphorylation of AChE, like that of the cystic fibrosis trans-membrane receptor protein (CFTR) [38], takes place also at non-consensus serine/threonine residues.

4. Discussion

We have shown that AChE can be phosphorylated in vitro, employed different methods suggesting that part of the AChE molecules in preparations from various mammalian cell types and *Torpedo* electric organ are phosphorylated, and showed that such phosphorylation can be physiologically relevant, particularly under exposure to various natural and man-made AChE inhibitors. That this phosphorylation is a general phenomenon was indicated by the fact that PKA was able to incorporate phosphate from ATP into purified AChE from different animal and tissue sources. Moreover, AP treatment of AChE modified the isoelectric focusing pattern of the active enzyme from various sources and enhanced the electrophoretic migration of a significant fraction of the treated enzyme under denaturing conditions, similarly to the effects on other in vivo phosphorylated proteins, e.g. Cdc25 [9].

The mechanism through which phosphorylation increases the activity of AChE remains obscure. Possible explanations include hyperactivation of fully active catalytic subunits, for instance by increasing product release. Alternatively, this activation could be due to a phosphorylation-induced refolding of poorly active enzyme molecules, bringing them to a more active state. Two-state transition between 'molten globule' and unfolded states of AChE has indeed been demonstrated by electron paramagnetic resonance spectroscopy [20]. This explanation is particularly attractive for the recombinant enzyme, and is in agreement with the fact that the catalytic properties of the phosphorylated enzyme (e.g. K_m and K_i) are identical to those of untreated AChE. In any event, phosphorylation of AChE is independent of either glycosylation or C-terminal variation in the enzyme, as it occurs with the non-glycosylated *E. coli*-produced enzyme as well as with the erythrocyte and brain-derived forms which differ in their 40 C-terminal amino acids due to alternative mRNA splicing [39,18]. However, the observation that alkaline phosphatase does not extensively modify the electrophoretic migration of recombinant human AChE produced in *E. coli* implies that mammalian kinase(s) are primarily required to exert this effect. While the location where this in vivo phosphorylation takes place is still unknown, that it does not depend upon glycosylation implies that it may occur intracellularly, as is the case for most of the known PKA phosphorylations [51]. An alternative possibility is that of extracellular phosphorylation [40,50]. PKA phosphorylation in the synaptic cleft would provide more rapid response to reduced enzyme activity than that provided by intracellular phosphorylation.

Phosphorylation of many key elements of the nervous system demonstrates the importance of protein kinases for synaptic functioning. For example, PKA phosphorylation of synapsin down-regulates pre-synaptic release [34]. Within the cholinergic synapse, choline acetyltransferase was shown to be a substrate for a calcium-dependent kinase [36] and PKA phosphorylation of the nicotinic acetylcholine receptor [13] was shown to take place in vivo. Receptor phosphorylation leads to channel desensitization and to a reduced sensitivity to acetylcholine [23,13]. It is possible that AChE phosphorylation, accelerating acetylcholine hydrolysis, participates in this phenomenon. Conversely, specific phosphatases might enhance synaptic transmission in response to cholinergic cues by suppressing AChE's activity. That phosphatase inhibitors reinforce physiological properties associated with cholinergic circuits (e.g. long-term potentiation, [29]) is in line with this prediction.

The fact that AChE phosphorylation affects neither the K_m of the enzyme for ATCh nor its affinity for active and peripheral site inhibitors, excludes the possibility that the attraction of ligands to the active site or intermediary complex were affected. Rather, these suggest that the activation may be due to a faster product release. Negative charges of phosphate groups on peripheral AChE sites could also affect the enzyme's dipole moment, which has been considered to be an important contribution to AChE catalytic rate [35]. Phosphorylation can further modulate enzyme activities under anti-cholinesterase therapies, with special importance for patients with genetic predisposition for adverse responses to such therapies [24].

It is intriguing that ^{33}P incorporation appeared comparable in the different preparations whereas the increase in activity was quite distinct for each enzyme source. For example, we observed activation factors of 2.5 in the case of human brain AChE, 4 for the red blood cell enzyme and 9.3 for the recombinant enzyme. This may indicate that the in vitro phosphorylation by PKA occurs at many sites, only a small fraction of which are catalytically effective; and that the extent to which this (these) site(s) remain phosphorylated differs among the different purification protocols. This, in conjunction with the predicted in vivo phosphorylation, could also explain the fact that the AP-modified band represents $< 3\%$ of total activity, while phosphorylation increases activity by up to 10-fold. Also, the existence of a consensus PKA motif was insufficient to ensure the examined cholinesterase phosphorylation, as was evident from the fact that BuChE failed to be phosphorylated. However, this could reflect a prior state of complete phosphorylation or steric hindrance due to the excessive glycosylation characteristic of BuChE (reviewed

in [44]). Subsequent experiments demonstrated that a consensus PKA site was not necessary for the observed effect: PKA was able to activate AChE in vitro, even when prepared from *Torpedo*, which lacks the consensus site or when the single T249 consensus PKA motif on human AChE was mutated. This suggested that PKA can phosphorylate AChE at non-consensus sites.

The cerebrospinal fluid (CSF) of Alzheimer's disease patients, both in vivo and post mortem, showed an anomalous AChE band following isoelectric focusing and activity staining [30,33,42]. If the hyperphosphorylation of tau in the Alzheimer's disease brain [47] reflects a general state of excess kinase activity, it is possible that AChE is also hyperphosphorylated under these circumstances. This could explain the appearance of the new AChE species in the CSF of Alzheimer's disease patients.

Several lines of evidence [8,22,41,18,16] demonstrate non-catalytic activities for AChE which may also be affected by its phosphorylation. The sequence homologies between AChE and the family of neurexin ligands, including neuroligins-1, 2 and 3 [15], raise the possibility that the non-catalytic properties of AChE may be due to its capacity to interact with neurexins. Phosphorylation of surface amino-acid residues is likely to be of primary importance to such protein-protein interactions, as is the case for cyclin interactions [32]. Neurotactin, one of these non-catalytically active nervous system proteins with sequence homology to AChE is indeed phosphorylated in vivo [2]. AChE phosphorylation is thus a key process with the potential to control numerous functions, both within cholinergic synapses and in the developing nervous system.

Acknowledgements

We thank Drs. G. Robinson (Urbana, IL) for critically reviewing this manuscript, A. Shafferman and A. Fischer (Ness Ziona, Israel) for the gifts of purified recombinant human AChE, U. Brodbeck (Bern, Switzerland) for purified native AChEs and monoclonal antibodies and Y. Gruenbaum (Jerusalem) for COS-1 cells. This study was supported by the US Army Medical Research and Development Command (Contract DAMD 17-97-1-7007, to H.S.).

References

[1] D. Barak, A. Ordentlich, A. Bromberg, C. Kronman, D. Marcus, A. Lazar, N. Ariel, B. Velan, A. Shafferman, Allosteric modulation of acetylcholinesterase activity by peripheral ligands involves a conformational transition of the anionic subsite, Biochemistry 34 (1995) 15444–15452.

[2] Y. Barthalay, R. Hipeau-Jacquotte, S. De la Escalera, F. Jimenez, M. Piovant, *Drosophila* neurotactin mediates heterophilic cell adhesion, EMBO J. 9 (1990) 3603–3609.

[3] R. Ben Aziz-Aloya, S. Seidman, R. Timberg, M. Sternfeld, H. Zakut, H. Soreq, Expression of a human acetylcholinesterase promoter-reporter construct in developing neuromuscular junctions of *Xenopus* embryos, Proc. Natl. Acad. Sci. USA 90 (1993) 2471–2475.

[4] D.M. Bolag and S.J. Edelstein, Protein Methods, Wiley-Liss, New York, 1991, pp. 161–174.

[5] Y. Bourne, P. Taylor, P. Marchot, Acetylcholinesterase inhibition by fasciculin: crystal structure of the complex, Cell 83 (1995) 503–512.

[6] J.-P. Changeux, Responses of acetylcholinesterase from *Torpedo marmorata* to salts and curarizing drugs, Mol. Pharmacol. 2 (1966) 369–392.

[7] M. Fischer, A. Ittah, I. Liefer, M. Gorecki, Expression and reconstitution of biologically active human acetylcholinesterase from *Escherichia coli*, Cell. Mol. Neurobiol. 13 (1993) 25–38.

[8] S. Greenfield, Acetylcholinesterase may have novel functions in the brain, Trends Neurosci. 7 (1984) 364–368.

[9] E. Gross, D. Goldberg, A. Levitzki, Phosphorylation of *S. cerevisiae* Cdc25 in response to glucose results in its dissociation from Ras, Nature 360 (1992) 762–765.

[10] M. Harel, G.J. Kleywegt, R.B. Ravelli, I. Silman, J.L. Sussman, Crystal structure of an acetylcholinesterase–fasciculin complex: interaction of a three-fingered toxin from snake venom with its target, Structure 3 (1995) 1355–1366.

[11] E. Harlow, D. Lane, Antibodies: A Laboratory Manual, Cold Spring Harbor Laboratory, Cold Spring Harbor, NY, 1988, pp. 488–495.

[12] R. Higuchi, Recombinant PCR, in: M.A. Innis, D.H. Gelfand, J.J. Sninsky, T.J. White (Eds.), PCR Protocols: A Guide to Methods and Applications, Academic Press, San Diego, CA, 1990, pp. 177–183.

[13] P.W. Hoffman, A. Ravindran, R.L. Huganir, Role of phosphorylation in desensitization of acetylcholine receptors expressed in *Xenopus* oocytes, J. Neurosci. 14 (1994) 4185–4195.

[14] E.G. Hyde, W.W. Carmichael, Anatoxin-a(s), a naturally occurring organophosphate, is an irreversible active site-directed inhibitor of acetylcholinesterase (EC 3.1.1.7), J. Biochem. Toxicol. 6 (1991) 195–201.

[15] K. Ichtchenko, T. Nguyen, T.C. Sudhof, Structures, alternative splicing and neurexin binding of multiple neuroligins, J. Biol. Chem. 271 (1996) 2676–2682.

[16] N.C. Inestrosa, A. Alvarez, C.A. Perez, R.D. Moreno, M. Vicente, C. Linker, O.I. Casanueva, C. Soto, J. Garrido, Acetylcholinesterase accelerates assembly of amyloid-β-peptides into Alzheimer's fibrils: possible role of the peripheral site of the enzyme, Neuron 16 (1996) 881–891.

[17] I.M. Johansson, A. Nordberg, Pharmacokinetic studies of cholinesterase inhibitors, Acta Neurol. Scand. Suppl. 149 (1993) 22–25.

[18] R. Karpel, M. Sternfeld, D. Ginzberg, E. Guhl, A. Graessmann, H. Soreq, Overexpression of alternative human acetylcholinesterase forms modulates process extensions in cultured glioma cells, J. Neurochem. 66 (1996) 114–123.

[19] M.J. Knapp, D.S. Knopman, P.R. Solomon, W.W. Pendlebury, C.S. David, S.I. Gracon, A 30-week randomized controlled trial of high-dose tacrine in patients with Alzheimer's disease, J. Am. Med. Assoc. 271 (1994) 985–991.

[20] D.I. Kreimer, R. Szosenfogel, D. Goldfarb, I. Silman, L. Weiner, Two-state transition between molten globule and unfolded states of acetylcholinesterase as monitored by electron paramagnetic resonance spectroscopy, Proc. Natl. Acad. Sci. USA 91 (1994) 12145–12149.

[21] U.K. Laemmli, Cleavage of structural proteins during the assembly of the head of bacteriophage T4, Nature (London) 227 (1970) 680–683.

[22] P. Layer, E. Willbold, Novel functions of cholinesterases in development, physiology and disease, Prog. Hisotchem. Cytochem. 29 (1995) 1–92.

[23] C. L'Na, J.-P. Changeux, Allosteric modulation of the nicotinic acetylcholine receptor, Trends Neurolog. Sci. 16 (1993) 181–186.

[24] Y. Loewenstein-Lichtenstein, D. Glick, N. Gluzman, M. Sternfeld, H. Zakut, H. Soreq, Overlapping drug interaction sites of human butyrylcholinesterase dissected by site-directed mutagenesis, Mol. Pharmacol. 50 (1996) 1423–1431.

[25] J. Massoulié, L. Pezzementi, S. Bon, E. Krejci, F.M. Vallette, Molecular and cellular biology of cholinesterases, Prog. Neurobiol. 41 (1993) 31–91.

[26] K. Meflah, S. Bernard, J. Massouli', Interaction with lectins indicates differences in the carbohydrate composition of the membrane-enzymes acetylcholinesterase and 5'-nucleotidase in different cell types, Biochemie 66 (1984) 59–69.

[27] C.B. Millard, C.A. Broomfield, Anticholinesterases: medical applications of neurochemical principles, J. Neurochem. 64 (1995) 1909–1918.

[28] S. Miller, J. Janin, A.M. Lisk, C. Chothia, Interior and surface of monomeric proteins, J. Mol. Biol. 196 (1987) 641–656.

[29] W. Muller, J.J. Petrozzino, L.C. Griffith, W. Danho, J.A. Connor, Specific involvement of Ca(2+)-calmodulin kinase II in cholinergic modulation of neuronal responsiveness, J. Neurophysiol. 68 (1992) 2264–2269.

[30] D.S. Navaratnam, J.D. Priddle, B. McDonald, M.M. Esiri, J.R. Robinson, A.D. Smith, Anomalous molecular form of acetylcholinesterase in cerebrospinal fluid in histologically diagnosed Alzheimer's disease, Lancet 337 (1991) 447–450.

[31] L.F. Neville, A. Gnatt, Y. Loewenstein, S. Seidman, G. Ehrlich, H. Soreq, Intramolecular relationships in cholinesterases revealed by oocyte expression of site-directed and natural variants of human BCHE, EMBO J. 11 (1992) 1641–1649.

[32] C. Patriotis, A. Makris, J. Chernoff, P.N. Tsichlis, Tpl-2 acts in concert with Ras and Raf-1 to activate mitogen-activated protein kinase, Proc. Natl. Acad. Sci. USA 91 (1994) 9755–9759.

[33] E.K. Perry, B.E. Tomlinson, G. Blessed, K. Bergman, P.H. Gibson, R.H. Perry, Cholinergic correlates of cognitive impairment in Parkinson's disease: comparison with Alzheimer's disease, J. Neurol. Neurosurg. Psychiat. 48 (1985) 413–422.

[34] V.A. Pieribone, O. Shupliakov, L. Brodin, S. Hifiker-Rothenfluh, A.J. Czernik, P. Greengard, Distinct pools of synaptic vesicles in neurotransmitter release, Nature (London) 375 (1995) 493–497.

[35] D.R. Ripoll, C.H. Faerman, P.H. Axelsen, I. Silman, J.L. Sussman, An electrostatic mechanism for substrate guidance down the aromatic gorge of acetylcholinesterase, Proc. Natl. Acad. Sci. USA 90 (1993) 5128–5132.

[36] B.M. Schmidt, R.J. Rylett, Phosphorylation of rat brain choline acetyltransferase and its relationship to enzyme activity, J. Neurochem. 61 (1993) 1774–1781.

[37] M. Schwarz, D. Glick, Y. Loewenstein, H. Soreq, Engineering of human cholinesterases explains and predicts diverse consequences of administration of various drugs and poisons, Pharmacol. Ther. 67 (1995) 283–322.

[38] F.S. Seibert, J.A. Tabcharani, X.-B. Chang, A.M. Dulhanty, C. Mathews, J.W. Hanrahan, J.R. Riordan, cAMP-dependent protein kinase-mediated phosphorylation of cystic fibrosis transmembrane conductance regulator residue Ser-753 and its role in channel activation, J. Biol. Chem. 270 (1995) 2158–2162.

[39] S. Seidman, M. Sternfeld, R. Ben Aziz-Aloya, R. Timberg, D. Kaufer, H. Soreq, Synaptic versus epidermal accumulation of human acetylcholinesterase is encoded by alternative 3'-terminal exons, Mol. Cell. Biol. 14 (1995) 459–473.

[40] S. Shaltiel, I. Schwartz, B. Korc-Grodzicki, T. Kreizman, Evidence for an extra-cellular function for protein kinase A, Mol. Cell Biochem. 127 (1993) 283–291.

[41] D.H. Small, G. Reed, B. Whitefield, V. Nurcombe, Cholinergic regulation of neurite outgrowth from isolated chick sympathetic neurons in culture, J. Neurosci. 15 (1995) 144–151.

[42] A.D. Smith, K.A. Jobst, D.S. Navaratnam, Z.X. Shen, J.D. Priddle, B. McDonalds, E. King, M.M. Esiri, Anomalous acetylcholinesterase in lumbar CSF in Alzheimer's disease, Lancet 338 (1991) 1538.

[43] H. Soreq, R. Miskin, A. Zutra, U.Z. Littauer, Modulation in the levels and localization of plasminogen activator in differentiating neuroblastoma cells, Dev. Brain. Res. 7 (1983) 257–259.

[44] H. Soreq, H. Zakut, Human Cholinesterases and Anticholinesterases, Academic Press, San Diego, CA, 1993, 300 pp.

[45] J.L. Sussman, M. Harel, F. Frolow, C. Oefner, A. Goldman, L. Toker, I. Silman, Atomic structure of acetylcholinesterase from *Torpedo californica*: a prototypic acetylcholine-binding protein, Science 253 (1991) 872–879.

[46] P. Taylor, Cholinergic agonists, anticholinesterase agents, in: A.G. Gilman, T.W. Rall, A.S. Nies, P. Taylor (Eds.), Pharmacological Basis of Therapeutics, Pergamon, New York, NY, 1990, pp. 122–130, 131–149.

[47] J.Q. Trojanowski, V.M. Lee, Phosphorylation of paired helical tau filaments in Alzheimer's disease neurofibrillary lesions: focusing on phosphatases, FASEB J. 9 (1995) 1570–1576.

[48] B. Velan, C. Kronman, H. Grosfeld, M. Leitner, Y. Gozes, Y. Flashner, T. Sery, S. Cohen, R. Ben-Aziz, S. Seidman, A. Shafferman, H. Soreq, Recombinant human acetylcholinesterase is secreted from transiently transfected 293 cells as a soluble globular enzyme, Cell. Mol. Neurobiol. 11 (1991) 143–156.

[49] B. Velan, C. Kronman, A. Ordentlich, Y. Flashner, M. Leitner, S. Cohen, A. Shafferman, < it > N < /it > -Glycosylation of human acetylcholinesterase: effects on activity, stability and biosynthesis, Biochem. J. 296 (1993) 649–656.

[50] C. Volonte, D. Merlo, M.T. Ciotti, P. Calissano, Identification of an ecto-kinase activity in cerebellar granule primary neuronal cultures, J. Neurochem. 63 (1994) 2028–2037.

[51] D.A. Walsh, S.M. Van Patten, Multiple pathway signal transduction by the cAMP-dependent protein kinase, FASEB J. 8 (1994) 1227–1236.

Elsevier Science B.V.

Fax: (31) (20) 485 3271
Phone: (31)(20) 485 3474

Postal Address:
Brain Research
Elsevier Science B.V.
P.O. Box 2759, 1000 CT Amsterdam
The Netherlands

Courier Service Address:
Brain Research
Elsevier Science B.V.
Molenwerf 1, 1014 AG Amsterdam
The Netherlands

* * *

If you need information about your accepted manuscript, proof, etc. then phone or FAX us at the above numbers, stating the journal name and article code number. We can also FAX this journal's Instructions to Authors to you.

SUBSCRIPTION AND PUBLICATION DATA 1997

Brain Research (including **Molecular Brain Research, Developmental Brain Research, Cognitive Brain Research Brain Research Protocols** and **Brain Research Reviews**) will appear weekly and be contained in 57 volumes (120 issues): **Brain Research, Volumes 743–778** (36 volumes in 72 issues), **Molecular Brain Research, Volumes 41–50** (10 volumes in 20 issues), **Developmental Brain Research, Volumes 98–104** (7 volumes in 14 issues), **Cognitive Brain Research, Volume 5** (1 volume in 4 issues) **Brain Research Protocols, Volume 1** (1 volume in 4 issues) and **Brain Research Reviews, Volumes 24–25** (2 volumes in 6 issues). Please note that **Volumes 41–43** of **Molecular Brain Research, Volume 743** of **Brain Research** and **Volume 5 (Issues no. 1 and 2)** of **Cognitive Brain Research** were published ahead of schedule in 1996, in order to reduce publication time. The volumes remain part of the 1997 subscription year.

Separate subscriptions: Molecular Brain Research, Vols. 41–50, Developmental Brain Research, Vols. 98–104, Cognitive Brain Research, Vol. 5, Brain Research Protocols, Vol. 1 and **Brain Research Reviews, Vols. 24 and 25,** may also be ordered separately. Prices are available from the Publisher upon request. Subscriptions are accepted on a prepaid basis only, unless different terms have been previously agreed upon.

Subscription orders can be entered only by calender year (Jan.-Dec.) and should be sent to Elsevier Science B.V., Order Fulfillment Department, P.O. Box 211, 1000 AE Amsterdam, The Netherlands, Tel.: (31) (20) 485 3642, Fax: (31) (20) 485 3598, or to your usual subscription agent.

Postage and handling charges include surface delivery except to the following countries where air delivery via SAL (Surface Air Lift) mail is ensured: Argentina, Australia, Brazil, Canada, Hong Kong, India, Israel, Japan, Malaysia, Mexico, New Zealand, Pakistan, P.R. China, Singapore, South Africa, South Korea, Taiwan, Thailand and USA. For all other countries airmail rates are available upon request.

Claims for missing issues must be made within six months of our publication (mailing) date, otherwise such claims cannot be honoured free of charge.

Orders, claims, and product enquiries: please contact the Customer Support Department at the Regional Sales Office nearest you: **New York,** Elsevier Science, P.O. Box 945, New York, NY 10159-0945, USA. Tel: (+1) 212-633-3730, [Toll free number for North American customers:1-888-4ES-INFO (437-4636)], Fax: (+1) 212-633-3680, e-mail: usinfo-f@elsevier.com; **Amsterdam,** Elsevier Science, P.O. Box 211, 1000 AE Amsterdam, The Netherlands. Tel: (+31) 20-485-3757, Fax: (+31) 20-485-3432, e-mail: nlinfo-f@elsevier.nl; **Tokyo,** Elsevier Science, 9-15, Higashi-Azabu 1-chome, Minato-ku, Tokyo 106, Japan. Tel: (+81) 3-5561-5033, Fax: (+81) 3-5561-5047, e-mail: kyf04035@niftyserve.or.jp; **Singapore,** Elsevier Science, No. 1 Temasek Avenue, #17-01 Millenia Tower, Singapore 039192. Tel: (+65) 434-3727, Fax: (+65) 337-2230, e-mail: asiainfo@elsevier.com.sg

Advertising Information: Advertising orders and enquiries may be sent to: *International:* Elsevier Science, Advertising Department, The Boulevard, Langford Lane, Kidlington, Oxford, OX5 1GB, UK; Tel.: (+44) (0) 1865 843565; Fax: (+44) (0) 1865 843976. *U.S.A. & Canada:* Weston Media Associates, Dan Lipner, P.O. Box 1110, Greens Farms, CT 06436-1110, USA, Tel.: (203) 261 2500; Fax: (203) 261 0101. *Japan:* Elsevier Science Japan, Marketing Services, 1-9-15 Higashi-Azabu, Minato-ku, Tokyo 106, Japan; Tel.: (+81) 3 5561 5033; Fax: (+81) 3 5561 5047.

ADONIS Identifier. This Journal is in the **ADONIS** Service, whereby copies of individual articles can be printed out from CD-ROM on request. An explanatory leaflet can be obtained by writing to **ADONIS** B.V., P.O. Box 17005, 1001 JA Amsterdam, The Netherlands.

⊗ The paper used in this publication meets the requirements of ANSI/NISO Z39.48-1992 (Permanence of Paper).

The Journal of Neuroscience, February 15, 1998, 18(4):•–•

Acetylcholinesterase Enhances Neurite Growth and Synapse Development through Alternative Contributions of Its Hydrolytic Capacity, Core Protein, and Variable C Termini

Meira Sternfeld,[1] Guo-li Ming,[2] Hong-jun Song,[2] Keren Sela,[1] Rina Timberg,[1] Mu-ming Poo,[2] Hermona Soreq[1]

[1]*Department of Biological Chemistry, The Life Sciences Institute, The Hebrew University of Jerusalem, 91904, Israel,*
[2]*Department of Biology, University of California at San Diego, La Jolla, CA 92093-0357*

Accumulated indirect evidence suggests nerve growth-promoting activities for acetylcholinesterase (AChE). To determine unequivocally whether such activities exist, whether they are related to the capacities of this enzyme to hydrolyze acetylcholine and enhance synapse development, and whether they are associated with alternative splicing variants of AChEmRNA, we used four recombinant human AChEDNA vectors. When *Xenopus laevis* embryos were injected with a vector expressing the synapse-characteristic human AChE-E6, which contains the exon 6-encoded C terminus, cultured spinal neurons expressing this enzyme grew threefold faster than cocultured control neurons. Similar enhancement occurred in neurons expressing an insertion-inactivated human AChE-E6-IN protein, containing the same C terminus, and displaying indistinguishable immunochemical and electrophoretic migration properties from AChE-E6, but incapable of hydrolyzing acetylcholine. In contrast, the nonsynaptic secretory human AChE-I4, which contains the pseudointron 4-derived C terminus, did not affect neurite growth. Moreover, no growth promotion occurred in neurons expressing the catalytically active C-terminally truncated human AChE-E4, demonstrating a dominant role for the E6-derived C terminus in neurite extension. Also, AChE-E6 was the only active enzyme variant to be associated with *Xenopus* membranes. However, postsynaptic length measurements demonstrated that both AChE-E6 and AChE-E4 enhanced the development of neuromuscular junctions *in vivo*, unlike the catalytically inert AChE-E6-IN and the nonsynaptic AChE-I4. These findings demonstrate an evolutionarily conserved synaptogenic activity for AChE that depends on its hydrolytic capacity but not on its membrane association. Moreover, this synaptogenic effect differs from the growth-promoting activity of AChE, which is unrelated to its hydrolytic capacity yet depends on its exon 6-mediated membrane association.

Key words: acetylcholinesterase; alternative C termini; neurogenesis; neurite extension; noncatalytic function; Xenopus *spinal neurons; synaptogenesis; neuromuscular junctions*

Acetylcholinesterase (AChE) hydrolyzes the neurotransmitter acetylcholine (ACh) released from nerve terminals at neuromuscular junctions (NMJs) and brain cholinergic synapses, thus terminating synaptic transmission (Salpeter, 1967). Potential noncatalytic functions of AChE were implicated by findings that certain AChE inhibitors decrease chick neurite outgrowth in culture and that externally added AChE stimulates this process regardless of the presence of specific inhibitors (Layer et al., 1993; Jones et al., 1995; Small et al., 1995). Sequence homology between AChE and several adhesion molecules (de La Escalera et al., 1990; Auld et al., 1995; Ichtchenko et al., 1995) and the early appearance of AChE in developing embryos before the onset of cholinergic neurotransmission (Layer and Willbold, 1995) also suggest that AChE may play a developmental function in cellular development and neuronal growth that is unrelated to its classic ACh hydrolyzing activity. However, experiments aimed at the noncatalytic nature of the neurogenic activity of AChE were all based on the indirect use of inhibitors or involved external addition of AChE to the culture medium (Jones et al., 1995) or solid substrate (Layer et al., 1993; Small et al., 1995). This called for studies in which the activity levels of AChE would be changed within the tested neurons themselves.

Human pre-AChEmRNA may be alternatively spliced at its 3′ end to yield three mature AChEmRNAs encoding protein products with three distinct C termini (Ben Aziz-Aloya et al., 1993; Karpel et al., 1994). These include the brain-abundant exon 6-encoded C-terminal peptide, the hematopoietic exon 5-encoded C terminus, which enables glycophospholipid attachment, and the C terminus derived from the open reading frame of the tumor-abundant pseudointron 4. The brain and muscle human (h) AChE form (hAChE-E6), expressed in developing *Xenopus laevis* embryos, accumulates in and enlarges the postsynaptic length of neuromuscular junctions (NMJs) (Seidman et al., 1994; 1995). Transgenic mice expressing hAChE-E6 show NMJ enlargement and late onset neuromotor deterioration (Andres et al., 1997). In contrast, DNA encoding the read-through form of hAChEmRNA (ACHE-I4/E5) causes production and secretion of an enzyme C terminated by the I4-encoded peptide (hAChE-I4) in ciliated and secretory epidermal cells of *Xenopus* embryos. Moreover, hAChE-I4 did not reach NMJs or affect their length (Seidman et

Received Oct. 2, 1997; revised Nov. 21, 1997; accepted Nov. 26, 1997.

This work was supported by grants from National Institutes of Health (NS 31923) to M-m.P., and USARMED (DAMD 17-97-1-7007), the Israeli Ministry of Defense, and the Binational Science Foundation United States-Israel (96/00110/1) to H.S. We thank Dr. U. Brodbeck, Bern, Switzerland, for anti-AChE antibodies, and Ms. Daniela Kaufer for help with experiments.

M.S. and G.M. contributed equally to this work.

Correspondence should be addressed to Hermona Soreq, Department of Biological Chemistry, The Life Sciences Institute, The Hebrew University of Jerusalem, 91904, Israel.

al., 1995). When transfected into glioma cells, ACHE-I4/E5 caused the appearance of small, processless round cells, whereas hAChE-E6 transfection induced process extension (Karpel et al., 1996). To explore the involvement of the catalytic activity and the alternative C termini of AChE in its neurogenic or synaptogenic activities, we constructed two novel hAChEDNA vectors. One of these encodes a truncated form of the enzyme, devoid of any of the natural C termini; the other encodes an insert-disrupted form of the enzyme, incapable of hydrolyzing ACh yet recognized by anti-AChE antibodies. These two constructs and the above hACHE-E6 and hACHE-I4/E5 DNAs were microinjected into *Xenopus* oocytes and embryos. The biochemical and hydrodynamic properties of the resultant proteins were then compared with the effects of each of these AChE variants on neurite extension from spinal neurons and on *in vivo* NMJ development in *Xenopus*.

MATERIALS AND METHODS

Construction of vectors. The plasmids referred to here as ACHE-E6 and ACHE-I4/E5 have been described in detail (Ben Aziz-Aloya et al., 1993; Seidman et al., 1995). To create a DNA construct encoding a truncated form of hAChE, lacking either of the native C termini, we used a two-phase PCR engineering procedure (Higuchi, 1990) using the recombinant human ACHE cDNA and genomic clones (Soreq et al., 1990). In the first PCR phase, performed essentially as described (Karpel et al., 1994), ACHE-E6 served as template. Two partially overlapping products were produced in which ACHE exon 4 and the SV40 polyadenylation signal were joined together, using primers containing the overlapping sequence: E3/1522+ 5′-CGGCTCTACGCCTACGTCTTTGAACAC CGTGCTTC-3′; E4del4–5′-TAACGTCGACTATCAGGTGGCGCT GAGCAATTTGGGGG-3′; E4del3+ 5′-TTGCTCAGCGCCACCTGAT AGTCGACGTTAACTTGTTTATTGCAGCTTATAATGG-3′; SV40 PolyA-5′ ATGATTTGGACAAACCACAACTAGAATGCAGTG-3′. Primers were named according to their position in the human ACHE alternative sequences and vectors. After removal of the primers, the two products were combined into one longer product by a second PCR reaction in which they served as templates. External primers E3/1522+ and SV40 polyA- were used in the second phase to create a fragment consisting of the 3′ end of exon 3, exon 4, and the polyA signal. PCR reaction was as above except that in the first cycle the denaturing step was at 94°C for 5 min and the annealing step was from 94 to 50°C (slope rate of 1°C per 30 sec). The product and the original ACHE-E6 plasmid were restricted using enzymes *Not*I and *Sal*I, and the two products were then ligated.

To construct the disrupted ACHE coding sequence we inserted an in-frame sequence of 21 nucleotides, six bases downstream of the codon for the active site serine, located in exon 2. The technique used was the same two-phase PCR described above. In the first PCR phase we used primers containing the inserted sequence. Primers used were E2/340+ 5′-GCTTTCCTGGGCATCCCCTTTGCGGAGCCA-3′; E2ins2–5′-TCCaccgaattgaggatgtcgccacgcgctCTCCCCAAACAGCGT-3′; E2ins1+ 5′-AGCGCCGtggcgacatcctcaattcggtggaGCCGCCTCGGCGGGCAT-3′; 1212–5′-GAAGTCTCCCGCGTTGATCAGGGCCTCTGG-3′. The inserted sequence is designated by lower case letters. Primers E2/340+ and E2ins2- were used to link the inserted sequence to the upstream PCR product, and primers E2ins1+ and E2/1212- were used to link it to the downstream product. The second PCR phase was performed using external primers E2/340+ and E2/1212-. Stage II PCR products and ACHE-E6 were restricted using enzymes *Bst*EII and *Sph*I and ligated. First and second phase PCR reactions were as above. After construction, the accuracy and integrity of both constructs was validated by DNA sequencing.

Recombinant AChE production and assays of hydrolytic activity. Xenopus oocytes were microinjected with 10 ng of DNA of each recombinant AChE plasmid, incubated for 48 hr, and homogenized in high-salt–detergent buffer as described previously (Neville et al., 1990). Homogenates were frozen until use. AChE activity was measured by evaluating acetylthiocholine (ATCh) hydrolysis using 96-well microtiter plates. pH dependence of AChE activity was assessed using phosphate buffer at the pH range 5.8–8.0, with intervals of 0.2. For K_m and substrate inhibition experiments, we used ATCh in the concentration range of 0.05–60 mM and the GraFit 3.0 program (Erithacus Software limited, Staines, UK). For enzyme stability studies, oocyte homogenates were incubated at 19–42°C for 0–5 hr, after which AChE catalytic activities in each of the homogenates were assessed as above.

Xenopus *embryo microinjection and subcellular fractionation. In vitro* fertilization of mature *Xenopus* eggs and blastomere microinjection were performed as described elsewhere (Seidman et al., 1994), except that embryos were raised in 19–21°C. Subcellular fractionation of 1-, 2-, and 3-d-old embryos into low-salt (0.01 M Tris-HCl, pH 7.4, 0.05 M $MgCl_2$, 144 mM NaCl), low-salt–detergent (1% Triton X-100 in 0.01 M sodium phosphate, pH 7.4), and high-salt (1 M NaCl in 0.01 M sodium phosphate, pH 7.4) buffers was performed as described previously (Seidman et al., 1994).

Protein blot analyses and immunocytochemistry. Denaturing SDS-PAGE and blotting were essentially as described elsewhere (Seidman et al., 1994), except that after transfer the blots were washed with 1× PBS (80 mM NaH_2PO_4, 20 mM Na_2HPO_4, pH 7.4), 0.5% Tween-20, 18% glucose, 10% glycerol, 2.5% bovine serum albumin, and 1% skim milk. Immunodetection was performed using a pool of monoclonal antibodies (132–1,2,3; 6 μg/ml each) raised against denatured human brain AChE, and a $1:2 \times 10^4$ dilution of a horseradish–peroxidase-conjugated sheep anti-mouse IgG (Jackson Laboratories, Bar Harbor, ME). Chemiluminescent detection was performed with the ECL kit (Amersham Life Sciences) as instructed. Ten microliter samples of oocyte homogenate (equivalent to ~50 ng AChE) were loaded on each lane. For enzyme activity blots, we used nondenaturing gel electrophoresis followed by incubation in ATCh staining mixture (Seidman et al., 1995), using similar amounts of oocyte homogenates.

For immunochemical AChE detection *in situ*, cells were fixed with 2% paraformaldehyde in PBS for 30 min at room temperature and then permeabilized with 0.1% Triton X-100 (20 min). After they were washed with TBST (10 mM Tris-HCl, pH 7.0, 150 mM NaCl, 0.05% Tween-20), cells were incubated with anti-human AChE antibodies (mouse monoclonal antibody 132–1; 1:1000 dilution in TBST containing 10% normal goat serum) at 4°C overnight. After washes with TBST (5 × 30 min), cells were incubated with goat anti-mouse IgG conjugated to fluorescein (Sigma) (1:100 in TBST containing 10% normal goat serum) at 22°C for 2 hr. After the same washing procedure as described above, cells were mounted and observed under a Nikon Diaphot microscope with a 20×/1.25 objective.

Culture preparation. Xenopus nerve–muscle cultures were prepared according to previously reported methods (Spitzer and Lamborghini, 1976; Anderson et al., 1977; Tabti and Poo, 1995). Briefly, neural tubes and the associated myotomal tissue of 1-d-old *Xenopus* embryos (stage 20–23 according to Nieuwkoop and Faber, 1967) were dissociated in Ca^{2+}-Mg^{2+}-free saline supplemented with EDTA (115 mM NaCl, 2.6 mM KCl, 10 mM HEPES, 0.4 mM EDTA, pH 7.6) for 15–20 min. The cells were plated on glass coverslips and used for experiments after 6 hr of incubation at room temperature. The culture medium consisted (vol/vol) of 49% Leibovitz L-15 medium (Life Technologies, Gaithersburg, MD), 1% bovine serum (Life Technologies), and 50% Ringer's solution (115 mM NaCl, 2 mM $CaCl_2$, 2.6 mM KCl, 10 mM HEPES, pH 7.6).

Neurite length measurements. Line drawings of isolated neurons and their neuritic processes were traced from the video monitor display of recorded microscopic images. The tip of the growing neurite was defined as the distal leading edge of the phase-dark palm of the growth cone, without considering the filopodial extension. The entire trajectory of the neurite, including all of its branches, was measured with a digitizing pad (Houston Instruments), and the total length of each neurite was calculated by a microcomputer. The rate of extension (micrometers per hour) was determined by dividing the net increase in neurite length (in micrometers) by the duration of observation (in hours).

Electron microscopy and morphometric analyses. Histochemical staining, transmission electron microscopy, and morphometric analyses were performed as described previously (Ben Aziz-Aloya et al., 1993; Seidman et al., 1995).

RESULTS

Construction and analyses of hAChE variants

To delineate functions and domains of AChE variants that are involved in neuron growth and synaptogenesis, two novel hAChEDNA vectors were constructed by a two-phase PCR procedure (see Materials and Methods). One of these constructs, ACHE-E4 (Fig. 1*A*), carries a truncated coding sequence containing exons 2, 3, and 4 of the human ACHE gene. The other construct, ACHE-

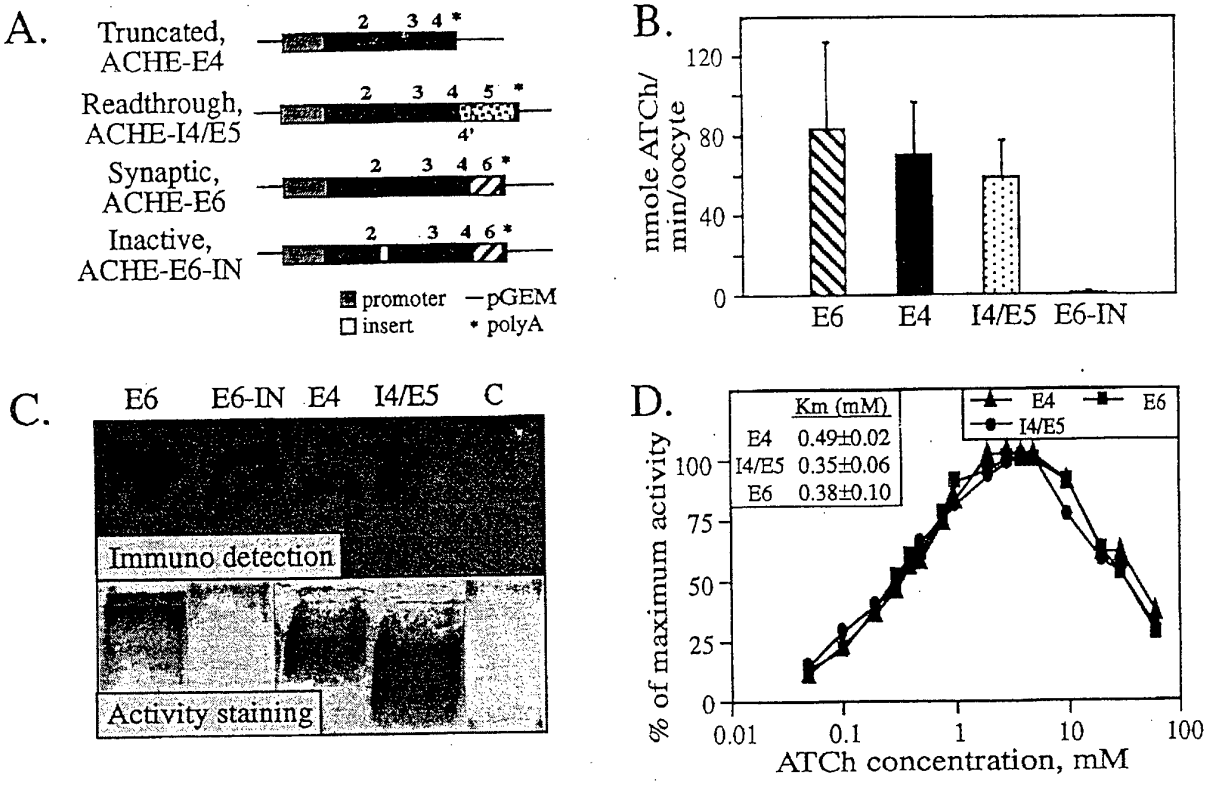

Figure 1. Biochemical properties of recombinant AChE variants. *A*, Analyzed AChE DNAs and the DNA constructs encoding each of the examined AChE variants. Common exons are designated by *black boxes*, exon 6 by a *hatched box*, and pseudointron 4 and exon 5 by *dotted boxes*. See Materials and Methods for details on the construction of these vectors. *B*, Hydrolytic cholinesterase activities. ATCh hydrolyzing activities of each of the enzyme forms encoded by the above ACHE constructs were tested in homogenates of microinjected *Xenopus* oocytes. Presented are average results of three experiments for each construct. Endogenous *Xenopus* AChE activities were subtracted from activities found for cDNA-injected oocytes. Note that AChE-E4 activity levels are comparable with those of AChE-E6 and AChE-I4 and that AChE-E6-IN displayed no significant catalytic activity. *C*, Electrophoretic properties and antibody recognition of the AChE variants. Homogenates of *Xenopus* oocytes microinjected with each of the ACHE cDNA constructs and of control buffer-injected oocytes (*C*) were subjected to denaturing gel electrophoresis followed by protein blot and immunodetection (*top*) and to nondenaturing gel electrophoresis followed by AChE activity staining (*bottom*). Each lane represents ~50 ng AChE. Note that AChE-E6-IN is highly immunoreactive but displays no catalytic activity and that AChE-E4 migrates faster than the other variants in the denaturing gel. In the *bottom panel*, note that AChE-I4 displays heterogeneous bands and migrates faster than AChE-E6 and AChE-E4. *D*, Substrate inhibition. The above oocyte homogenates were assayed for cholinesterase activity in the presence of 0.05–60 mM ATCh as substrate. Cholinesterase activity in each substrate concentration is shown as percentage of the highest activity for each homogenate, after subtraction of spontaneous ATCh hydrolysis. Shown is one representative of two experiments. *Inset*, K_m values of the recombinant hAChE variants.

E6-IN (Fig. 1*A*), encodes a protein identical to the synapse-accumulating AChE-E6, except that it carries an in-frame insert of seven amino acids near the active site protein sequence, which should render it inactive. Similar to the previously used ACHE-E6 (Ben Aziz-Aloya et al., 1993) (Fig. 1*A*) and ACHE-I4/E5 (Seidman et al., 1995) (Fig. 1*A*), transcription of both these constructs was regulated by the cytomegalovirus promoter, and they both contain the SV40 polyadenylation signal. Together, this set of four constructs enabled us to explore the biochemical and morphogenic activities of AChEs with three distinct C termini (encoded by E6, I4, or E4) and of the synaptic AChE-E6 enzyme with or without catalytic capacity.

For biochemical characterization of their protein products, all four plasmids were microinjected into *Xenopus* oocytes. The catalytic activity of the resultant proteins was then assessed by measuring the hydrolysis rate of acetylthiocholine (ATCh) in oocyte homogenates. As predicted, oocytes expressing the disrupted form, ACHE-E6-IN, displayed exceedingly low activity levels (Fig. 1*B*), which were similar to those of the two experimental controls: buffer-injected and uninjected oocytes (not shown), most probably reflecting the endogenous *Xenopus* AChE activity levels. As expected, both natural AChE variants, terminated with the E6-encoded C terminus or with that encoded by I4, showed high activity levels (Fig. 1*B*), confirming previous results (Schwarz et al., 1995a; Seidman et al., 1995). The novel truncated form of AChE, encoded by ACHE-E4, displayed activity levels within the range of the other two variants (Fig. 1*B*). This demonstrated that neither of the natural C termini encoded by E6 or I4 is essential for the ACh hydrolytic activity of AChE.

Electrophoretic distinctions and hydrolytic similarities

In consideration of the possibility that the low activity levels observed for the ACHE-E6-IN homogenates did not reflect inactivation but were caused by impaired production of this protein in oocytes, we subjected the various recombinant hAChEs to denaturing gel electrophoresis followed by immunoblotting. Selective immunodetection of hAChE bands (Fig. 1*C*, *top panel*) demonstrated that the *Xenopus* system is capable of producing AChE-E6-IN in size and amounts comparable to those of the other AChE variants. The electrophoretic migration distance of

all variants except AChE-E4 matched the expected molecular weight of 66 kDa, whereas AChE-E4 migrated somewhat faster, consistent with its truncated C terminus. Minor amounts of an immunopositive protein, with a migration distance similar to that of AChE-E4, could also be seen in the lanes loaded with the protein products of ACHE-E6 and ACHE-E6-IN (Fig. 1*C*, *top panel*). Catalytic activity and intact C termini are therefore not obligatory requirements for production and stability of this protein in the *Xenopus* milieu.

When subjected to nondenaturing gel electrophoresis followed by AChE activity staining, the enzyme produced by ACHE-E6-IN showed no detectable catalytic activity, as opposed to the other variants, which were all highly active (Fig. 1*C*, *bottom panel*). The migration of AChE-E6 was considerably slower and the band was much sharper than those of AChE-I4, which displayed faster migrating heterogeneous bands. AChE-E4 showed an intermediate band. The four tested hAChE variants thus differed in their Stokes radius and charge and active site conformation, whereas they maintained similar primary folding and production efficiency.

Having shown that ACHE-E6, ACHE-I4/E5, and ACHE-E4 all encode for active enzymes, we wished to examine whether changing the C terminus of AChE did not affect its catalytic properties in a more subtle manner. Interestingly, the *Xenopus* enzyme retained its full catalytic activity after 5 hr at 42°C, whereas all hAChE variants lost 50% of their activity (not shown). However, all three hAChE variants were found to have K_m values within the same range of the previously reported value (0.3 mM for AChE-E6 in *Xenopus* oocytes) (Seidman et al., 1994) and were similarly inhibited by high substrate concentrations (Fig. 1*D*). Also, substrate hydrolysis by all AChE forms was similarly enhanced within the pH range of 5.8–8.0 (data not shown), in agreement with reports of others (for review, see Schwarz et al., 1995b). There was therefore no indication whatsoever for involvement of the variable C termini of AChE in its catalytic properties, consistent with previous reports in which proteolytic cleavage of the C terminus was used to obtain a homogeneous catalytically active AChE preparation for x-ray diffraction analysis (Sussman et al., 1991).

Expression of human AChE in *Xenopus* spinal neurons

Expression of hAChE in *Xenopus* embryonic neurons was examined after injection of each of the above hAChEDNA constructs into one of the blastomeres of two-cell stage *Xenopus* embryos. To facilitate identification of living neurons expressing hAChE during neurite growth assays, fluorescent dextran was co-injected with the DNA. The progeny neurons of the injected blastomere could then be identified by the presence of fluorescent dextran. Confirmation of AChE expression in individual spinal neurons was then obtained by immunocytochemical staining of the dissociated neurons from 1-d-old embryos, using monoclonal antibodies specific for hAChE (Seidman et al., 1995). The reliability of fluorescent dextran as a marker for neurons overexpressing AChE was examined in the following experiment. Nerve–muscle cultures were prepared from embryos injected with ACHE-E6 cDNA and rhodamine–dextran. Dextran-positive neurons in 1-d-old cultures were identified and recorded. The same cultures were then processed for immunocytochemical staining with antibodies against AChE. In control cultures prepared from embryos not injected with AChE-E6 cDNA, there was a negligible level of AChE staining. In cultures prepared from AChE-E6 cDNA and dextran-injected embryos, we found that 92% (36 of 39 cells) of dextran-positive neurons exhibited AChE staining, whereas 95% (55 of 58 cells) of dextran-negative neurons exhibited undetectable AChE staining. Figure 2 depicts examples of (AChE+) and (AChE−) neurons, together with their bright-field images at 7, 8, and 9 hr in culture, before the staining of AChE. In this culture, dextran-positive muscle cells also showed, as expected, elevated staining with AChE. Thus, immunostaining for hAChE shows that hAChE-E6 is expressed in these spinal neurons and that dextran fluorescence is a reliable marker for AChE expression.

Effects of expressing human AChE on neurite growth

Six hours after plating of dissociated *Xenopus* neural tube cells in culture, many spinal neurons exhibit active neurite outgrowth. Only isolated neurons not in contact with any other cell were used in this study, on which two types of neurite growth assays were made. First, the total neurite length of each neuron in the culture was measured. Second, extension of individual neurites was measured for a 3–4 hr period at 1 hr intervals (from 6 to 10 hr after plating). The hAChE-expressing (AChE+) neurons were identified by the presence of fluorescent dextran in the cell. To reduce culture-to-culture variation, similar numbers of (AChE+) and control neurons in the same culture or cultures from the same batch of embryos were examined. This analysis revealed that the average neurite length (the entire trajectory of the neurite, including all its branches) was 124.0 ± 11.7 μm (SEM; $n = 32$) in (AChE-E6+)-expressing neurons, which is significantly longer ($p < 0.001$; two-tailed t test) than that observed for noninjected neurons (88.2 ± 10.3 μm; SEM; $n = 33$) or AChE-I4-expressing neurons (77.5 ± 8.2 μm; SEM; $n = 27$). To illustrate the overall difference in neurite growth for a large number of neurons, composite drawings were made by superimposing tracings of the video images of randomly chosen neurons, 15 from each of the noninjected control, (AChE-E6+), and (AChE-I4+) groups, respectively (Fig. 3). It is clear from this figure that the net neurite extension over the first 9 hr in culture was substantially longer in (AChE-E6+) neurons.

The higher total neurite length at a particular time in culture may reflect a higher growth rate of each neurite, an earlier onset of neurite outgrowth from the soma after cell plating, or both. Direct measurements of the growth rate of individual neurites during the 6–10 hr period revealed that (AChE-E6+) neurites indeed exhibit a higher growth rate. As shown in Table 1, in the same group of cultures, the average growth rate was 12.9 ± 2.7 μm/hr (SEM; $n = 33$) for noninjected control neurons but was elevated to 37.9 ± 5.2 μm/hr (SEM; $n = 32$) for (AChE-E6+) neurons, the difference being highly significant ($p < 0.005$; two-tailed t test). In contrast, neurons expressing the read-through form AChE-I4 did not show any difference in growth rate compared with the noninjected controls. The enhanced growth rate of (AChE-E6+) neurons was sufficient to account for the difference in the overall neurite length described above, although earlier neurite initiation could also have occurred. In addition to the growth rate, we also measured the number of neuritic branches in each group of neurons. As shown in Table 1, no significant difference was found between any of the groups.

Growth promotion is unrelated to ACh hydrolytic activity

Whether the growth-promoting effect on *Xenopus* neurons was partially or entirely caused by the catalytic activity of the enzyme in hydrolyzing ACh was tested by expressing AChE-E6-IN, the insertion-inactivated form of AChE-E6, which lacks ACh hydro-

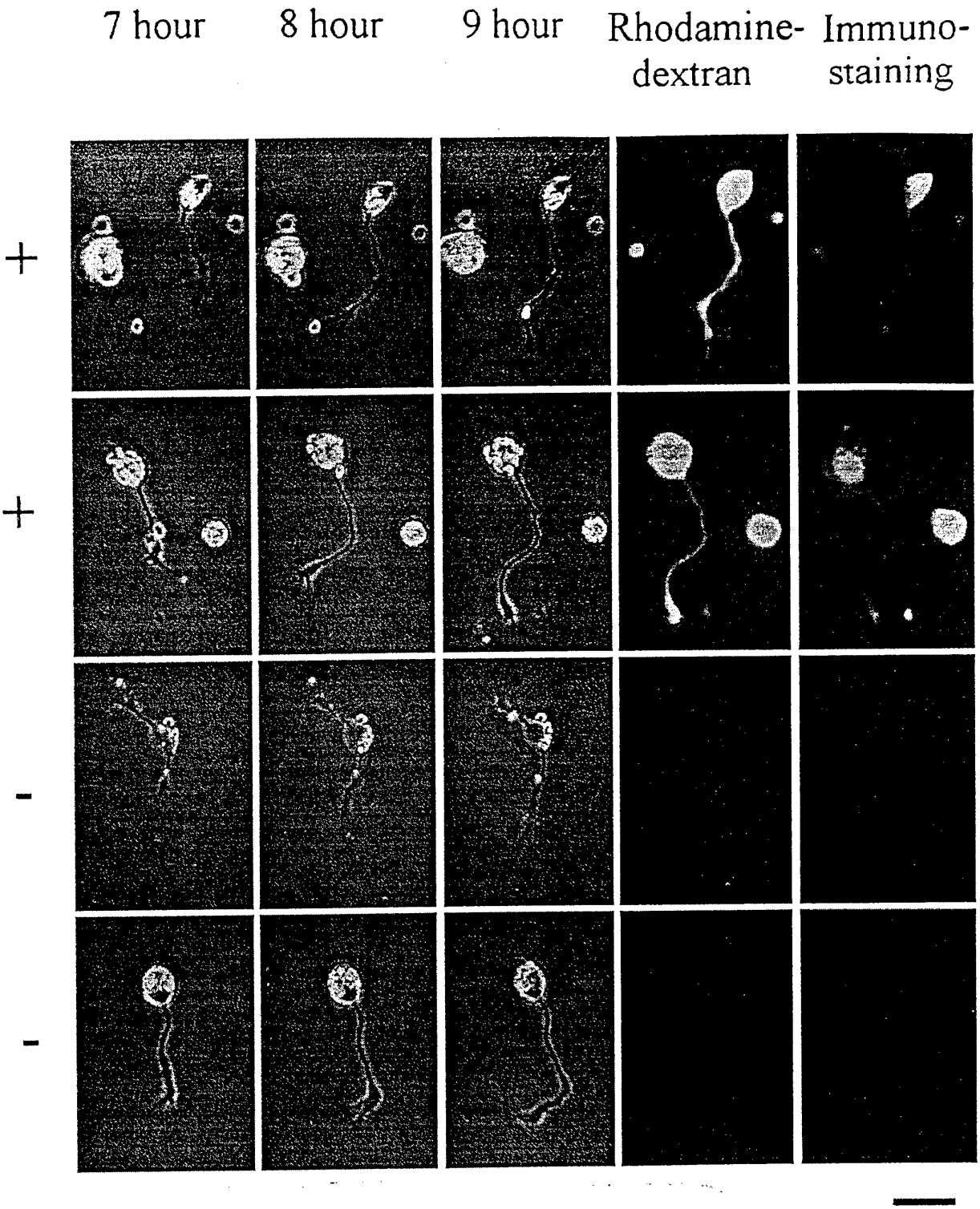

Figure 2. Neurons expressing human AChE-E6 (+) and control neurons (−) in *Xenopus* cultures. *Xenopus* embryos were co-injected with AChE-E6 DNA and rhodamine–dextran complexes, and their spinal neurons were dissociated into culture 1 d later. Bright-field images were taken at 7, 8, and 9 hr after cell plating. Both the total neurite length and the rate of neurite growth were measured during this period. Fluorescence micrographs on the right of the 9 hr photographs depict the rhodamine fluorescence of dextran complexes, which were co-injected with the cDNA. Indirect fluorescein immunofluorescence staining of AChE observed at the end of the experiment is shown on the last *right panel*. Note the correlation between dextran fluorescence and AChE staining. Staining and imaging conditions were identical for all four cells, which were from the same culture. Fluorescently labeled cells (+) were positive with both red and green filters, whereas negative (−) cells remained invisible in both. Scale bar, 20 μm.

Orig. Op.	OPERATOR:	Session	PROOF:	EDs:	AAs:	COMMENTS:	ARTNO:	INIT:
1st disk, 2nd YY(v)	taylorp	6	GH/R				482123	ea

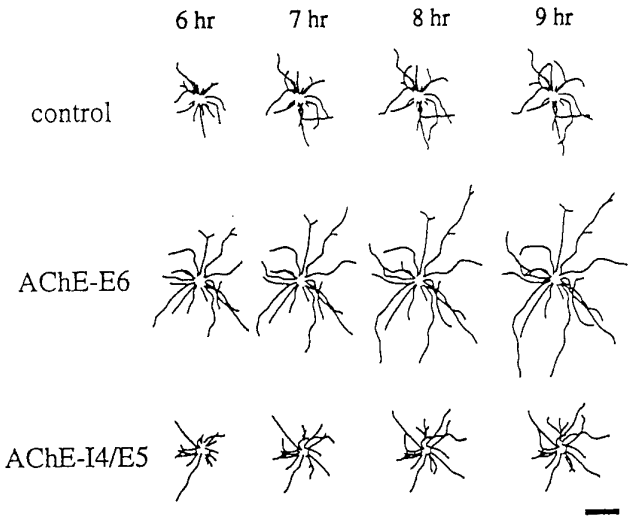

Figure 3. Effects of expressing human AChE on the growth of *Xenopus* spinal neurons. Composite concentric line drawings were made from video images of 12 isolated spinal neurons at 6, 7, 8, and 9 hr after cell plating. The center of the neuronal soma (deleted from this image) was placed in the center of each drawing. Note consistent overall neurite length promotion in neurons that expressed AChE-E6 but not AChE-I4. Neurons derived from uninjected blastomeres served as controls. Scale bar, 20 μm.

lytic activity (see above). As shown in Table 1, (AChE-E6+) and (ACHE-E6-IN+) neurites were similar both in the total neurite length after 9–10 hr in culture and in the rate of neurite growth during this period. Thus, the ability of hAChE to promote growth was associated with the presence of the E6-derived C terminus, regardless of the catalytic activity.

The E6-derived C terminus is essential for growth promotion

The ability of AChE-E6 but not AChE-I4 to promote neurite growth could be attributable to a dominant-positive effect of the AChE-E6 C terminus (conferred by a sequence and/or structural element present in this domain), or to a dominant-negative effect exerted by the I4-encoded C terminus (i.e., the I4 peptide could interfere with the growth-promoting properties of other domain(s) in the AChE core protein). This problem was examined by expressing the truncated AChE-E4 form of AChE, which retains the ACh hydrolytic activity yet lacks either the E6- or the I4-derived natural C-terminal peptides. The inability of AChE-E4 to promote growth (Table 1) proved the first option correct. Therefore, growth promotion of *Xenopus* spinal neurons by AChE did not require ACh hydrolytic activity; neither was it affected by the presence or absence of the I4-derived C terminus. Rather, to exert this growth-promoting activity the E6-derived synapse-characteristic C terminus must be present.

The growth promotion activity of AChE is associated with membrane interaction

Despite their sequence and biochemical similarities, AChE-E6 and AChE-I4 have previously been shown to be differentially localized in *Xenopus* embryos, both intra- and intercellularly (Seidman et al., 1995). AChE-E6 was found to be associated with NMJs and AChE-I4 localized in epidermis and secreted therefrom. To compare the hydrodynamic and membrane association properties of the different recombinant hAChE variants in relation to their growth-promoting capacities, we microinjected ACHE-E4, ACHE-E6, or ACHE-I4/E5 DNAs into *in vitro* fertilized *Xenopus* eggs. Sequential extractions of injected embryos into low-salt, low-salt–detergent, and high-salt buffers yielded hAChE-containing homogenates from 1-, 2-, and 3-d-old injected *Xenopus* embryos. AChE catalytic activities measured in these homogenates ranged 2- to 10-fold higher than those of homogenates from uninjected embryos (data not shown) (Seidman et al., 1995). Most importantly, the recombinant hAChE variants differed in their membrane association. Catalytically active AChE in homogenates from ACHE-E4-injected embryos was 92–95% soluble in low-salt buffer, and AChE-I4 was 74–91% low-salt soluble (Fig. 4), as compared with 33–53% for low-salt-soluble AChE-E6. A major fraction (20–50%) of hAChE-E6, but no other active variant, partitioned into the low-salt–detergent fraction, reconfirming our previous reports (Seidman et al., 1995) and resembling the solubility pattern of the endogenous *Xenopus* enzyme (Fig. 4). Thus, although AChE-E6 could be membrane-associated, AChE-E4 and AChE-I4 appear to be soluble proteins that could be secreted from the cells expressing them. Moreover, in all cases except AChE-E4, but including the endogenous *Xenopus* enzyme, there seemed to be a shift in solubility with development, from the low-salt fraction to the detergent and high-salt fractions. This shift may reflect a progressive increase in membrane interaction and association with other components, such as the extracellular matrix, at the time these components are being formed and neurites extend their neurites *in vivo*.

The synaptogenic and neurite growth-promoting activities of AChE are distinct

To compare the synaptogenic effect of AChE (Seidman et al., 1995) with its neurite growth-promoting capacity, we examined neuromuscular junctions (NMJs) from myotomes of 2-d-old embryos injected with the above four vectors. AChE activity staining (Seidman and Soreq, 1996) followed by transmission electron microscopy was used to assess the *in vivo* localization of AChE and its synaptogenic activity in *Xenopus* NMJs. As is apparent from the representative images of NMJs presented in Figure 5, both AChE-E6 and the truncated AChE-E4 accumulated in NMJs in amounts exceeding those in control NMJs. High levels of catalytically active AChE, most likely of endogenous *Xenopus* origin, were also detected in NMJs from embryos expressing AChE-E6-IN. In contrast, AChE-I4 was absent from NMJs, confirming previous observations (Seidman et al., 1995). These analyses demonstrated that although the E6-encoded C terminus may promote the interaction of AChE with NMJ components, it is not obligatory for NMJ accumulation of catalytically active AChE. Rather, the I4-encoded C terminus appeared to interfere dominantly with the accumulation of AChE in NMJs. Moreover, postsynaptic length measurements in 2-d-old embryos showed that transgenic expression of both AChE-E6 and the soluble AChE-E4 enlarged NMJs from an average length of 1.82 ± 0.16 μm (SEM; $n = 55$) to significantly larger synapses with averages of 2.29 ± 0.16 μm (SEM; $n = 66$) and 2.68 ± 0.36 μm (SEM; $n = 16$), respectively ($p < 0.05$; two-tailed t test). In contrast, NMJs from embryos expressing AChE-I4 or AChE-E6-IN displayed average postsynaptic lengths that were somewhat smaller yet not significantly different from that of control NMJs (1.69 ± 0.19 μm, SEM, $n = 43$, and 1.41 ± 0.23 μm, SEM, $n = 31$, respectively). The columns in Figure 5 depict this change, which is reflected by a shift in NMJ distribution between two groups: synapses with postsynaptic lengths smaller or larger than 2.5 μm. Thus, both the

Table 1. Effects of AChE on neurite growth *in vitro*

Construct injected[a]		Total neurite length per cell (μm) at 6–7 hr.	Total neurite length per cell (μm) at 9–10 hr.	Growth rate (μm/hr)	Number of branches	Number of cells (embryos)
ACHE-E6	+	64.6 ± 6.5	124.0 ± 11.7*	37.9 ± 5.2*	1.8 ± 0.1	32 (7)
	–	55.2 ± 5.9	88.2 ± 10.3	12.9 ± 2.7	1.6 ± 0.1	33 (7)
ACHE-I4/E5	+	62.0 ± 10.6	77.5 ± 8.2	11.6 ± 2.1	1.7 ± 0.1	27 (8)
	–	52.9 ± 5.0	92.7 ± 6.2	14.7 ± 1.9	1.6 ± 0.1	31 (8)
ACHE-E6-IN	+	91.2 ± 9.8*	156.9 ± 13.6*	33.6 ± 3.7*	2.0 ± 0.1	25 (3)
	–	47.4 ± 5.1	62.5 ± 9.6	11.2 ± 2.1	1.5 ± 0.1	28 (3)
ACHE-E4	+	48.0 ± 7.0	94.2 ± 9.1	11.9 ± 3.7	1.7 ± 0.2	16 (4)
	–	51.6 ± 7.4	126.2 ± 20.4	13.0 ± 4.2	1.8 ± 0.2	20 (4)

[a] cDNA vectors were injected into *Xenopus* embryos at the two-cell stage using rhodamine–dextran as a marker. Cultures were made from injected embryos 1 d later. "+" indicates rhodamine–detran-positive neurons; "–" indicates rhodamine–dextran-negative neurons in the same cultures.

* Significant difference was found between + and – groups (two-tailed t test; $p < 0.005$).

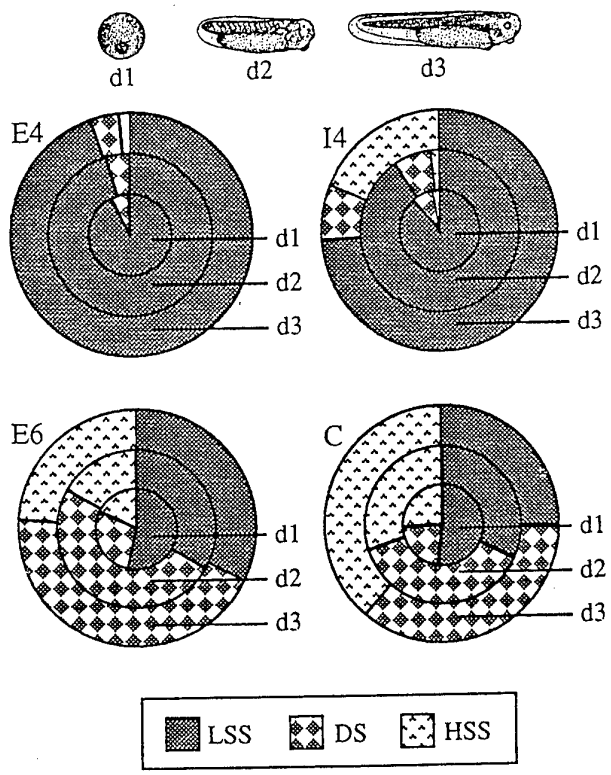

Figure 4. AChE-E6 exhibits developmentally increased membrane association *in vivo*. Cleaving *Xenopus* embryos were injected with the various ACHE DNA vectors or with buffer (*C*) and sequential extractions into low-salt-soluble (*LSS*), low-salt–detergent-soluble (*DS*), and high-salt-soluble (*HSS*) fractions were performed. Endogenous *Xenopus* AChE activities were subtracted from activities of all other embryo samples. Slices therefore represent the net relative fractions of the total summed activities for the host enzyme and each hAChE variant. Note that AChE-E6 is similar to *Xenopus* AChE in its lower solubility under low-salt extraction, whereas AChE-E4 and AChE-I4 are both predominantly low-salt soluble. *Top*, Schematic drawings of 1,- 2-, and 3-d-old *Xenopus* embryos modeled after those of Deuchar (1966).

synaptic accumulation and the hydrolytic capacity of the transgenic enzyme were found to be obligatory requirements for its ability to enhance NMJ development. In contrast, the synaptogenic activity of AChE was found to be unrelated to membrane association, unlike its neuritic growth-promoting function.

DISCUSSION

We used four recombinant hAChE variants to demonstrate that the neurite growth-promoting activity of AChE in cultured *Xenopus* neurons depends on the E6-encoded C terminus but not on catalytic activity, whereas its synaptogenic property in live *Xenopus* embryos depends both on its ability to accumulate within the synapse and on its hydrolytic capacity. Thus, AChE plays two distinct roles, with different mechanistic requirements, during nervous system development.

That the C terminus of hAChE modifies the electrophoretic migration properties of the enzyme under both native and denaturing conditions demonstrated that it constitutes an independent domain in the AChE protein, affecting its Stokes radius and surface charge. Human AChE-E6, AChE-I4, and AChE-E4, all of which differ in their C termini, are catalytically active and enzymatically indistinguishable (this report) (Schwarz et al., 1995a). Cleavage of the E6-encoded C terminus does not affect the catalytic activity of *Torpedo* AChE (Duval et al., 1992), which demonstrates that the C terminus is not necessary for substrate hydrolysis *in vitro*. Our current results further reveal that the intact catalytic activity of AChE in *Xenopus laevis* is C terminus independent also *in vivo*. Furthermore, an in-frame insertion of a foreign septapeptide near the active site serine abolished the catalytic activity of the enzyme, consistent with predictions of others (Taylor and Radic, 1994). Neither of these alterations had an apparent effect on the amounts or the immunoreactivity of the enzyme produced in *Xenopus* oocytes or embryos.

The minor fast-migrating immunoreactive band produced from the hAChE-E6 and hAChE-E6-IN proteins implies partial cleavage of the C terminus encoded by E6, yielding a protein that is identical to hAChE-E4. The electrophoretic heterogeneity of hAChE-I4 and the fact that part of the hAChE-I4 protein migrated similarly to hAChE-E4 under nondenaturing gel electrophoresis further suggested that the I4-encoded C terminus could be positioned in several orientations relative to the core domain and be accessible to proteases, consistent with findings of others (Sussman et al., 1991). However, because only minor parts of hAChE-E6 or hAChE-I4 co-migrate with hAChE-E4, we conclude that most of the former proteins indeed possessed their complete C termini.

Sequential extraction experiments demonstrated that the endogenous *Xenopus* enzyme and hAChE-E6 partitioned mainly between the low-salt and the low-salt–detergent fractions, whereas hAChE-E4 and hAChE-I4 were almost completely sol-

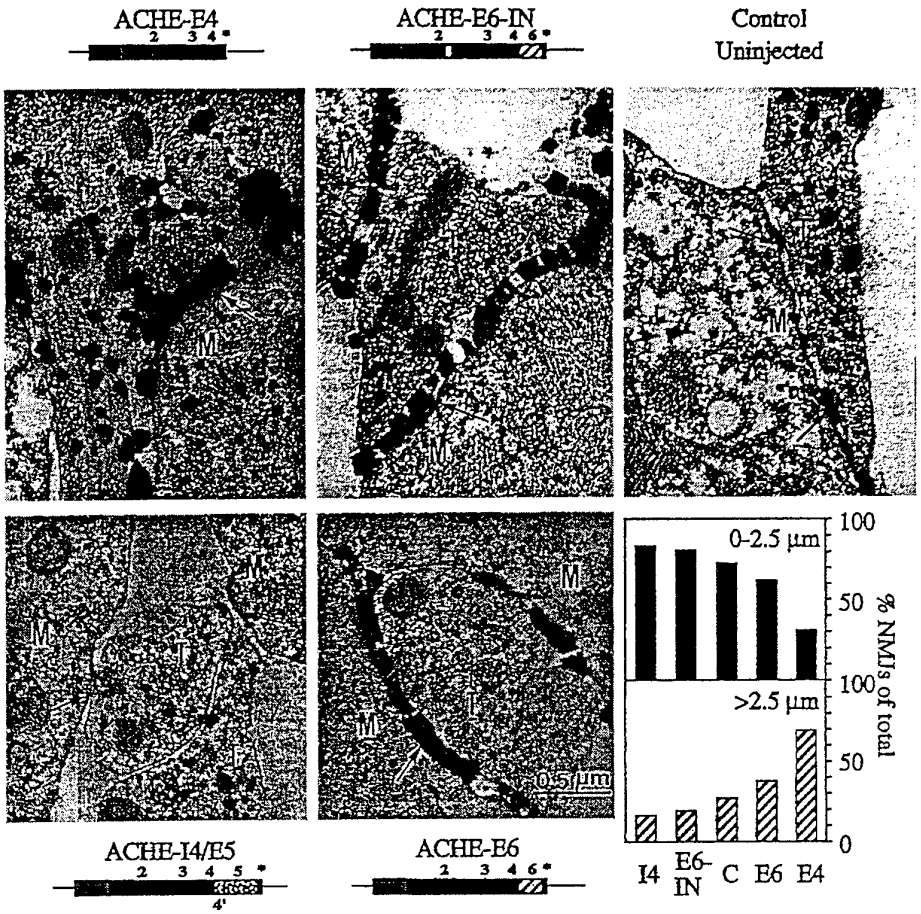

Figure 5. AChE-E6 and AChE-E4 enhance NMJ length, whereas AChE-I4 and AChE-E6-IN do not. Two-day-old DNA-injected and control uninjected *Xenopus* embryos were stained for catalytically active AChE and examined by electron microscopy. Representative images of NMJs from embryos with each of the vectors are shown. Note the enhanced staining apparent as dark electron-dense deposits in NMJs from AChE-E6-, AChE-E6-IN-, and AChE-E4-injected embryos as compared with controls. *T*, Nerve terminal; *M*, muscle cell; *arrows* points at synaptic clefts. *Bottom right panel*, NMJ population analysis. Electron microscope NMJ images (16, 31, 43, and 66 sections from AChE-E4, -E6-IN, -I4, and -E6 injected and 55 sections from control uninjected embryos, respectively) were used for postsynaptic length measurements. The percentage of synapses with lengths shorter or longer than 2.5 μm are presented for NMJs from embryos injected with each vector. Note that expression of AChE-E6 and AChE-E4 increases postsynaptic length as compared with controls.

ubilized in low salt. These observations extend previous findings (Seidman et al., 1995) that unlike hAChE-E6, hAChE-I4 is secreted to the medium by *Xenopus* embryos and imply that the C terminus encoded by I4 does not contribute to the membrane interaction properties of this enzyme. Furthermore, these results are in agreement with the well known membrane association of AChE-E6 (for review, see Massoulie et al., 1993). Therefore, of all AChE forms tested, only proteins containing the E6-derived C terminus could associate with neuronal membranes and support growth through such association.

The endogenous *Xenopus* enzyme, which has not yet been extensively characterized or molecularly cloned, displayed hydrodynamic properties and subcellular interactions similar to those of transgenic hAChE-E6 and resembles the synaptic form of mammalian AChE encoded by ACHE-E6. *Xenopus* AChE is more resistant to heat and to the anticholinesterase echothiophate than the human enzyme and does not form heteromeric multimers with hAChE (this report) (Seidman et al., 1994). However, despite these distinctions, *Xenopus* neurons and NMJs respond to the morphogenic activities of hAChE in an evolutionarily conserved manner. This emphasizes the importance of these functions and may allude to their early emergence in evolution.

In addition to its extracellular function in the hydrolysis of synaptic ACh, we demonstrate here that when intracellularly expressed, the membrane-associated AChE-E6 protein but not the alternatively spliced AChE-I4-secreted protein promotes autologous neurite extension of *Xenopus* neurons. Similar neurite growth activity can be induced by mutation-inactivated AChE-E6 but not by the enzymatically active truncated AChE-E4 enzyme. In cultures of chick sympathetic neurons, rat hippocampus, or retinal ganglion cells, AChE inhibitors interacting with the peripheral site of the enzyme prevented the neurite growth effect and fasciculation exerted by externally added AChE (Layer et al., 1993; Jones et al., 1995; Small et al., 1995). However, the active site organophosphate inhibitor echothiophate, which totally inhibits cholinesterase activity, did not block AChE-induced growth. This indicated that the neurite promotion effects were not caused by enzyme activity per se. However, the effect of these pharmacological agents could be unrelated to their binding to AChE, whereas elevation of the levels of intracellularly produced AChE protein unequivocally establishes a novel noncatalytic function for this protein. Like the process extension in rat glioma cells microinjected with ACHE-E6 DNA (Karpel et al., 1996), the neurite growth-promoting effect was spatially limited to those cells expressing the enzyme and did not extend to adjacent, non-hAChE-expressing neurons. This suggests that it involves the detergent-extractable fraction of AChE-E6 and that it is associated with membrane protein signaling.

How does AChE promote neurite growth? A group of adhesion molecules, such as neurotactin, neuroligin, and gliotactin, contain extracellular domains showing a uniformly distributed homology to cholinesterases. Their cysteine positions correspond to those involved in the formation of AChE intramolecular disulfide bonds, suggesting that these adhesion molecules may resume

tertiary structure similar to that of cholinesterases. Although none of these proteins is a catalytically active esterase, replacement of the extracellular domain of *Drosophila* neurotactin with the core domain of AChE created a chimeric protein promoting cell adhesion (Darboux et al., 1996). *Drosophila* AChE itself or neurotactin lacking most of its intracellular or extracellular domains failed to do so, suggesting membrane-associated signaling operable with the AChE core domain. Thus, AChE may promote neurite extension by modulating the adhesion capacity of neurites.

β-Neurexins have been identified as the neuronal membrane partners interacting with neuroligins (Ichtchenko et al., 1995). This indicates that the core AChE domain encoded by exons 2–4 and corresponding to the cholinesterase-like domains of neurotactin and neuroligins could also operate by supporting recognition of neurexins and related ligand(s). In mammals, it has been postulated that association between β-neurexins and neuroligins contributes to axon growth and cell–cell and cell–extracellular matrix interactions (Puschel and Betz, 1995). Unlike the core polypeptide of AChE, the E6-derived C terminus does not share homology with the neurotactin family members (Seidman et al., 1995) but could associate the enzyme with the cell membrane. Both hAChE-E6 and hAChE-E6-IN, but not hAChE-E4 or hAChE-I4, could potentially associate with the cell membrane through the E6 C terminus and interact, through the core AChE domain, with a β-neurexin-like ligand expressed on the surface of the same or other cells or associated with the extracellular matrix. This would elicit signal transduction by the intracellular domain of the ligand, which can induce neurite extension. Likewise, the process extension effect exerted by hAChE-E6 on glia (Karpel et al., 1996) can be attributed to interaction with the corresponding ligand of the AChE homologous protein gliotactin (Auld et al., 1995). Moreover, the recent discovery of the novel Neurexin 4 expressed in epithelial cells (Baumgartner et al., 1996) extends this hypothesis also to non-neuronal sites. This theory is strengthened further by our recent observation that transgenic expression of hAChE in mice modulates the production of β-neurexins in the mouse spinal cord (Andres et al., 1997). Molecular cloning of *Xenopus* neurexins would be required to further investigate this mechanism.

The novel function of AChE in promoting neurite growth explains the early developmental involvement for this protein before synaptogenesis, supporting descriptive theories based on its spatiotemporal expression pattern in avian embryogenesis (Layer et al., 1995). It presents an interesting example of multiple, seemingly unrelated functions for one protein. That such functional duality in various tissues may be a more general phenomenon than we are currently aware of is indicated from findings with other proteins, such as lactate dehydrogenase (LDH), which is both a hepatic enzyme (Baumgart et al., 1996) and a structural crystallin protein in the lens (Chiou et al., 1991; Voorter et al., 1993). Although ACh hydrolysis was the first and foremost identified function of AChE, distinct elements on the surface of this protein might have been preserved during evolution because of their interaction capacities with specific diverse molecules, which serve for different cellular functions.

Unlike its neurite growth-promoting activity, our current findings demonstrate that the synaptogenic activity of AChE is tightly related with its catalytic activity yet not dependent on the E6-derived C terminus. Thus the synaptic accumulation of the catalytically active, truncated AChE-E4 sufficed to enhance NMJ development *in vivo*, whereas the inert AChE-E6-IN did not enlarge these synapses, although its biochemical properties suggest distribution similar to that of the native enzyme. This in turn suggests that the I4-derived C terminus is actively involved in the exclusion of AChE-I4 from the synaptic cleft and attributes an important role to the effective termination of cholinergic neurotransmission in synapse development. Altogether, one should view AChE as a modular macromolecule, designed to transduce neurite growth signals as well as synapse development ones by virtue of a concerted combination of its core protein domain, alternative C termini and its ACh hydrolytic capacity.

REFERENCES

Anderson MJ, Cohen MW, Zorychta E (1977) Effects of innervation on the distribution of acetylcholine receptors on cultured muscle cells. J Physiol (Lond) 268:731–756.

Andres C, Beeri R, Friedman A, Lev-Lehman E, Henis S, Timberg R, Shani M, Soreq H (1997) Acetylcholinesterase-transgenic mice display embryonic modulations in spinal cord choline acetyltransferase and neurexin Iβ gene expression followed by late-onset neuromotor degeneration. Proc Natl Acad Sci USA 95:8173–8178.

Auld VJ, Fetter RD, Broadie K, Goodman CS (1995) Gliotactin, a novel transmembrane protein on peripheral glia, is required to form the blood-nerve barrier in *Drosophila*. Cell 81:757–767.

Baumgart E, Fahimi H, Stich A, Volki A (1996) L-lactate dehydrogenase A4- and A3B isoforms are bona fide peroxisomal enzymes in rat liver. Evidence for involvement in intraperoxisomal NADH reoxidation. J Biol Chem 271:3846–3855.

Baumgartner S, Littleton JT, Broadie K, Bhat MA, Harbecke R, Lengyel JA, Chiquet-Ehrismann R, Prokop A, Bellen HJ (1996) A *Drosophila* neurexin is required for septate junction and blood-nerve barrier formation and function. Cell 87:1059–1068.

Ben Aziz-Aloya R, Seidman S, Timberg R, Sternfeld M, Zakut H, Soreq H (1993) Expression of a human acetylcholinesterase promoter-reporter construct in developing neuromuscular junctions of *Xenopus* embryos. Proc Natl Acad Sci USA 90:2471–2475.

Chiou SH, Lee HJ, Huang SM, Chang GG (1991) Kinetic comparison of caiman epsilon-crystallin and authentic lactate dehydrogenases of vertebrates. J Protein Chem 10:161–166.

Darboux I, Barthalay Y, Piovant M, Hipeau-Jaczquotte R (1996) The structure-function relationships in *Drosophila* neurotactin show that cholinesterasic domains may have adhesive properties. EMBO J 15:4835–4843.

de La Escalera S, Bockamp EO, Moya F, Piovant M, Jimenez F (1990) Characterization and gene cloning of neurotactin, a *Drosophila* transmembrane protein related to acetylcholinesterase. EMBO J 9:3593–3601.

Deuchar EM (1966) Biochemical aspects of amphibian development. London: Methuen.

Duval N, Massoulie J, Bon S (1992) H and T subunits of acetylcholinesterase from *Torpedo*, expressed in COS cells generate all types of globular forms. J Cell Biol 118:641–653.

Higuchi R (1990) Recombinant PCR. In: PCR protocols (Innis MA, Gellfand DH, Sninsky JJ, White TJ, eds), pp 177–183. San Diego: Academic.

Ichtchenko K, Hata Y, Nguyen T, Ullrich B, Missler M, Moomaw C, Sudhof TC (1995) Neuroligin 1: a splice site-specific ligand for β-neurexins. Cell 81:435–443.

Jones SA, Holmes C, Budd TC, Greenfield SA (1995) The effect of acetylcholinesterase on outgrowth of dopaminergic neurons in organotypic slice culture of rat midbrain. Cell Tissue Res 279:323–330.

Karpel R, Ben Aziz-Aloya R, Sternfeld M, Ehrlich G, Ginzberg D, Tarroni P, Clementi F, Zakut H, Soreq H (1994) Expression of three alternative acetylcholinesterase messenger RNAs in human tumor cell lines of different tissue origins. Exp Cell Res 210:268–277.

Karpel R, Sternfeld M, Ginzberg D, Guhl E, Graessman A, Soreq H (1996) Overexpression of alternative human acetylcholinesterase forms modulates process extensions in cultured glioma cells. J Neurochem 66:114–123.

Layer PG, Willbold E (1995) Novel functions of cholinesterases in development, physiology and disease. Prog Histochem Cytochem 29:1–99.

Layer PG, Weikert T, Alber R (1993) Cholinesterases regulate neurite growth of chick nerve cells in vitro by means of a non-enzymatic mechanism. Cell Tissue Res 273:219–226.

Orig. Op.	OPERATOR:	Session	PROOF:	EDs:	AAs:	COMMENTS:	ARTNO:	INIT:

Massoulie J, Pezzementi L, Bon S, Krejci E, Vallette F-M (1993) Molecular and cellular biology of cholinesterases. Prog Neurobiol 41:31–19.

Neville LF, Gnatt A, Padan R, Seidman S, Soreq H (1990) Anionic site interactions in human butyrylcholinesterase disrupted by two adjacent single point mutations. J Biol Chem 265:20735–20738.

Nieuwkoop PD, Faber J (1967) Normal table of *Xenopus laevis*, Ed 2. Amsterdam: North Holland.

Puschel AW, Betz H (1995) Neurexins are differentially expressed in the embryonic nervous system of mice. J Neurosci 15:2849–2856.

Salpeter M (1967) Electron microscope radioautography as a quantitative tool in enzyme cytochemistry. I. The distribution of acetylcholinesterase at motor endplates of a vertebrate twitch muscle. J Cell Biol 32:379–389.

Schwarz M, Loewenstein-Lichtenstein Y, Glick D, Liao J, Norgaard-Pedersen B, Soreq H (1995a) Successive organophosphate inhibition and oxime reactivation reveals distinct responses of recombinant human cholinesterase variants. Mol Brain Res 31:101–110.

Schwarz M, Glick D, Loewenstein Y, Soreq H (1995b) Engineering of human cholinesterases explains and predicts diverse consequences of administration of various drugs and poisons. Pharmacol Ther 67:283–322.

Seidman S, Soreq H (1996) Transgenic *Xenopus* microinjection methods and developmental neurobiology. Neuromethods series (Boulton A, Baker GB, eds), pp 000–000. Totowa, NJ: Humana.

Seidman S, Ben Aziz-Aloya R, Timberg R, Loewenstein Y, Velan B, Shafferan A, Liao J, Norgaard-Pedersen B, Brodbeck U, Soreq H (1994) Overexpressed monomeric human acetylcholinesterase induces subtle ultrastructural modifications in developing neuromuscular junctions of *Xenopus laevis* embryos. J Neurochem 62:1670–1681.

Seidman S, Sternfeld M, Ben Aziz-Aloya R, Timberg R, Kaufer-Nachum D, Soreq H (1995) Synaptic and epidermal accumulation of human acetylcholinesterase are encoded by alternative 3′-terminal exons. Mol Cell Biol 15:2993–3002.

Small DH, Reed G, Whitefield B, Nurcombe V (1995) Cholinergic regulation of neurite outgrowth from isolated chick sympathetic neurons in culture. J Neurosci 15:144–151

Soreq H, Ben Aziz R, Prody CA, Seidman S, Gnatt A, Neville L, Lieman-Hurwitz J, Lev-Lehman E, Lapidot-Lifson Y, Zakut H (1990) Molecular cloning and construction of the coding region for human acetylcholinesterase reveals a G+C-rich attenuating structure. Proc Natl Acad Sci USA 87:9688–9692.

Spitzer NC, Lamborghini JC (1976) The development of the action potential mechanism of amphibian neurons isolated in culture. Proc Natl Acad Sci USA 73:1641–1645.

Sussman JL, Harel M, Frolow F, Oefner C, Goldman A, Toker L, Silman I (1991) Atomic structure of acetylcholinesterase from *Torpedo californica*: a prototypic acetylcholine-binding protein. Science 253:872–879.

Tabti N, Poo, M-m (1995) Study on the induction of spontaneous transmitter release at early nerve-muscle contacts in *Xenopus* cultures. Neurosci Lett 173:21–26.

Taylor P, Radic Z (1994) Cholinesterases: from genes to proteins. Annu Rev Pharmacol Toxicol 34:281–320.

Voorter CE, Wintjes LT, Heinstra PW, Bloemendal H, De-Jong WW (1993) Comparison of stability properties of lactate dehydrogenase B4/epsilon-crystalline from different species. Eur J Biochem 211:643–648.